PETROGRAPHY AND STABLE ISOTOPE GEOCHEMISTRY OF ALTERATION AND MINERALIZATION IN THE RAMBLER VOLCANOGENIC MASSIVE SULPHIDE DEPOSIT, BAIE VERTE, NEWFOUNDLAND

REINHOLD JAMES WEICK

NOTICE

The quality of this microform is heavily dependent upon the quality of the original thesis submitted for microfilming. Every effort has been made to ensure the highest quality of reproduction possible.

If pages are missing, contact the university which granted the degree.

Some pages may have indistinct print especially if the original pages were typed with a poor typewriter ribbon or if the university sent us an inferior photocopy.

Reproduction in full or in part of this microform is governed by the Canadian Copyright Act, R.S.C. 1970, c. C-30, and subsequent amendments.

AVIS

La qualité de cette microforme dépend grandement de la qualité de la thèse soumise au microfilmage. Nous avons tout fait pour assurer une qualité supérieure de reproduction.

S'il manque des pages, veuillez communiquer avec l'université qui a conféré le grade.

La qualité d'impression de certaines pages peut laisser à désirer, surtout si les pages originales ont été dactylographiées à l'aide d'un ruban usé ou si l'université nous a fait parvenir une photocopie de qualité inférieure.

La reproduction, même partielle, de cette microforme est soumise à la Loi canadienne sur le droit d'auteur, SRC 1970, c. C-30, et ses amendements subséquents.

Canada

PETROGRAPHY AND STABLE ISOTOPE GEOCHEMISTRY OF ALTERATION AND MINERALIZATION IN THE RAMBLER VOLCANOGENIC MASSIVE SULPHIDE DEPOSIT, BAIE VERTE, NEWFOUNDLAND

BY

REINHOLD JAMES WEICK ©

A thesis submitted to the School of Graduate Studies in partial fulfilment of the requirements for the degree of

Master of Science

Department of Earth Science

Memorial University of Newfoundland

April, 1993

St. John's, Newfoundland

ISBN 0-315-91608-7

Canada

Abstract

The Rambler is one of the five VMS deposits of the Consolidated Rambler Mines properties which occur in the Pacquet Harbour Group; a deformed and metamorphosed sequence of volcanic and sedimentary rocks located on the east half of the Baie Verte Peninsula in Central Newfoundland. The deposit contains alteration and base metal sulphide assemblages typically associated with VMS mineralization, but is highly deformed and occurs as a northeast trending, shallow dipping, ellipsoidal body, above a prominent imbricate shear zone. The syn-kinematic quartz + muscovite ± chlorite assemblages in the shear zone are of uncertain origin, but similar to the alteration in several epigenetic / mesothermal gold prospects which occur throughout the Baie Vert region. The alteration and sulphide assemblages associated with the deposit and its shear zone are cut by quartz-carbonate veins which contain their own characteristic alteration assemblages. All alteration assemblages are overprinted by disseminated biotite related to a late metamorphic event.

Oxygen isotope thermometry and calculated $\delta^{18}O$ and δD fluid values confirm a complex thermal and fluid history in the Rambler deposit. An early high temperature event is recorded by the isotopic composition of a dark green variety of chlorite in massive sulphide horizons, which equilibrated with a high ^{18}O magmatic fluid; $\delta^{18}O$ and δD values of +9.0 to +9.4‰ and -39‰ at 430 to 480°C. A decrease in temperature (~200 to 300°C) and shift in $\delta^{18}O$ and δD fluid values to +4.4 and +4.6‰, and -26 to -37‰, respectively, are associated with the occurrence of a pervasive secondary light green chlorite which may have equilibrated with a mixture of seawater and metamorphic fluids during greenschist metamorphism and deformation of the Pacquet Harbour Group. The presence of an additional low ^{18}O (< +5‰) low D (< -60‰) fluid during deformation is suggested by $\delta^{18}O$ and δD mineral values of +6.4 to +8.2‰ and -55 to -70‰ for muscovite which are out of equilibrium with values of +2.9 to +7.5‰ and -57 to -73‰ for coexisting chlorite. Low $\delta^{18}O$ chlorite fluid values of 0 to +4.1‰ at 180 to 200°C may be related to an influx of meteoric waters during the formation of quartz-carbonate

veins.

Metamorphic biotite in the stratigraphy of the deposit appears to have equilibrated with a high ^{18}O fluid, with $\delta^{18}O$ values as high as +7.5 ‰ and δD values of -41 to -49‰ at temperatures of 540 and 560°C. Similar biotite occurs in contact metamorphic assemblages along the margin of the Burlington Granodiorite to the west of the Consolidated Rambler Mines properties.

Alteration mineralogy and isotopic composition of the low ^{18}O-low D fluid which affected the Rambler is distinct from the isotopic composition of the CO_2-rich, low D fluids in equilibrium with chlorite and muscovite during the formation of two epigenetic / mesothermal gold deposits in the Baie Verte and Springdale regions. The replacement of seafloor assemblages in massive sulphide horizons by syn-kinematic assemblages in the footwall shear zone suggests the distinct low ^{18}O-low D hydrothermal fluid may have evolved from the influx and mixing of formational and meteoric fluids during the obduction and imbrication of the Pacquet Harbour Group and its emplacement over the Laurentian continental margin.

Acknowledgements

Financial support for the field work in the summer of 1989 was provided by the Newfoundland Department of Mines and Energy as part of the Federal -Provincial, Mineral Development Agreement. Further financing of the project was provided by Dr. Mark Wilson through his NSERC operating grant at Memorial University.

I would like to gratefully acknowledge the assistance of a number of people, without whose help and support this project would not have been completed. Dr. Mark Wilson as the chair of my supervisory committee was a constant source of ideas and enthusiasm throughout the project. Dr. Scott Swinden of the Newfoundland Department of Mines and Energy is thanked whole-heartedly for his patient criticism and continued review of submitted manuscripts, during the early and latter stages of the study. A review of petrography sections of the thesis by Dr. Roger Mason of Memorial University is gratefully acknowledged. Gert Andrews, Adrian Timball and Gerry Pulchan are thanked for their time and efforts during the completion of the major element and stable isotope analyses. Mervin Goodyear is thanked for his help during the final printing(s) of the thesis.

My colleagues are also thanked for the support they provided during the years I attended Memorial in St. John's. Finally, I would like to thank my wife Alison, for her patience and devotion during a project which consumed a significant amount of my time.

Table of Contents

		page
Abstract		ii
Acknowledgments		iv
Table of Contents		v
List of Tables		viii
List of Figures		ix
List of Plates		xi
Introduction and Purpose of Study		xiii
Chapter 1: Formation and Alteration of Volcanogenic Massive Sulphide (VMS) Deposits		
1.1	Introduction	1
1.2	Volcanogenic Massive Sulphide (VMS) Deposits	2
1.3	Epigenetic Deposits	4
1.4	Alteration Processes related to Syngenetic VMS and Epigenetic Mineralization	8
1.5	Metamorphism and Alteration of VMS Deposits in Orogenic Belts	15
1.6	Implications for the Source of Gold in VMS Deposits	19
Chapter 2: Regional Setting of VMS Deposits on the Consolidated Rambler Mines Properties		
2.1	Introduction	20
2.2	Geology and Metallogeny of the Newfoundland Dunnage Zone	23
2.3	Geology of the Baie Verte Peninsula	29
	2.3.1 Fleur de Lys Belt	29
	2.3.2 Baie Verte Belt	31
2.4	Geology of the Pacquet Harbour Group	33
2.5	VMS and Epigenetic Deposits on the Baie Verte Peninsula	34

Table of Contents

		page
Chapter 3: Geologic Setting and Distribution of Alteration in the Rambler VMS Deposit		
3.1	Introduction	37
3.2	Previous Geological Work	40
3.3	Geologic Setting of the Rambler VMS Deposit	41
3.4	VMS and Gold Mineralization on the Consolidated Rambler Mines Properties	47
3.5	Stratigraphy of the Rambler VMS Deposit	47
Chapter 4: Petrography of Alteration and Mineralization in the Rambler Deposit		
4.1	Introduction	55
4.2	Alteration	55
	4.2.1 Stage 1: Seafloor / Greenschist Metamorphism	56
	4.2.2 Stage 2: Syn-kinematic Alteration	63
	4.2.3 Stage 3: Vein Alteration	67
4.3	Massive and Disseminated Sulphide Mineralization	69
	4.3.1 Secondary Sulphides	71
	4.3.2 Gold	73
	4.3.3 Telluride	73
4.4	Biotite	76
Chapter 5: Major and Trace Element Geochemistry		
5.1	Introduction	78
5.2	Analytical Methods	79
	5.2.1 Assays	79
	5.2.2 Major Element Analyses	79
	5.2.3 Trace Element Analyses	80
5.3	Results and Interpretations	80
	5.3.1 Assay Data	81
	5.3.2 Major Element Chemistry	81
	5.3.3 Trace Element Chemistry	85

Table of Contents

		page
Chapter 6: Stable Isotope Geochemistry		
6.1	Introduction	88
6.2	Analytical Methods	88
6.3	Data Summary	89
	6.3.1 $\delta^{18}O$ and δD Data: Alteration	89
	6.3.2 $\delta^{34}S$ Data: Mineralization	93
6.4	Calculations	93
	6.4.1 Thermometry	95
	6.4.2 $\delta^{18}O$ and δD Fluid Compositions	97
	6.4.3 $\delta^{34}S$ Mineralization	98
Chapter 7: Discussions		
7.1	Introduction	100
7.2	Setting, and Geologic and Petrographic Relationships	101
	7.2.1 Paragenesis	102
	7.2.2 Alteration Chemistry	103
7.3	Isotope Geochemistry of Silicate and Sulphide Assemblages	108
	7.3.1 ^{18}O Thermometry	112
	7.3.2 $\delta^{18}O$ and δD Fluid Values and Source Variations	113
7.4	Chlorite-Muscovite Isotopic Equilibria	119
7.5	Evidence for a Low D Fluid in the Rambler Deposit	121
Conclusions		126
References		130
Appendix 1: Analytical Techniques / Sample Descriptions		152
Appendix 2: Stable Isotope Theory		161
Appendix 3: Major and Trace Element Data		166

List of Tables

page

Table 6.1 $\delta^{18}O$ and δD silicate analyses of silicates. 90

Table 6.2 $\delta^{34}S$ sulphide analyses. 92

Table 6.3 $\Delta^{18}O$ thermometry. 96

Table 6.4 Calculated $\delta^{18}O$ and δD fluid values from silicate analyses. 98

Table 7.4 $\delta^{18}O$ and δD chlorite and muscovite analyses from the Blue Hill, Rio Tinto, and Ducktown VMS deposits. 137

Appendix 1 : Analytical Methods

Table A1.1 Atomic Absorption Spectrophotometry for BE-N (basalt). 159

Appendix 3 : Major and Trace Element Data

Table A3.1 Major and trace element analyses of whole-rock samples from the hangingwall, deposit and footwall of the Rambler VMS deposit. 167

Table A3.2 Major element analyses of volcanic rocks. 168

Table A3.3 Major element analyses of Pacquet Harbour basalt. 169

Table A3.4 Mineral analyses from select studies. 170

Table A3.5 Trace element analyses from seafloor VMS deposits 171

List of Figures

		page
Figure 1.1	"Ideal" VMS deposit.	3
Figure 1.2	Alteration associated with mesothermal gold mineralization.	7
Figure 1.3	Schematic diagram: seafloor hydrothermal system.	9
Figure 1.4	Alteration in VMS deposits.	12
Figure 1.5	Source of fluids related to mesothermal gold mineralization.	14
Figure 1.6	Geologic / structural setting of the Ducktown VMS deposit.	18
Figure 2.1	Tectono-stratigraphic subdivisions of Newfoundland.	21
Figure 2.2	Volcanogenic massive sulphide deposits in Newfoundland.	26
Figure 2.3	Epigenetic gold deposits and prospects in Newfoundland.	28
Figure 2.4	Geology of the Baie Verte Peninsula.	30
Figure 3.1	Location Map: Consolidated Rambler Mines Properties.	39
Figure 3.2	Geological Map: Consolidated Rambler Mines Properties.	48
Figure 3.3	Lithological and structural trends in the vicinity of the Rambler VMS deposit; drillhole locations.	50
Figure 3.4	Vertical cross-section through the Rambler deposit.	51
Figure 5.1	Drill section (MZ89-28): base metal concentrations.	(pocket)
Figure 5.2	Variation diagrams: a) basalt geochemistry, b) alteration.	82
Figure 5.3	Variation diagrams: a) alteration, b) molar plot.	84
Figure 5.4	Trace element concentrations in the Rambler and in seafloor VMS deposits.	86
Figure 7.1	Paragenetic sequence of silicate alteration, sulphide and gold mineralization.	104

List of Figures

page

Figure 7.2 $\delta^{18}O$ and δD mineral data from the oceanic crust, ophiolites and VMS deposits. 109

Figure 7.3 $\delta^{34}S$ values from the Rambler, other VMS deposits, and epigenetic - mesothermal gold deposits. 111

Figure 7.4 $\delta^{18}O$ and δD fluid values: a) vent, pore and inclusion fluids, b) calculated values from VMS deposits. 114

Figure 7.5 Calculated $\delta^{18}O$ and δD fluid values: a) chlorite analyses, and b) muscovite analyses from the Rambler deposit. 116

Figure 7.6 $\delta^{18}O$ and δD fluid values: a) amphibole and biotite analyses, and b) $\delta^{18}O$ quartz fluid values from the Rambler deposit. 118

Figure 7.7 $\delta^{18}O$ and δD chlorite and muscovite, and b) chlorite - muscovite disequilibria in the Rambler deposit. 122

Figure A2.1 δD and $\delta^{18}O$ variations: crustal fluid reservoirs (Kyser, 1987). 165

List of Plates

		page
Plate 3.1	Rambler (Main Mine) mine site.	38
Plate 3.2	Uncle Theodore prospect.	42
Plate 3.3	Schist and mylonite: Rambler Brook Thrust.	42
Plate 3.4	Schist and mylonite: Discovery Outcrop.	44
Plate 3.5	Deformed agglomerate ("mill rock").	46
Plate 3.6	Pillow lava.	46
Plate 3.7	Stage 1 and stage 2 alteration in drill core.	54
Plate 4.1	Photomicrograph: stage 1 alteration in gabbro.	57
Plate 4.2	Photomicrograph: stage 1 alteration in basalt.	57
Plate 4.3	Photomicrograph: stage 1 alteration ; epidotized basalt.	59
Plate 4.4	Photomicrograph: quartz-chlorite breccia.	59
Plate 4.5	Photomicrograph: stage 1 silicates in massive sulphide sample.	61
Plate 4.6	Photomicrograph: stage 1 silicates in massive sulphide sample; light green chlorite and euhedral epidote.	61
Plate 4.7	Photomicrograph: silicates in massive sulphide sample. tourmaline inclusions in quartz and chalcopyrite.	62
Plate 4.8	Photomicrograph: chert; recrystallized quartz and disseminated magnetite.	62
Plate 4.9	Photomicrograph: stage 2 alteration in sheared gabbro: muscovite replacing chlorite.	64

List of Plates

		page
Plate 4.10	Photomicrograph: stage 2 alteration: footwall schist: chlorite with fractured epidote.	64
Plate 4.11	Photomicrograph: stage 2 alteration: contorted shear bands in footwall schist.	66
Plate 4.12	Photomicrograph: stage 2 alteration: quartz and pyrite in footwall mylonite.	66
Plate 4.13	Photomicrograph: stage 3 alteration: silicate assemblages in footwall quartz-carbonate vein.	68
Plate 4.14	Photomicrograph: stage 3 alteration: wallrock alteration along large footwall vein.	68
Plate 4.15	Photomicrograph: massive sulphide mineralization.	70
Plate 4.16	Photomicrograph: massive sulphides; light yellow and dark red varieties of sphalerite.	70
Plate 4.17	Photomicrograph: secondary sulphides.	72
Plate 4.18	Photomicrograph: secondary sulphides; arsenopyrite and electrum.	72
Plate 4.19	Photomicrograph: massive sulphides; deformed grain of electrum.	74
Plate 4.20	SEM photograph: chalcopyrite, Fe and Au-telluride.	75
Plate 4.21	SEM photograph: Ni and Au-telluride.	75
Plate 4.22	Photomicrograph: metamorphic biotite.	77

Introduction and Purpose of Study

The Rambler project was initiated in 1989 to contribute to the research initiatives of the Newfoundland Department of Mines and Energy focused on characterising the occurrence of base metal and gold mineralization in the volcanic terrains in Central Newfoundland. The main objective of the study was to determine whether a late alteration event was superimposed on volcanogenic massive sulphide (VMS) mineralization in the Rambler deposit, and whether stable isotope geochemistry could be used to distinguish between VMS, and the possible epigenetic alteration silicate and sulphide assemblages in the deposit. A secondary objective was to attempt to correlate gold occurrences in the deposit with either the syngenetic or epigenetic event(s).

VMS and epigenetic gold deposits and prospects occur in close proximity in several areas of Central Newfoundland. Hudson and Swinden (in prep) have described syn-volcanic base metal and syn-kinematic gold mineralization in the VMS deposits of the Gullbridge area. Weick et al. (1989) describe similar VMS and mesothermal gold occurrences on the Consolidated Rambler Mines properties in the Pacquet Harbour Group at the centre of the Baie Verte Peninsula.

The Rambler VMS deposit is intensely deformed. Its massive and stockwork alteration and sulphide assemblages occur in a northeast trending, shallow-dipping linear orebody above a prominent imbricate shear zone which cuts through the footwall of the deposit. Imbricate shears overprint regional greenschist and seafloor hydrothermal alteration assemblages and massive sulphide horizons with local quartz + chlorite $\pm$ muscovite, and quartz + muscovite $\pm$ chlorite schists and mylonites throughout the stratigraphy of the deposit. Syn- to post-kinematic quartz veins cut the syngenetic alteration assemblages and occur within the overprinting syn-kinematic alteration assemblages in the stratigraphy of the deposit.

Alteration in the footwall shear zone of the Rambler deposit is similar to the alteration

described in the stockworks of many other deformed VMS deposits (Franklin et al., 1981). It is also similar to local shear-related auriferous disseminated sulphides associated with several gold prospects to the south of the Rambler mine site, and the alteration commonly associated with epigenetic shear-hosted mesothermal gold mineralization (Mueller and Groves, 1992; Dubé, 1990). During preliminary examinations of drill core from the deposit, it was not entirely certain whether the disseminated sulphides in the footwall were intensely deformed VMS stockwork alteration, or subsequent alteration and mineralization associated with a subsequent (epigenetic) alteration event related to the complex tectonic history of the Pacquet Harbour Group.

To accomplish the objectives of the study, 300 metres of drill core were examined and relogged to constrain the occurrence and distribution of alteration and mineralization in the Rambler deposit. 300 core samples were collected for petrographic and geochemical analyses. Samples with high assayed gold contents were examined using a Scanning Electron Microscope (SEM) to define the setting of gold in relation to its surrounding alteration and sulphide assemblages. Samples with "end-member" alteration and mineralization were analyzed for a suite of standard major and trace elements to constrain the chemistry of the different types of alteration. Selected core samples were crushed and separated into their pure mineral fractions for subsequent oxygen, hydrogen, and sulphur isotope analyses.

Chapter 1: Formation and Alteration of Volcanogenic Massive Sulphide (VMS) Deposits

1.1 Introduction

Volcanogenic massive sulphide (VMS) and epigenetic gold deposits are common varieties of mineralization in orogenic belts. VMS deposits occur as syngenetic stratabound and/or stratiform accumulations of base metal sulphides which in response to the circulation of seawater through the oceanic crust. Epigenetic gold deposits, including the mesothermal and epithermal varieties are generated by the migration of crustal fluids during or after peak regional metamorphism along the shear zones and thrust faults within volcanic terrains in orogenic belts (Hutchinson, 1987; Kerrich, 1987; Colvine, 1988). Both types of mineralization are the products of distinct hydrothermal systems which develop in seafloor mid-ocean ridge (MOR) and in continental margin orogenic belts.

VMS and epigenetic deposits frequently occur together in the same volcanic terrains, and actually appear to be superimposed in some ore deposits (Addy and Ypma, 1977; Franklin et al., 1981). In some VMS deposits, syngenetic seafloor alteration and sulphide assemblages are overprinted by syn-kinematic sericitic gold-bearing assemblages commonly associated with the central alteration zones of epigenetic shear-hosted mesothermal deposits (Gjelsvik, 1968; Rui, 1973, Franklin et al., 1981). Some epigenetic deposits contain high concentrations of base metals, attributed by some workers to the presence of pre-existing VMS mineralization (Tourigny et al., 1989). Implicit in the descriptions of some of these deposits is a gradation between end-member syngenetic seafloor and epigenetic / mesothermal mineralizing events; generations of alteration and mineralization related to specific geologic settings and specific orogenic environments.

VMS and epigenetic deposits are formed by the interaction of rocks and fluids in the

crust. Isotopic analyses suggest that fluids associated with the formation of VMS deposits include seawater, ^{18}O-shifted seawater, and magmatic and/or metamorphic fluids (Ohmoto and Rye, 1974; Urabe and Sato, 1978; Pisutha-Arnond and Ohmoto, 1983). Meteoric fluids are introduced during the incorporation of VMS deposits in orogenic belts (Hattori and Sakai, 1979). Similar high ^{18}O magmatic and metamorphic, and low ^{18}O meteoric fluids are also present during epigenetic mineralization, including mesothermal gold deposits (Kerrich, 1987; Nesbitt et al., 1989). The commonality of these fluids, and the occurrence of distinct generations of alteration and mineralization in many VMS deposits is consistent with the complexities among the metamorphic, structural and metallogenic events related to the formation of orogenic belts (Kerrich, 1987).

1.2 Volcanogenic Massive Sulphide (VMS) Deposits

VMS deposits are defined as conformable stratiform and/or stratabound accumulations of massive sulphides ($\geq 60\%$) generated by the circulation of fluids through the oceanic crust (Franklin et al., 1981; Lydon, 1988; Kappel and Franklin, 1989). They belong to a larger class of deposits which include all exhalative stratiform sulphide deposits which form in subaqueous environments. VMS hydrothermal systems are common near centres of active volcanism in mid-ocean ridge (MOR), oceanic island, and arc-related tectonic environments.

VMS deposits occupy specific stratigraphic intervals in volcanic, and pelitic to semi-pelitic strata in Archean and Phanerozoic greenstone, volcanic and/or ophiolite terrains (Spence and deRosen-Spence, 1975). In some Phanerozoic volcanic belts they cluster near felsic intrusions or near fault intersections in the crust (Lapierre et al., 1985). In ophiolites they can occur at specific stratigraphic intervals, such as sheeted dyke to pillow lava transitions, and between repeated rock sequences associated with volcanic cycles (Sangster, 1972; Lambert and Sato, 1974; Sawkins, 1976; Scott, 1978; Franklin et al.,

1981).

Base metal ratios and tectonic settings were the dominant criteria used in early studies to distinguish between the Pb-rich mineralization associated with the Kuroko deposits of Japan, and Cu-Zn mineralization associated with the ophiolite-hosted deposits of Cyprus (Hutchinson, 1973; Sangster and Scott, 1976). More recent classifications of the VMS deposits in the Appalachians of Newfoundland have focused on the tectonic settings of the deposits as determined from the rare earth element (REE) geochemistry of host volcanic rocks (Swinden et al., 1988; Dunning et al., 1991; Swinden, 1991).

VMS deposits typically consist of one or more massive sulphide lenses ($\geq$60 per cent sulphides) which overlie discordant "pipe-shaped" stockwork alteration zones (Figure 1.1). In plan stockworks are concentrically zoned, consisting of altered rocks which contain disseminated sulphide mineralization (Franklin et al., 1981; Lydon, 1988). In vertical cross-section, contacts between the deposits and their overlying strata are sharply defined, and frequently marked by a layer of chert or exhalite. Contacts below the deposit are diffuse and gradational with respect to the underlying stockwork alteration zones (Constantinou and Govet, 1973).

VMS deposits are morphologically diverse. Deposits can vary from steep, inverted cylindrical cones to conformable sheets (Sato, 1974; Kappel and Franklin, 1989; Large et al., 1988). Sedimentary fabrics and textures are rare, but complete Bouma sequences are described in the massive sulphide horizons of exceptionally well-preserved deposits (Roberts, 1975; Swanson et al., 1981). Talus blocks and brecciated rocks are common below massive sulphide horizons (Constantinou and Govet., 1973). Colloform fabrics and textures are common at macro and microscopic scales (Yui, 1983; Graham et al., 1988). Breccia, folds, and shear bands are dominant fabrics and textures in deformed deposits (Knuckey et al., 1982).

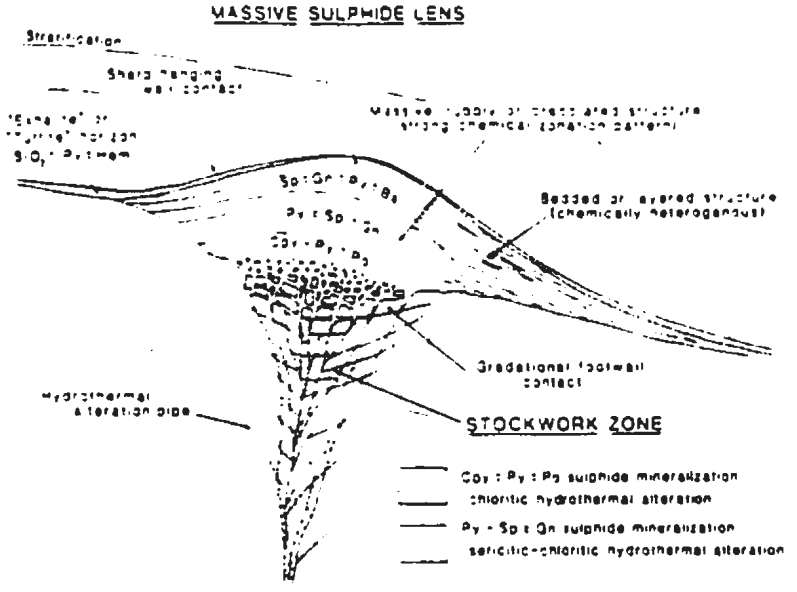

Figure 1.1. Architecture of an "ideal" VMS deposit (Lydon, 1988).

1.3 Epigenetic Deposits

Epigenetic is a term used to refer to a wide variety of ore deposits, which include epithermal, porphyry and mesothermal varieties of mineralization. Epithermal and porphyry deposits are formed by the circulation of fluids near igneous intrusions at relatively shallow crustal depths ($\leq$5km; MacMillan and Panteleyev, 1988; Panteleyev, 1988). Of greatest relevance to this study are the mesothermal or lode varieties of epigenetic mineralization, recently recognized on the Baie Verte peninsula and throughout the volcanic terrains of Central Newfoundland (Swinden, 1991). These deposits are characterised by their structurally controlled setting, diagnostic alteration assemblages, low base metal concentrations and relatively high precious metal contents. Initially described in Archean terrains, they are currently recognized as common forms of sulphide and gold mineralization in all orogenic settings (Roberts, 1988).

Mesothermal deposits are frequently associated with shear zones, generated as subsidiary structures to larger regional structural discontinuities between accreted gneissic, ophiolitic / volcanic, and sedimentary terrains. (Kerrich, 1987). Heterogeneous strain in these structures, results in complex anastomosing shears which surround less deformed structural blocks. As a result, deposits form near extensional dilational zones in overall compressional regimes (Kerrich, 1987). Mineralization is frequently concentrated as tabular or sheeted bodies or cylindrical chutes parallel to local shears, foliations, and/or extension lineations. Morphological variations typically include the disseminated-stratabound, and vein and shear-hosted disseminated varieties of mineralization. The former occur in permeable strata which focus the migration of fluids. The latter occur in shear zones which cut through stratigraphy. Mineralization is generally associated with brittle-ductile transitions in deformed volcanic and sedimentary sequences (Poulsen and Robert, 1988).

In contrast to VMS deposits, epigenetic deposits are characterised by low base metal concentrations and relatively high concentrations of Au, and Ag and other metals

including As, W, B, Mo and Sb (Kerrich and Fryer, 1981; Kerrich and Hodder, 1982). Rock fabrics and structures in some deposits are consistent with multiple fluid events where $P_{fluid} \geq P_{lithostatic}$ (Kerrich, 1987). Sulphide assemblages typically include disseminated pyrite or pyrrhotite ($\leq 30\%$), along with trace chalcopyrite, arsenopyrite, sphalerite, galena, molybdenite, and stibnite. Oxides include magnetite, rutile, sphene, scheelite and leucoxene. Telluride and selenides are common in many deposits (Dubé et al., 1987; Mueller and Groves, 1992). Gold occurs in native form, and as electrum and telluride (Mueller and Groves, 1992).

Alteration associated with epigenetic epithermal and mesothermal deposits is variable, but dominated by a few common alteration minerals and assemblages. The alteration and sulphide mineralization associated with epithermal and porphyry style deposits occurs as concentric zones surrounding a central fluid conduit or intrusive body. Silicification / carbonatization are common froms of alteration associated with the other argillic, phyllic, propyllitic, potassic and aluminous silicate assemblages, and the sulphide, sulphate, and telluride assemblages in these deposits (Beane and Titley, 1981; Berger, 1982; Cox, 1982). Common alteration products include quartz as adularia or opaline silica, albite, epidote, chlorite, muscovite, carbonate, and zeolite.

Alteration in mesothermal deposits occurs at temperatures of approximately 350°C, is typically characterised by high concentrations of carbonate, and concentrated in zones parallel to structural conduits which focus the migration of hydrothermal fluids (Figure 1.2, after Dubé et al., 1987). Typical alteration assemblages include chlorite + calcite ± magnetite, mixed kinematic ankerite + muscovite ± chlorite, ankerite + fuchsite ± chlorite, and ankerite + muscovite assemblages associated with disseminated sulphide mineralization. Mineral analyses in central alteration zones show consistent enrichments in K, Na, Al, and Cr, and CO_2, and depletions in Fe and Mg with respect to the surrounding less altered rocks (Dubé et al., 1987).

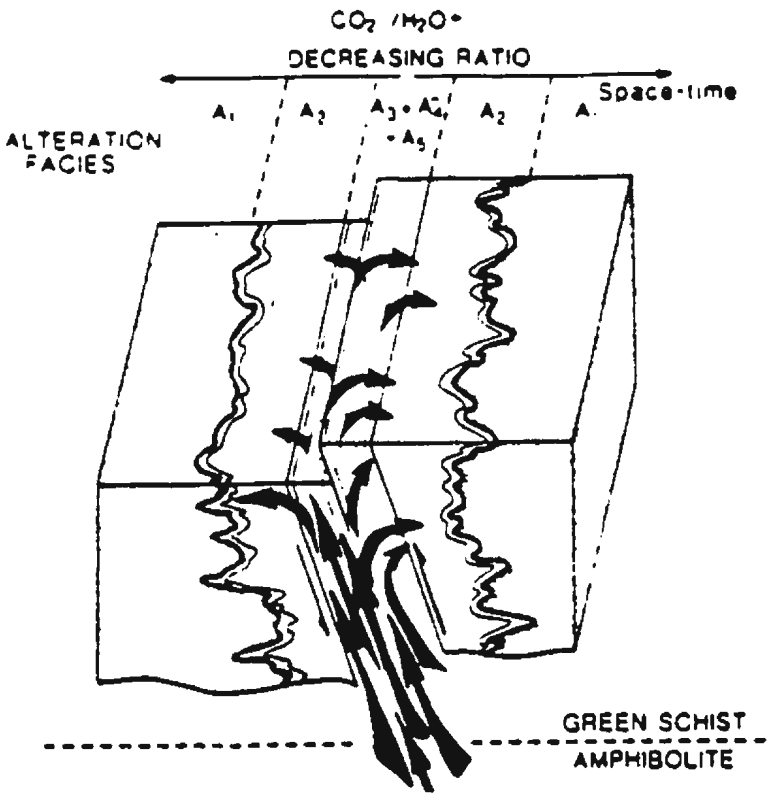

Figure 1.2. Typical alteration and sulphide assemblages in a shear-hosted mesothermal gold deposit: A1) greenschist metamorphism, A2) chlorite + calcite + magnetite, A3) ankerite + muscovite + chlorite, A4) ankerite + fuchsite + chlorite, and A5) ankerite + muscovite + pyrite (Dubé et al., 1987).

1.4 Alteration Processes related to Syngenetic VMS and Epigenetic Mineralization

Alteration associated with VMS base metal sulphide, and epigenetic mineralization is produced by similar fluid-rock reactions in different geologic environments. The two varieties of mineralization are products of distinct hydrothermal systems which develop near seafloor mid-ocean ridge (MOR) settings and during the formation of continental margin orogenic belts. Although there are differences in the geologic setting of these deposits, their associated hydrothermal systems are frequently composed of similar rocks and fluids, and as such, capable of producing similar alteration. As a result, VMS and epigenetic deposits frequently contain chemically similar syn-volcanic and syn-kinematic silicate assemblages.

The hydrothermal systems associated with VMS deposits have been modelled in the laboratory by reacting basalt, seawater and evolved hydrothermal fluids over a variety of temperatures and pressures (Mottl, 1983). Data from these studies suggests that seawater changes from a slightly basic, Na^{+}, Mg^{+2}, Cl^{-}, SO_4^{-2} rich solution, to a hot acidic, Na^{+}, Ca^{+2}, K^{+}, Cl^{-} enriched brine capable of dissolving and transporting significant quantities of metals (ppm) during its reaction with basalt (Rona et al., 1983). The changes occur in three distinct sub-seafloor hydrothermal environments (Figure 1.2):

1) upper sections ($\leq$3km) of the oceanic crust altered by low temperature ($\leq$200°C) hydration reactions as seawater moves downward to recharge circulating hydrothermal fluid cells,

2) deep sections (3-5km) of the oceanic crust characterised by high temperature (200-450°C) and pressure (400-500 bars) greenschist to amphibolite metamorphic transitions, and

3) active mid-ocean ridge (MOR) volcanic centres where hot ($\geq$350°C), reduced, metalliferous brines generated at depth, vent directly to the seafloor (Rosenbauer and Bischoff, 1983).

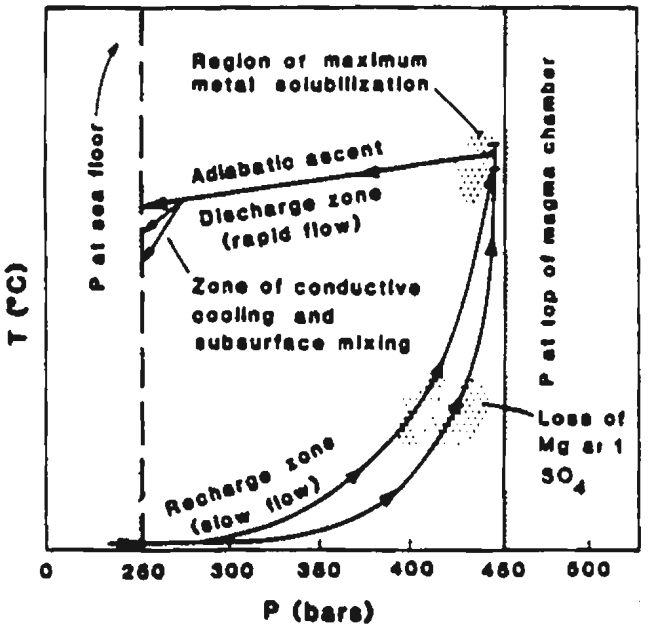

Figure 1.3. Schematic diagram: seafloor hydrothermal system (Rosenbauer and Bischoff, 1983).

Initial changes in seawater chemistry are dominated by the removal of sulphate, through the precipitation of anhydrite, and the almost complete removal of Mg^{2+} at temperatures $\geq$ 150°C and water - rock (W/R) ratios $\leq$ 50. Mg^{2+} precipitation is compensated for by the transfer of Na^{+}, K^{+} and Ca^{2+} to solution. Na^{+} is dissolved from basalt at 300°C at W/R ratios $\approx$ 10, but precipitates as secondary minerals at $\approx$ 350°C and W/R ratios $\leq$ 5 (Hajash, 1975). Ca^{2+} dissolves at temperatures $\geq$ 150°C, but is incorporated in Ca-rich minerals such as epidote and amphibole. K^{+} dissolves at $\geq$ 200°C, and precipitates as K-rich alteration minerals, such as illite or muscovite at temperatures $\leq$ 200°C.

Basalt-seawater reactions ultimately result in a highly acidic brine, depleted in Mg^{2+} and enriched in Ca^{2+} and K^{+} (Rosenbauer and Bischoff, 1983). The reaction of these fluids with unaltered basalt at low pressures, high W/R ratios ($\leq$1000) and temperatures $\geq$ 350°C, may actually decrease fluid pH further, causing a substantial increase in the solubility of the base metals during the formation of epidosites; altered volcanics consisting of $\geq$ 80% epidote and lesser quartz and albite (Seyfried et al., 1988). Epidosites and "epidotized" rocks are common in the seafloor alteration zones in numerous ophiolites, and volcanic terrains.

Brines in seafloor hydrothermal systems are silica saturated, and in simulated seafloor systems, silica precipitates at 150 to 500°C (Mottl, 1983). High silica concentrations are common in the high temperature geothermal centres of the Red Sea (Pottorf and Barnes, 1983), and also in low temperature "off-axis" seafloor hydrothermal systems at the Galapagos Ridge, where ^{18}O thermometry suggests silica precipitation at temperatures as low as 30°C to 40°C (Herzig et al., 1988).

The mixing of seafloor brine with seawater results in the precipitation of sulphides during the discharge of hydrothermal fluids through vents, or accumulating sulphide mounds (Goldfarb et al., 1983; Lydon, 1988; Kappel and Franklin, 1989). Mineralization occurs in response to decreases in temperature and pressure, the reduction of seawater SO_4^{-2},

increases in pH, fO_2 and decreases in fS_2, and to a lesser extent; reactions with organically generated H_2S. The resulting sulphide mineralization typically consists of up to 30% pyrite or pyrrhotite, with lesser amounts of sphalerite, chalcopyrite and galena.

VMS mineralization is frequently zoned. High temperature pyrrhotite, marcasite, pyrite and chalcopyrite assemblages typically occur near the centre of massive sulphide horizons, and stockwork alteration zones. Low temperature sphalerite ± galena assemblages occur toward the periphery of individual deposits. Other common sulphides include pyrrhotite, arsenopyrite, bornite, pentlandite, wurtzite and marcasite (Sangster and Scott, 1976). Common sulphates include barite, gypsum and anhydrite. Magnetite, hematite and geothite are common oxides.

Variations in temperature, fluid-rock chemistry and W/R ratios result in different alteration assemblages in individual deposits. Thermodynamic models at temperatures of 300°C, pressures of 500 to 600 bars, and W/R ratios of 1, 3, 10, 50, 62 and 125 predict the following:

W/R = 0 to 2:	chl + alb + ep + act,
2 to 35:	chl + alb + ep + act + qtz,
35 to 50:	chl + alb + qtz, and
> 50:	chl + qtz

(Mottl and Holland, 1978). In natural VMS hydrothermal systems, talcose, chloritic, and Mg-enriched alteration assemblages near the periphery of individual deposits, are gradational to sericitic alteration assemblages near the centre and top of stockwork alteration zones (Figure 1.4; Lydon, 1988). Alteration associated with massive sulphide horizons commonly includes siliceous, aluminous, carbonate, talcose, or oxide enriched assemblages (Constantinou and Govet., 1973; Franklin et al., 1981; Lydon, 1988). The mineralogy and chemistry of the alteration is frequently modified by subsequent metamorphic and structural events.

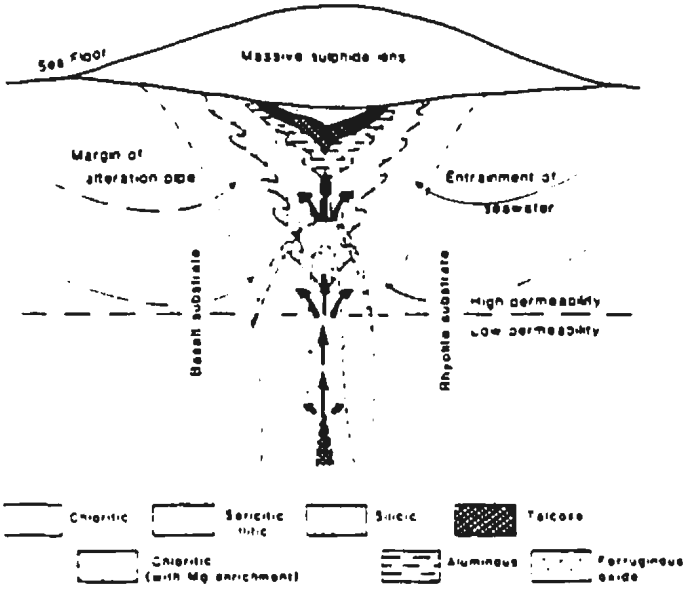

Figure 1.4 Distribution of VMS alteration in mafic and felsic volcanic rocks (Lydon, 1988).

In contrast to the extensively modelled VMS hydrothermal systems, fluid processes associated with the formation of epigenetic mesothermal varieties of mineralization are not well constrained. Epigenetic mineralization is frequently constrained in terms of the shallow circulation of magmatic, metamorphic and meteoric fluids through the crust (Fyfe and Kerrich, 1984). However, fluids associated with the formation of mesothermal deposits originate in deep crustal reservoirs, where they equilibrate with large volumes of rock at low W/R ratios at depths of up to 10 kilometres (Kerrich, 1987). Fluid inclusion studies suggest the fluids are enriched in CO_2 and slightly saline: $\leq 4\%$ $NaCl_{eq}$ (Roedder, 1969, 1984).

Studies relate the generation of epigenetic / mesothermal fluids to the dehydration reactions associated with lateral secretion, magmatic degassing, structurally focused metamorphic outgassing, meteoric water circulation (Boyle, 1979; Nesbitt et al., 1986), mantle degassing-granulitization (Fyon et al., 1984; Colvine et al., 1988) or suggest a direct link with the ortho-magmatic processes in nearby felsic igneous rocks (Hattori, 1987). Other studies relate the fluids to dehydration reactions associated with the assimilation of subducted oceanic crust in supra-subduction zone tectonic settings (Fyfe and Kerrich, 1985; Goldfarb et al., 1988; Kyser and Kerrich, 1992).

Fluids generated by metamorphic or magmatic dehydration reactions in deep crustal reservoirs ascend through the crust along structural conduits into overlying rocks (Figure 1.4). Studies suggest metals are extracted at the source or derived from surrounding rocks during the upward migration of fluids at low W/R ratios (Kerrich and Fryer, 1981). Mineralization can occur either in response to fluid mixing and/or fluid-rock disequilibria, which influence temperature, pressure, W/R ratio, pH, fO_2, and fS_2, resulting in the precipitation of sulphides, oxides, gold and other metals. The correlation of high metal concentrations with specific lithologies is common in some epigenetic deposits. In other deposits, high metal concentrations may occur in several different rock types (Kerrich, 1987).

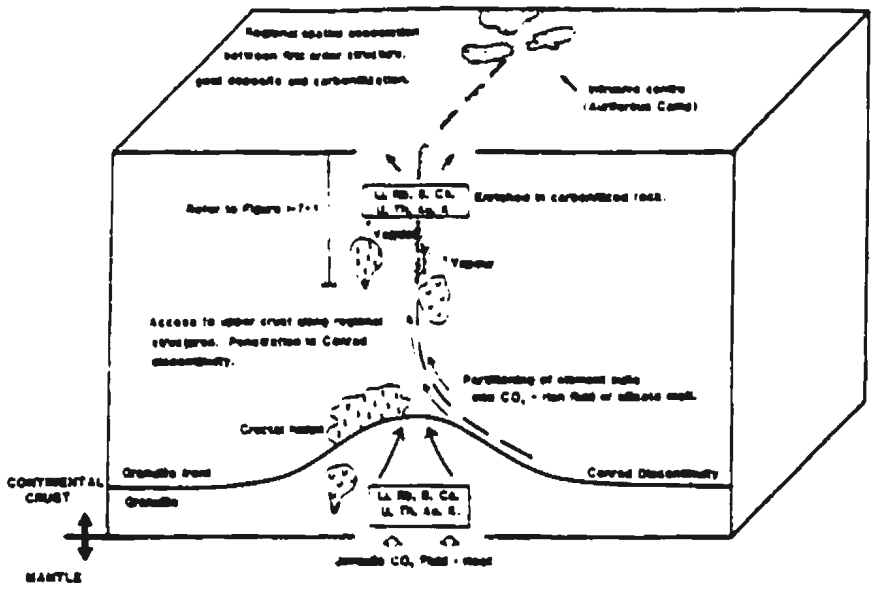

Figure 1.4. Source and migration of fluids associated with mesothermal gold mineralization (Colvine et al., 1988).

1.5 Metamorphism and Alteration of VMS Deposits in Orogenic Belts

The different generations of alteration and sulphide mineralization in VMS deposits are composed of distinct alteration assemblages which form in response to reactions between pre-existing syngenetic mineral assemblages and crustal fluids. Assemblages vary in response to local physical and chemical conditions influenced by regional metamorphism, deformation and local fluid alteration during orogeny. The result is a complete spectrum of deposits which range from relatively intact recrystallized orebodies, to intensely deformed deposits which contain overprinting "kinematic" alteration. Examples of the former, though rare, include the Millenbach, and Kuroko VMS deposits (Franklin et al., 1981). Examples of the latter include the Caledonide deposits of Norway, some of the Cretaceous deposits in western Australia and Tasmania, and VMS deposits in the Appalachian orogen including those associated with the Consolidated Rambler Mines properties (Franklin et al., 1981; Large et al., 1988: this study).

Alteration and sulphide assemblages in most "fossil" VMS deposits; the deposits incorporated in orogenic settings, are affected to some extent by local and regional metamorphic events during their incorporation in orogenic belts (Addy and Ypma, 1977; Franklin et al., 1981). In the absence of deformation, regional metamorphism is essentially isochemical, so while alteration assemblages are recrystallized, there is very little change in the chemistry of the original alteration assemblages (Spence and de Rosen-Spence, 1975). The isochemical nature of metamorphism is well illustrated by the alteration and metamorphic assemblages associated with the stockworks of the Millenbach VMS deposit near Noranda, Quebec (Knuckey et al., 1982). The Millenbach greenschist chlorite and sericitic stockwork assemblages are overprinted by amphibolite contact metamorphic assemblages associated with the intrusion of the Lac Dufault Granodiorite (Spence and de Rosen-Spence, 1975; Riverin and Hodgson, 1980; Franklin et al., 1981). The amphibolite assemblages retrograde back to chlorite + muscovite + albite + epidote $\pm$ carbonate assemblages which are similar to the original seafloor assemblages during post-intrusive regional metamorphism. Locally preserved pre-contact and contact

metamorphic domains in post-intrusive regional greenschist assemblages offer compelling evidence of the isochemical nature of metamorphism in the stratigraphy of the Millenbach deposit (Riverin and Hodgson, 1980).

Other VMS deposits are affected by deformation in addition to regional metamorphism during their incorporation in orogenic belts. Many are incorporated into the shear zones which develop in less competent stratigraphic transitions in ophiolites and volcanic terrains (Lydon, 1988). Deformation and alteration in these structures results in the development of syn-kinematic alteration assemblages which envelope and overprint regional greenschist metamorphic, and seafloor hydrothermal alteration assemblages associated with VMS mineralization (Franklin et al., 1981). As an example, the Killingdal VMS deposit in west Norway occurs in a syn-kinematic alteration (shear) zone consisting of quartz + muscovite schist (Gjelsvik, 1968). Similar assemblages in the nearby Skorovass VMS deposit are also attributed to the kinematic destruction of greenschist albite + amphibole $\pm$ epidote seafloor greenschist assemblages during late Caledonide deformation (Rui, 1973).

In highly deformed deposits, it becomes difficult to distinguish between deformed syngenetic seafloor, and later epigenetic syn-kinematic alteration and sulphide assemblages. Many of these are overprinted by the same K and CO_2 rich, Na, Ca and Fe depleted assemblages characteristic of the alteration assemblages in the central alteration zones of epigenetic shear-hosted mesothermal gold deposits (Dubé et al., 1989). In addition to the intensely deformed VMS deposits which appear to develop mesothermal characteristics, some mesothermal deposits appear to contain abnormally high concentrations of base metal sulphides, linked in some studies to pre-existing seafloor volcanogenic hydrothermal processes (Tourigny et al., 1989). In such deposits, it would be difficult to determine whether quartz + muscovite $\pm$ chlorite $\pm$ disseminated sulphide assemblages are the products of syngenetic seafloor and/or later overprinting epigenetic syn-deformational fluid alteration.

Combined syngenetic and epigenetic alteration asseblages are described in several VMS deposits. The Que River deposit, in Tasmania contains syngenetic VMS remnants overprinted by epigenetic syn-kinematic alteration assemblages (Large et al., 1988). Sulphide banding in the deposit is attributed to primary depositional layering (Young, 1980). Quartz + sericite ± fuchsite + disseminated pyrite alteration zones on either side of the orebody are interpreted as folded stockworks to the original massive sulphide lens. However, galena occurs in an axial planar foliation contemporaneous with recrystallization and mylonitization related to subsequent deformation.

While visible gold in the Que River deposit is attributed to the "remobilization" of syngenetic alteration and sulphide assemblages (Large et al., 1988), the mineralogy and chemistry of some of the gold-rich zones is similar to that associated with adularia-sericite style epithermal mineralization (Heald et al., 1987; White and Hedenquist, 1990). McGoldrick and Ross (1992) suggest the deposit is part of a "spectrum" of "hybrid" VMS and epithermal deposits; a model consistent with the overprinting of syngenetic VMS alteration assemblages by epigenetic and syn-kinematic alteration assemblages in a deformed deposit.

In other studies, epigenetic alteration in VMS deposits has been linked to specific orogenic events. For example, the Ducktown deposit in Tennessee is similar to the Rambler VMS deposit in terms of its tectonic and geologic setting (Figure 1.4; Rankin, 1975; Addy and Ypma, 1977). The Ducktown was affected by regional metamorphism and structural events associated with the formation of the Blue Ridge mountains. Its alteration is described in terms of a prograde syn-tectonic phase, a post-tectonic prograde phase which occured during peak regional metamorphism, and a retrograde cooling phase accompanied by brittle deformation. As a result, its silicate and sulphide assemblages are recrystallized to the extent that it is difficult to distinguish between uniquely syngenetic and epigenetic alteration assemblages (Kallioski, 1965).

Local alteration in the Ducktown VMS deposit is characterised by the replacement of

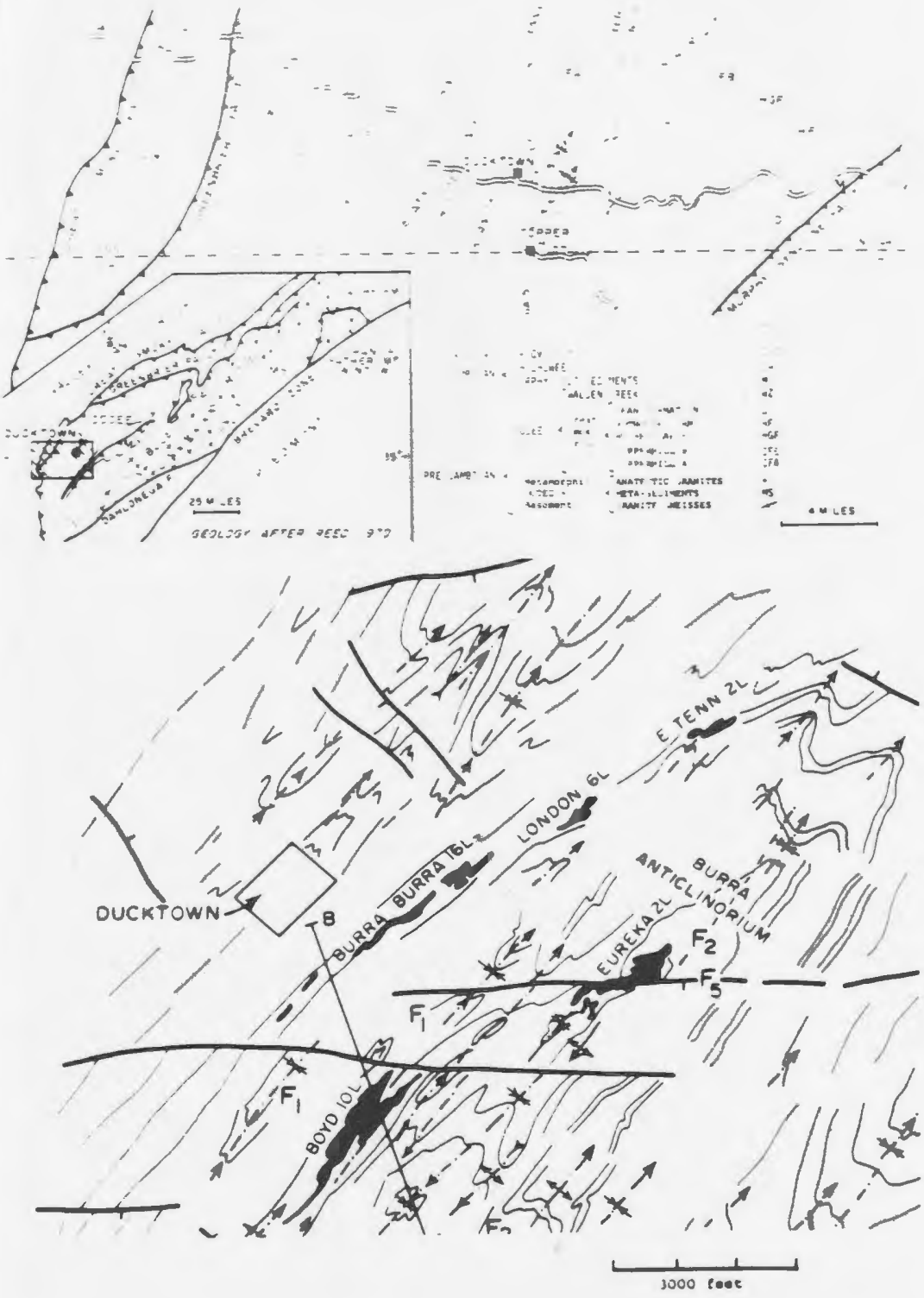

Figure 1.6 Regional geological setting of the Ducktown area, and detailed structural map of the Ducktown Mining District showing the occurrence and structural disposition of eight orebodies with the Burra anticlinorium and Coletown synclinorium as major structures (after Addy and Ypma, 1977).

biotite and garnet by chlorite, and of staurolite and kyanite by muscovite; alteration which is accompanied by high carbonate concentrations, and ^{18}O enrichments in quartz of +0.6‰ (Taylor, 1967). As such, an epigenetic overprint in the Ducktown deposit is related to the presence of high ^{18}O and CO_2-rich mesothermal fluids, which occured sometime after the original formation of the deposit, and during or after the regional metamorphism and deformation related to the formation of the Blue Ridge mountains.

1.6 Implications for the Source of Gold in VMS Deposits

The potential coincidence of syngenetic seafloor and epigenetic alteration in VMS deposits raises important questions concerning the origin of gold. Gold is common in its native state and as electrum and telluride in numerous fossil VMS and mesothermal gold deposits, but visible gold, while expected to be present, has never actually been observed in the deposits actively forming on the seafloor (Hannington et al., 1990).

A favoured mechanism for the formation of visible gold is its remobilization and reconcentration during low temperature annealing and sulphide recrystallization (Boyle, 1979). Other studies, however, suggest that the gold is enriched; an interpretation consistent with an external (epigenetic) source for the gold in some deposits (Guha et al., 1988). Implicit in both interpretations is the presence of different crustal fluids which remobilize gold during later metamorphic and structural events (Guha et al. 1988, Huston and Large, 1989). The interpretations are also consistent with petrographic and mineralogical criteria, and isotopic data which demonstrate the presence and interaction of different crustal fluids during the formation of VMS deposits on the seafloor and during their incorporation in orogenic belts.

Chapter 2: Regional Geology

2.1 Introduction

The island of Newfoundland comprises the northeastern portion of the Appalachian Orogen, a late Precambrian to middle Palaeozoic mountain belt extending from Alabama to Newfoundland. Rocks in the Orogen record a "Wilson cycle"modelled as a "two-sided" symmetrical system (Williams, 1964) related to the opening and closing of the proto-Atlantic or Iapetus Ocean (Wilson, 1966; Harland and Gayer, 1972). The Appalachians in Newfoundland have been affected by four orogenic events; referred to as the early Cambrian to Palaeozoic Taconian, the mid to late Silurian Salinic, the mid Palaeozoic Acadian, and the late Palaeozoic Alleghanian orogenies (Harland and Gayer, 1972; Dunning et al., 1991).

The Appalachians in Newfoundland include the Avalon, Gander, Dunnage and Humber tectono-stratigraphic zones (Figure 2.1). The Humber and Avalon zones are remnants of the North American / Laurentian and Pan African continental margins, respectively (Williams and Hatcher, 1983). The Humber Zone, consists of Precambrian continental basement overlain by Palaeozoic shelf-facies clastic sediments and platform carbonates. The continental basement exposed in the Long Range Mountains and as a series of related inliers to the south along the south west coast of Newfoundland is correlated with the eastern edge of the Grenville Orogenic Province in the Canadian Shield (Rivers and Chown, 1986).

The Humber Zone contains mafic dykes and alkalic basalts related to Early Cambrian rifting as a precursor to the opening of the Iapetus Oceanic tract(s) (Williams and Hiscott, 1987). The initial collision of inboard terrains with the Laurentian continental margin was recorded in the Humber Zone by structures associated with the Taconian Orogeny. Subsidence of the continental margin during collision, was accompanied by

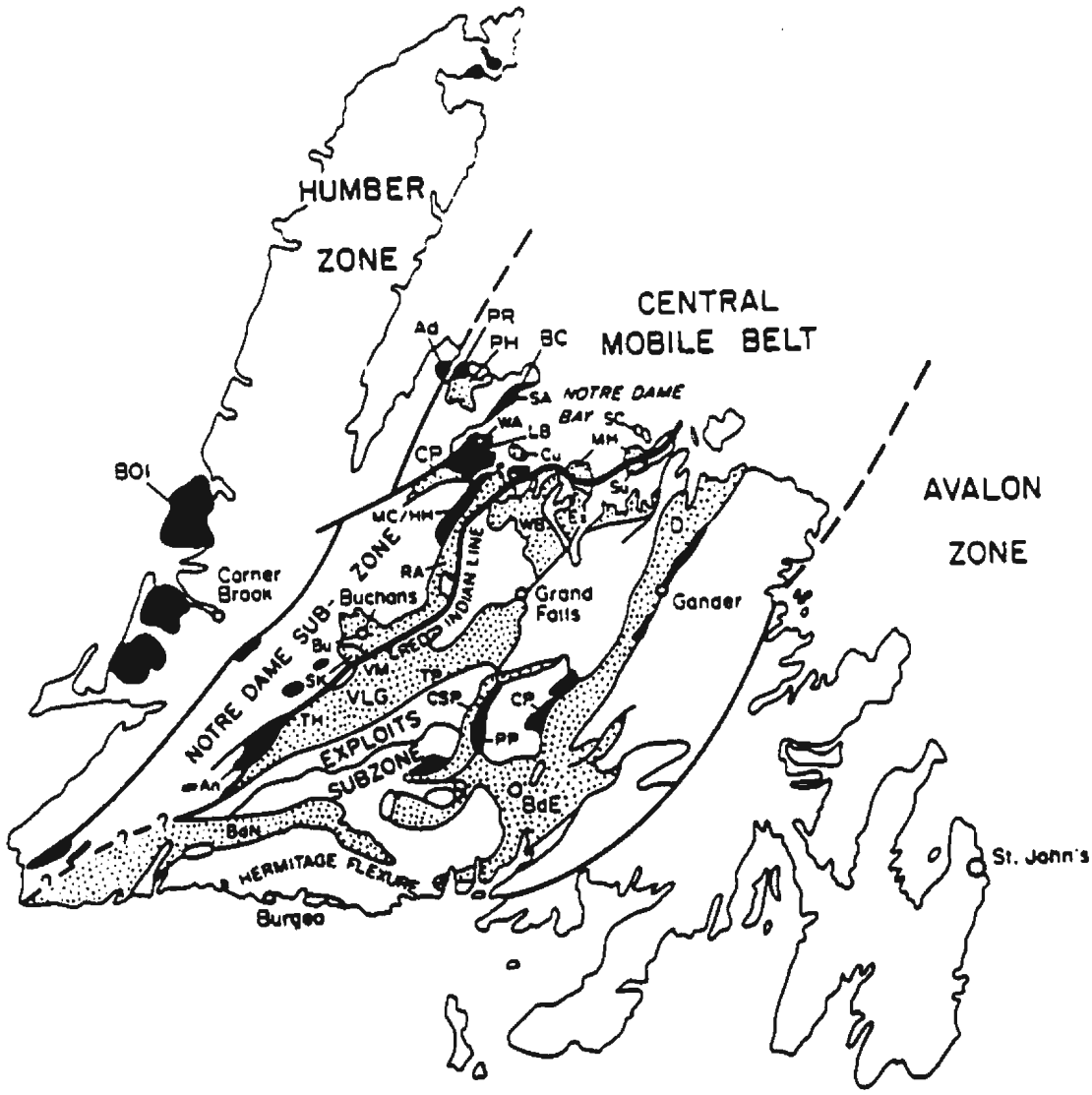

Figure 2.1. Tectono-stratigraphic subdivisions of Newfoundland. Stippled areas are underlain by Iapetan volcanic/epiclastic rocks, the solid black areas by ophiolites. Ophiolite complexes have been abbreviated as follows: Ad - Advocate Ophiolite Cplx., An - Annieopsquotch Ophiolite Cmplx., BC - Betts Cove Ophiolite Cplx., BOI - Bay of Islands Cplx. Other complexes, groups and formations include: Bde - Baie D'Espoir Gp., BdN - Baie du Nord Gp., Bu - Buchans Gp., CP - Coy Pond Cplx., CSP - Cold Spring Pond fm., CW - Cutwell Gp., Ex - Exploits Gp., LB - Lushs Bight Gp., MC/HH - Mansfield Cove/Hall Hill Cplx., MH - Moreton's Harbour Gp., PH - Pacquet Harbour Gp., PP - Pipestone Pond Cplx., PR -Point Rousse Cplx., RA - Robert's Arm Gp., SA -Snook's Arm Gp., SC - Sleepy Cove Gp., Sk - Skidder basalt, Su - Summerford Gp., TH - Tulks Hill volcanic belt, TP - Tally Pond volcanic belt, VLG - Victoria Lake Gp., Vm - Victoria Mine sequence, WA - Western Arm Gp., and WB - Wild Bight Gp (Swinden., 1991).

the emplacement of allochthonous oceanic sediments and ophiolites of the Humber Arm and Hare Bay allochthons (Church and Stevens, 1971, Dewey and Bird, 1971, Williams, 1979).

The Avalon Zone on the east side of the Appalachian orogen consists of late Precambrian volcanic and sedimentary rocks overlain by early Palaeozoic strata of shallow marine origin. Its western contact with the Gander Zone is the Dover - Hermitage Bay Fault; a trans-crustal fault with a major strike-slip component of displacement (Brown and Colman-Sadd, 1976).

The Humber and Avalon zones are separated by Palaeozoic rocks of the Gander and Dunnage zones which comprise the Central Mobile Belt. The Gander zone consists of substantial thicknesses of highly deformed and metamorphosed pre-Silurian clastic sedimentary rocks deposited near a continental margin (Colman-Sadd, 1980). The Gander sediments are overthrust and exposed as "structural windows" through the oceanic rocks of the Dunnage Zone (Colman-Sadd and Swinden, 1984; Williams et al., 1988).

The Dunnage Zone consists dominantly of ophiolites and marine volcanic-sedimentary sequences related to a series of Cambrian to mid-Ordovician island arc and back arc tectonic settings. It is allochthonous to the Precambrian crustal blocks which comprise the structural basement of most of central Newfoundland (Colman-Sadd and Swinden, 1984). The present distribution of volcanic terrains in the Dunnage Zone, partly reflects trans-current structural movements during the late evolution of the orogen.

Accretion of Iapetan oceanic terrains to the Laurentian continental margin began near the end of the early Ordovician, with the emplacement of imbricate thrust stacks over the continental shelf. Lower crustal slices were composed of continental margin sediments. Higher crustal slices consisted of ophiolitic fragments of the Dunnage Zone oceanic crust and mantle (Church and Stevens, 1971; Williams, 1979). Ophiolitic detritus was shed

westward across the miogeocline during the emplacement of the allochthon (Steven, 1970; Stevens and Williams, 1973). Accretion was accompanied by deformation, metamorphism and widespread tonalitic plutonism (Dunning and Chorlton, 1985).

The accretion of the outboard Dunnage and Gander terrains to the Humber Zone was almost complete by the early Silurian (Williams and Hatcher, 1983). Widespread volcanism, sedimentation, plutonism and metamorphism occurred across the newly accreted continental margin during the mid-Silurian (Coyle, 1990). Similar orogenic pulses recorded in the rocks of Cape Breton, Nova Scotia, and in the west European Caledonides are attributed to a thermal and kinematic maximum currently associated with the mid-Silurian Salinic orogeny (pers. comm., Dunning et al., 1991).

The Early Devonian Acadian orogeny is characterised by widespread deformation, metamorphism and by granitoid plutonism associated with the final collision of the Avalon Zone, or Avalon composite terrane (Swinden, 1991). Strike-slip faulting during the late Devonian and Carboniferous eras resulted in the formation of pull-apart basins which filled with late Devonian and Carboniferous sediments.

2.2 Geology and Metallogeny of the Newfoundland Dunnage Zone

The Dunnage Zone consists dominantly of ophiolites and thick marine volcanic / epiclastic terrains which are unconformably overlain by post-accretionary terrestrial volcanic and fluviatile sediments. Volcanism is recorded in these terrains from as early as Late Cambrian, and continued sporadically up to the mid Ordovician. Most fluviatile sequences are unconformable with respect to the pre-accretionary basement and appear to be related to a series of epicontinental volcanoes and/or successor basins (Williams, 1979).

Rifting and calc-alkalic magmatism as early as 620 Ma is consistent with the geological evidence which suggests a rift-drift transition at approximately 500 Ma (Williams et al.,

1985; Kamo et al., 1989). The evidence is consistent with a maximum time of 30-40 Ma or less between the development of oceanic crust and the initiation of subduction. Temporal constraints and geochemical signatures, and a lack of "major basin" oceanic crust, suggest volcanism was associated with a complex succession of island arc and back arc basins at or near the margin of the Iapetus ocean basin (Dunning et al., 1991).

U/Pb zircon dating indicates at least two distinct ages of ophiolites in the central and western portions of Newfoundland (Dunning et al., 1991). Ophiolites in the eastern portion of the Dunnage Zone were formed in the Tremadoc (ca. 494 Ma); while those to the west, were formed in the Arenig (ca. 488-474 Ma) (Dunning and Krogh, 1985). Most have geochemical signatures consistent with supra-subduction zone magmatism and are therefore not related to a major oceanic basin or its spreading centre (Sun and Nesbitt, 1978, Dunning et al., 1991). Many are interpreted as the products of arc and back arc rifting in a supra-subduction zone (SSZ) tectonic environment (Coish et al., 1982; Jenner et al., 1988; Swinden et al., 1989).

The Dunnage Zone is divided into the western Notre Dame and eastern Exploits subzones by the Red Indian Line. Although the two Subzones were previously related to island arc environments (Wilson, 1966, Bird and Dewey, 1970), REE signatures are consistent with their formation in back-arc tectonic settings (Jenner et al., 1988; Swinden et al., 1990). Thick marine volcanic and epiclastic sequences in these subzones include rocks of late-Cambrian to mid-Ordovician age, which extend the relative age of Dunnage volcanic terrains (Bell and Blenkinsop, 1981; Bostock et al., 1979; Dunning et al., 1991).

The diverse history of the Appalachian orogen is reflected in a complex multi-stage metallogeny during which different varieties of deposits formed at different times, in different tectonic settings (Swinden, 1991). As is the case with other volcanic belts, VMS and mesothermal gold mineralizing events were important components of this history, which formed in the pre-accretionary Iapetus basins and in syn to post-

accretionary structures during the development of the orogen.

In early classifications, the VMS deposits of Central Newfoundland were compared directly to the Kuroko, and Cyprus VMS deposits (Mitchell and Bell 1973; Franklin et al., 1981). Recent detailed geochemical and geochronological studies, however, recognize a diversity in the tectonic setting of these deposits. The REE signatures of the basalts which contain these deposits suggest the presence of back-arc, primitive arc, mature arc, and continental rift tectonic settings (Swinden et al., 1988; Swinden et al., 1989). The presence of both tholeiitic and boninitic basalts near the centre of the Pacquet Harbour suggests that the Rambler formed during the Ordovician in a primitive arc tectonic setting (Swinden, 1991).

Primitive arc volcanic settings are among the most prolific hosts to VMS deposits in Central Newfoundland. Structures within the volcanic terrains in these settings are frequently associated with the occurrence of epigenetic gold mineralization. REE signatures of volcanic rocks in these settings indicate the presence of a subduction zone (Sun et al., 1978; Coish et al., 1982), and volcanic lithologies are dominated by island arc tholeiites with minor calc-alkalic rocks and boninites. Ophiolite-hosted Cu $\pm$ Zn $\pm$ Au deposits in Central Newfoundland include the Tilt Cove, Betts Cove, Whalesback and Rendell-Jackman deposits in addition to the Ming, Ming West, East Mine, Rambler and Big Rambler Pond deposits which occur on the Consolidated Rambler Mines properties. Cu $\pm$ Zn $\pm$ Au deposits in mafic volcanic rocks in mixed volcanic / epiclastic sequences in primitive arc tectonic settings include the Point Leamington and Indian Cove deposits. Cu $\pm$ Zn $\pm$ Pb $\pm$ Ag $\pm$ Au VMS deposits in mixed mafic/felsic volcanic / epiclastic rocks include the Burnt Pond, Duck Pond and Tally Pond deposits (Figure 2.2; Swinden et al., 1989; 1991).

In contrast to the detailed tectonic framework developed for VMS deposits, the classification of epigenetic mineralization in Central Newfoundland is still largely

1	York Harbour	15	Lockport	28	Oriental #1
2	Skidder	16	Tulks Hill	29	Oriental #2
3	Terra Nova	17	Tulks East	30	Lucky Strike - Main
4	Tilt Cove	18	Jacks Pond	31	Lucky Strike - New Year
5	Betts Cove	19	Ott Islands	32	Lucky Strike - North
6	Little Bay	20	Boundary	33	Two Level
7	Whalesback	21	Duck Pond	34	Rothermere #1
8	Little Deer	22	Great Burnt Lake	35	Rothermere #2
9	Miles Cove	23	Bobby's Pond	36	MacLean
10	Colchester	24	Strickland	37	MacLean Extension
11	Rambler	25	Lake Bond	38	Clementine
12	Ming	26	Guilbridge	39	Engine House
13	East Mine	27	Pilley's Island	40	Ming West
14	Point Leamington			41	Daniel's Pond

Figure 2.2 Volcanogenic massive sulphide deposits in central and western Newfoundland with greater than 200,000 tonnes production and/or reserves. Stippled areas are ophiolitic and volcanic terrains associated with the remnants of Iapetus oceanic basins (after Swinden, 1991).

descriptive. These deposits, many of which are of uncertain origin, occur in structures in the same ophiolite and volcanic sequences, as the VMS deposits (Figure 2.3; Tuach, 1990). Dubé (1990) proposed a descriptive classification system to distinguish among different types of "gold-only" deposits in western Newfoundland. The system identifies different varieties of disseminated stratabound, and structurally controlled mesothermal Au deposits. Stratabound deposits are separated into silicified wallrock and sedimentary host-rock sub-types. The structurally controlled deposits are separated into vein and altered wall rock subtypes.

Recent geological and geochronological studies link some of the epigenetic deposits in Central Newfoundland to specific orogenic events. The existence of a Late Precambrian event is suggested by the stratigraphic ages of several Au prospects in the northern region of the Burin peninsula (Huard, 1989). U/Pb dating has recently provided Silurian ages for the Stog'er Tight and Hammer Down Au deposits in the Baie Verte and Springdale regions (Ramezani, 1992; Ritcey, 1992). Both gold deposits appear to have formed during the mid to late Silurian Salinic orogeny, a tectonic event associated with the final "cratonization" of the Iapetus oceanic tract. The age of the Stog'er Tight deposit is discussed in detail in section 2.5. Relative ages of the volcanogenic and disseminated mineralization on the Consolidated Rambler Mines properties have not been accurately determined.

Figure 2.3 Epigenetic gold deposits and prospects in relation to major structural linears in Newfoundland (Tuach, 1990). VMS (Figure 2.2) and epigenetic gold deposits (this Figure) in Central Newfoundland are frequently associated with the same volcanic terrains, groups, formations and structures.

2.3 Geology of the Baie Verte Peninsula

The Consolidated Rambler Mines properties occur near the centre of the Baie Verte Peninsula located along the north coast of Newfoundland, between 49° 15' and 50° 10' north latitude, and 55° 20' and 57° 00' east longitude. The most recent geological compilation of the peninsula separates regional stratigraphy into the Fleur de Lys and Baie Verte Belts as portions of the Humber and Dunnage Zones, respectively (Figure 2.4; Hibbard, 1983).

The Fleur de Lys and Baie Verte Belts are separated by the Baie Verte Line, a major structural linear which separates the accreted oceanic crust, and the continental platform sediments and gneiss associated with the ancient Laurentian continental margin. Recent studies suggest the Baie Verte Line was active from the Ordovician through to the Carboniferous, with west directed thrusting followed by several episodes of strike-slip movement (Goodwin and Williams, 1990).

2.3.1 Fleur de Lys Belt

The Fleur de Lys Belt comprises the west half of the Baie Verte Peninsula. Its stratigraphy consists of the East Pond Metamorphic Suite, the Fleur de Lys Supergroup, and several large plutons (Hibbard, 1983). The East Pond Metamorphic Suite along the west coast of the peninsula comprises a basal sequence of migmatites, overlain by banded gneiss and psammitic to semi-pelitic schists which contain small bodies of eclogite and metaconglomerate.

The Fleur de Lys Supergroup is exposed to the north and east of the East Pond Metamorphic Suite. Units defined in previous studies include the White Bay, Old House Cove, Rattling Brook and Ming's Bight groups. These typically consist of psammitic, semi-pelitic and graphitic schist, marble, greenschist and amphibolite (Betz, 1948; Watson, 1947; Fuller, 1941; Baird, 1951; Hibbard and Bursnall, 1979). Units at the top

Figure 2.4 Geology of the Baie Verte Peninsula.

Intrusive Rocks

CB - Cape Brule Porphyry, **KP** - King's Point Complex, **WC** - Wild Cove Igneous Suite: granite porphyry.

Bg - Burlington Granodiorite: granite and granodiorite.

Baie Verte Belt

ML - Mimac Lake Group, **CJ** - Cape St. John Group: subaerial mafic to felsic volcanic rocks.

PH - Pacquet Harbour Group, **FP** - Flatwater Pond Group, **SA** - Snook's Arm Group: volcanic flows, pillowed basalts, felsic volcanic and volcaniclastic sediments.

AC - Advocate Complex, **PR** - Point Rousse Complex, **BC** - Betts Cove Complex: ophiolite sequences and gabbro.

Fleur de Lys Belt

FdL - Fleur de Lys Supergroup: psammitic to pelitic schist and gneiss, and amphibolite:

EP - East Pond Metamorphic Suite: gneiss and schist.

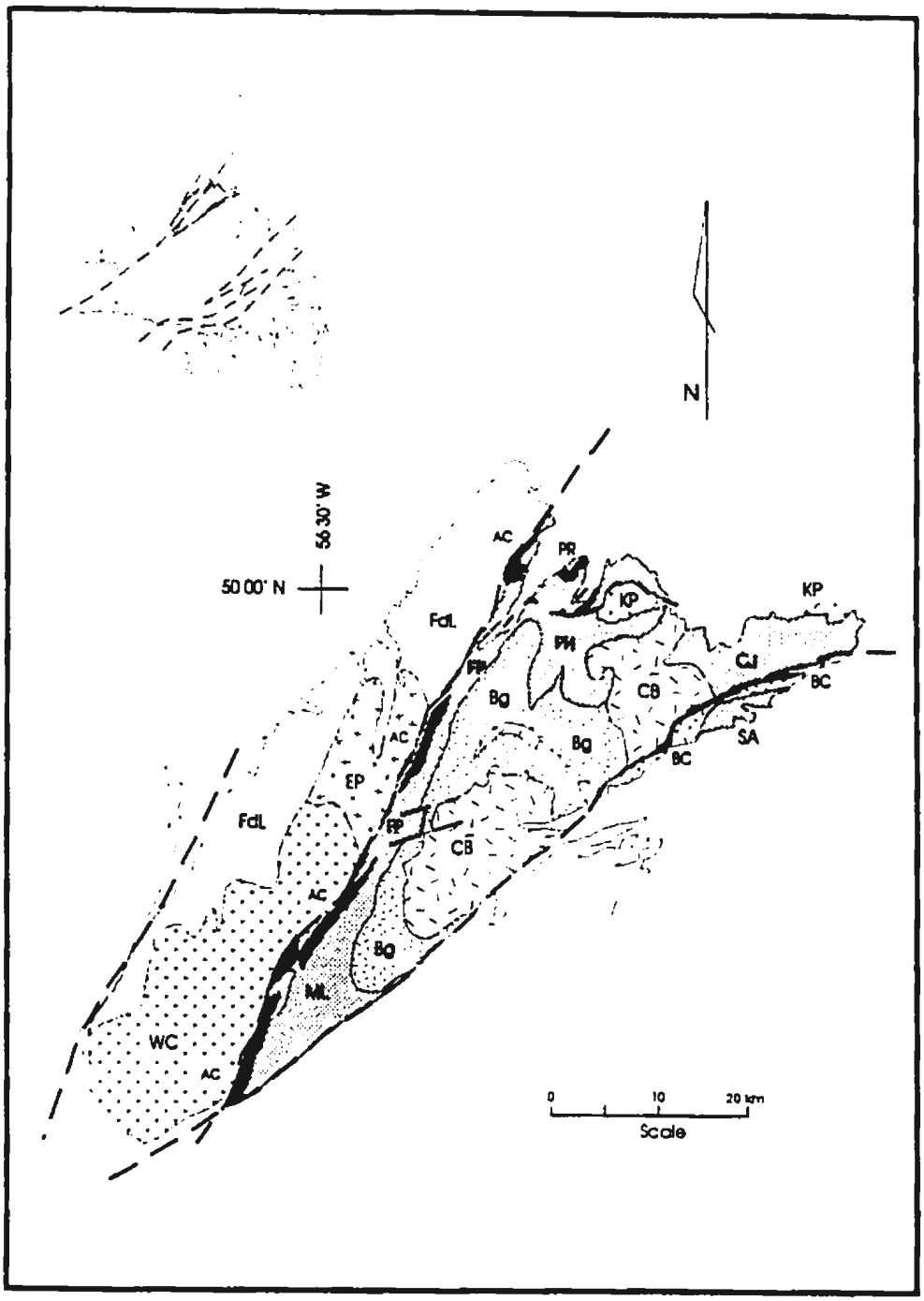
N
56 30' W
50 00' N
AC
PR
KP
KP
FdL
PH
PH
CJ
BC
Bg
CB
AC
Bg
SA
BC
EP
FdL
PP
CB
AC
Bg
ML
WC
AC
0
10
20 km
Scale

of the supergroup include the Birchy Complex, metasediments and greenschists of the Horse Islands Group, and schists correlated with rocks to the south of the Baie Verte peninsula (Hibbard, 1983).

Intrusive bodies in the Fleur de Lys Belt include the Wild Cove Pond Igneous Suite and the Partridge Point Granite. These are described as a "granitic" batholith, and garnetiferous, muscovite-bearing leucogranite, respectively (Kidd, 1974; Fuller, 1941; Hibbard, 1983).

2.3.2 Baie Verte Belt

The Baie Verte Belt is exposed to the south and east of the Baie Verte Line. Its stratigraphy is divided into an ophiolitic basement, and overlying volcanic and sedimentary cover sequences (Hibbard, 1983). The ophiolitic basement consists of three disrupted ophiolitic sequences which include the Betts Cove, Point Rousse and Advocate Complexes, and the Pacquet Harbour Group.

The Betts Cove Complex is an intact sequence of ultramafic units, mafic dykes and volcanic flows (Upadhyay, 1973; Coish, 1977). It provides the type section for most of the basement stratigraphy west of the Baie Vert Belt. A U/Pb zircon age determination from gabbro in the ophiolite provides a minimum age of 488.6 +3.1 -1.2 Ma for the oceanic crust in the Baie Verte Belt (Dunning and Krogh, 1985).

In contrast to the Betts Cove, other ophiolites on the Baie Verte Peninsula are variably disrupted and incomplete. The Point Rousse Complex along the north coast of the peninsula is a south directed, imbricate thrust stack of mixed ultramafic, volcanic and volcaniclastic rocks (Norman, 1973; Norman and Strong, 1975; Kidd et al., 1978). The Advocate Complex along the Baie Verte Line is a dismembered sequence of deformed and altered ultramafic and volcanic units (Kidd, 1974; Bursnall, 1975). The Pacquet Harbour Group, not considered a complete ophiolite, consists of deformed volcanic and

sedimentary rocks correlated with the upper portion of the Betts Cove Ophiolite Complex (Gale, 1971, 1973; Hibbard, 1983).

Conformably overlying the ophiolites are Ordovician marine volcanic and sedimentary rocks which are associated with upper sections of the ophiolite complexes (Kidd et al., 1978). These include the Snook's Arm Group which overlies the Betts Cove Complex. The Betts Cove may be equivalent to rocks exposed as the upper part of the Pacquet Harbour and the Flatwater Pond groups (Swinden, 1991). The marine volcanic and sedimentary rocks are overlain unconformably by the Cape St. John and Mic Mac Lake groups, which are Silurian in age, and terrestrial in origin (pers. comm., H.S. Swinden, 1991). Ordovician and Silurian strata are unconformably overlain by Carboniferous sediments in the southeast corner of the Peninsula, correlated with similar rocks in the Deer Lake Basin to the south (Dean and Strong, 1975; Hibbard, 1983).

Intrusive rocks comprise greater than half the outcrop in the Baie Verte Belt. These include the Burlington Granodiorite, Dunamagon Granite, and Cape Brulé Porphyry and smaller intrusive bodies such as the Reddit's Cove Gabbro, the La Scie Intrusive Suite, and the granite and syenite of the Middle Arm Ridge area (Baird, 1951; Neal et al., 1960, 1963). Recent U/Pb zircon age determinations provide Silurian ages for the formation of these intrusive bodies (pers com., Dunning, 1993).

The regional metamorphic grades in the Baie Vert Belt are typically greenschist. The grades decrease to lower greenschist facies with increasing proximity to the Baie Verte Line (Kennedy, 1973, 1975b; De Wit, 1974; Kidd, 1974; Bursnall, 1975). The grades frequently increase to mid to upper amphibolite facies near large plutonic bodies such as the Burlington Granodiorite and some structures including the Scrape Thrust which may represent a metamorphic sole to the Point Rousse Ophiolite Complex (Hibbard, 1983). Metamorphic grades are dominantly greenschist on the Consolidated Rambler Mines Properties and in the south portion of the Pacquet Harbour Group (Hibbard, 1983).

2.4 Geology of the Pacquet Harbour Group

The Pacquet Harbour Group is exposed as an imbricate sequence of volcanic, intrusive and sedimentary rocks near the centre of the Baie Verte Peninsula (Figure 2.4; after Hibbard, 1983).

External contacts between the Pacquet Harbour Group and other litho-stratigraphic units in the Baie Verte Belt are poorly constrained. The Group is correlated with similar volcanic units in the upper portion of the Betts Cove Complex (Gale, 1971; Hibbard, 1983; Swinden et al., 1989). It is bound to the west by the Burlington Granodiorite, to the east by the Cape Brulé Porphyry, and to the north by the Dunamagon Granite. It is overthrust from the north by imbricate ultramafic, volcanic, and sedimentary units of the Point Rousse Complex along the Scrape Thrust (Hibbard, 1983). Its contacts with volcanic units of the Cape St. John and ultramafic units to the east and northeast are probably thrusts as well (per. comm. Norman, 1990).

The extent to which internal stratigraphy can be identified in the Pacquet Harbour Group is a matter for continuing debate. Many workers document several generations of structure on the Consolidated Rambler Mines properties and in the south portion of the Group (Gale, 1971; Tuach and Kennedy, 1973; Tuach, 1976; Hibbard, 1983). Recent mapping on the Consolidated Rambler Mines properties provide structural orientations consistent with those to the north along the Scrape Thrust (pers. comm., T.J. Calon, 1989).

A study by Coates (1990) divided mixed volcanic and sedimentary sequences on the Consolidated Rambler Mines properties into the Rambler Sequence and Uncles' Sequence; two structural blocks separated by the west to northwest trending, shallow northeast dipping Rambler Brook Fault. Internal stratigraphic relationships within, and between the sequences are uncertain, but stratigraphic continuity is noted in the vicinity

of some VMS deposits on the Consolidated Rambler Mines properties. The rocks in both sequences are dominated by greenschist and upper greenschist grades of metamorphism.

Whole-rock analysis of volcanic rocks in the Pacquet Harbour Group distinguish tholeiitic basalts from high magnesian, incompatible element depleted basalts identified as boninites (Gale, 1971; Cameron et al., 1979; Hibbard, 1983). In subsequent studies, extended REE plots and Nb / Th ratios plotted against Y were used to relate the chemistry of these units to primitive or transitional arc palaeotectonic settings (Swinden et al., 1988). The REE chemistry suggests complex multi-stage melting from a refractory source related to the presence of an immature subduction zone in a primitive arc tectonic setting (Swinden et al., 1988).

2.5 VMS and Epigenetic Deposits of the Baie Verte Peninsula

Mining and exploration on the Baie Verte Peninsula have made significant contributions to the economy of Newfoundland since 1864. Eight of nine orebodies on the peninsula are past-producing VMS deposits including the Terra Nova, Tilt Cove, and Betts Cove deposits, and the VMS deposits on the Consolidated Rambler Mines properties (Figure 2.2). The Tilt Cove deposit is the second largest ophiolite-hosted VMS deposit in the Caledonide - Appalachian orogen. Approximately 8 million tonnes of Cu ore was mined intermittently from it between 1864 and 1957. The Betts Cove deposit, which occurs to the south of Tilt Cove deposit is smaller, with reserves estimated at $\leq$ 1 million tonnes.

Melange fabrics, and a lack of alteration in the Terra Nova deposit have been attributed to its structural emplacement along with the Advocate Ophiolite Complex in the Baie Verte Line (Hibbard, 1983). The Tilt Cove and Betts Cove deposits are structurally intact in comparison and occur in the Betts Cove Ophiolite Complex on the east coast of the peninsula. The base metal sulphide mineralization in all th. : deposits consists of pyrite, pyrrhotite, chalcopyrite, sphalerite and arsenopyrite with trace amounts of galena and magnetite with significant gold and silver (Strong and Saunders, 1988). Altered

rocks below intact deposits including the Betts Cove consist of well defined stockwork zones which contain core assemblages of quartz and chlorite, gradational to peripheral assemblages of quartz + albite + chlorite + calcite (Saunders, 1985). The extensive alteration associated with the Tilt Cove deposit has been attributed to the presence of a large seafloor fluid convection system associated with the high thermal gradients present during the rifting of an island arc (Strong and Saunders, 1988).

Exploration during the 1980's in central Newfoundland resulted in the discovery of additional VMS and numerous epigenetic Au prospects (Tuach et al., 1988; Tuach, 1990). Exploration from 1986 to 1991 resulted in the discovery of the Ming West VMS deposit on the Consolidated Rambler Mines properties, and several gold deposits in the ophiolites of the Baie Verte peninsula, including the Deer Cove, Pine Cove and Stog'er Tight deposits in the Point Rousse Complex and the Dorset prospect in the Flatwater Pond Group, Other recent epigenetic gold discoveries include the Nugget Pond deposit in the Betts Cove Complex, the Brass Buckle and Uncles' prospects in the Pacquet Harbour Group. The Uncles' prospects include several small occurrences to the south of the Rambler deposit, including the Uncle Theodore prospect which is exposed along the northwest shoreline of Big Rambler Pond.

The mesothermal deposits in the Point Rousse Complex occur in thrusts and are hosted by a variety of altered ultramafic rocks, gabbros, mixed mafic and felsic volcanics, and sediments. Related disseminated mineralization generally occurs in dilational veins, stockwork breccia, or sheared quartz veins along brittle-ductile transitions. It consists of disseminated pyrite, pyrrhotite and magnetite with trace amounts of chalcopyrite, sphalerite, and galena (Gower et al., 1988; Ramezani, 1992). Local thrust faults and shear zones associated with these deposits mimic structural trends and orientations associated with the Scrape Thrust which separates the Point Rousse Complex from the underlying Pacquet Harbour Group (pers. comm., T.J. Calon, 1991).

The Stog'er Tight gold prospect in the Point Rousse Complex consists of mineralization which is typical of the "altered wall-rocks type" of mesothermal shear-hosted Au mineralization (Dubé, 1990). The deposit occurs along a shallow thrust, which is similar in orientation to the Deer Cove thrust to the north (Ramezani, 1993). Four alteration zones have been defined. These include a chlorite + calcite zone, calcite + muscovite zone, a red albite + pyrite + gold zone and a chlorite + magnetite zone. Gold mineralization occurs with pyrite, red albite, and muscovite in altered gabbro in the margins of syn-deformational quartz + albite + ankerite veins. U/Pb ages for igneous zircon yields an Early Ordovician crystallization age of 483 +3/-2 Ma (edit) for the host Stog'er Tight gabbro. Hydrothermal zircons provide a minimum age of 420 $\pm$ 5 Ma for the gold mineralization in the deposit (Ramezani, 1992).

Chapter 3: Geologic Setting and Distribution of Alteration in the Rambler VMS Deposit

3.1 Introduction

The Consolidated Rambler Mines properties are located 18 kilometres east of the town of Baie Verte (near the intersection of Highways 414 and 418) at the centre of the Baie Verte Peninsula (Figure 3.1). VMS deposits including the Rambler, a concentrating mill and camp facilities at the centre of the properties (Plate 3.1) are readily accessible by well maintained mine roads (Figure 3.2).

Mines on the properties are currently idle with total production from 1962 to 1982 estimated at over 4 million tonnes of Cu-Au ore (Tuach, 1988). Recent exploration by MPH Exploration Limited has confirmed the presence of gold in the deposits. The discovery of the Ming West VMS deposit and numerous other prospects and mineralized alteration zones highlights the potential for future discoveries in the immediate area.

Two distinct types of mineralization occur on the Consolidated Rambler Mines properties. VMS deposits occur as parallel northeast trending, shallow dipping, structurally attenuated orebodies along specific stratigraphic transitions within, and above the Rambler Sequence (Coates, 1990). Auriferous disseminated sulphide mineralization typified by some of the Uncles' prospects and the Discovery Outcrop occur south of the Rambler mine site in shear zones which appear to be related to the Rambler Brook Fault. The two types of mineralization coincide in the Rambler deposit, offering a unique opportunity to examine their effects on the distribution and concentration of base metals, gold and trace metals in an intensely deformed VMS deposit.

Plate 3.1 Rambler (Main) Mine, mill and concentrator.

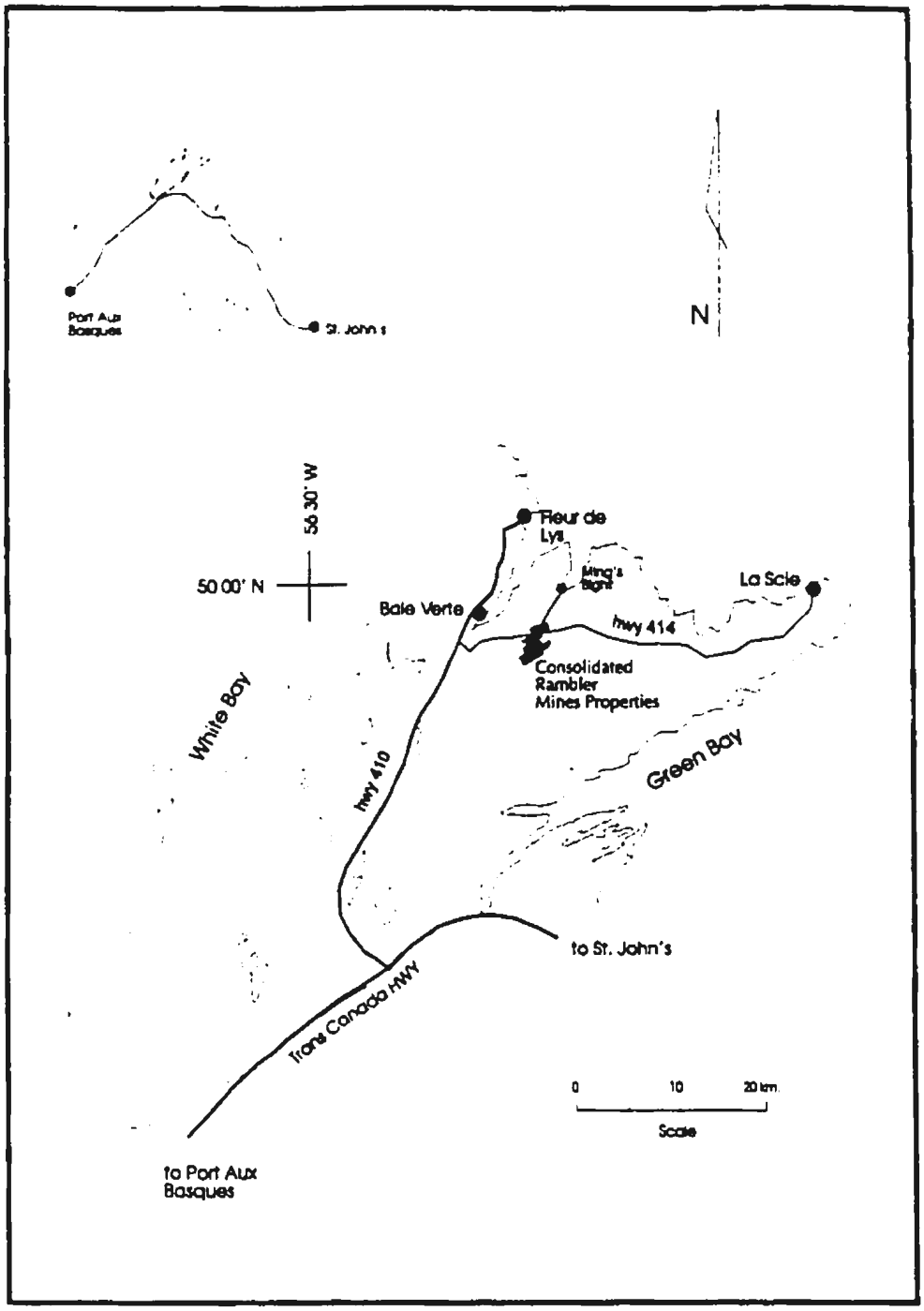

Figure 3.1 Location of the Consolidated Rambler Mines properties on the Baie Verte Peninsula in North Central Newfoundland.

3.2 Previous Geological Work

The Rambler VMS deposit occurs at the centre of the Consolidated Rambler Mines properties. Originally referred to as the Rambler during its discovery by Enos England, a local trapper and prospector. It was subsequently listed as one of the "main" deposits of Rambler Mines Limited and Rambridge Mines Limited from 1944 to 1960. The deposit has more recently been referred to as the Main Mine on the Consolidated Rambler Mines properties (Coates, 1990). The deposit is herein referred to as the Rambler Mine to be consistent with the name provided by Enos England.

Early interpretations of the geology of the Consolidated Rambler Mines properties are presented in studies by Baragar (1954), Gale (1971, 1973), Heenan (1973), Tuach (1976), Tuach and Kennedy (1978), Hibbard (1983), and Tuach et al. (1988). Gale (1971) utilized an existing geochemical grid, to create a geological map at 1" to 800' scale Gale (1971) identified three phases of deformation and two different styles of folding.

The Consolidated Rambler Mines properties were re-mapped by Tuach (1976), who subdivided the Pacquet Harbour Group into five gradational litho-facies units in a conformable, lithologic succession. Stratigraphy was interpreted in terms of a north-facing, arcuate, mixed sequence of volcanic and sedimentary lithologies, surrounding a central felsic volcanic "dome". Generations of structure were interpreted in terms of two deformational events. Hibbard (1983) questioned the validity of these interpretations citing additional structural complexities.

Recent interpretations of the stratigraphy are quite different. Mixed intrusive, volcanic, and sedimentary lithologies are separated into the Rambler and Uncles' "Sequences", which are juxtaposed along the arcuate northwest to east trending, shallow northeast dipping Rambler Brook Fault (Coates, 1990). The Uncles' Sequence to the southwest, occurs as a series of mafic volcaniclastic units, massive flows, and pillow basalts which

host the Uncles' prospects to the south of the Rambler mine site. The Rambler Sequence northeast of the fault, is described as a basal volcaniclastic pile, which is overlain by mafic to intermediate flows, pillows and volcaniclastic rocks, succeeded in turn by epiclastic and pyroclastic lithologies (Coates, 1990).

3.3 Geologic Setting of the Rambler VMS Deposit

Rocks assigned to the Uncles' and Rambler sequences were examined during field work in the summer of 1989. Mafic volcanic and volcaniclastic rocks of the Uncles' Sequence were examined along a road cut to the south of the Rambler camp, and in the immediate vicinity of the Uncle Theodore prospect along the western shore of Big Rambler Pond. Mafic and felsic volcanic, intrusive, and pyroclastic units assigned to the Rambler Sequence were examined in several outcrops along the Rambler Brook Fault, and in the vicinity of the Rambler mine site.

Mafic volcanic units associated with the Uncles' Sequence south of the Rambler camp site consist of dark green, medium to fine grained, massive, pillowed, variably foliated and altered volcanic rocks. Outcrops with pillows (up to 3m) contain well defined selvages ($\leq$5cm) and flow breccia. Silicification and carbonatization are common forms of local alteration.

Volcanic rocks in the vicinity of the Uncles' prospects are intensely altered and silicified. Cleared exposures of the Uncle Theodore prospect occur as structurally intercalated, northeast trending, light green to grey silicified quartz, chlorite, and light green quartz $\pm$ muscovite schists which contain variably deformed quartz veins (Plate 3.2). Disseminated pyrite occurs in shear bands throughout the cleared exposures.

The base of the Rambler Sequence is dominated by structurally intercalated felsic and mafic volcanic units succeeded by a series of volcaniclastic, pyroclastic and epiclastic sediments (Coates, 1990). Felsic and mafic volcanic units occur as a series of low

Plate 3.2 Uncle Theodore Prospect; exposures of silicified quartz + chlorite, and quartz + muscovite schist with disseminated pyrite.

Plate 3.3 Exposures of schists and mylonite associated with the Rambler Brook Thrust in Rambler Brook along the south margin of tailings dump. Chloritized volcanic units near the structural footwall of the Rambler Sequence.

exposures approximately 200 metres northwest of the Rambler mine site along the north margin of the tailings dump. Outcrops in this location consist of light grey to buff, fine to medium grained rocks with fragmental textures. Deformed volcanic rocks exposed along Rambler Brook in the thrust south of the tailings dump occur as dark green, fine grained chlorite schist with a well developed northwest trending, shallow northeast dipping planar schistosity (Plate 3.3). Sulphide mineralization occurs as disseminated pyrite and chalcopyrite ($\leq$ 30%).

Outcrops near the Rambler mine site consist of mixed volcanic and sedimentary units. Schists and mylonites of the Discovery outcrop are exposed approximately 50 metres southwest of the mine, adjacent to an abandoned shaft (Plate 3.4). The mixed volcanic and sedimentary units are intruded by a gabbro sill and small mafic dykes. The sill, intersected over a thickness of 100 metres during drilling on the Rambler deposit, occurs in a series of small exposures on the north side of the mill, and outcrops in an island near the centre of England's Steady; a small pond at the centre of the property. Exposures typically consist of a variety of undeformed pegmatitic, cummulate, massive and porphyritic textured gabbro. The dark green fine to medium grained randomly oriented mafic dykes typically range from several metres to a metre in thickness.

Volcanic, volcaniclastic, pyroclastic and epiclastic sequences associated with the upper portion of the Rambler Sequence were examined in a series of exposures immediately south and southwest of the mine buildings. Exposures typically consist of mixed polymictic conglomerate, fine to medium grained wacke, a light grey to green agglomerate (Plate 3.5) with prominent deformed felsic fragments ($\leq$ 10cm), and light grey to green, fine grained tuffaceous sediment. These units are succeeded by pillow lavas along a road cut approximately 150 metres east of the mine site (Plate 3.6).

Transposed bedding and cleavage orientations on the Consolidated Rambler Mines properties are consistent with the disposition of lithologies along an openly folded, shallow northeast plunging thrust fault system (pers. comm., D. Duncan, 1989).

Plate 3.4 Schist and mylonite exposed as the "Discovery Outcrop"; the exposed footwall of the Rambler VMS deposit.

Structural orientations are consistent with those defined along the Scrape Thrust to the north of the Consolidated Rambler Mines properties (pers. comm. T. J. Calon and N. Ryburn, 1990). Deformed units exposed near the centre of the properties are disposed along a series of folded bedding-parallel imbricate shears which create zones of low strain surrounded by "anastomosing" high strain shear zones typified by the Rambler Brook Thrust Fault (pers. comm. T. J. Calon, 1990).

Metamorphic grades in local outcrops on the Consolidated Rambler Mines properties are typically greenschist. Exposures of volcanic rock are dominated by spilitic assemblages of quartz + albite + chlorite + calcite $\pm$ epidote. Upper greenschist grades are indicated by the presence of biotite porphyroblasts in the less deformed and altered intrusive and volcanic lithologies.

Plate 3.5 Felsic agglomerate ("mill rock") with stretched felsic and mafic volcanic fragments ($\leq$ 10cm) exposed in outcrop approximately 100 metres southeast of the Rambler mine site.

Plate 3.6 Pillow lavas exposed in a road cut approximately 150 metres east of the Rambler mine site.

3.4 VMS and Gold Mineralization on the Consolidated Rambler Mines Properties

VMS deposits including the Rambler, Ming Mine and Ming West deposits occur in stratigraphic intervals which are characterised by the presence of chert and tuffaceous exhalite (Coates, 1990). The Rambler (Main), Ming, and Ming West VMS deposits occur as attenuated, parallel, northeast-trending shallow-dipping (30°) ore chutes in the Rambler Sequence (Figure 3.2). The East Mine of less certain origin is exposed as quartz + muscovite schist in the mafic volcanic rocks exposed to the east of the Rambler mine site.

Sulphide assemblages in the VMS deposits are completely recrystallized. Fabrics observed in massive sulphide horizons of the Rambler deposit vary from breccia-textured to shear-banded ore. Massive sulphide assemblages generally consist of high percentages ($\leq$80%) of pyrite and sphalerite, with trace chalcopyrite. Galena occurs along the margins of quartz veins which cut through some of the massive sulphide horizons.

Disseminated auriferous sulphide associated with the Uncles' prospects occurs near the top of the Uncles' Sequence to the south of the Rambler Brook Fault. Similar mineralization also occurs in the Discovery Outcrop; the exposed footwall of the Rambler deposit (Plate 3.4). Outcrops in these locations typically consist of light green to grey, fine grained, quartz + chlorite, and quartz + muscovite schist to mylonite. Bright green shear bands ($\leq$2cm) suggest the presence of a Cr-rich mica. Sulphides in the Uncle Theodore prospect typically consist of disseminated cubes and fine pyrite ($\leq$30%), with trace pyrrhotite, chalcopyrite, and sphalerite.

3.5 Stratigraphy of the Rambler VMS Deposit

The Rambler deposit occurs as a deformed, northeast trending, shallow plunging ellipsoidal orebody consisting of recrystallized massive and disseminated sulphide. The deposit occurs above and is parallel to a sheared transition from felsic to mafic volcanic

Figure 3.2 Lithological and structural trends on the Consolidated Rambler Mines properties showing the location of Rambler and Uncles' Sequences, VMS deposits, and the Uncles' prospects.

Rambler (Main) deposit: volcanogenic massive sulphide mineralization.

Mine tailings.

Rambler Brook Thrust.

Approximate lithological and structural trends.

Bedding / cleavage orientations.

Extension lineations.

Prospect locations.

Location of mine shaft.

Buildings.

Roads.

Mineral claim boundaries.

Geochemical grid stations.

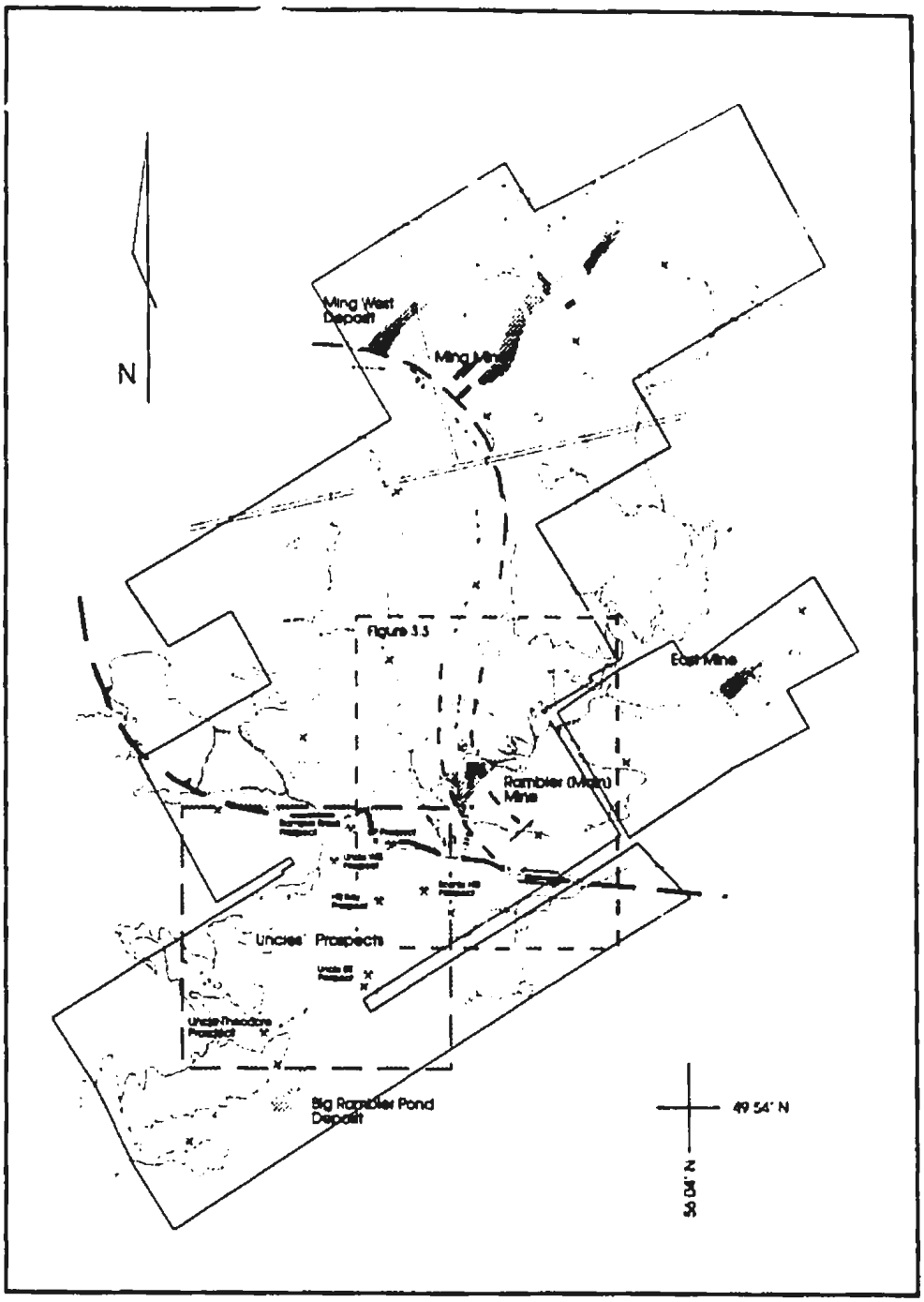
N
Ming West Deposit
Ming Mine
Figure 3.3
East Mine
Rambler (Main) Mine
Uncles' Prospects
Big Rambler Pond Deposit
49 54' N
56 04' W

and volcaniclastic lithologies in the Rambler Sequence (Figure 3.3). Drilling in 1989 intersected sulphide mineralization along strike for approximately 90 metres, tracing the deposit approximately 640 metres down plunge from the original mine workings (pers com., D. Duncan, 1989). Mineralization has been intersected in widths of up to 30 metres.

Correlation of lithologies between drill holes was not possible due to the intense deformation and alteration in the stratigraphy of the deposit. Core logging and sampling was restricted to two drill fences; MZ88-20 to MZ88-28 (Figure 3.3). Core data is consistent with a structurally intercalated, but upright stratigraphic succession, which was separated into the footwall, deposit and hangingwall stratigraphic sections for the purposes of this study (Figure 3.4).

The footwall section of the stratigraphy occurs as the first 50 metres at the base of the of most longitudinal drill sections and consists of mixed intervals of mylonite, schist, and their less deformed and altered volcanic, sedimentary and intrusive protoliths. Mylonites and schists occur as light to dark grey to green, fine grained, foliated to massive recrystallized units with bands of disseminated sulphides ($\leq$2m). Intervals of volcanic and intrusive rock occur as dark green, fine to medium grained, massive to cummulate textured rocks. The altered intrusive rocks at the bottom of drillhole MZ89-28 are cut by a large ($\leq$15m) quartz vein in the base of the footwall. Rocks immediately adjacent to the vein ($\leq$1m) are intensely silicified.

The deposit is the most consistent stratigraphic marker in the drilled stratigraphy. It averages 15 metres in thickness and consists of mixed intervals of quartz + chlorite $\pm$ epidote breccia, disseminated ($\leq$5m) and massive sulphides ($\leq$2m), and chert. Intervals of quartz + chlorite $\pm$ epidote breccia define the base of the deposit. These occur as dark green to grey, fine to medium grained, brecciated siliceous units cut by irregular fractures with massive to disseminated sulphides with irregular light to dark green chloritic fractures ($\leq$3mm). The breccia is mixed with, and gradationally succeeded by

Figure 3.3 Lithological and structural trends in the vicinity of the Rambler (Main) deposit, showing approximate extent of VMS mineralization, prospect and drillhole locations, and location of section line for Figure 3.4.

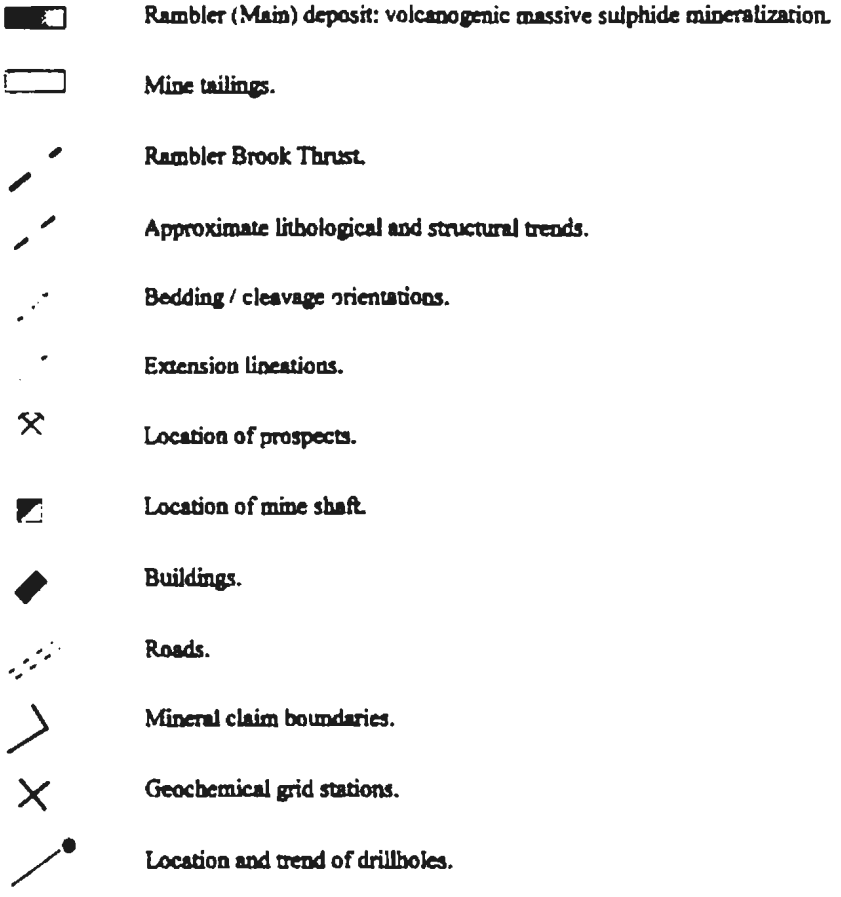

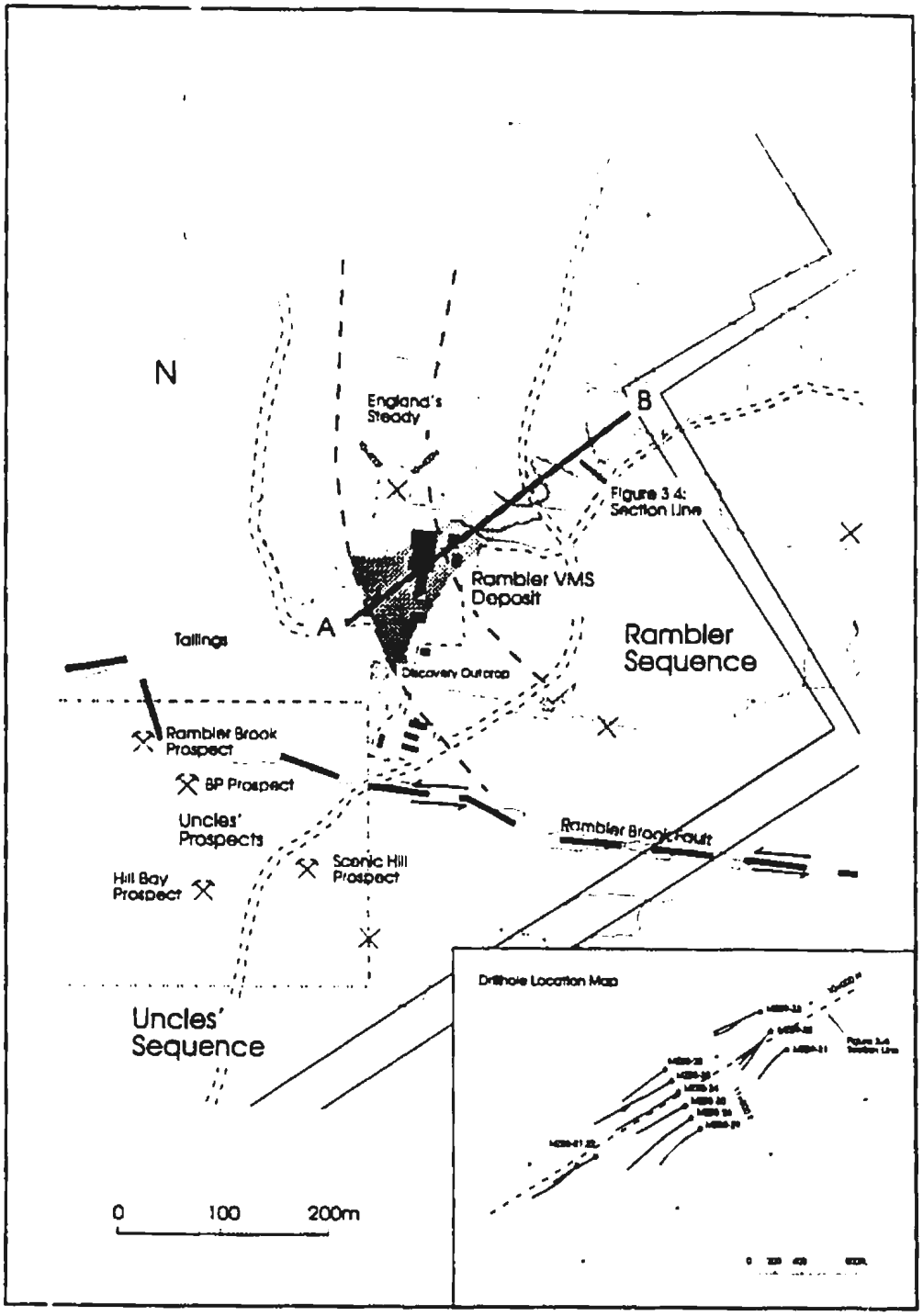
N
England's Steady
B
Figure 3.4: Section Line
Rambler VMS Deposit
A
Tailings
Rambler Sequence
Discovery Outcrop
Rambler Brook Prospect
BP Prospect
Uncles' Prospects
Rambler Brook Fault
Scenic Hill Prospect
Hill Bay Prospect
Uncles' Sequence
0
100
200m
Drillhole Location Map

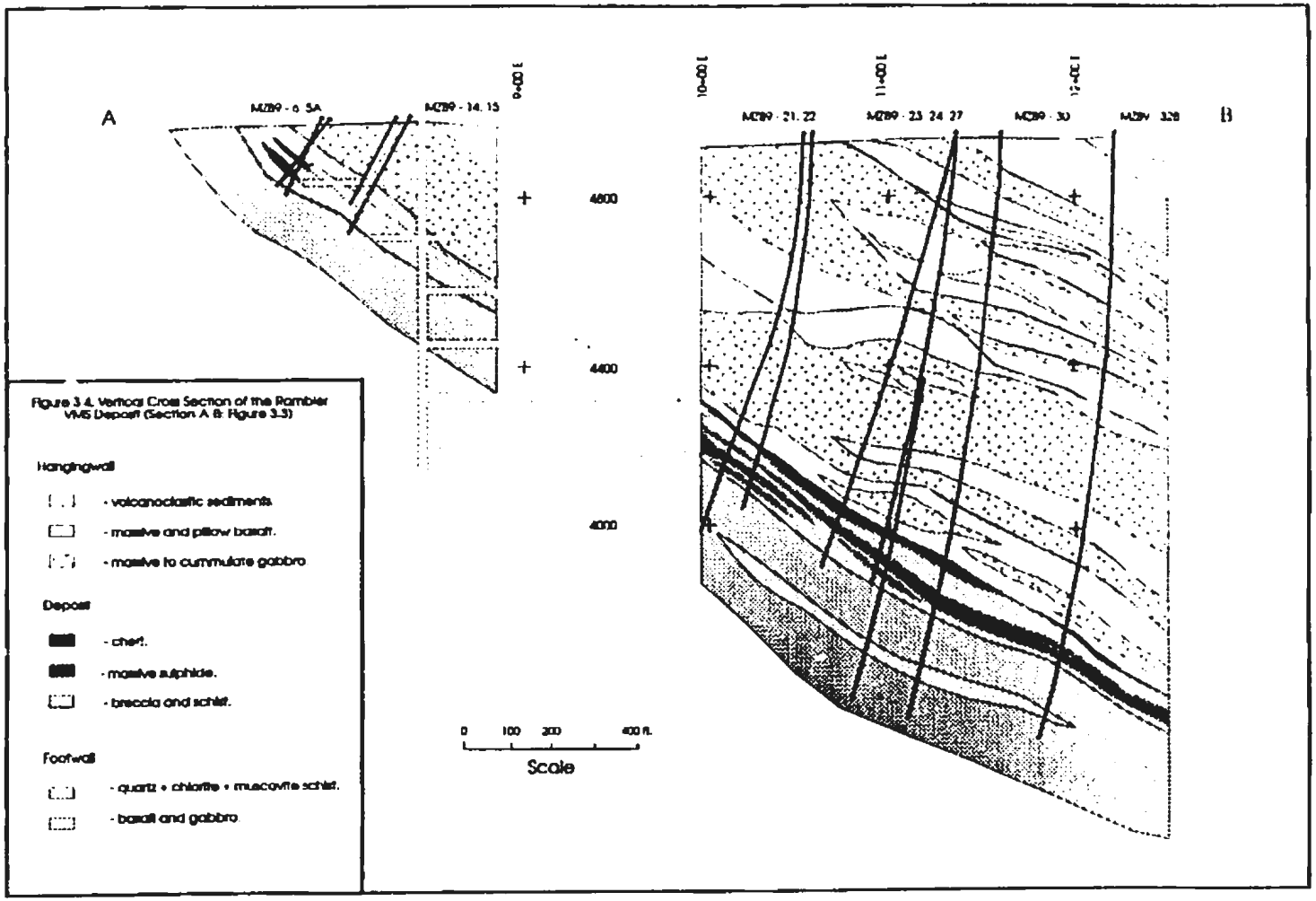

Figure 3.4. Vertical Cross Section of the Rambler VMS Deposit (Section A-B; Figure 3.3)

intervals (≤ 2m) of massive and disseminated sulphides, which are succeeded in turn by intact to deformed and brecciated intervals (≤ 1m) of dark red to black, amorphous, magnetic chert. Breccia, massive sulphides and chert in the deposit are structurally intercalated with intervals of schist and mylonite, which are the dominant lithologies in the footwall section of the stratigraphy (Plate 3.7).

A chert unit (≤ 1m) intersected in several drill holes above massive sulphide mineralization marks the transition from the deposit to the hangingwall section of the stratigraphy. Rocks near the base of the hangingwall consist of altered gabbros (≤ 100m) which are correlated with similar units exposed on the island at the centre of England's Steady. In core the gabbro consists of mixed coarse cummulate, fine massive, and porphyritic rocks which contain disseminated leucoxene. Intrusive contacts near the top and bottom of the sill are variably altered and tectonized.

The upper section of the hangingwall contains a variety of volcanic and intrusive rocks, and volcaniclastic and pyroclastic sediments. The gabbro sill at the base of the hangingwall is overlain by basalt mixed with volcaniclastic and pyroclastic sediment. Intervals of basalt typically occur as dark to light green, fine massive, to variably foliated altered units which contain pillow selvages (≤ 3cm) and amygduales (≤ 2mm). The basalts are gradational to mixed volcaniclastic and pyroclastic units at the top of the drill section.

The mixed volcaniclastic and pyroclastic units at the top of the hangingwall contain intervals (≤ 3m) of felsic agglomerate, volcanic sediment and tuff. Agglomerates contain distinctive rounded to subangular, intact, stretched, or brecciated, pebble to cobble-sized fragments of mafic and felsic volcanic rock and chert. The fragments and clasts are generally suspended in a matrix of light grey to green, fine to medium grained (≤ 2mm), recrystallized sediment. Other intervals (≤ 2m) contain similar dark green, fine to medium grained, bedded, granular textured wacke. Tuff intervals (≤ 0.5m) occur as light grey to green, finely banded fragmental units, near the top of the hangingwall.

Small ($\leq$ 2m) mafic dykes intrude the altered lithologies throughout the drilled section, with the exception of the footwall mylonite and schists. In core, these occurred as dark green, fine grained massive intervals of intrusive rock. The dykes were distinguished from similar extrusive rocks by the presence of definitive intrusive contacts and the absence of visible leucoxene.

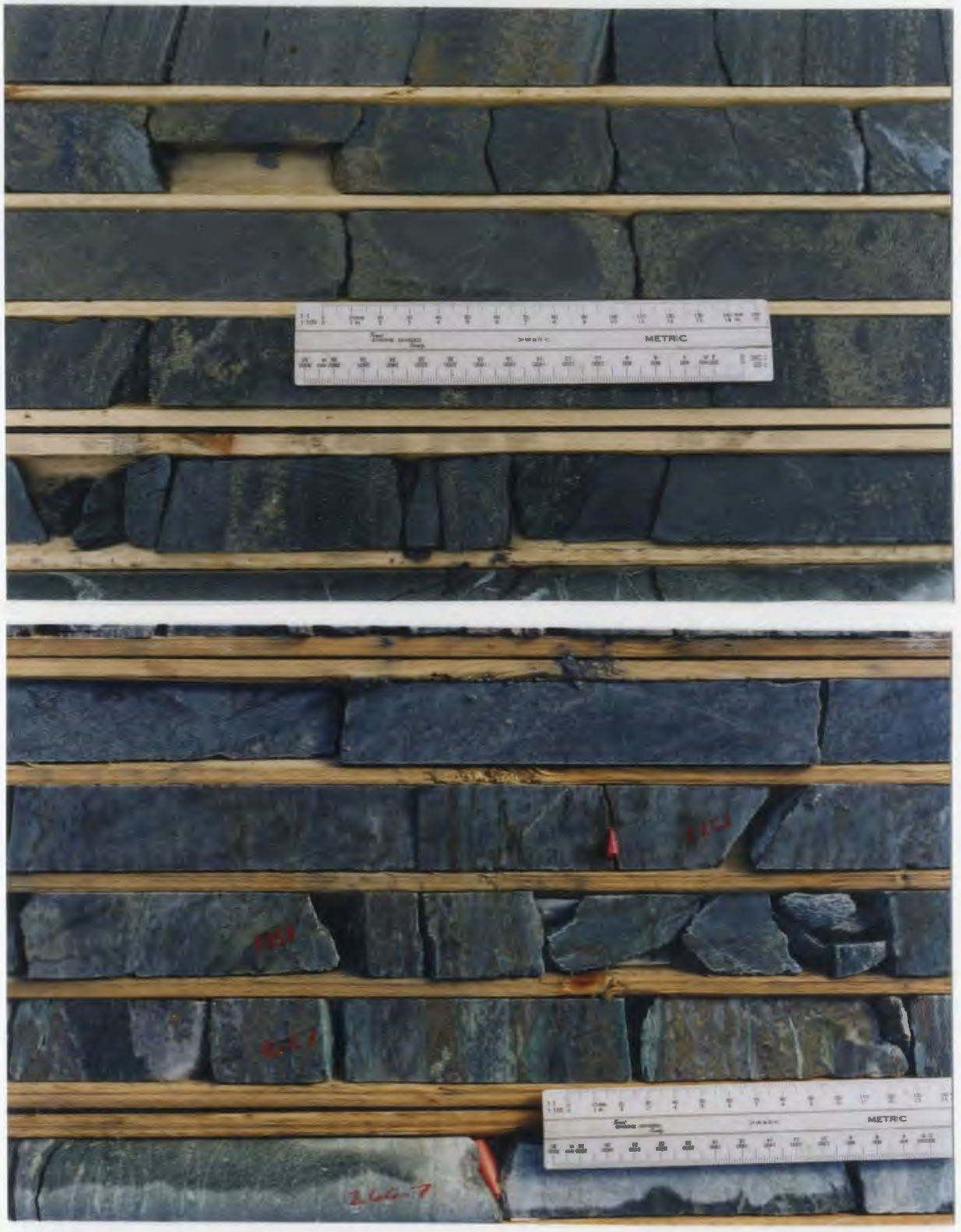

Plate 3.7 Drill core from the Rambler deposit. Contrasting brecciated volcanogenic massive sulphide mineralization (top) from the deposit and shear-related syn-kinematic disseminated sulphide mineralization (bottom) in the footwall.

Chapter 4: Petrography of Alteration and Mineralization in the Rambler VMS Deposit

4.1 Introduction

Intact VMS deposits typically consist of one or more concordant massive sulphide horizons above discordant stockwork alteration zones (Franklin et al., 1981; Lydon, 1988). Upper contacts between the massive sulphide and overlying strata are generally sharp, and frequently marked by thin layers of chert. Lower contacts are gradational to the stockwork alteration in underlying lithologies. The primary fabrics and textures in intact VMS deposits are consistent with the static alteration related to the fluid circulation and sedimentary processes associated with seafloor hydrothermal systems. These definitive stratigraphic and petrographic relationships are rarely preserved in deformed VMS deposits.

In order to look for evidence of possible mesothermal alteration in the Rambler deposit, 300 metres of core was (re)logged and sampled, with emphasis on the nature and occurrence of the different varieties of alteration, and spatial distribution of VMS and the mesothermal-looking varieties of disseminated sulphide mineralization. Three hundred core samples were selected from the different varieties of alteration and mineralization for petrographic analyses. Of these, 100 were selected for standard thin sections, and another 50 for polished thin sections. Twenty polished thin sections from samples with high assayed gold contents were carbon coated and examined with a Scanning Electron Microscope (SEM) to locate and determine the setting of gold, and to determine its occurrence in relation to other silicate and sulphide assemblages.

4.2 Alteration

Three common alteration assemblages occur in the drill core of the Rambler deposit. To compensate for their gradational nature, the main varieties were defined as "stages" in

on the basis of their overprinting relationships, and by the dominance of specific end-member fabrics, textures and silicate assemblages in the different sections of the stratigraphy.

Stage 1 alteration was defined as pervasive regional greenschist facies metamorphism. It is common throughout the Pacquet Harbour Group and in the stratigraphy of the Rambler VMS deposit, where it was defined as regional greenschist metamorphic, and deformed seafloor hydrothermal silicate assemblages in the hangingwall and deposit sections of the stratigraphy. Stage 2 alteration was defined by overprinting syn-kinematic assemblages which comprise the schists and mylonites in the footwall shear zones and in the shear zones in other areas of the stratigraphy. It is similar to the dominant alteration exposed in the Discovery Outcrop and alteration exposed in the Uncles' prospects. Stage 3 alteration was defined as the quartz veins throughout the stratigraphy of the deposit and in several outcrops on the Consolidated Rambler Mines properties.

The main stages of alteration, stage 1 and stage 2, were intimately associated with the "seafloor" massive and "epigenetic-looking" disseminated sulphide mineralization in the deposit and footwall sections of the stratigraphy. All three stages of alteration were overprinted by biotite porphyroblasts.

4.2.1 Stage 1: Seafloor / Greenschist Metamorphism

Stage 1 alteration assemblages in the deposit occur as quartz + chlorite $\pm$ epidote $\pm$ muscovite assemblages in intervals of massive sulphide. Variable amounts of quartz + epidote + chlorite $\pm$ muscovite occur in intervals of epidotized volcanic rock, quartz-chlorite breccia and chert.

Stage 1 alteration assemblages in samples of coarse cumulate textured hangingwall gabbro occur as equigranular ($\leq$0.8mm) intergrowths of albite and subhedral to anhedral

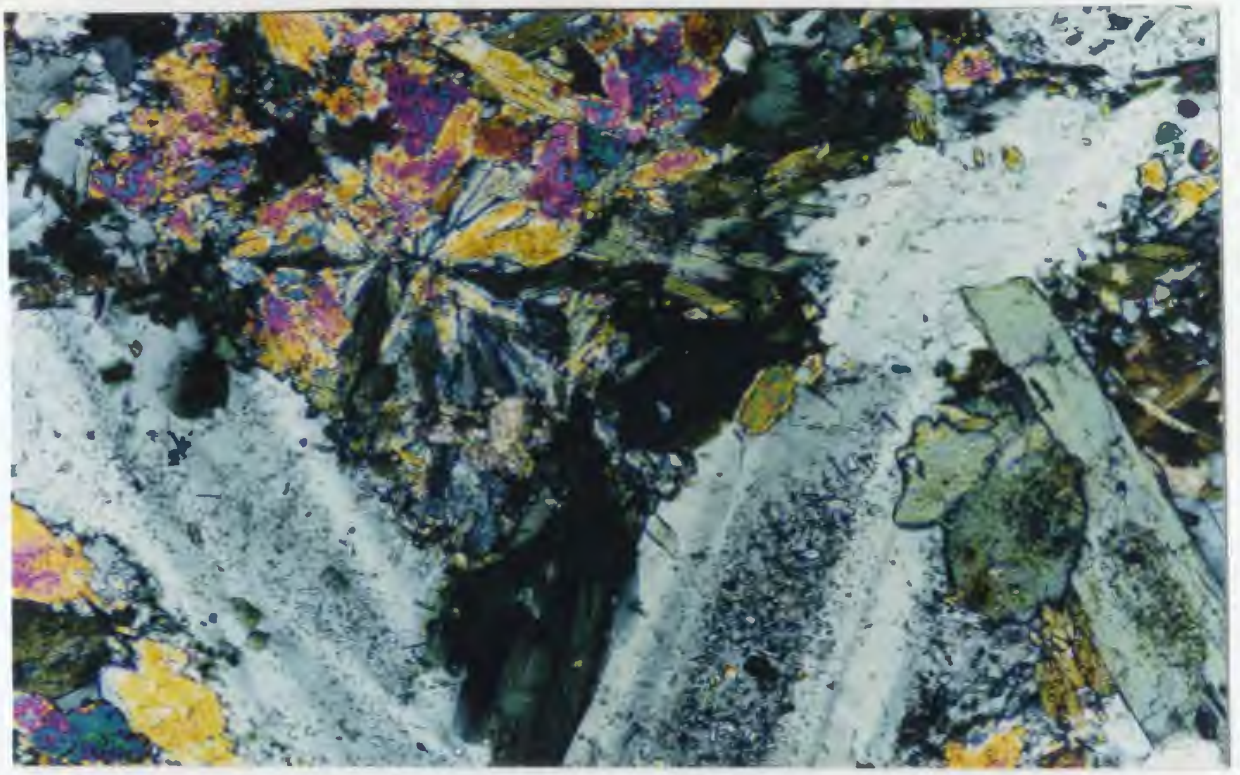

Plate 4.1 Typical stage 1 groundmass silicate assemblages in gabbro: altered albite, amphibole (light green), and radiating prismatic epidote (yellow, birefringent), with interstitial chlorite, sphene [28-2709, crossed polarized light, magnification = 100 X].

Plate 4.2 Stage 1 silicate assemblages in basalt. Random albite microlites (white) in a fine groundmass of chlorite, epidote and sphene [26-1948, crossed polarized light, magnification = 100 X].

blue-green amphibole (≤0.5mm; Plate 4.1). The albite contains fine inclusions of epidote (≤0.1mm). Amphibole is overprinted by radiating prismatic acicular epidote (0.2mm). It is surrounded by fine recrystallized quartz (≤0.1mm) intergrown with isolated subhedral sphene (≤0.04mm) associated with drusy to skeletal masses of leucoxene (≤0.4mm), and laths (≤0.4mm) of subhedral chlorite and biotite.

Stage 1 silicate assemblages in basalts are mineralogically similar, but texturally distinct from those observed in gabbro (Plate 4.2). In thin section, subhedral to euhedral albite grains (≤0.1mm) are surrounded by a matrix of fine recrystallized quartz (≤0.03mm), subhedral epidote (≤0.05mm), and pleochroic light to pale green chlorite laths (≤0.01mm) with isolated clustered subhedral grains of sphene (≤0.05mm). Chlorite is frequently overprinted and replaced by dark brown subhedral biotite (≤0.01mm).

Stage 1 assemblages in epidotized volcanic and sedimentary rocks contain high modal percentages of quartz, epidote and chlorite in comparison to less altered volcanic and sedimentary rocks. Assemblages in intervals of epidotized basalt consist of recrystallized quartz (≤0.3mm) with disseminated (≤40%) to massive (≥60%) epidote (≤0.1mm). Relict amygdules (≤3mm) occur as concentric aggregates of polygonal quartz (≤1mm) which surround recrystallized "cores" of calcite (Plate 4.3).

Stage 1 assemblages are common as both the clast and matrix constituents in volcanic sediments. Stage 1 assemblages in the mafic volcanic clasts (≤4cm) are similar to the stage 1 alteration assemblages in intervals of gabbro. Assemblages in felsic agglomeratic clasts (≤2cm) are similar to the assemblages in epidotized volcanic rocks, which consist dominantly of granoblastic quartz (≤0.2mm) with interstitial epidote (≤0.05mm) and chlorite (≤0.1mm). Detrital grains in the matrix consist of poorly to moderately-sorted, subangular albite (≤0.5mm) and recrystallized magnetite (≤0.2mm).

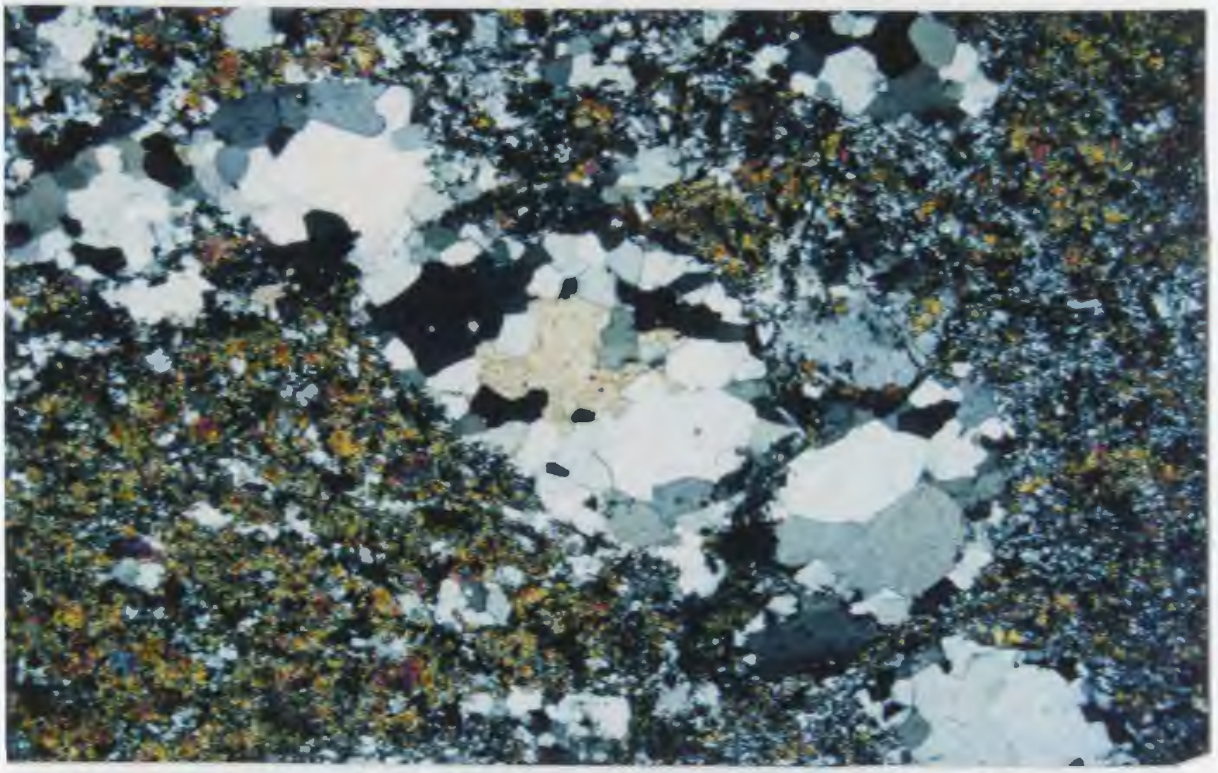

Plate 4.3 Stage 1 alteration: recrystallized amygdules (≤3mm) in epidotized basalt with "cores" of calcite [26-1962, crossed polarized light, magnification = 25 X].

Plate 4.4 Quartz-chlorite breccia: siliceous breccia fragments (≤1cm) surrounded by fractures (≤2mm) with masses of light green chlorite overprinted by biotite [26-1945, crossed polarized light, magnification = 100 X].

Stage 1 assemblages in breccia and massive sulphide horizons typically consist of high modal percentages of quartz, chlorite, and muscovite. Intervals of chert are dominated by recrystallized quartz and disseminated magnetite. Siliceous angular fragments ($\leq$5cm) in intervals of breccia consist of granoblastic quartz ($\leq$1mm) and fine ($\leq$0.01mm) disseminated subhedral to anhedral grains of epidote. The fragments are surrounded by irregular dark green fractures, ($\leq$2mm in width) which contain masses of the light green chlorite ($\leq$0.1mm) (Plate 4.4). Other fracture minerals include isolated to clustered masses of subhedral epidote ($\leq$1mm), sphene ($\leq$0.05mm), and magnetite ($\leq$0.1mm).

Stage 1 alteration in samples of massive sulphides ($\geq$60%) consist of several textural varieties of quartz ($\leq$1mm), epidotized and sericitized albite ($\leq$0.5mm), and a dark green, fine ($\leq 5\mu$m) variety of chlorite locally overgrown and replaced by the pale to light green variety of chlorite which is pervasive throughout the remainder of the stratigraphy. Both varieties of chlorite are intergrown with pale green to white muscovite ($\leq$0.1mm) (Plate 4.5) which occurs in fractures and shears with euhedral prismatic epidote ($\leq$0.2mm) (Plate 4.6). Rare tourmaline occurs as radiating acicular inclusions ($\leq$0.01mm) in quartz and recrystallized chalcopyrite (Plate 4.7). Cherts contain polygonal to granoblastic aggregates of quartz ($\leq$0.5mm) intergrown with disseminated to massive recrystallized magnetite ($\leq$0.01mm; Plate 4.8).

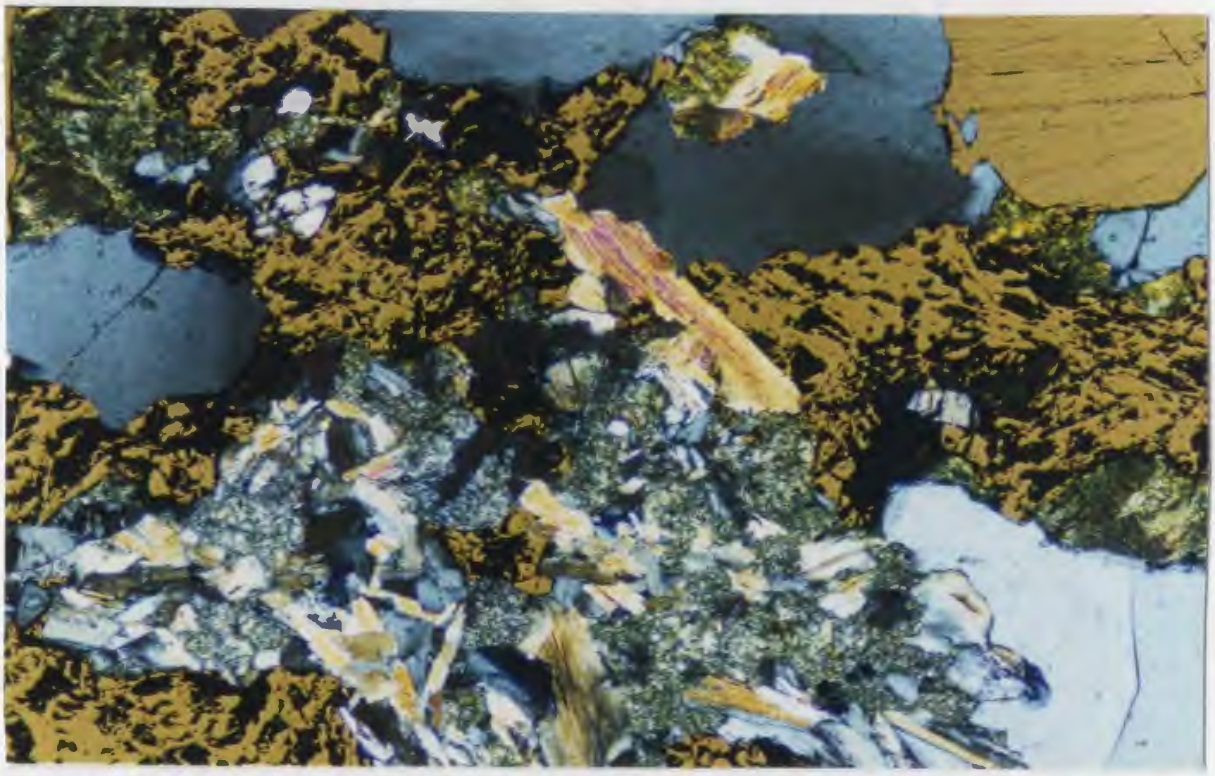

Plate 4.5 Alteration silicates in massive sulphides.: Fine ($\leq 5\mu m$) chlorite (dark green) intergrown and overprinted by light green chlorite (≤ 0.1mm, coarse, pale green), and muscovite (≤ 0.1mm, high birefringence). Quartz occurs as large (≤ 4mm) polygonal grains (dark to light grey) Sulphides include chalcopyrite (irregular, dark yellow) and pyrite (light yellow, upper right corner [21-2760, crossed polarized transmitted and reflected light, magnification = 200 X].

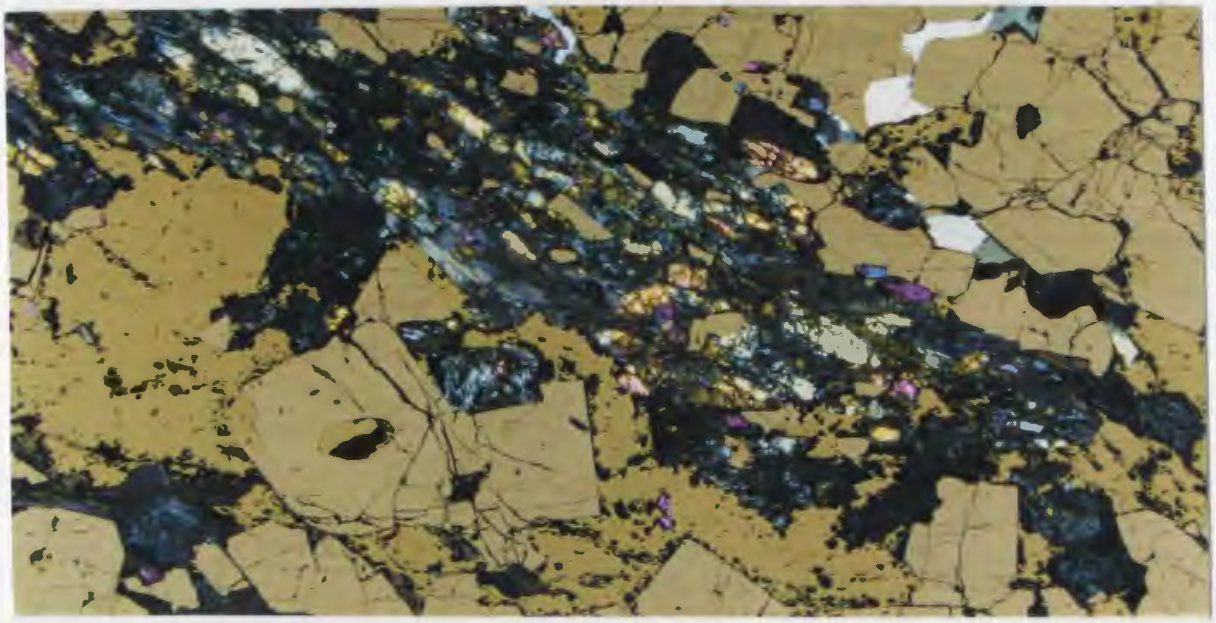

Plate 4.6 Silicates in sheared massive sulphides: chlorite (≤ 0.1mm: dark green) intergrown with subhedral to euhedral epidote (acicular). Sulphides along the margin of the shear consist of pyrite (light yellow polygonal grains) and chalcopyrite (dark yellow interstitial masses between pyrite) [21-2760, crossed polarized transmitted and reflected light, magnification = 25 X].

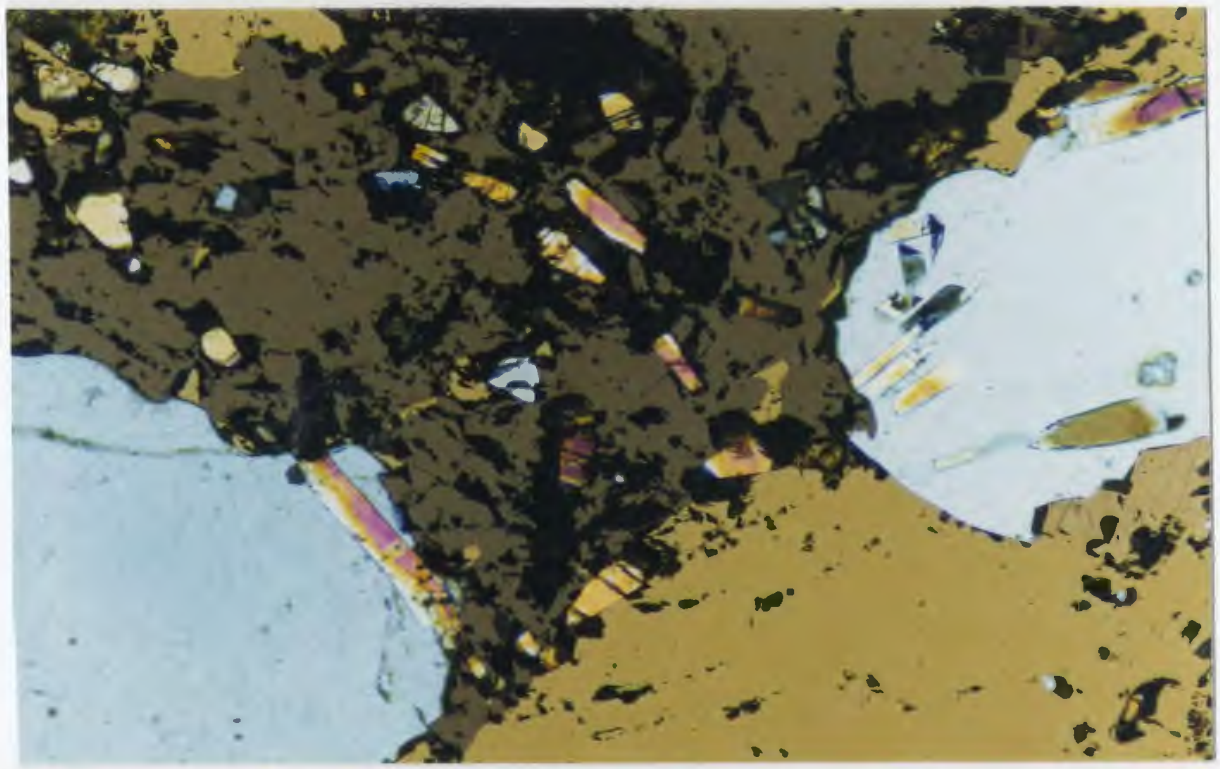

Plate 4.7 Alteration silicates in massive sulphide: inclusions ($\leq$0.01mm) of tourmaline (acicular, high birefringence) in recrystallized quartz (light grey), and recrystallized chalcopyrite (dark yellow) and sphalerite (dark greenish brown) [21-2760, crossed polarized transmitted and reflected light, magnification = 100 X].

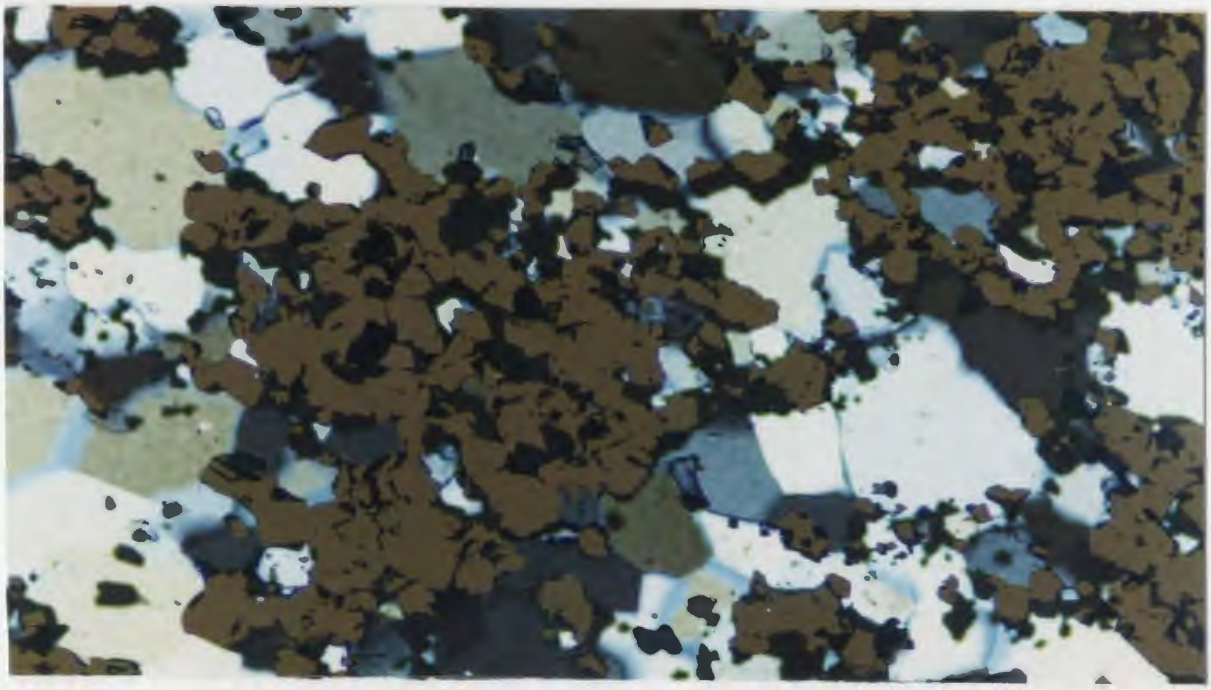

Plate 4.8 Recrystallized chert: granoblastic quartz ($\leq$0.5mm, light grey) with irregularly disseminated to massive recrystallized magnetite ($\leq$0.01mm, dark brown) [28-2719, crossed polarized transmitted and reflected light, magnification = 100 X].

4.2.2 Stage 2: Syn-kinematic Alteration

Stage 1 assemblages of quartz + albite + chlorite + epidote ± magnetite / sphene / leucoxene are replaced by stage 2 syn-kinematic quartz + chlorite ± epidote, quartz + chlorite ± muscovite, and quartz + muscovite ± chlorite assemblages with increasing deformation in the Rambler deposit. These alteration assemblages occur in shear zones throughout the stratigraphy, but are most abundant in the footwall, where they dominate intervals of schist and mylonite.

Stage 1 assemblages are replaced by stage 2 assemblages in a shear zone (≤1m) which cuts through the gabbro sill near the base of the hangingwall. In a thin section of quartz + chlorite ± muscovite schist, stage 2 assemblages consist of intervals of recrystallized quartz (≤0.05mm) with anastomosing shear bands (≤1mm) of light green chlorite (≤0.4mm) which contain rare subhedral to anhedral grains (≤0.01mm) of sphene. The chloritic shear bands are consistently overprinted by foliation parallel to oblique laths (≤0.2mm) of muscovite (Plate 4.9).

The stage 2 assemblages in the shear zone in the hangingwall gabbro are similar to stage 2 assemblages throughout the deposit and footwall sections of the stratigraphy. Thin sections of schist samples from the base of the deposit, reveal fractured to brecciated euhedral megacrystic epidote (≤0.4mm) in a groundmass of recrystallized quartz (≤0.1mm) intergrown with parallel to anastomosing laths (≤0.1mm) of light green chlorite (Plate 4.10). Footwall schists contain shear bands (≤3mm) consisting of polygonal quartz and pyrite (≤0.3mm) alternating with contorted shear bands (≤0.5cm) of fine (≤0.01mm) light to pale green chlorite (Plate 4.11).

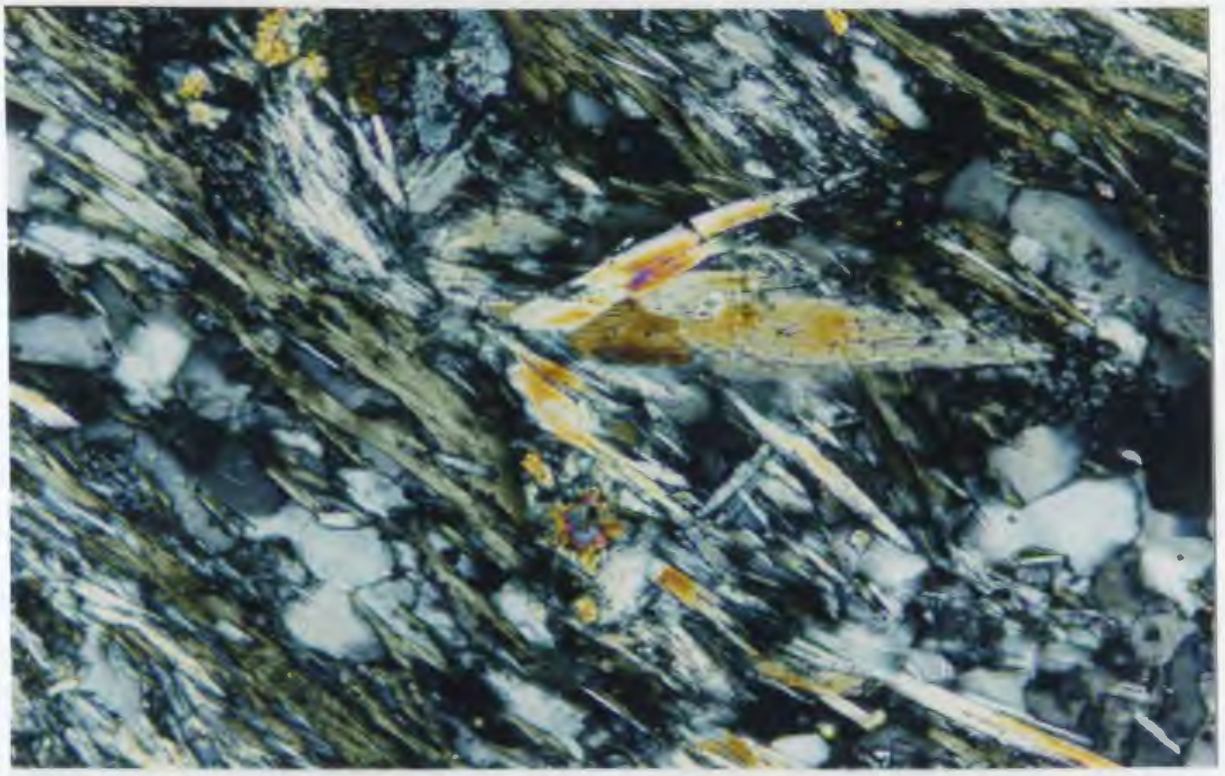

Plate 4.9 Stage 2 alteration; quartz + chlorite ± muscovite schist in gabbro: quartz with anastomosing chlorite overprinted by oblique muscovite ($\leq$0.2mm, high birefringence) [28-2702, crossed polarized light, magnification = 200 X].

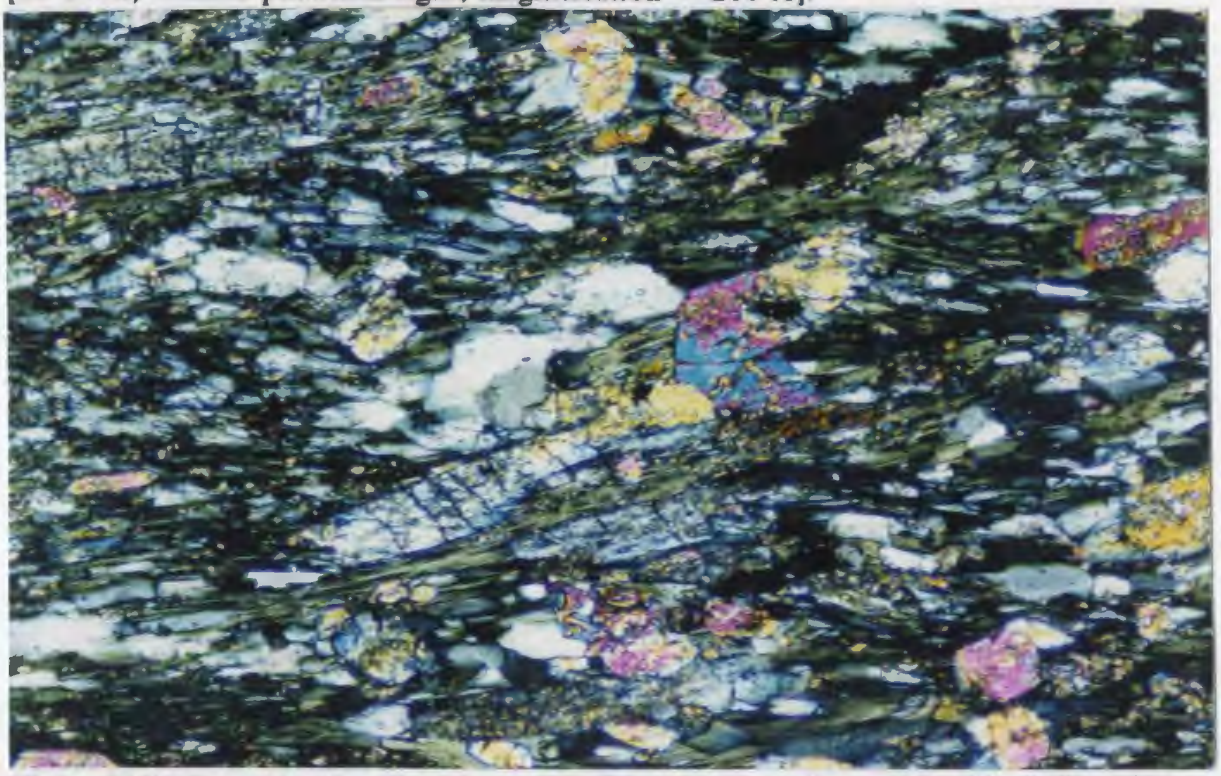

Plate 4.10 Stage 2 alteration: footwall schist; intact to fractured subhedral epidote ($\leq$0.4mm, high birefringence) in a groundmass of recrystallized quartz (light grey to white) and anastomosing chlorite ($\leq$0.1mm, light green) [28-2724, cross polarized light, magnification = 100 X].

Stage 2 alteration assemblages in intervals of footwall mylonite consist of finely comminuted and recrystallized grains of quartz with fine anastomosing laths of muscovite ($\leq$0.1mm) (Plate 4.12). These quartz + muscovite $\pm$ disseminated pyrite assemblages comprise the stage 2 end-member alteration as it occurs in the footwall section of the stratigraphy.

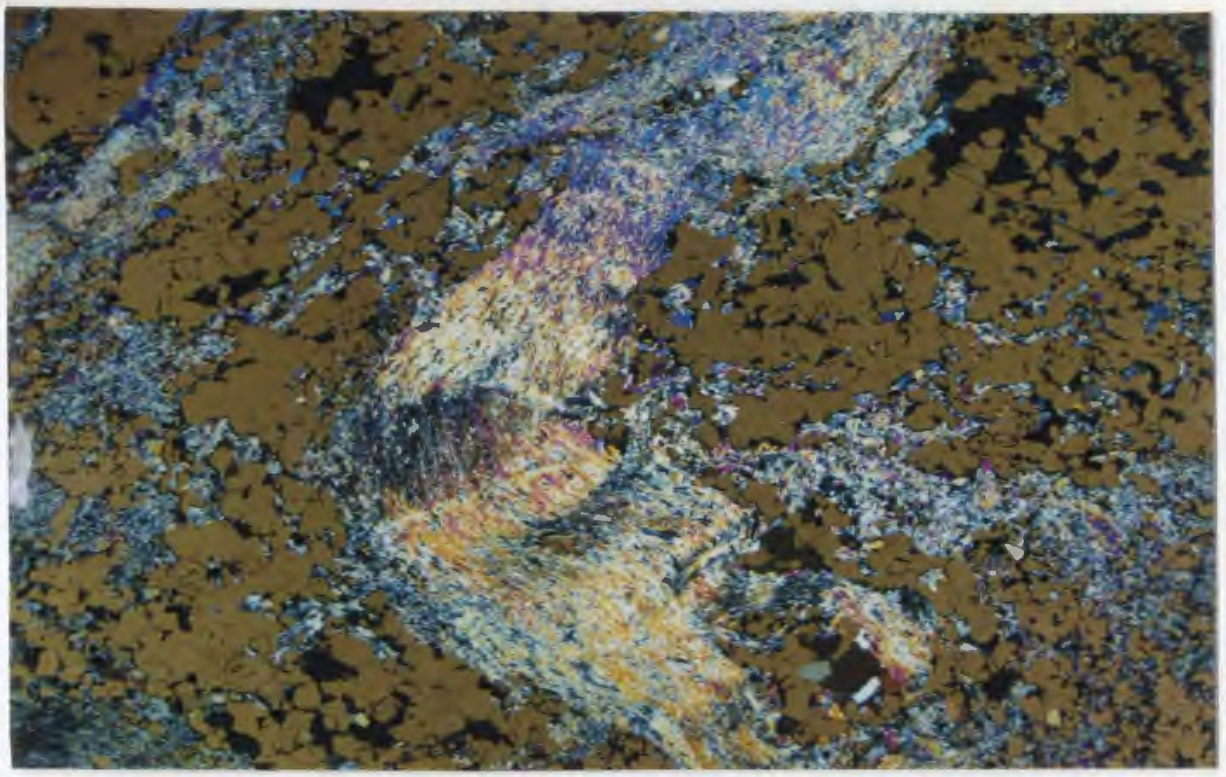

Plate 4.11 Stage 2 alteration: recrystallized quartz, chlorite and muscovite in a small ($\leq$ 1cm) crenulation fold [24-1925, cross polarized transmitted and reflected light, magnification = 100 X].

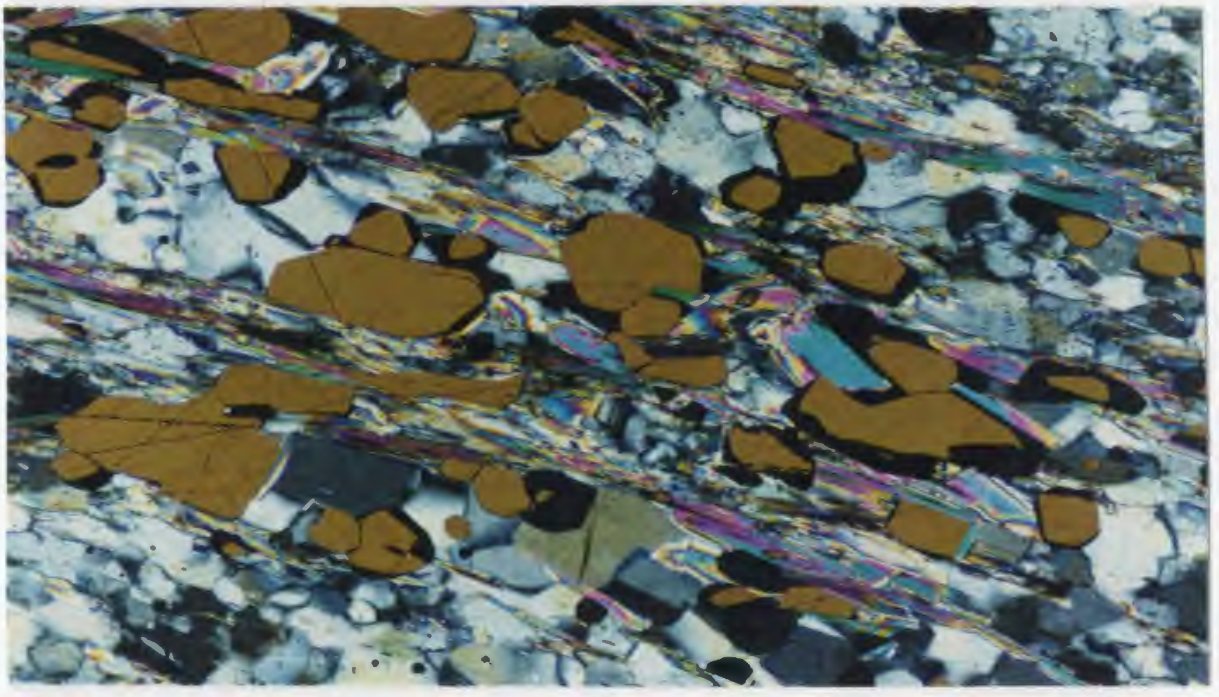

Plate 4.12 Stage 2 alteration: footwall mylonite; quartz with fine anastomosing lathes of muscovite (birefringent laths) and recrystallized polygonal disseminated pyrite (yellowish brown) [24-1925; cross polarized transmitted and reflected light, magnification = 200 X].

4.2.3 Stage 3: Vein Alteration

Stage 3 alteration assemblages occur in quartz veins which cut stage 1 and stage 2 assemblages throughout the stratigraphy of the deposit. The veins ($\leq$5m) are dominated by assemblages which include albite + quartz $\pm$ calcite $\pm$ chlorite, or quartz + calcite $\pm$ chlorite. Adjacent silicified rocks contain alteration consisting of quartz + chlorite with lesser epidote and sphene. Smaller veins contain assemblages consisting dominantly of calcite $\pm$ quartz $\pm$ chlorite. Their adjacent rocks are often weakly carbonatized.

A large (15m) quartz vein intersected in an interval of brecciated intrusive rock in the footwall of hole MZ89-28, contains coarse polygonal to euhedral grains ($\leq$6mm) of quartz and unaltered albite. Polygonal syntaxial overgrowths of quartz and albite (0.4mm) are common along the interior margin of the vein. Fractures ($\leq$4mm) contain coarse ($\leq$1mm) aggregates of light green chlorite and calcite ($\leq$2mm) (Plate 4.13). Altered rocks along the vein margins contain polygonal intergrowths of quartz and albite (0.2mm) with interstitial pleochroic light to pale green chlorite ($\leq$0.3mm) and euhedral epidote ($\leq$0.2mm). Sphene occurs as clustered subhedral to euhedral grains ($\leq$0.02mm) and aggregates ($\leq$0.3mm). Chlorite ($\leq$0.1mm) is frequently overprinted and replaced by laths of muscovite (Plate 4.14).

Assemblages in smaller silicate-dominated veins occur as polygonal aggregates of quartz ($\leq$3mm) and masses of dark brown biotite ($\leq$0.2mm) which replaces the pervasive secondary light green chlorite ($\leq$0.5mm). The vein assemblages are cut by fractures ($\leq$0.2mm) which contain fine to amorphous ($\leq$0.01mm) calcite. Carbonate veins are dominated by recrystallized polygonal to granoblastic calcite ($\leq$0.5mm), with scattered polygonal ($\leq$0.2mm) grains of quartz and aggregate clumps ($\leq$0.1mm) of light green chlorite.

Plate 4.13 Stage 3 alteration: typical assemblages in large footwall quartz - carbonate vein; quartz and albite cut by chloritic fracture [28-2733, crossed polarized light, magnification = 25 X].

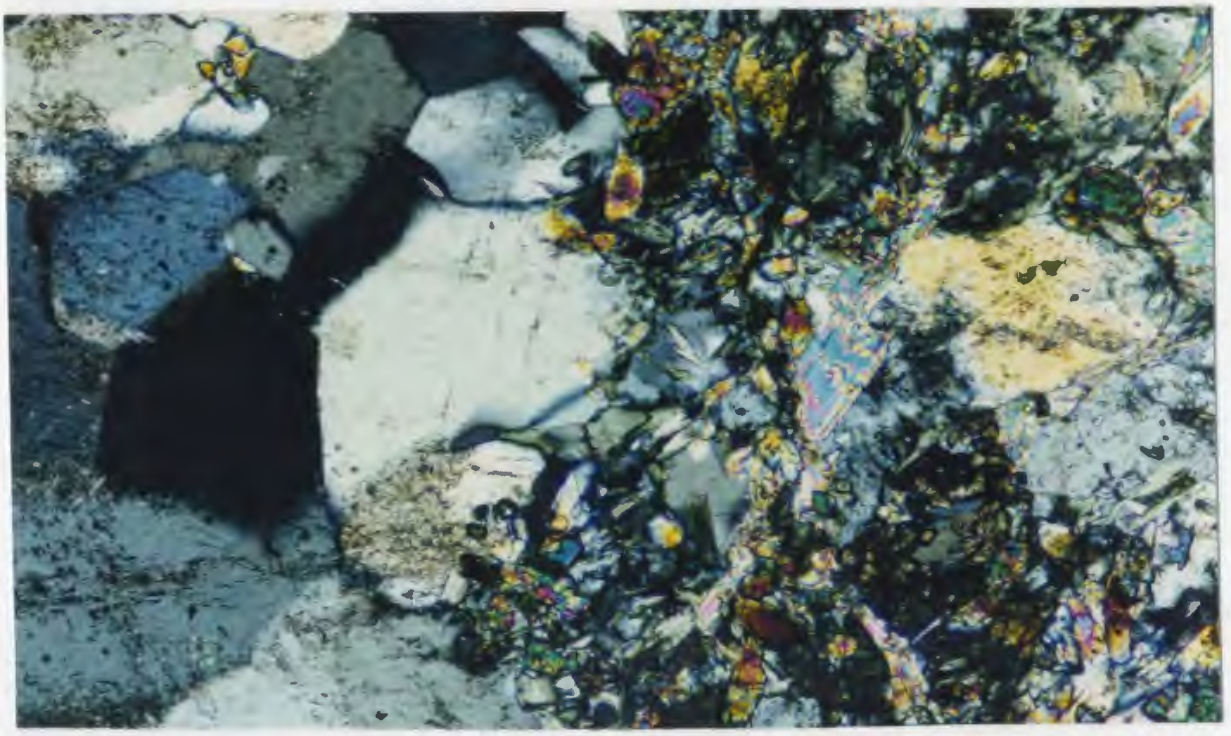

Plate 4.14 Stage 3 alteration: wallrock alteration along margin of large footwall vein; quartz + chlorite + epidote ±biotite ± sphene assemblages [28-2731, crossed polarized light, magnification = 100 X].

4.3 Massive and Disseminated Sulphide Mineralization

Intervals of massive sulphide mineralization ($\geq 80\%$ sulphides) were intersected over widths of up to 15 metres in holes MZ89-21 to MZ89-28. Sulphide assemblages invariably consist of recrystallized pyrite ($\geq 60\%$), with variable amounts of chalcopyrite and sphalerite ($\leq 35\%$), and trace amounts of galena (up to 5%). The disseminated sulphides in the footwall consist dominantly of pyrite ($\geq 80\%$), with lesser amounts of chalcopyrite and sphalerite ($\leq 20\%$).

The massive sulphides in the deposit section of the stratigraphy are texturally and mineralogically diverse. Euhedral cubic, polygonal / granoblastic, and colloform pyrite were noted in thin section. In most specimens, massive sulphides are dominated by recrystallized polygonal pyrite (≤ 0.4mm) and sphalerite intergrown with irregular interstitial chalcopyrite (≤ 0.2mm), which frequently contain inclusions (≤ 0.05mm) of galena (Plate 4.15). Polyphase inclusions (≤ 0.01mm) in recrystallized pyrite grains contain chalcopyrite, galena and pyrrhotite.

Two varieties of sphalerite are common in thin sections of massive and disseminated sulphide (sample 21-2750). A light yellow variety occurs as rounded inclusions and recrystallized grains in samples dominated by stage 2 quartz + muscovite $\pm$ chlorite alteration assemblages. A dark red variety occurs as irregular grains and interstitial masses with fine inclusions (≤ 0.01mm) of chalcopyrite in massive sulphide samples which contain both stage 1 and stage 2 alteration assemblages. Examples of both are shown in plate 4.16.

Texturally diverse massive sulphide assemblages near the top of the deposit are replaced with increased deformation by auriferous disseminated sulphide ($\leq 30\%$) in the lower portion of the deposit and footwall sections of the

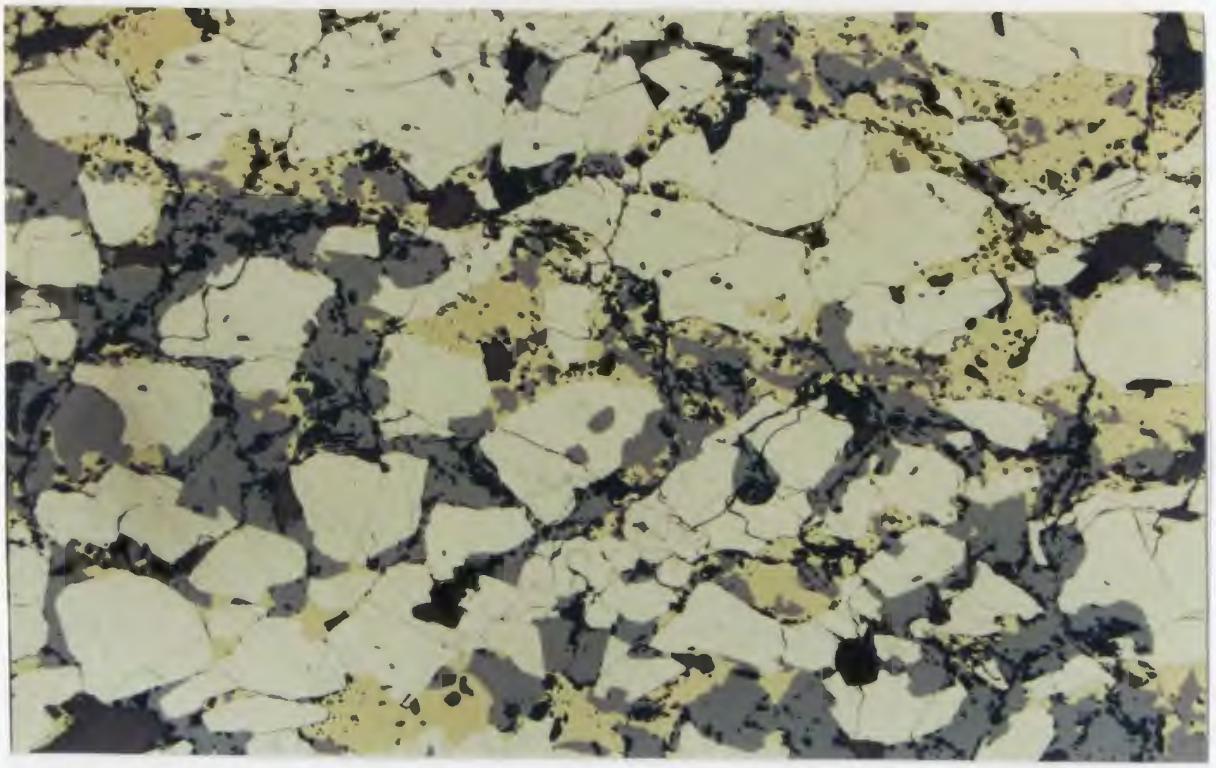

Plate 4.15 Sulphide assemblages in a massive sulphide sample: pyrite ($\leq$0.4mm, light yellow, polygonal) with sphalerite ($\leq$0.3mm, light grey, angular polygonal) and irregular recrystallized chalcopyrite ($\leq$0.3mm, dark yellow) [21-2753, transmitted and reflected light, magnification = 25 X].

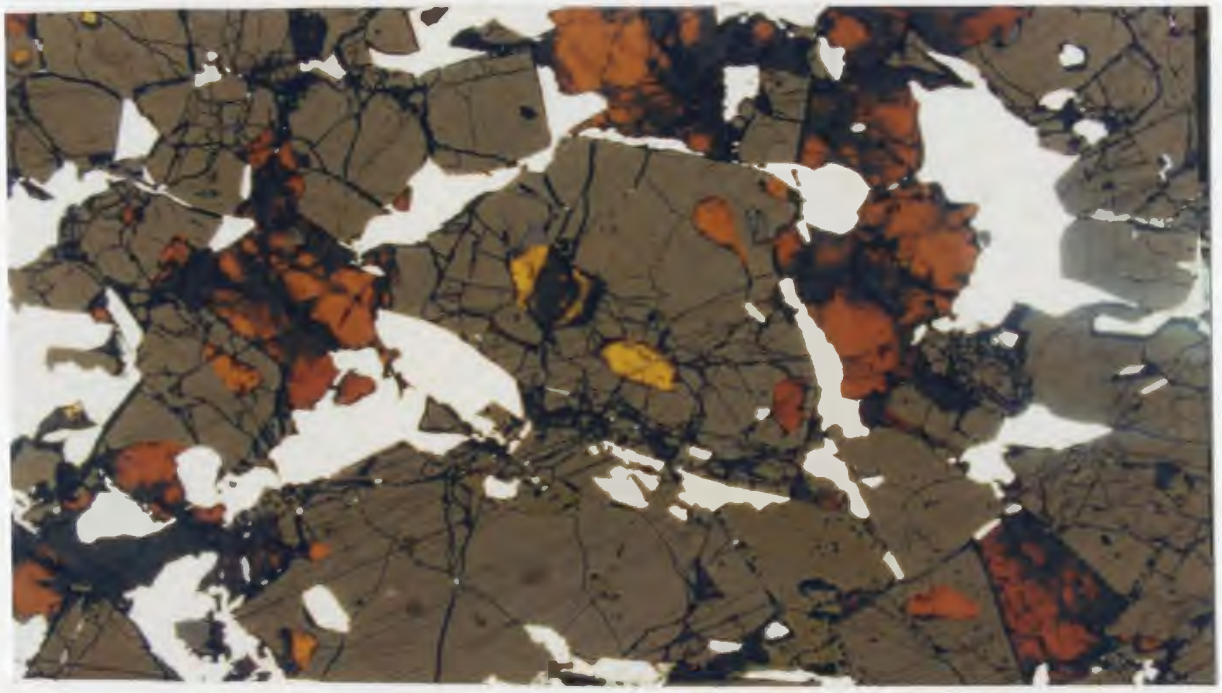

Plate 4.16 Assemblages in massive sulphide sample: light yellow (inclusion) and dark red (interstitial) sphalerite [21-2750; transmitted and reflected light, magnification = 100 X].

stratigraphy. Mixed intervals of brecciated and sheared ore with variably folded to contorted shear bands of massive and semi-massive sulphides ($\leq 80\%$) occur within the gradational transition from the deposit to the footwall section of the stratigraphy.

Hand specimens of footwall schist and mylonite contain disseminated sulphides, which are dominated in thin section by recrystallized pyrite ($\leq 30\%$). Individual sections reveal polygonal euhedral grains of pyrite (≤ 0.2mm) with traces of light coloured sphalerite (≤ 0.1mm) and irregular masses of recrystallized chalcopyrite (≤ 0.2mm) (Plates 4.11 and 4.12).

4.3.1 Secondary Sulphides

Secondary sulphide assemblages were discovered in samples 21-2721 and 26-1974, which were selected for their anomalously high gold contents. These sulphide assemblages overprint stage 1 and 2 silicate alteration and associated recrystallized sulphide assemblages. Secondary sulphides include chalcopyrite + pyrrhotite $\pm$ galena $\pm$ Pb telluride, and chalcopyrite + arsenopyrite $\pm$ sphalerite assemblages, respectively.

The secondary sulphide assemblages in 21-2721, a recrystallized massive sulphide sample, occur in an irregular vein (≤ 5mm) as masses of chalcopyrite and pyrrhotite (≤ 1mm). The pyrrhotite contains inclusions (≤ 0.2mm) of galena and equant polygonal grains (≤ 0.5mm) of pyrite. The galena inclusions enclose, and are frequently associated with round to irregular inclusions (≤ 0.1mm) of Pb-telluride (Plate 4.17).

Secondary sulphides in 26-1974; a sample of semi-massive sulphide mineralization, occur in a shear band (≤ 0.5cm) which contains irregular fractures (≤ 0.4mm) associated with numerous grain interstices which contain quartz and chalcopyrite. Many of the interstices contain small ($\leq 8\mu$m) sulphide and silicate inclusions. Some contain arsenopyrite, pyrrhotite and electrum (Plate 4.18).

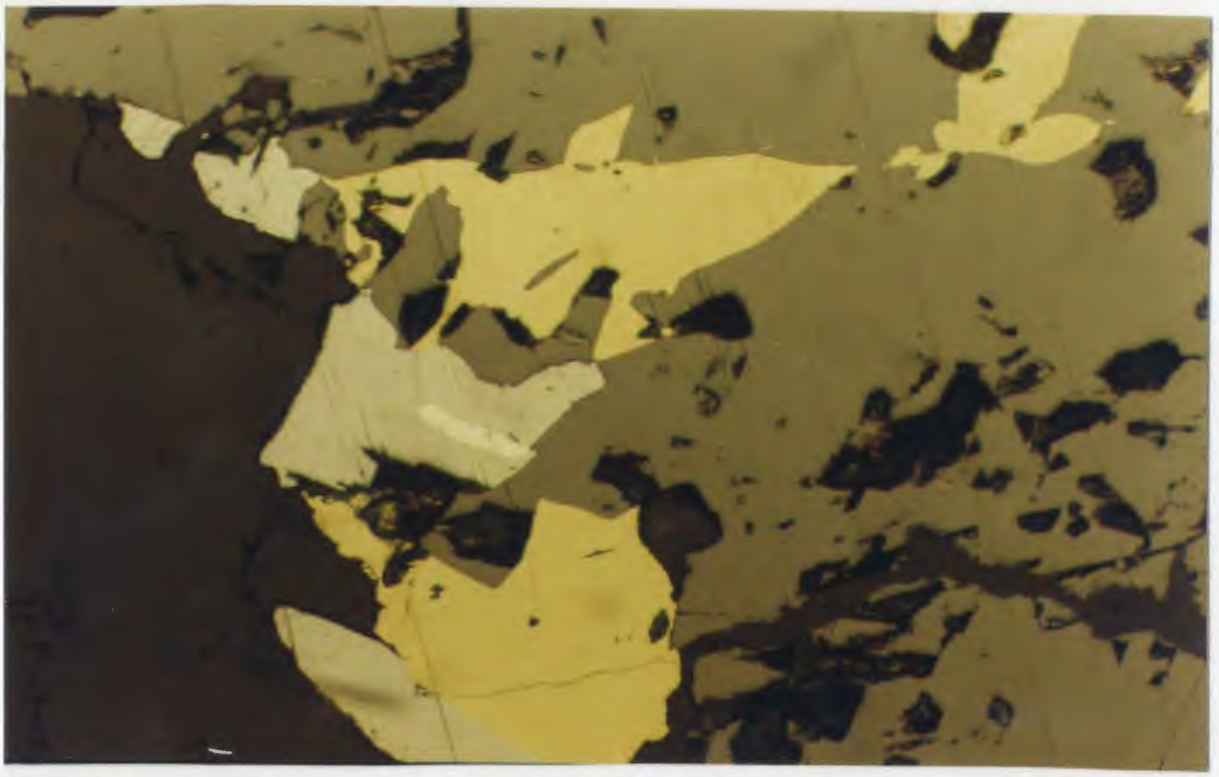

Plate 4.17 Secondary sulphide assemblages; pyrrhotite with inclusions (≤0.2mm) of galena and equant polygonal grains (≤0.5mm) of pyrite. Galena (light grey) inclusions with irregular inclusions (≤0.1mm) of Pb-telluride [21-2721, reflected light, magnification = 100 X].

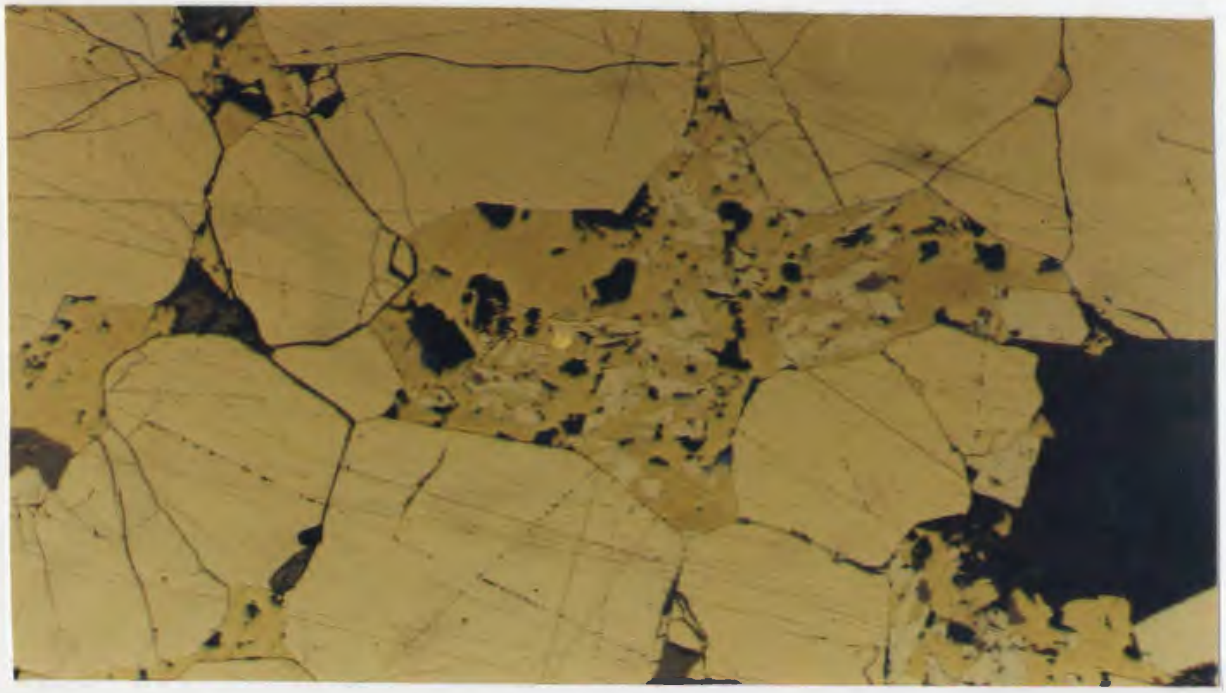

Plate 4.18 Secondary sulphide in interstitial chalcopyrite; inclusions of arsenopyrite (≤0.04mm, small light yellow, angular euhedral prisms) and electrum (≤0.02mm, small, bright yellow grains) [26-1974, reflected light, magnification = 200 X].

4.3.2 Gold

Semi-quantitative probe analyses using SEM revealed the presence of electrum, a gold - silver alloy, in two of ten samples with high assayed gold contents. It occurs in sample 26-1974 as irregular to rounded grains (0.008-0.02mm) near rounded inclusions of sphalerite and euhedral bladed inclusions ($\leq$ 0.04mm) of arsenopyrite in interstitial chalcopyrite ($\leq$0.2mm, Plate 4.18). It occurs in sample 21-2824 as a flattened grain (0.02mm) between two polygonal grains of pyrite along a short grain boundary ($\sim$0.15mm) enclosed by chalcopyrite (Plate 4.19). Gold occurs as telluride in 26-1925, a sample of quartz + muscovite $\pm$ chlorite schist from the footwall of the deposit.

4.3.3 Telluride

SEM backscatter electron imaging of a thin section of auriferous quartz + muscovite $\pm$ chlorite schist (sample 24-1925) revealed numerous irregular polygonal grains ($\leq$0.03mm) of Fe, Ni, Bi and Au-telluride in the interstices of silicate and sulphide assemblages (Weick et al., 1990). The different telluride and sulphide phases were identified using SEM semi-quantitative probe analyses.

Au-telluride in one area of the thin section was observed in a rounded grain ($\sim 11\mu m$) with Fe-telluride adjacent to an irregular inclusion ($\sim 4\mu m$) of chalcopyrite between three larger grains ($\leq$0.7mm) of polygonal quartz (plate 4.20). In another area of the section, Au-telluride (0.003mm) occurs in the corner of an irregular grain ($\sim 35\mu m$) of Ni-telluride between two larger grains ($\leq$0.1mm) of recrystallized pyrite (plate 4.21).

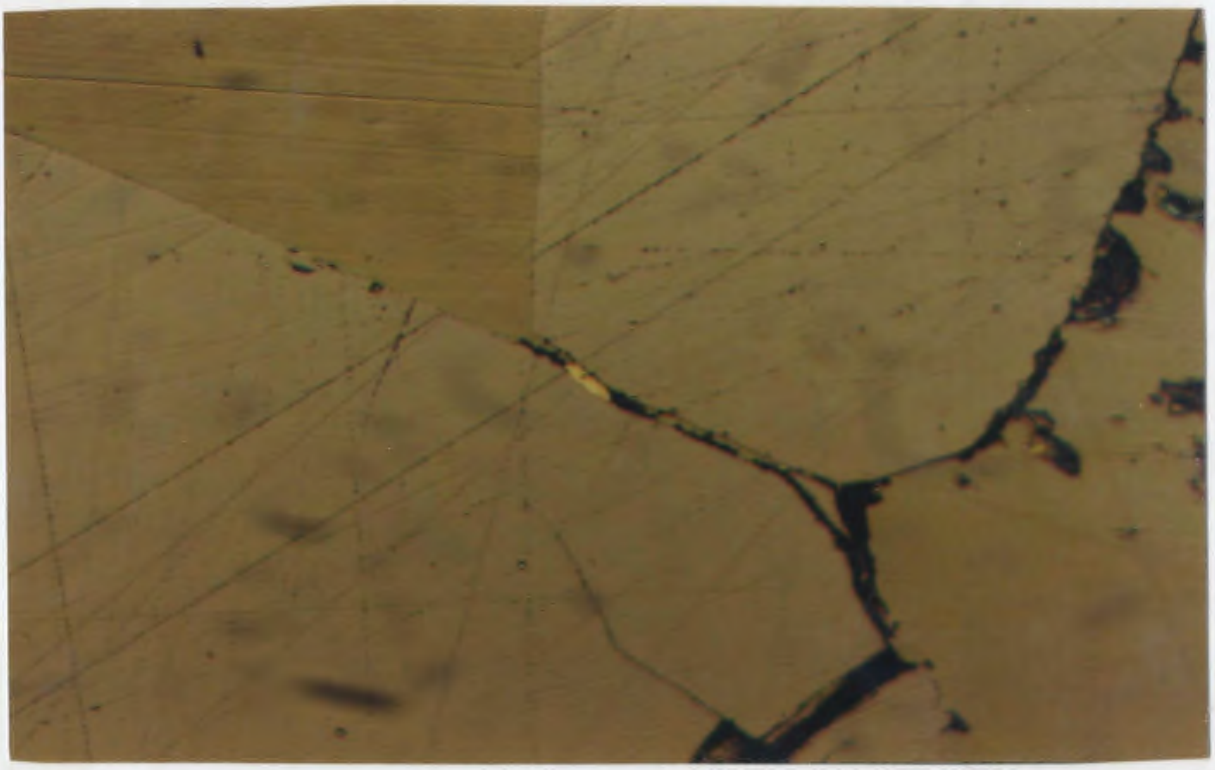

Plate 4.19 Grain (0.02mm) of electrum between two larger grains of recrystallized pyrite [21-2824, reflected light, magnification = 200 X].

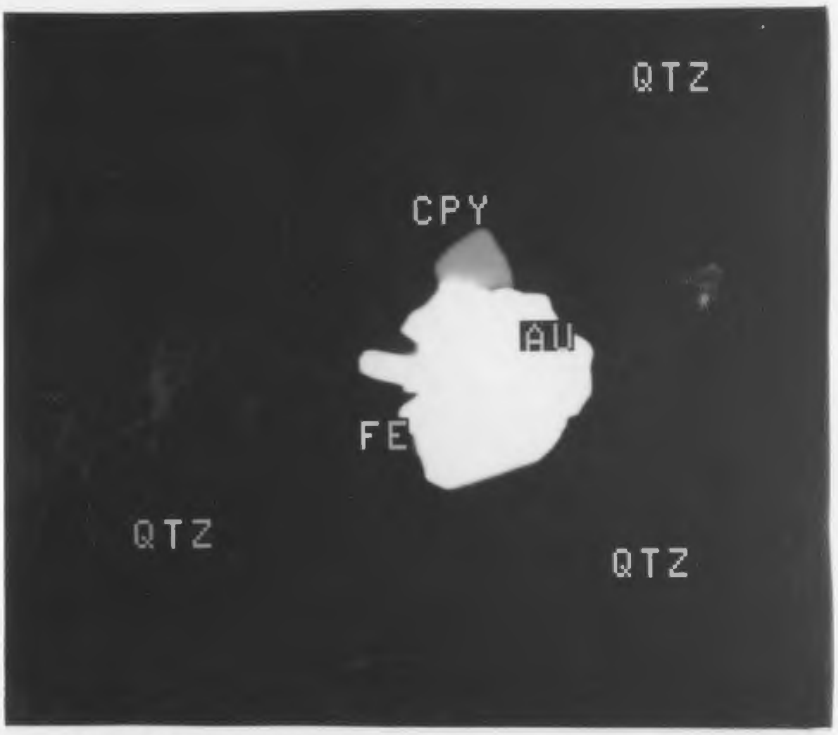

Plate 4.20 SEM photograph; rounded composite grain (~11μm) of chalcopyrite, Fe and Au-telluride (~4μm) between three polygonal grains (≤0.7mm) of quartz in footwall mylonite [24-1925, SEM backscatter electron image, magnification = 1,300 X].

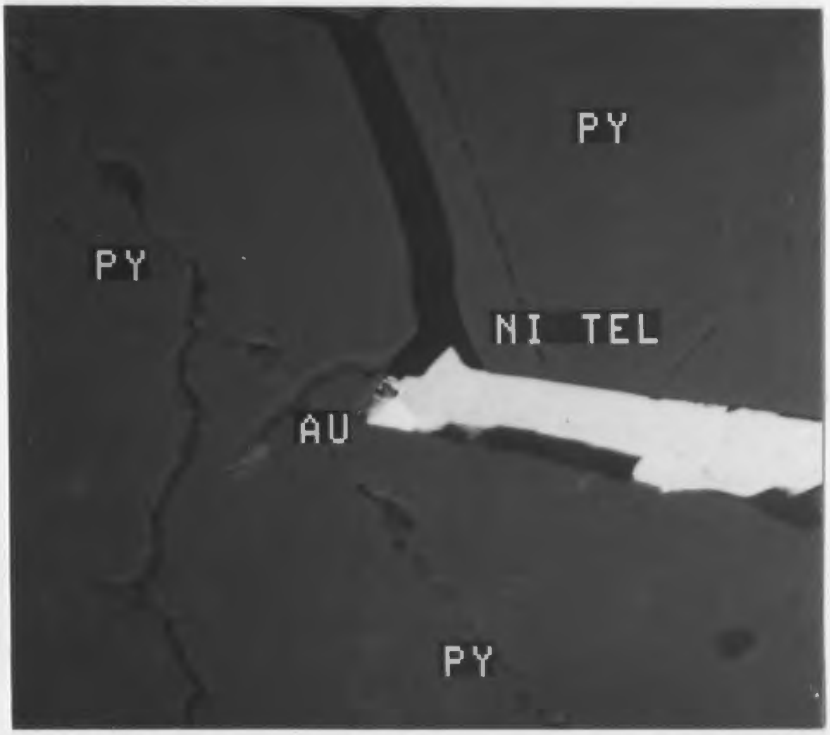

Plate 4.21 SEM photograph of footwall mylonite; Au-telluride as an inclusion (~3μm) in polygonal grain (~35μm) of Ni-telluride between two larger polygonal grains (≤0.1mm) of pyrite [24-1925, SEM backscatter image, magnification = 800 X].

4.4 Biotite

Stage 1 and stage 3 alteration assemblages are overprinted by biotite. In the hangingwall, biotite occurs as well developed porphyroblasts ($\leq$1.5mm) which overprint stage 1 quartz and epidote assemblages ($\leq$0.2mm) in epidotized basalt (Plate 4.22). Subhedral lathes ($\leq$0.3mm) of dark brown biotite also replace light green chlorite in the matrix of agglomeratic rocks.

Biotite occurs as large porphyroblasts ($\leq$2.0mm) in the chloritic fractures of quartz-chlorite breccia in the deposit section of the stratigraphy. It also overprints altered wall-rock assemblages associated with stage 3 quartz-carbonate veins, which occur within stage 2 footwall schists and mylonites. It was absent in massive sulphide samples and was not observed in any of the high strain footwall schists and mylonites.

Plate 4.22 Biotite porphyroblast (≤ 1.5mm) in quartz-chlorite breccia [sample 23-2817, crossed polarized light, magnification = 100 X].

Chapter 5: Major and Trace Element Geochemistry

5.1 Introduction

Major and trace element geochemistry have been used to constrain the chemistry and source of fluids associated with alteration and mineralization. Early studies focused on establishing the identity and distribution of the "pathfinder elements" (Levinson, 1974; Boyle, 1979; Fyon et al., 1983). Other studies have examined the chemistry, volume and mass changes related to fluid-rock reactions in ore-forming hydrothermal systems (Gresens, 1976; Mottl, 1983). The studies suggest that base metal sulphides, gold and other metals are transported by chemically similar fluids and processes in different geologic environments (Barnes, 1969). The different generations of alteration and mineralization in VMS and mesothermal gold deposits are products of multiple fluid "events", indicated by variations in the chemistry of alteration minerals, and the contrasting mineral, fluid and gaseous phases in different generations of fluid inclusions (Roedder, 1969, 1984; Kashida and Kerrich, 1987).

Major and trace element geochemistry was used in this study only to describe alteration trends, not to provided a quantitative account of the petrogenesis of the volcanic rocks in the stratigraphy of the Rambler deposit. Fifteen whole-rock samples of the stage 1 and stage 2 alteration were selected from the hangingwall, deposit and footwall sections of the stratigraphy in addition to the samples previously submitted for commercial assay. Two of the whole-rock samples were split and submitted as blind duplicates. Samples included whole-rock powders from the hangingwall and footwall, and assay pulps from mineralized horizons in the deposit section of the stratigraphy.

5.2 Analytical Methods

Commercial assays were performed by Eastern Analytical Limited at their laboratory in Springdale, Newfoundland. Whole-rock samples were analyzed for a standard suite of major element oxides using the Atomic Absorption facilities in the Department of Earth Science at Memorial University. Splits of the whole-rock powders were sent to Chemex Laboratories Limited of Pasedena, Newfoundland for trace element analyses. Two blind duplicates were submitted to assess analytical precision.

5.2.1 Assays

Gold, silver, copper and zinc assays were performed by Eastern Analytical Laboratories as part of the 1988-1989 drilling exploration program supervised by MPH Exploration Limited. Gold and silver were analyzed by standard fire assay techniques with a gravimetric finish. Copper and zinc were analyzed using aqua-regia dissolution followed by absorption spectroscopy. Details of the techniques are summarized in Appendix 1.

5.2.2 Major Element Analyses

Major element oxides were determined using standard procedures. A 0.1 g aliquot of 100 mesh rock powder was dissolved in a concentrated HF + 50 mL saturated boric acid solution. MgO and CaO analyses required further dilution with a lanthanum oxide and distilled water. Sample absorptions were compared to known standards during absorption spectroscopy (AAS). Loss on ignition (LOI) was determined by weighing a portion of the sample in a crucible before and after ignition at 1000°C. Details of the analyses and related uncertainties are presented in Appendix 1. Major element and trace element data from these analyses are reported in Table A3.1 (Appendix 3).

5.2.3 Trace Element Analyses

Te, Ag, As, Bi, Cu, Cd, Hg, Mo, Sb, and Se concentrations of the whole-rock samples were also determined by AAS. Details of the analyses are presented in Appendix 1. The concentration of these elements in the hangingwall, deposit and footwall sections of the stratigraphy are reported in Table A3.1 (Appendix 3).

5.3 Results and Interpretations

Data from whole-rock analyses include major element oxide totals from 91 to 98% (Appendix 3, Table A3.1). These variations were particularly high among samples from the deposit and footwall sections of the stratigraphy, where they are attributed to intensely altered nature, and high concentrations of sulphides in individual samples. As a result, the whole-rock data can only be used to demonstrate trends in a qualitative fashion, in an attempt to illustrate some of the previously described trends among the different alteration stages.

Major and trace element data from the analyses of whole-rock samples from the Rambler deposit were compared with similar geochemical data from previous studies of similarly altered volcanic rocks in the Pacquet Harbour Group and in similar geologic environments (Appendix 3). Major element data from the analyses of altered basalts (Table A3.2) from studies by Gale (1971), Sun and Nesbitt (1978), and Hibbard (1983) are compiled in Table A3.2. Major and trace element analyses of Pacquet Harbour samples collected to the south of the Consolidated Rambler Mines properties are presented in Table A3.3. Mineral analyses from Deer et al., (1967), Saunders (1985), Swinden (1988), and Swinden et al. (1988) are compiled in Table A3.4. Trace element data compiled by Hannington (1989) from seafloor sulphide deposits is presented in Table A3.5.

5.3.1 Assay Data

Assays were plotted in longitudinal section to establish the base and precious metal concentrations associated with intervals of massive and disseminated sulphide mineralization in the stratigraphy of the deposit. A representative section showing the distribution of lithologies, alteration and sulphide assemblages, and reported assay values is presented in Figure 5.1 (back pocket).

Cherts and massive sulphide horizons in the deposit section of the stratigraphy coincide with reported assays of $\geq$0.075 ounces/ton Au, 0.500 wt% Cu, 0.500 wt% Zn and 0.075 ounces/ton Ag (3, 5000, 5000 and 3 ppm, respectively). Concentrations of these metals in intervals of footwall schist and mylonite which contain disseminated sulphide are generally lower at $\leq$0.075 oz/ton Au, 0.500 wt% Cu, 0.500 wt% Zn and 0.075 ounces/ton Ag (3, 5000, 5000 and 3 ppm) with enrichments of up to 0.075 ounces/ton Au, 0.050 wt% Cu, 0.050 wt% Zn and 0.250 ounces/ton Ag (3, 500, 500 and 1 ppm) along the large quartz vein near the base of hole MZ89-28 (Figure 5.1). Au, Cu, Zn and Ag concentrations in less altered volcanic and sedimentary rocks of the hanging wall are generally $\leq$ 0.010 ounces/ton Au, 0.05 wt% Cu, 0.10 wt% Zn and 0.01 ounces/ton Ag (0.3, 500, 100 and 0.3 ppm, respectively).

5.3.2 Major Element Chemistry

The major element chemistry of less altered volcanic rocks in the hangingwall of the Rambler deposit is consistent with the presence of both tholeiitic and boninitic basalts in the stratigraphy of the Rambler deposit (Gale, 1971; Hibbard, 1983; Swinden et al., 1988). In Figure 5.2.a low Al_2O_3/TiO_2 ratios of the high Ti basalts cluster in the tholeiitic (MORB) field. Low Ti (<0.6%), high Mg lavas with high Al_2O_3/TiO_2 ratios plot in the boninitic lava field (modified after Sun and Nesbitt, 1978).

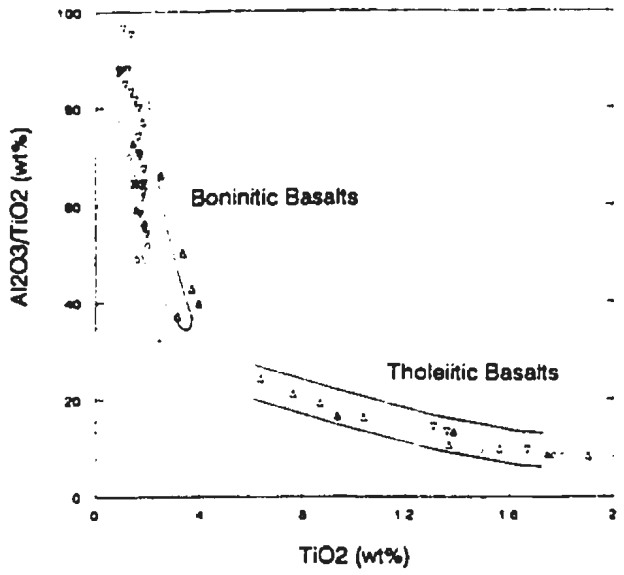

Figure 5.2.a) A comparison of basalt geochemistry from the hangingwall of the Rambler deposit with the geochemistry of boninitic and tholeiitic basalts from other studies. Data from Sun and Nesbitt (1978) ○, Gale (1971) △, Hibbard (1983) ◇, and Swinden (unpub. data, 1992) ▽, Rambler hangingwall volcanic rocks ▲ (this study).

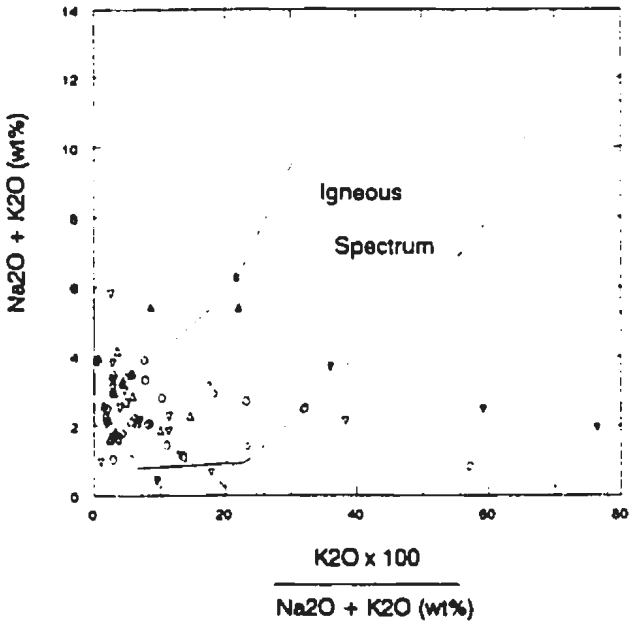

Figure 5.2.b) Alteration trends in the stratigraphy of the Rambler deposit compared with the chemistry of unaltered (igneous spectrum) and altered volcanic rocks (after Hughes 1972). Data from Sun and Nesbitt (1978) ○, Gale (1971) △, Hibbard (1983) ◇ and Swinden (unpub. data, 1992) ▽. Rambler hangingwall ▲, footwall ▼ (this study).

An increase in the modal percentage of muscovite during stage 1 and stage 2 alteration in Rambler stratigraphy is consistent with K enrichments of up to 2.88 wt% in highly altered, sericitized rocks in the deposit and footwall sections of the stratigraphy. These K enrichments are accompanied by Na and Ca depletions, with individual values as low as 0.29 and 0.06 wt%, respectively. K, Na and Ca concentrations of 0.05-1.36, 2.14-4.92, and 5.02-9.70 wt% from less altered volcanic rocks in the hangingwall of the deposit are more consistent with the 0.01-0.82, 0.55-5.65 and 6.61-12.52 wt% range of values reported from the analyses of unaltered basalts in the Pacquet Harbour Group to the south of the Consolidated Rambler Mines properties (unpub. data, H.S. Swinden, 1992).

The mobility of K, Na and Ca is common among unaltered and altered volcanic rock compositions reported in geochemical studies by Swinden (1988), Saunders (1985), and MacLean and Hoy (1991). In Figure 5.3 unaltered and spilitic rock compositions (Gale, 1971; Sun and Nesbitt, 1978; Hibbard, 1983; Swinden, 1988) plot within, or to the left of the "igneous spectrum" defined by the composition of unaltered tholeiitic to calc-alkaline volcanic rocks (after Hughes, 1972).

The composition of less altered volcanic rocks in the hangingwall of the deposit is consistent with those of unaltered and spilitic volcanic rock compositions reported in other studies (Sun and Nesbitt, 1978; Gale, 1971; Hibbard, 1983 and unpub. data, H.S. Swinden, 1992). However, a linear trend among the Rambler hangingwall and footwall samples above and to the right of the igneous spectrum is consistent with K enrichments and Na depletions during stage 1 and stage 2 alteration in the stratigraphy of the deposit (Figure 5.2.b).

The mobility of Na and Ca during hydrothermal alteration of volcanic rocks has been assessed by comparing Na_2O and CaO contents of altered and unaltered volcanic rocks from the Wild Bight Group and the Pipestone Pond areas in Central Newfoundland by Swinden (1988) and in similar volcanic rocks of the Cape St. John Group near the Tilt

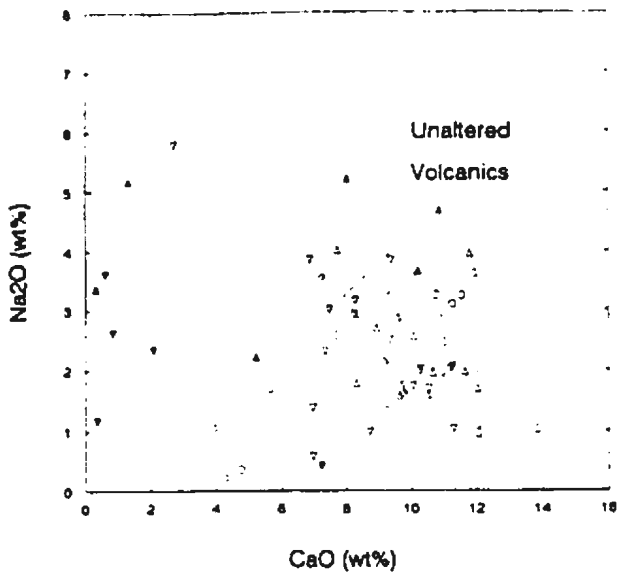

Figure 5.3.a) Alteration chemistry in the stratigraphy of the Rambler deposit compared with the compositions of altered and unaltered (diagonal field) volcanic rocks (after Miyashiro, 1975). Data from Sun and Nesbitt (1978) ○, Gale (1971) △, Hibbard (1983) ◇, Swinden (unpub. data, 1992) ▽. Rambler hangingwall ▲, footwall ▼ (this study). The distribution of the Rambler data is consistent with Na and Ca depletions during stage 1 and stage 2 alteration.

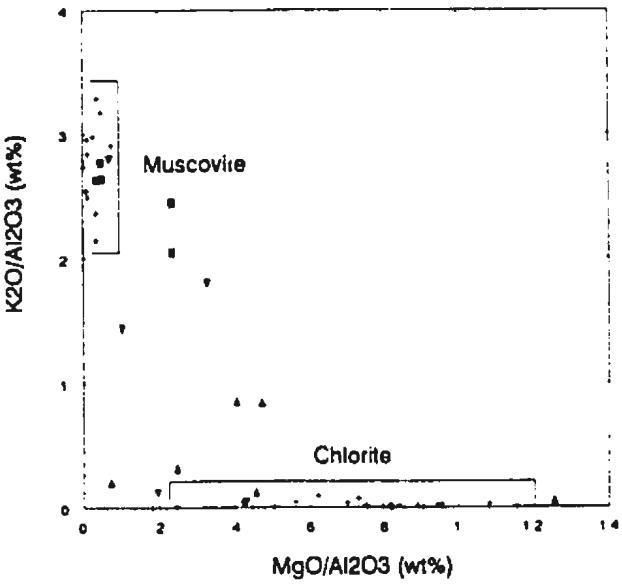

Figure 5.3.b) Molar plot comparison of whole-rock and chlorite and muscovite K_2O/Al_2O_3 (wt%) vs. MgO/Al_2O_3 ratios. Mineral data from Deer et al. (1966), Henley et al. (1981), Swinden (1988), Saunders (1985), MacLean and Hoy (1991) +. Rambler hanging wall ▲, deposit ■, footwall ▼ (this study). The distribution of Rambler analyses between the chlorite and muscovite fields suggests rock chemistries are influenced by the presence of these minerals.

Cove VMS deposit by Saunders (1985). In Figure 5.3.a only a few (~20%) of the reported analyses from studies by Gale (1971), Hibbard (1983) and Swinden (unpub. data, 1992) plot within, or close to a diagonal field which defined the Na and Ca contents of unaltered volcanic rocks to within approximately 1 to 4 and 7 to 12 wt%, respectively (Miyashiro, 1975). Most of the Rambler data (filled symbols) with the exception of two of the hangingwall samples, plot along the left side of the diagram and towards its origin consistent with the depletions in Na and Ca during alteration (Gale, 1971; Hibbard, 1983; Swinden, 1988).

A molar plot of K and Mg in Figure 5.3.b compares whole-rock analyses of volcanic rocks from the Rambler deposit to the major element oxide composition of common alteration minerals observed in thin section. The K and Mg contents are normalized to Al_2O_3 to reduce the affects of volume changes related to alteration (Gresens, 1967, 1974). In Figure 5.5, K/Al and Mg/Al ratios of altered volcanic rocks in Rambler deposit fall between end-member muscovite and chlorite fields suggesting whole-rock compositions are influenced by the presence of chlorite and muscovite.

5.3.3 Trace Element Chemistry

Scatter plots of trace element concentrations from whole-rock samples collected from the Rambler deposit suggest high concentrations of Te, As, Bi, Cd, and Hg coincide with the high sulphide concentrations in the massive sulphide horizons in the deposit section of the stratigraphy. Concentrations in massive sulphide samples collected from the deposit are 9.0 to 34.5ppm for Te, 170 to 270ppm for As, 0.1 to 2.7ppm for Bi, 8.3 to 54.0ppm for Cd, and 0.13 to 0.64ppm for Hg. Lower concentrations 1.4 to 7.6ppm, 12 to 69ppm, 0.1 to 1.2ppm, 0.1 to 2.3ppm, and 0.01 to 0.02ppm, respectively, are associated with the disseminated mineralization in footwall schists and mylonites. The concentrations of Te, As, Bi, and Cd are close to, or below reported detection limits; $\leq$ 0.05ppm, $\leq$ 2ppm, $<$ 0.1ppm, and $<$ 0.1ppm, respectively in the hangingwall, with the exception of Hg which varies from 0.01 to 0.04 ppm.

Figure 5.4 Comparison of the Te, Ag, As, Bi, Cd, Hg, Mo, Sb and Se contents of massive and disseminated sulphide in the Rambler deposit with the concentration ranges of the same elements in seafloor VMS deposits. Data from black smoker vents (b.s.), Axial Seamount (A.S.), Explorer Ridge (E.R.), TAG Hydrothermal Field (TAG), Snakepit Vent Field (S.V.F.) (Hannington, 1989, 1990). Rambler hangingwall ▲, deposit ■, footwall ▼ (this study).

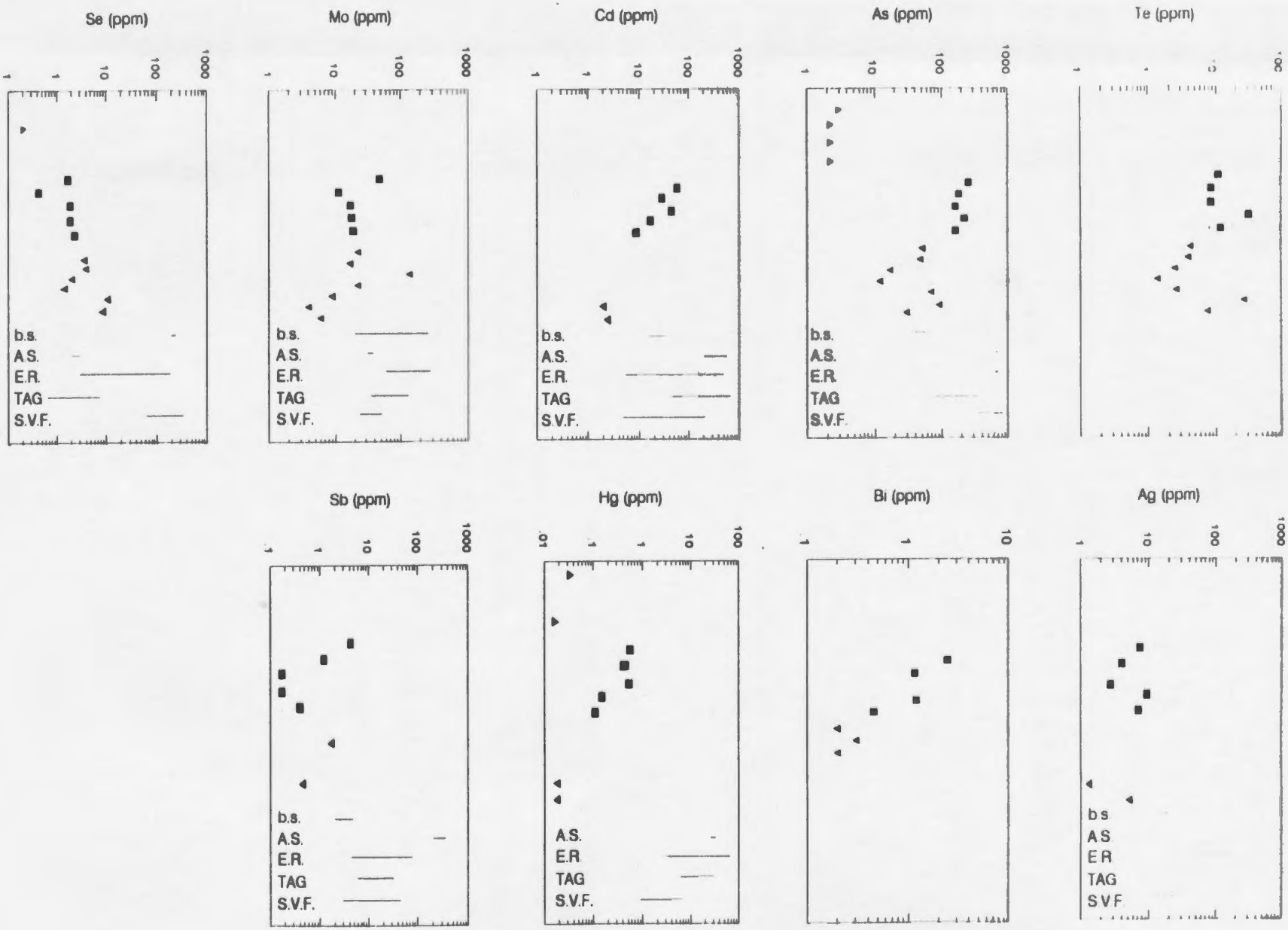
Se (ppm)
Mo (ppm)
Cd (ppm)
As (ppm)
Te (ppm)
Sb (ppm)
Hg (ppm)
Bi (ppm)
Ag (ppm)
b.s.
A.S.
E.R.
TAG
S.V.F.
1
10
100
1000

In contrast to Te, As, Bi, Cd, and Hg, concentrations of Mo and Se are similar in massive and disseminated sulphide in the deposit and footwall, respectively. Concentrations of Ag and Sb in the footwall are similar to those in the deposit in only two of the schist and mylonite samples. Other Ag and Sb analyses from the footwall were below detection limits. Concentrations of these elements in both types of mineralization vary from 1.4 to 9.4ppm for Mo, 4 to 135ppm for Se, 0.4 to 4.0ppm for Ag, and 0.4 to 7.0ppm for Sb (Figure 5.6). The same elements are below reported detection limits; < 1ppm, < 0.2 ppm and < 0.2 ppm, respectively, in the hangingwall.

Te, Ag, As, Bi, Cd, Hg, Mo, Sb, and Se contents of sulphide in the Rambler deposit are generally within two to three orders of magnitude of the concentration of these elements in sulphides associated with seafloor hydrothermal settings (Figure 5.6; Hannington, 1989; Hannington et al., 1991). As, Cd, Mo and Se concentrations of 12 to 270ppm, ≤ 54ppm, 4 to 135ppm, and 0.4 to 0.7ppm, respectively, in the Rambler deposit are similar to the analyses of sulphides associated with seafloor hydrothermal (black smoker) vents, and seafloor VMS deposits (Figure 5.6; Hannington, 1989, Hannington et al., 1991). In contrast Ag, Hg, and Sb concentrations of ≤ 9.4ppm, 0.01 to 6.4ppm, and ≤ 4.0ppm, respectively, are depleted in relation to the seafloor sulphide concentrations (Hannington, 1989, 1990). Concentrations of Te and Bi in seafloor sulphides are not available in the data compiled by Hannington (1989, Hannington et al., 1991). Petrographic relationships and textural evidence suggest Te was remobilized and reconcentrated during the syn-kinematic alteration and the metamorphic recrystallization of the Rambler deposit.

Chapter 6: Stable Isotope Geochemistry

6.1 Introduction

Stable isotope geochemistry has been used extensively to determine formation temperatures and W/R ratios, and to characterize the source of fluids related to hydrothermal processes (Taylor, 1974). Oxygen and hydrogen isotopes are particularly useful for distinguishing among fluids and tracing the influence of crustal fluid reservoirs deposits during the formation of hydrothermal ore deposits (Taylor, 1974; Valley et al., 1987; Kyser, 1987).

To determine the $\delta^{18}O$, δD and $\delta^{34}S$ values of silicate and sulphide assemblages in the Rambler deposit, thirty-six core samples were crushed, and separated into pure mineral separates for isotopic analyses. The mineral separates were prepared using a combination of heavy liquid and magnetic separation techniques. Sample purities were determined using X-ray diffraction (XRD). Silicate and sulphide mineral separates were converted into CO_2, H_2, and SO_2 using vacuum line extraction facilities at Memorial University.

Techniques and sample descriptions are presented in Appendix 1 and 4. $\delta^{18}O$, δD and $\delta^{34}S$ data are presented in Table 6.1 and 6.2. Oxygen isotope temperatures from quartz-mineral pairs, and the $\delta^{18}O$ and δD values of fluids in equilibrium with silicates at the indicated alteration temperatures are presented in Tables 6.3 and 6.4. Background information on fractionation theory, notation conventions and calculations is summarized in Appendix 2.

6.2 Analytical Methods

O_2 was extracted from silicates by reaction with BrF_5 at 600°C for 6 to 8 hours. The oxygen was converted to CO_2 by combustion with a carbon rod at 800°C (Clayton and

Mayeda, 1963). Structural H_2O was liberated from chlorite, muscovite and biotite through inductive heating to ~ 1300°C using a Leppel radio frequency (RF) generator (Godfrey, 1962) and subsequently converted to H_2 gas by reaction with metallic Zn at 460° C for approximately 30 minutes (Tanweer et al., 1988). SO_2 gas was evolved through the combustion of sulphides and CuO in a vacuum line at 1000°C (Rafter, 1957).

Oxygen and deuterium analyses were performed on a Finnigan Mat 252 gas source mass spectrometer. Deuterium analyses were corrected for the formation of H^{3+} in the ion source and machine (Craig, 1957, 1961). Sulphur analyses were performed on a VG 903E mass spectrometer. Internal standards AGS, MUN_{illite}, and $NBS\text{-}123_{sph}$ were analyzed periodically to insure the accuracy of $\delta^{18}O$, δD and $\delta^{34}S$ analyses. Analyses of AGS yeilded consistent values of 9.6 $\pm$ 2σ ‰. MUN_{illite}, an internal standard, provided values of -90 ‰. NBS-123 was analysed at 16.9 ‰. Duplicate samples were continually submitted to confirm analytical precision. δ values of mineral separates contaminated slightly by the presence of other minerals were corrected using standard mass balance calculations (Ohmoto and Rye, 1974; Taylor, 1974).

6.3 Data Summary

$\delta^{18}O$, δD and $\delta^{34}S$ analyses are reported using standard δ notation in relation to appropriate SMOW and CDT reference standards (Craig, 1957, 1961). Uncertainties for oxygen, hydrogen and sulphur analyses are estimated at $\pm$ 0.2 ‰, $\pm$ 2 ‰, and $\pm$ 0.2 ‰, respectively. $\delta^{18}O$, δD and $\delta^{34}S$ data are presented in Tables 6.1 and 6.2, respectively.

6.3.1 $\delta^{18}O$ and δD Data: Alteration

$\delta^{18}O$ values of quartz were consistent throughout the stratigraphy of the deposit. The $\delta^{18}O$ values of quartz separated from stage 1 assemblages in the hangingwall and deposit

Table 6.1 Oxygen and hydrogen isotope analyses of stage 1, stage 2 and stage 3 alteration assemblages in the stratigraphy of the Rambler VMS deposit. Rock types include; gbbr = gabbro, cht = chert, vms = massive sulphide, myl = schist-mylonite, vn = quartz carbonate veins. Analysed minerals include; qtz = quartz, alb = albite, amp = amphibole, chl = chlorite, se = sericite and bio = biotite. Isotopic compositions of mineral separates contaminated by other minerals were recalculated using a standard mass balance corrections (Taylor 1974). The recalculated value is reported in brackets below the original values. All values are reported in standard delta notation (per mill) relative to SMOW

			qtz	alb	amp		chl		se		bio	
		rock	O	O	O	D	O	D	O	D	O	D
stage 1 alteration												
hangingwall	28 2713	gbbr	11.8	8.0	5.8	-63						
	21 2749	gbbr	11.2									
deposit	21 2719	cht	10.9									
	21 2751,52	vms	11.1									
	21 2751	vms							8.3	-63		
	21 2752	vms					7.5		8.2	-55		
	21 2754	vms	11.5				5.2	-73	7.9			
	21 2760	vms	10.6				7.4	-70				
	21 2720	vms	10.6				5.2	-63				
stage 2 alteration												
footwall	24 1911	myl	10.4									
	20 2762	myl	10.4				4.3	-60	6.4	-72		
	26 1974	myl	10.1									
	24 1925	myl	11.0						7.1	-70		
	28 2728	myl	10.7				1.7	-78				
	24 1930	myl	10.1				4.0	-57				
stage 3 alteration												
	23 2520	vn	11.9				6.3	-62				
							(3.9)					
	23 2518	vn	11.6				3.5	-63				
	24 1963	vn	11.9				2.9	-61				
	23 2514	vn	12.0									
	21 2835	vn	10.7								5.0	-84
	24 1908	vn	10.9	8.0								
	23 2512	vn	11.1									
	28 2542	vn	10.4									
	28 2730	vn	10.1									
	24 1934	vn	8.7								3.2	-76

varied from +10.6 to +11.8 ‰. The $\delta^{18}O$ value of stage 1 quartz in chert was +10.9 ‰. Stage 1 quartz separated from massive sulphide samples yielded $\delta^{18}O$ values of +10.6 to +11.6 ‰ (Table 6.1). The $\delta^{18}O$ values of stage 2 quartz from the footwall were similar to those of the stage 1 quartz, with individual values in schist and mylonite samples from +10.1 to +11.0 ‰. $\delta^{18}O$ values of stage 3 quartz were more variable than stage 1 and stage 2 quartz with values of +10.1 to +12.0 ‰. A $\delta^{18}O$ quartz value of +8.7 ‰ was rejected.

The $\delta^{18}O$ values of albite separated from hangingwall and footwall samples were the same. Groundmass albite from the gabbro sill in the hangingwall and from a stage 3 vein in the footwall yielded $\delta^{18}O$ values of +8.0 ‰.

$\delta^{18}O$ values of stage 1 and stage 2 chlorites were variable in the deposit and footwall sections of the stratigraphy. Stage 1 chlorite separated from some of the sulphide samples in the deposit had $\delta^{18}O$ values of +7.4 and +7.5‰. $\delta^{18}O$ values of stage 1 chlorites separated from other massive sulphide samples in the deposit were lower at approximately +5.2‰. The δD values of stage 1 chlorite in samples of massive sulphide mineralization varied from -63 to -73 ‰.

The $\delta^{18}O$ values of all stage 2 chlorites were similar to those of the low ^{18}O stage 1 chlorites. The $\delta^{18}O$ values of stage 2 chlorites in schist and mylonite varied from +4.0 to 4.7, with δD values of -57 to -78 ‰. Stage 3 chlorites had $\delta^{18}O$ values of 6.3, 3.5, and 2.9 ‰ with δD values of -63, -63 and -61 ‰.

Muscovite could only be extracted in quantities sufficient for analysis from three samples of massive sulphide mineralization. The $\delta^{18}O$ values of these samples varied from 7.9 to 8.3 ‰. The δD values of the muscovite in two of the massive sulphide samples varied from -55 to -63 ‰. Insufficient material prevent the third sample from being analyzed for D.

Table 6.2 Sulphur isotope analyses of massive and disseminated sulphide from the deposit and footwall sections of the Rambler VMS deposit. Individual analyses values are reported using standard delta values (per mil CDT) with their average analytical uncertainties.

	sample	mineral	analytical runs	sample depth in feet	S(CDT)
massive sulphide mineralization					
deposit	21 2754	pyrite	2	735.1 – 735.6	5.8 –/+ 0.05
	21 2752		3	733.2 – 733.6	5.8 –/+ 0.06
	28 2720		3	972.3 – 972.5	7.5 –/+ 0.03
	21 2754	red sphalerite	1	735.1 – 735.6	6.1 –/+ 0.10
	21 2752		2	733.2 – 733.6	5.6 –/+ 0.09
	21 2760	chalcopyrite	2	774.1 – 774.4	6.6 –/+ 0.80
disseminated sulphide mineralization					
footwall	20 2761	pyrite	1	225.3 – 225.4	7.6 –/+ 0.01
	24 1930		1	1318.0 – 1318.3	6.5 –/+ 0.01
	24 1925		2	1018.4 1020.0	6.7 –/+ 0.07
	24 1911		3	970.2 970.5	5.5 –/+ 0.06
	20 2761	yellow sphalerite	1	225.3 – 225.4	6.8 –/+ 0.09

Two samples of stage 2 muscovite were collected from schists and mylonites in the footwall. The $\delta^{18}O$ values of these muscovites were similar to those obtained in stage 1 alteration assemblages. The $\delta^{18}O$ values were +6.4 and 7.1 ‰ with δD values -72 and -70 ‰, respectively.

Amphibole was separated from the gabbro sill in the hangingwall section of the stratigraphy. Analyses provided a $\delta^{18}O$ value +5.8 ‰, and a δD value of -63 ‰.

Biotite was recovered from two samples of altered volcanic rock in the footwall. Analyses of the biotite separates, yielded $\delta^{18}O$ values of +5.0 and +3.2 ‰, and δD values of -84 and -76 ‰.

6.3.2 $\delta^{34}S$ Data: Mineralization

Pyrite, the dark red variety of sphalerite and chalcopyrite were obtained from massive sulphide samples. The $\delta^{34}S$ values of the pyrite vary from +5.8 to 7.5 ‰. $\delta^{34}S$ values of the dark red sphalerite were +6.1 and 5.6 ‰. A single sample of chalcopyrite yielded a $\delta^{34}S$ value of +6.6 ‰.

Pyrite and a light yellow variety of sphalerite were separated from samples of disseminated sulphide mineralization from the footwall. $\delta^{34}S$ values of pyrite in the footwall vary from +5.5 to 7.6 ‰. A single sample of light yellow sphalerite yielded a $\delta^{34}S$ value of 6.8 ‰.

6.4 Calculations

Isotopic analyses were used to calculate a range of alteration and metamorphic temperatures using the $\Delta^{18}O$ quartz-mineral, and $\Delta^{34}S$ sulphide pair fractionation curves (Kyser, 1987; Valley et al., 1987). $\Delta^{18}O$ quartz-albite temperatures were estimated from combined equilibrium exchange data (Matthews et al., 1983) and quartz-fluid data

(Matsuhisa et al., 1979). Quartz-chlorite and quartz-muscovite temperatures were determined by combining $\Delta^{18}O_{chl,serp\text{-}H2O}$ curve of Wenner and Taylor (1971) and the $\Delta^{18}O_{illite\text{-}H2O}$ curve of Yeh and Savin (1976) with the $\Delta^{18}O_{qtz\text{-}H2O}$ curve of Clayton et al. (1972). Quartz-biotite temperatures were determined directly from the $\Delta^{18}O_{qtz\text{-}bio}$ curve of Bottinga and Javoy (1975).

$\delta^{18}O$ values of the fluids in equilibrium with stage 1, 2 and 3 silicate assemblages were calculated from the appropriate mineral-H_2O fractionation curves (Table 6.5; Valley et al., 1987; Kyser, 1987). The δD values of fluids in equilibrium with chlorite and biotite were determined in the same manner using the $\delta D_{chl/serp\text{-}H2O}$ curve of Graham et al. (1984) and the $\delta D_{bio\text{-}H2O}$ curve of Suzuoki and Epstein (1976). The δD values of the fluids in equilibrium with muscovite were estimated using the $\delta D_{smectite\text{-}H2O}$ curve of Yeh (1980).

$\delta^{18}O$ and δD fluid values were calculated as a range using the maximum and minimum formation temperatures of each mineral in the different alteration stages approximated to the nearest 10°C. $\delta^{18}O$ fluid values in equilibrium with quartz were calculated at the maximum and minimum quartz-mineral temperatures from each alteration stage using the fractionation curve of Clayton et al. (1972). The $\delta^{18}O$ fluid values in equilibrium with albite were calculated at maximum and minimum quartz-albite temperatures using the curve of Matsuhia et al. (1979). The $\delta^{18}O$ and δD compositions of fluids in equilibrium with biotite were calculated using the fractionation curves of Bottinga and Javoy (1973, 1975) and Suzuoki and Epstein (1970), respectively. The $\delta^{18}O$ and δD fluid values in equilibrium with the amphibole from the gabbro sill were calculated at temperatures consistent with the occurrence of the mineral in seafloor / greenschist metamorphic assemblages using combined fractionation curves of Clayton et al. (1972) and Bottinga and Javoy (1973, 1975) for oxygen, and the curve of Suzuoki and Epstein (1976) for D. Fluid data are discussed in Chapter 7.

6.4.1 Thermometry

Local alteration temperatures associated with specific quartz-mineral pairs in the different alteration assemblages of the Rambler deposit vary from 176 to 559°C. The single quartz-albite pair separated from stage 1 groundmass assemblages in the gabbro sill in the hangingwall provides an alteration temperature of 230°C. A quartz-albite pair in a quartz vein in the footwall yields a temperature of 297°C.

$\Delta^{18}O$ analyses of stage 1 quartz-chlorite pairs in the deposit suggest a range of alteration temperatures. Quartz-chlorite pairs with high $\delta^{18}O$ chlorite values from massive sulphide samples in the deposit yield high alteration temperatures of 436 and 483°C. Quartz-chlorite pairs with low $\delta^{18}O$ chlorite values (+5.2) provide lower alteration temperatures of 260 and 264°C.

Temperatures from the low temperature quartz-chlorite pairs in the deposit, quartz-chlorite pairs in stage 2 footwall schist / mylonites, and stage 3 veins are consistent. Quartz-chlorite pairs in footwall schist and mylonite samples yield concordant alteration temperatures of 269 to 277°C. Temperatures from quartz-chlorite pairs in stage 3 veins vary from 176 to 203°C.

Quartz-muscovite pairs from stage 1 and stage 2 alteration assemblages in the deposit and footwall provide equilibration temperatures which vary from 222 to 309°C. Stage 1 quartz-muscovite pairs provide temperatures of 243 to 309°C. Stage 2 quartz-muscovite pairs provided temperatures of 209 to 222°C.

Quartz-biotite temperatures were high in comparison to other quartz-mineral determinations. Quartz-biotite pairs from altered volcanic rocks in the footwall yield temperatures of 529 and 549°C.

Table 6.3 Oxygen isotope thermometry of quartz–mineral pairs separated from stage 1, stage 2 and stage 3 alteration assemblages in the Rambler VMS deposit. Fractionation equations are as follows: (q–a) Matsuhisa et al. (1979) and Matthews et al. (1983), (q–c) Clayton et al. (1972) and Wenner and Taylor (1971), (q–m) Clayton et al. (1972) and Eslinger et al. (1979) and (q–b) Bottinga and Javoy (1975). Fractionation equations are in Kyser (1987).

		rock	q–a	q–c	q–m	q–b	T°C	T°C
stage 1 alteration								
hangingwall	28 2713	gbbr	3.8				230 (q–a)	
	21 2749	gbbr						
deposit	21 2719	cht						
	21 2751.52	vms						
	21 2751	vms			2.8			309 (q–m)
	21 2752	vms		3.6	2.9		438 (q–c)	299 (q–m)
	21 2754	vms		6.3	3.6		264 (q–c)	243 (q–m)
	21 2760	vms		3.2			483 (q–c)	
	21 2720	vms		6.4			260 (q–c)	
stage 2 alteration								
footwall	24 1911	myl						
	20 2762	myl		6.2	4.1		269 (q–c)	209 (q–m)
	26 1974	myl						
	24 1925	myl			3.9			222 (q–m)
	28 2728	myl		6.0			277 (q–c)	
	24 1930	myl		6.1			273 (q–c)	
stage 3 alteration								
veins	23 2520	va		5.6			203 (q–c)	
	23 2518	va		8.1			200 (q–c)	
	24 1963	va		9.0			176 (q–c)	
	23 2514	va						
	21 2835	va				5.7	538 (q–b)	
	24 1908	va	2.9				297 (q–a)	
	23 2512	va						
	28 2542	va						
	28 2730	va						
	24 1934	va				5.5	559 (q–b)	

6.4.2 $\delta^{18}O$ and δD Fluid Compositions

Calculated $\delta^{18}O$ and δD values of fluids in equilibrium with the low temperature stage 1 chlorite at 260 to 270°C in the deposit section of the stratigraphy vary from +4.4 to +4.6 ‰, and from -26 to -37 ‰, respectively. The isotopic composition of fluids in equilibrium with high temperature stage 1 chlorites at 430 to 480°C are higher at +9.0 to +9.4 ‰, and have similar δD values of -39 ‰. $\delta^{18}O$ values of stage 2 chlorites at 270 to 280°C in the footwall vary from +3,4 to +4.3 ‰ with δD values of -20 to -42 ‰. Fluids in equilibrium with stage 3 vein chlorites at 180 to 200°C have $\delta^{18}O$ values of 0 to +4.1 ‰ and δD values of -19 to -28 ‰.

The $\delta^{18}O$ values of fluids in equilibrium with muscovite are consistent with those associated with chlorite, but calculated δD muscovite fluid values are lower by about -10 to -20 ‰ over a similar range of temperatures. The $\delta^{18}O$ values of fluids in equilibrium with stage 1 muscovites at temperatures of 240° to 310°C vary from +3.5 to +6.0 ‰, with δD values of -42 to -54 ‰. $\delta^{18}O$ and δD values of fluids in equilibrium with stage 2 muscovites at temperatures of 210 to 220°C are similar, but slightly lower at +0.8 to +1.9 ‰ and -55 to -57 ‰, respectively.

Fluids in equilibrium with the amphibole and biotite are ^{18}O-rich in comparison to the fluids which equilibrated with low temperature silicate assemblages. $\delta^{18}O$ values of fluids in equilibrium with amphibole varied from +8.2 to +8.6 ‰ with δD values of -74 to -78 ‰ at estimated temperatures of 300 to 550°C. The $\delta^{18}O$ and δD values of fluids in equilibrium with biotite vary from +5.7 to +7.5 ‰, and from -41 to -49 ‰, respectively. The fluid compositions are similar to those calculated for the high temperature stage 1 alteration assemblages.

$\delta^{18}O$ values of fluids in equilibrium with quartz vary from -3.0 to +5.3 ‰. The $\delta^{18}O$ values of fluids in equilibrium with stage 1 quartz at 200 to 310°C in the deposit and hangingwall vary from +0.7 to 5.3 ‰, with $\delta^{18}O$ values of +1.0 to +4.4 ‰ in samples

Table 6.4 Oxygen and hydrogen isotope composition of fluids in equilibrium with stage 1, stage 2 and stage 3 alteration minerals in the Rambler VMS deposit. Abbreviations are as follows: Oqtz = quartz oxygen (Clayton et al., 1972), Oalb = albite oxygen (Matsuhisa et al., 1979), Ochl = chlorite oxygen (Wenner and Taylor, 1971), Omu = oxygen muscovite (illite curve of Eslinger and Savin, 1973), Dchl = hydrogen chlorite (Wenner and Taylor, 1973), Dmu = hydrogen sericite (extrapolation of the smectite curve by Yeh, 1980), Oamp = oxygen amphibole (quartz–water and quartz–hornblende curves of Clayton et al., 1972 and Bottinga and Javoy, 1975), Damp = amphibole hydrogen (Suzuoki and Epstein, 1976), Obio = oxygen biotite (Bottinga and Javoy, 1973, 1975) and Dbio = hydrogen biotite (Suzuoki and Epstein, 1976). All values are expressed in standard delta notation relative to SMOW.

Alteration minerals		rock	Oqtz		Oalb	Ochl		Omu		Dchl		Dmu	
stage 1 alteration													
hangingwall	28 2713	gbbr	1.8	5.3	5.6								
	21 2749	gbbr	1.2	4.7									
deposit	21 2719	cbt	1.0	4.4									
	21 2751,52	vms	1.1	4.6									
	21 2751	vms						3.9	6.0			−50	−54
	21 2752	vms				9.0	9.4	3.8	5.9			−12	−66
	21 2754	vms	1.5	4.9		4.6	4.6	3.5	5.6	−56	−37		
	21 2760	vms	7.2	8.1 *		9.0	9.4				−39		
	21 2720	vms	1.6	5.1		4.4	4.6			−26	−27		
	– quartz @ 230–310°C and 430–460°C*, albite @ 230°C, chlorite @ 260–270 and 430–480°C, muscovite at 210–310°C												
stage 2 alteration													
footwall	24 1911	myl	−0.7	2.8									
	20 2762	myl	−0.6	2.8		3.7	3.9	0.8	1.2	−23	−23	−56	−57
	26 1974	myl	−0.9	2.5									
	24 1925	myl	−0.1	3.3				1.5	1.9				−55
	28 2728	myl	−0.4	3.1		4.1	4.3			−41	−42		
	24 1930	myl	−1.0	2.5		3.4	3.6			−20	−21		
	– quartz @ 210–260°C, chlorite @ 270–280°C, sericite at 210–220°C.												
stage 3 alteration													
	23 2520	vn	−1.1	0.2		3.4	4.1			−20	−22		
	23 2518	vn	−1.4	−0.1		0.6	3.5			−21	−28		
	24 1963	vn	−1.1	0.2		0	2.9			−19	−25		
	24 1908	vn	−2.1	−0.8	6.3								
	– quartz @ 180–200°C, albite @ 300°C, chlorite @ 180–200°C.												

Metamorphic Minerals		Oamp		Obio	Damp		Dbio	
28 2713	gbbr	8.2	8.6		−74	−78		
21 2835	volc			7.5			−49	
24 1934	volc			5.7			−41	
– amphibole @ 300–550°C (estimated temperatures only), biotite @ 540–560°C.								

of chert to values of +0.7 to 5.1 ‰ for the quartz extracted from samples of massive sulphide mineralization. $\delta^{18}O$ fluid values in equilibrium with stage 2 quartz at 210 to 280°C are lower at -1.0 to +3.3 ‰. Fluids in equilibrium with stage 3 vein quartz yield $\delta^{18}O$ values near 0 ‰ at 180 to 200°C. Two samples of albite yield $\delta^{18}O$ fluid values of +5.6 and +6.3 at 200 and 300°C, respectively.

6.4.3 $\delta^{34}S$: Mineralization

Most sulphide isotopic analyses from massive and disseminated sulphide mineralization in the deposit and footwall were not in isotopic equilibrium. $\delta^{34}S$ pyrite values of +5.7 and +5.8 ‰ are lower, and therefore not in equilibrium with the $\delta^{34}S$ sphalerite values of 6.1 and 5.6 ‰ of dark red sphalerite in sulphide samples 21-2754 and 21-2752 (Sakai, 1968; Kyser, 1987). A single $\delta^{34}S$ chalcopyrite value of +6.6 is not in equilibrium with the lower sphalerite values in other sulphide samples. Pyrite and sphalerite, in equilibrium in footwall sample 20-2761 provide a temperature estimate of 425°C using the combined pyrite-galena and sphalerite-galena sulphide fractionation curves of Kajiwara and Krouse (1971).

Chapter 7: Discussions

7.1 Introduction

$\delta^{18}O$ and δD analyses of seafloor hydrothermal fluids and fluid inclusions consistently suggest the presence of different fluids in the hydrothermal systems which generate VMS deposits. Chemical analyses and thermodynamic modelling of vent fluids from 21°N East Pacific Rise (EPR) suggest that the $\delta^{18}O$ and δD values of seawater (SMOW) increase to +2.0 and +2.5 ‰, respectively in isolated MOR hydrothermal systems (Craig et al., 1980; Bowers and Taylor, 1985). However, vent fluids at rift and SSZ tectonic settings seldom achieve these isotopic values, due in part to the variations among MOR hydrothermal systems, and the possible presence of other fluids of different isotopic compositions in addition to seawater and ^{18}O-shifted seawater in the hydrothermal systems (Schoell and Faber, 1978).

Fluid source variations are also recorded by the isotopic diversity of fluid inclusions in VMS deposits. $\delta^{18}O$ fluid values of -6 to +4 ‰, and δD values of -30 to +15 ‰, were originally modelled in terms of the mixing between seawater and high ^{18}O magmatic fluids, and/or by the mixing of diagenetic and hydrothermal pore fluids in the hydrothermal systems of the Kuroko deposits (Ohmoto and Rye, 1974; Hattori and Meuhlenbachs, 1980; Pisutha-Arnond and Ohmoto, 1983; Urabe and Sato, 1978; Marumo, 1989). In another study, Hattori and Sakai (1979) establish the role of meteoric fluids during the formation of epigenetic Neogene Au-Ag and Cu-Pb-Zn vein deposits which occur in the same volcanic terrains as the Kuroko deposits.

The isotopic compositions of common alteration minerals reflect the influence of several isotopically distinct fluids in VMS hydrothermal systems. $\delta^{18}O$ and δD values associated with the analyses of seafloor alteration assemblages in ophiolites and VMS deposits vary from 0 to +8 ‰, and from -30 to -65 ‰, respectively. However, the $\delta^{18}O$ values of amphiboles in the Raul deposit are unusually high at +8 to +14 ‰ (Ripley and

Ohmoto, 1979), respectively. The δD values of chlorite and biotite in the Ducktown VMS deposit are low at -60 ‰ to -80 ‰ (Addy and Ypma, 1977). Unusually low δD values of -60 to -75 ‰ are also seen in amphibole and chlorite from seafloor alteration assemblages in the East Liguria ophiolite (Barrett and Friedrichson, 1989). Calculated $\delta^{18}O$ and δD values of the fluids in equilibrium with these minerals in some of these deposits are consistent with the mixing of seawater and ^{18}O-shifted seawater with high $\delta^{18}O$, low D fluids (Ohmoto and Rye, 1974; Addy and Ypma, 1977; Ripley and Ohmoto, 1979; Hattori and Sakai., 1979; Urabe and Sato, 1978). Different syngenetic fractionation models have been used to explain the presence of these fluids in the seafloor hydrothermal systems which produce VMS deposits (Ohmoto and Rye, 1974; Addy and Ypma, 1977; Urabe and Sato, 1978).

7.2 Setting, and Geologic and Petrographic Relationships

Geologic relationships in local outcrops on the Consolidated Rambler Mines properties are consistent with a complex multi-stage alteration, structural and metamorphic history in the Pacquet Harbour Group (Gale 1971, 1973; Tuach, 1976; Tuach and Kennedy, 1978; Hibbard, 1983; Tuach et al., 1988). Major element analyses of the volcanic rocks in the hangingwall of the Rambler are consistent with regional REE data which suggest the presence of boninitic basalts, and therefore the possible origin of the deposit in a primitive arc volcanic setting (Swinden, 1991).

Regional greenschist / seafloor metamorphism occurs on the Consolidated Rambler Mines properties as the pervasive quartz + albite + epidote + chlorite ± magnetite / sphene / leucoxene assemblages in local outcrops of volcanic, intrusive and sedimentary rock. These assemblages are mineralogically and texturally identical to those recognized in hydrothermally altered seafloor basalts and in the volcanic rocks effected by regional greenschist facies metamorphism in all other volcanic belts (Miyashiro, 1975; Mottl,

1983). Intense hydrothermal alteration is associated with the presence of the VMS deposits and altered rocks which occur along a transition from felsic to mafic volcanic, intrusive and sedimentary rocks in the upper portion of the Rambler Sequence. If the Pacquet Harbour Group is indeed equivalent to the upper section of the Betts Cove Ophiolite (Hibbard, 1983), then the minimum age of the seafloor hydrothermal alteration and sulphide mineralization in the Rambler is approximately 490 Ma (Dunning and Krogh, 1985).

Seafloor hydrothermal alteration associated with the formation of the Rambler deposit and possibly, the alteration in the Discovery Outcrop (Coates, 1990), was followed by regional deformation associated with the formation of shear zones and thrust faults, such as the Scrape Thrust throughout the Pacquet harbour Group. Regional deformation resulted in shallow northeast plunging open folds with northeast trending fold axes and extension lineations, the deformation and extension of the VMS deposits in the Rambler Sequence, and the formation of local thrusts such as the Rambler Brook thrust. Subsequent fluid alteration along these structures may have generated additional disseminated sulphide mineralization in the Uncles' prospects.

Biotite prophyroblasts in the altered volcanic rocks of the Rambler stratigraphy are consistent with the influence of a late post-kinematic thermal event. Similar prophyroblasts have been noted in contact metamorphic assemblages near the margins of the Burlington Granodiorite (Hibbard, 1983; pers. comm. M. R. Wilson, 1993).

7.2.1 Paragenesis

Descriptions of modern VMS hydrothermal processes on the seafloor suggest massive sulphide mineralization form at the same time as seafloor / greenschist quartz + albite + epidote + chlorite $\pm$ muscovite assemblages (Franklin et al., 1981; Lydon, 1988).

Texture and fabric variations preserved in the recrystallized sulphide assemblages of seafloor VMS deposits are consistent with several generations of sulphide mineralization during seafloor hydrothermal alteration (Alt et al., 1985).

In the Rambler deposit, stage 1 alteration assemblages are replaced with increasing strain by the stage 2 kinematic quartz + chlorite ± muscovite assemblages in samples of schist and mylonite in the deposit and footwall sections of the stratigraphy. A tentative paragenetic sequence for the alteration and sulphide mineralization in the Rambler deposit is provided in Figure 7.1.

In comparison to main stage alteration and mineralization in the Rambler deposit, the timing of secondary sulphide and telluride assemblages in relation to other assemblages is problematic. The secondary sulphides in sample 24-1925 include comparatively high temperature interstitial chalcopyrite ± arsenopyrite ± pyrrhotite assemblages. The interstitial setting and euhedral habit of the telluride grains in sample 24-1925 is consistent with their formation after peak deformation. While both types of mineralization occur as post-kinematic phases with respect to stage 1 alteration and massive sulphide assemblages, implied correlations with other silicate alteration and sulphide assemblagse are even less certain.

7.2.2 Alteration Chemistry

Alteration in the Rambler deposit is similar to the alteration associated with numerous other VMS deposits (Gjelsvik, 1968; Rui, 1973; Addy and Ypma, 1977; Franklin et al., 1981; Large et al., 1988). There are numerous reactions and reaction pathways to describe the alteration in the deposit, but these should explain chemical trends which include enrichments in muscovite during the destruction of albite and replacement of chlorite consistent with K enrichments and Na and Ca depletions in the stratigraphy of

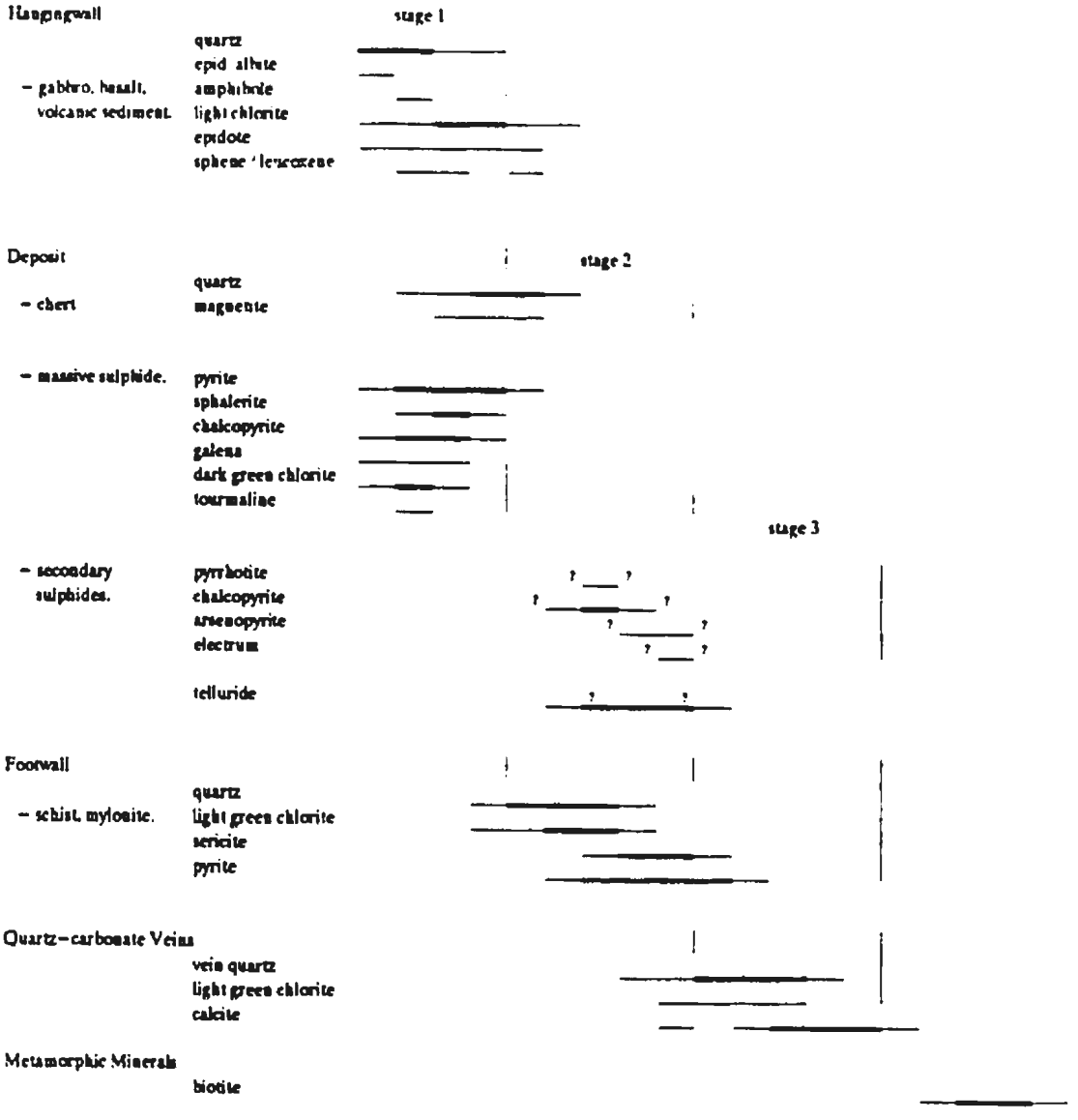

Figure 7.1 Paragenetic sequence of alteration, sulphide and gold mineralization from petrographic relationships in the Rambler VMS deposit.

the deposit. Of greatest relevance are common greenschist facies reactions which describe basalt hydration and metamorphism in the oceanic crust and seafloor hydrothermal systems, and/or the alteration associated with the formation of mesothermal gold deposits.

Several reactions have been used to describe the production of the greenschist "spilitic" assemblages during seafloor alteration or metamorphism. Lydon (1988) describes the hydration of basalt at W/R ratios of 1:30:

$$1.000\ \underset{\text{basalt}}{Na_{4.90}(Ca_{11.71}Mg_{1.73}Fe^{2+}_{0.83}Fe^{3+}_{1.55})Al_{17.18}Si_{49.33}O_{160}} + 0.009\ Mg^{2+}$$

$$+\ 10.379\ \underset{\text{fluid}}{H_2O} + 0.179\ O_2 \longrightarrow 1.604\underset{\text{chlorite}}{(Mg_{.51}Fe_{.49})_5Al_2Si_3O_{10}(OH)_8}$$

$$+\ 4.90\ \underset{\text{albite}}{NaAlSi_3O_8} + 2.075\ \underset{\text{amphibole}}{Ca_{2.0}(Mg_{.60}Fe_{.40})Si_{8.0}O_{22}(OH)_2}$$

$$+\ 3.776\underset{\text{epidote}}{Ca_{2.0}(Fe_{.60}Al_{2.40})Si_3O_{12}(OH)} + 1.893\ \underset{\text{quartz}}{SiO_2} + 0.009\ Ca^{2+}. \qquad (1)$$

The alteration assemblages produced by this and similar reactions are similar to the stage 1 alteration assemblages which dominate the hangingwall and deposit sections of Rambler stratigraphy. This particular reaction has amphibole as a product of seafloor hydrothermal alteration, suggesting that the hangingwall amphibole is also of seafloor origin. However, a later metamorphic origin is also a distinct possibility, especially in light of the sporadic occurrence of the porphyroblastic biotite throughout the stratigraphy of the deposit. Stage 1 assemblages of different modal compositions in epidotized volcanic rocks, quartz-chlorite breccia, and in samples of massive sulphide mineralization may have resulted from local variations in temperature, pH, fO_2 and W/R ratios in different areas of the deposit (Mottl, 1983; Seyfried et al., 1988). For example, the following are used to describe the production of the plagioclase-epidote assemblages

during the Ca and Na metasomatic reactions which buffer seawater chemistry in seafloor hydrothermal systems:

$$\underset{\text{anorthite}}{3\ CaAl_2Si_2O_8} + Ca^{2+} + \underset{\text{fluid}}{2\ H_2O} \longrightarrow \underset{\text{epidote}}{2\ Ca_2Al_3Si_3O_{12}(OH)} + 2H^+ \qquad (2)$$

$$\underset{\text{anorthite}}{4\ CaAl_2Si_2O_8} + 2\ Na^+ + \underset{\text{quartz}}{4\ SiO_{2(aq)}} + 2\ H_2O \longrightarrow \underset{\text{epidote}}{2\ Ca_2Al_3Si_3O_{12}(OH)}$$

$$+ \underset{\text{albite}}{2\ NaAlSi_3O_8} + 2\ H^+ \qquad (3)$$

(Seyfried et al., 1988). Alteration products in these reactions are similar to the stage 1 assemblages in the epidotized volcanic rocks and breccia which occur in the lower portion of the deposit section of the Rambler stratigraphy. Local and temporal variations in W/R ratios during these reactions are linked to the production of chlorite in epidotized volcanic rocks associated with seafloor hydrothermal alteration (Seyfried et al., 1988).

Models which describe the alteration associated with mesothermal gold deposits use reactions which describe the production of quartz + muscovite ± chlorite ± sulphide assemblages during the alteration of greenschist metamorphic assemblages in mafic volcanic rocks. The main reaction products are similar to the stage 2 quartz + muscovite ± chlorite assemblages in schists and mylonites which host disseminated sulphides in the footwall of the Rambler deposit. The following has been used, for example, to describe the alteration of gabbro during the formation of the Norbeau mesothermal gold deposit:

$$\underset{\text{actinolite}}{3\ Ca_2(Mg,Fe)_5Si_8O_{22}(OH)_2} + \underset{\text{epidote}}{2\ Ca_2Al_3Si_3O_{12}(OH)} + CO_2 + \underset{\text{fluid}}{H_2O}$$

$$\longrightarrow \underset{\text{chlorite}}{3\ (MgFe)_5Al_2Si_3O_{10}(OH)_8} + \underset{\text{calcite}}{10\ CaCO_3} + \underset{\text{quartz}}{21\ SiO_2}. \qquad (4)$$

(Dubé et al., 1987). The reaction produces secondary chlorite from greenschist amphibole and epidote assemblages, which may be analogous to the pervasive light green

chlorite in the altered rocks throughout the stratigraphy of the Rambler (section 4.x). Roberts (1988) uses a similar reaction to describe the production of muscovite + dolomite + quartz assemblages during the reaction of assemblages of chlorite, and calcite with a K-rich fluid:

$$\underset{\text{chlorite}}{3\,(Mg,Fe)_5Al_2SiO_3O_{10}(OH)_8} + \underset{\text{calcite}}{CaCO_3} + 2\,K^+ + \underset{\text{fluid}}{15\,CO_2}$$

$$\longrightarrow \underset{\text{muscovite}}{2\,KAl_3Si_3O_{10}(OH)_2} + \underset{\text{dolomite}}{15Ca(Mg,Fe)(CO_3)_2} + \underset{\text{quartz}}{3\,SiO_2}$$

$$+ \underset{\text{fluid}}{9\,H_2O} + 2\,H^+. \qquad (5)$$

An alternative describes the production of muscovite during the destruction of albite and its reaction with a K-enriched hydrothermal fluid:

$$\underset{\text{albite}}{3\,NaAlSiO_3O_8} + K^+ + \underset{\text{fluid}}{3H^+} + 3OH^- \longrightarrow \underset{\text{muscovite}}{KAl_3Si_3O_{10}(OH)_2} +$$

$$+ \underset{\text{quartz}}{6\,SiO_2} + \underset{\text{fluid}}{3\,Na^+} + 4\,O_2 + 6\,H^+ . \qquad (6)$$

(after Roberts, 1988). Other reactions could be used to model the production of specific mineralogical features associated with the alteration in the Rambler deposit. For example Spence and deRosen Spence (1975) react Fe^{2+} and Mg^{2+} with muscovite to form chlorite through the reaction:

$$\underset{\text{muscovite}}{3\,KAl_3Si_3O_{10}(OH)_2} + \underset{\text{fluid}}{10\,(Fe,Mg)^{2+}} + 32\,H_2O \longrightarrow$$

$$\underset{\text{chlorite}}{2\,(Mg,Fe)_5Al_2SiO_3O_{10}(OH)_8} + 3\,Si(OH)_4 + \underset{\text{fluid}}{5\,Al(OH)^{-4}} + 3\,K^+. \qquad (7)$$

The reaction is consistent with the presence of secondary chlorite observed in the pressure shadows surrounding recrystallized pyrite in some of the footwall schists and mylonites.

Fe and Mg carbonates are common in the central alteration zones of mesothermal gold deposits (Dubé et al. 1987), and similar carbonate-rich assemblages result when mesothermal fluids react with the alteration and sulphide assemblages of VMS deposits (Addy and Ypma, 1977). However, Fe and Mg carbonates are not present in either the stage 1 or the stage 2 alteration assemblages of the Rambler deposit. Calcite, the dominant carbonate, occurs only in late quartz + carbonate and carbonate assemblages of stage 3 veins. The lack of carbonate in stage 2 alteration assemblages is inconsistent with the presence of high CO_2 metamorphic or mesothermal fluids during the deformation of the Rambler deposit.

Further speculation concerning the exact chemical origin of the different alteration minerals and assemblages in the Rambler deposit is beyond the scope of the study. Alteration assemblages in the deposit are the products of common greenschist mineral reactions which occur during seafloor hydration and hydrothermal alteration, and regional metamorphism. Similar assemblages are also produced during the deformation of mafic volcanic rocks and the formation of epigenetic deposits. The reactions are non-unique in that they provide no evidence of the source of fluids related to the different generations of silicate alteration and sulphide mineralization observed in the Rambler and in other VMS deposits.

7.3 Isotope Geochemistry of Silicate and Sulphide Assemblages

The $\delta^{18}O$ values of quartz and albite from the Rambler deposit are consistent with those associated with seafloor / greenschist alteration and metamorphism in oceanic basalt, ophiolites and VMS deposits. Average $\delta^{18}O$ quartz and albite values of +10.8 and +8.0 ‰ are consistent with the range of reported quartz and albite $\delta^{18}O$ values which vary from +5 to +20 ‰, and from +6 to +9 ‰ (Figure 7.2; Heaton and Sheppard, 1977; Kowalik, 1979; Urabe and Sato, 1978; Pisutha-Arnond and Ohmoto, 1983; Munha et al., 1986; Beatty and Taylor, 1988). However, a total range of $\delta^{18}O$ and δD values of +2.9 to +8.3 ‰ and -55 to -84 ‰ from the analyses of the hydrous silicates in the Rambler

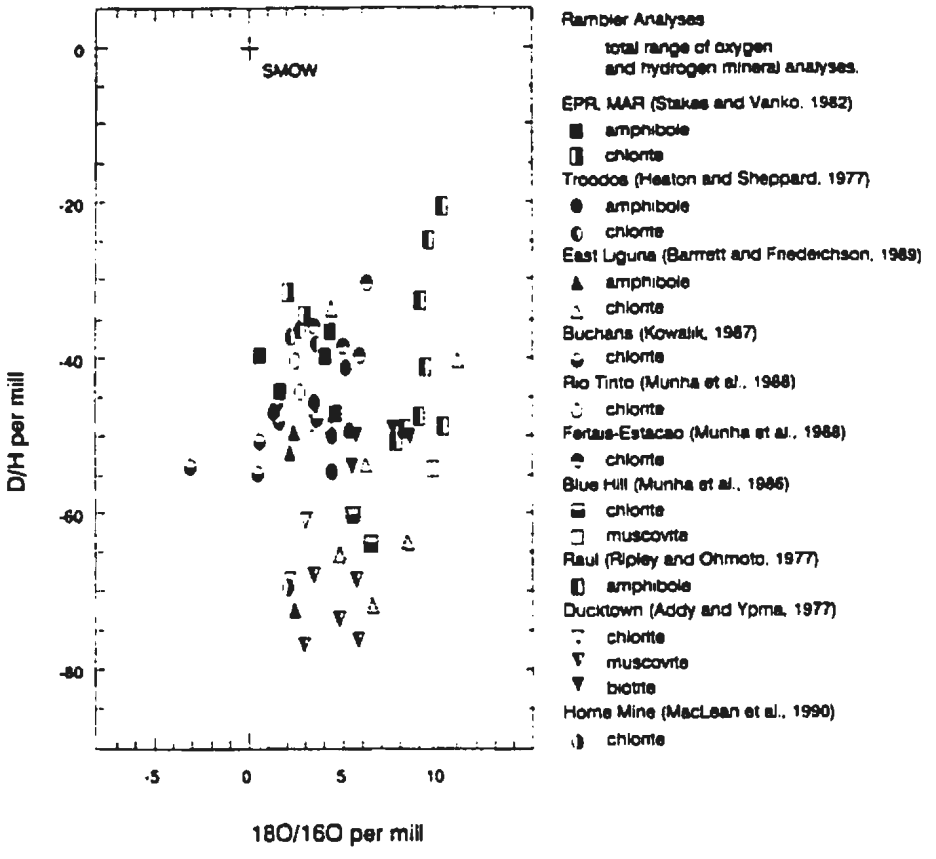

Figure 7.2. The total range of $\delta^{18}O$ and δD amphibole, chlorite, muscovite and biotite values from the Rambler deposit (stippled) compared with $\delta^{18}O$ and δD values of similar minerals from the oceanic crust, ophiolites and other VMS deposits.

deposit is similar and slightly lower, than the isotopic values obtained from seafloor alteration assemblages (Addy and Ypma, 1977; Heaton and Sheppard, 1977; Kowalik, 1979; Stakes and O'Neil, 1982; Munha et al., 1986; Barrett and Friedrichson, 1989; MacLean and Hoy, 1991; Urabe and Sato, 1978; Beatty and Taylor, 1988).

Chlorite $\delta^{18}O$ and δD values which vary from +2.9 to +7.5 ‰ and from -57 to -78 ‰ in the Rambler deposit are consistent with $\delta^{18}O$ and δD chlorite values of approximately 0 to +8 ‰ and -30 to -65 ‰ reported in other VMS deposits (Addy and Ypma, 1977; Heaton and Sheppard, 1977; Kowalik, 1979; Munha et al., 1986; Barrett and Friedrichson, 1989). $\delta^{18}O$ values of muscovite which vary from +6.4 to +8.3 ‰ in the Rambler are consistent with reported muscovite values of +5 to +10 ‰. However, δD muscovite values of -55 to -72 ‰ from the deposit and footwall are lower than available δD muscovite analyses which vary from -30 to -54 ‰ (Addy and Ypma, 1977; Munha et al., 1986).

A $\delta^{18}O$ and δD values of +5.8 ‰ and -36 ‰, respectively for the amphibole in the hangingwall sill are within the range of the $\delta^{18}O$ values of +2.2 to 7.0 ‰, and δD values of -36 to -56 ‰ associated with groundmass amphibole in samples of altered oceanic basalt (Stakes and O'Neil, 1982; Heaton and Sheppard, 1977; Barrett and Friedrichson, 1989), suggesting a seafloor origin for the amphibole in the Rambler deposit. The isotopic values are noticeably distinct from the high $\delta^{18}O$ values of +7.5 to +12 ‰ for the metamorphic amphibole in the Raul VMS deposit (Ripley and Ohmoto, 1977). Biotite $\delta^{18}O$ and δD values of +5.0 and -84 ‰, and +3.2 and -76 ‰ are similar to reported $\delta^{18}O$ values +3.4 to +5.0 ‰ and δD values of -60 to -77 ‰ from the Ducktown VMS deposit (Addy and Ypma, 1977).

A total range of $\delta^{34}S$ values of +5.8 to +7.6 ‰ from sulphide analyses in the Rambler is consistent with $\delta^{34}S$ values of -6 to +20 ‰, and -7 to +17 ‰ from sulphide analyses in Phanerozoic and Archean VMS deposits, and similar to $\delta^{34}S$ values of 0 to +15 ‰ obtained from sulphide analyses in the epigenetic / mesothermal gold deposits (Figure

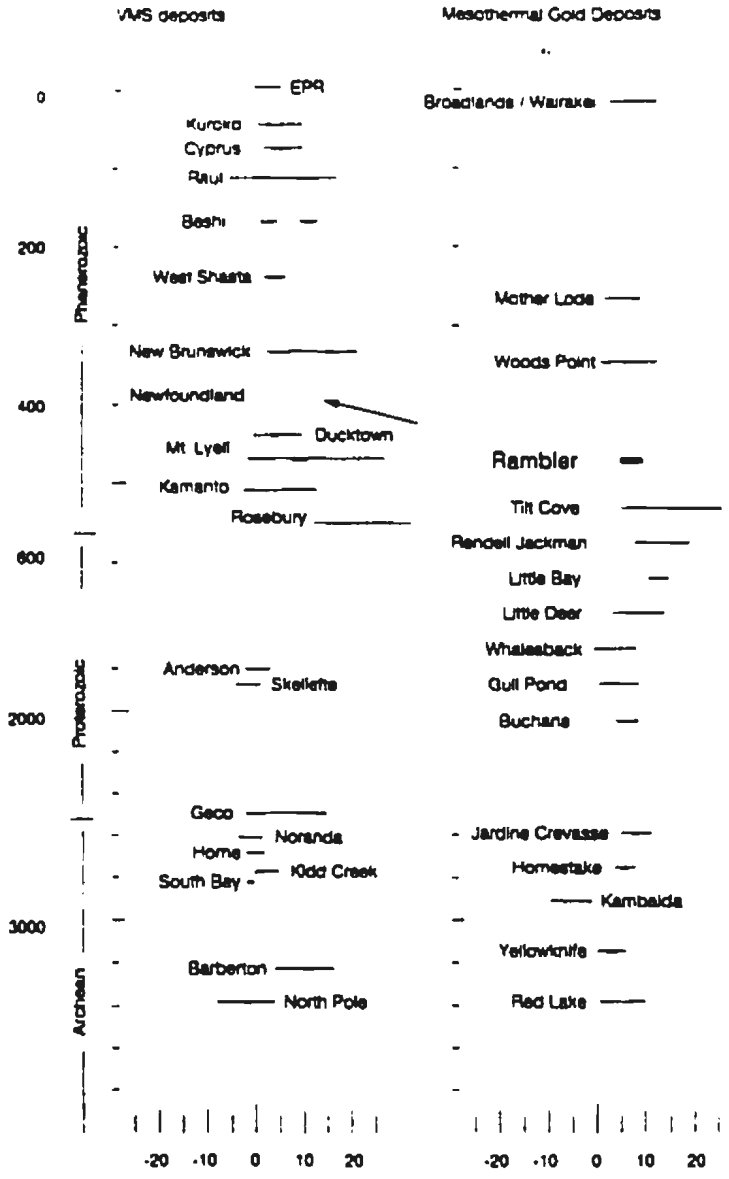

Figure 7.3 Range of $\delta^{34}S$ values (CDT) from sulphide analyses in the Rambler VMS deposit compared with the reported $\delta^{34}S$ values in Archean and Phanerozoic VMS and mesothermal gold deposits (modified after Kerrich, 1989). $\delta^{34}S$ values from Newfoundland VMS deposits (stippled box in mesothermal column) are from Bachinski (1978), Kowalik et al. (1981) and this study.

$\delta^{34}S$ values from the Rambler deposit are also similar to data reported from sulphide isotopic analyses in several other VMS deposits in Central Newfoundland. An average of $+6.3 \pm 0.6$ ‰ is similar to average $\delta^{34}S$ values of $+5.3 \pm 1.7$ ‰, $+4.2 \pm 1.8$ ‰ and $+5.5$ to $+8.7$ ‰ from the analyses of similar sulphide assemblages in the Whalesback, Gull Pond and Buchans VMS deposits (Bachinski, 1977, 1978; Kowalik et al., 1981). The similarity in $\delta^{34}S$ values may indicate that sulphide analyses are not useful for distinguishing between different events of alteration and mineralization in recrystallized ore deposits.

7.3.1 ^{18}O Thermometry

Oxygen isotope thermometry from quartz-mineral pairs confirms a complex thermal history during the alteration and metamorphism of the Rambler deposit. All thermal events are consistent with temperatures indicated by greenschist metamorphic assemblages in local outcrops of the Pacquet Harbour Group on the Consolidated Rambler Mines properties.

Quartz-chlorite pairs suggest a high and low temperature event for the alteration in the deposit and footwall sections of the stratigraphy. Petrographic evidence suggests a link between the dark green chlorite and high temperatures of 438 and 483°C obtained from quartz-chlorite pairs in samples of massive sulphide mineralization. Stage 2 and stage 3 samples dominated by the light green chlorite yield temperatures which show a total variation of 176 to 277°C. Replacement of the dark green chlorite by the light green chlorite (Plates 4.5 and 4.9) suggests the high te perature fluid event preceded low temperature syn-kinematic alteration in the Rambler deposit.

Quartz-muscovite pairs from stage 1 and stage 2 assemblages yield consistently low temperatures of 209 to 309°C roughly concordant with the low temperature quartz-chlorite determinations. However, these low temperatures may represent an artifact of sampling bias. Pure muscovite could only be obtained in quantities sufficient for

analyses by scraping sericitic shears and partings in massive sulphide, schist, and mylonite samples. It was not clear, therefore, if a pre-kinematic, but unsampled muscovite, was present in the recrystallized groundmass assemblages of the massive sulphide samples. Higher temperature determinations of 243 to 309°C from stage 1 quartz-muscovite pairs in massive sulphide samples support the presence of a higher temperature muscovite in the deposit section of the stratigraphy.

Quartz-biotite pairs from breccia vein assemblages in the footwall of the deposit provide unusually high temperatures of 539 and 559°C consistent with the influence of a late thermal event. Quartz-albite pairs yield temperatures of 230 and 297°C for stage 1 assemblages and stage 3 vein assemblages, which are in general agreement with the quartz-chlorite and quartz-muscovite temperatures obtained from stage 1 assemblages in the hangingwall and deposit sections of the stratigraphy.

7.3.2 $\delta^{18}O$ and δD Fluid Values and Source Variations

The $\delta^{18}O$ and δD values of fluids in equilibrium with different alteration minerals in the Rambler deposit are not entirely consistent with those associated with seafloor hydrothermal processes (Figure 7.4.a). $\delta^{18}O$ and δD fluid values of 0 to +9.4 ‰ and from -19 to -57 ‰, at temperatures of 176 to 559°C, are similar in ^{18}O and lower in D than a total range of fluid values of 0 to +3 ‰ and +32 to -5 ‰ from analyses of seafloor vent fluids (Craig et al., 1980; Schoell and Faber, 1984; Bowers and Taylor, 1985). Rambler fluid values are higher in ^{18}O and lower in D than values which vary from -9 to -1 ‰ and +5 to -12 ‰ associated with the isotopic analyses of pore fluids (Gieske, 1981), and higher in ^{18}O and lower in D than a range of $\delta^{18}O$ and δD fluid values of -9 to +4 ‰ and +20 to -30 ‰ from the analyses of fluid inclusions in the Kuroko VMS deposits (Ohmoto and Rye, 1974, Hattori and Sakai, 1979; Pisutha-Arnond and Ohmoto, 1983). The Rambler fluid values are similar to $\delta^{18}O$ and δD fluid values of -1.5 to +6.5 ‰ and -8 to -40 ‰ in equilibrium with similar alteration minerals in the Kuroko, Adjustrel,

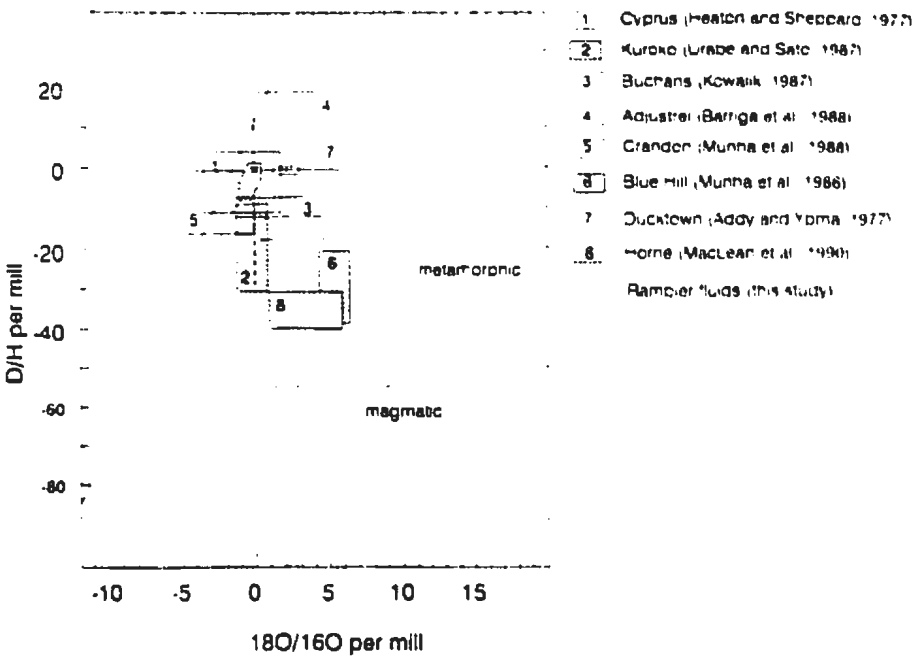

Figure 7.4.a) The total range of $\delta^{18}O$ and δD fluid values from the Rambler deposit (dashed) compared with isotopic analyses of seafloor vent fluids (shaded; Schoell and Faber., 1978, Craig et al., 1980; Stakes and O'Neil, 1982), pore fluids (stippled outline; Gieske, 1981), and the inclusion fluids associated with seafloor hydrothermal processes (stippled outline; Ohmoto and Rye, 1974; Hattori et al. 1979; Pisutha-Arnond and Ohmoto, 1983).

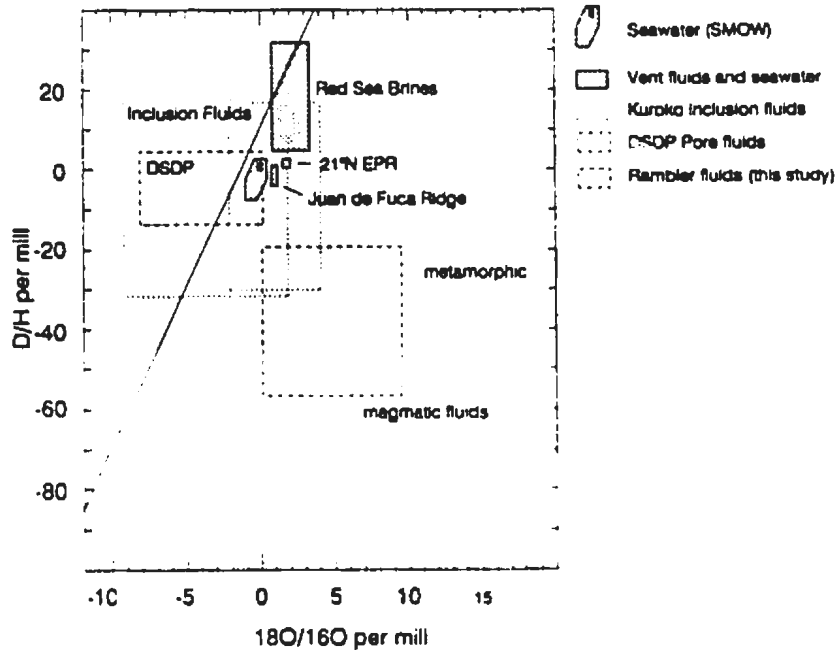

Figure 7.4.b) The total range of $\delta^{18}O$ and δD fluid values from the Rambler deposit (dashed) and the $\delta^{18}O$ and δD values of fluids in equilibrium with the seafloor hydrothermal alteration assemblages in VMS deposits (Addy and Ypma, 1977; Heaton and Sheppard, 1977; Urabe and Sato, 1978; Kowalik, 1979; Barriga and Kerrich., 1981; Munha et al., 1986; MacLean and Hoy, 1991).

Buchans and Horne VMS deposits (Figure 7.4.b; Urabe and Sato, 1978; Kowalik, 1979; Barriga and Kerrich, 1981; MacLean and Hoy, 1991). Isotopic variations among the calculated fluids in equilibrium with different alteration minerals are consistent with the influence of different fluids during the formation, alteration and metamorphism of the Rambler deposit. Mineral analyses and quartz-mineral temperatures suggest two isotopically distinct fluids equilibrated with chlorite. The $\delta^{18}O$ values of +9.0 to +9.4 ‰ and δD values of -39 ‰ of fluids in equilibrium with the high temperature (dark green) chlorite at 483 and 438°C are similar to the isotopic composition of high ^{18}O magmatic or metamorphic fluids (Taylor, 1974). $\delta^{18}O$ values of 0 to +4.6 ‰ and δD values of -19 to -37 ‰ for fluids in equilibrium with the lower temperature (light green) chlorite at 180 to 270°C are lower in ^{18}O and similar in D to the fluids associated with the high temperature chlorite, and similar in $\delta^{18}O$ and δD to calculated fluids values in equilibrium with chlorite analyses from VMS deposits and ophiolites at 200 to 300°C (solid outline in Figure 7.5.a).

The restricted occurrence of dark green chlorite in massive sulphide mineralization suggests its high ^{18}O fluid was either a magmatic fluid, or isotopically-evolved seawater introduced during seafloor hydrothermal alteration and sulphide mineralization (Gregory and Taylor, 1981). The replacement of dark green chlorite by syn-kinematic light green chlorite (Plate 4.5) is consistent with decreasing alteration temperatures, and a shift in fluid isotopic compositions from the high ^{18}O fluid to some mixture of seawater, and metamorphic and possibly meteoric fluids during the latter part of stage 1 and during stage 2 alteration.

Mineral analyses and quartz-mineral isotopic equilibration temperatures also confirm variations in the source of fluids in equilibrium with muscovite. Calculated $\delta^{18}O$ fluid values of +3.5 to +6.0 ‰ with δD values of -42 to -54 ‰ at 240 to 310°C, and $\delta^{18}O$ fluid values of +0.8 to +1.9 ‰ with δD values of -55 to -57 ‰ at 210 to 220°C, are similar in ^{18}O, but lower in D than the corresponding fluids in equilibrium with chlorite in the same alteration stages. The contrasting fluid isotopic compositions suggest the

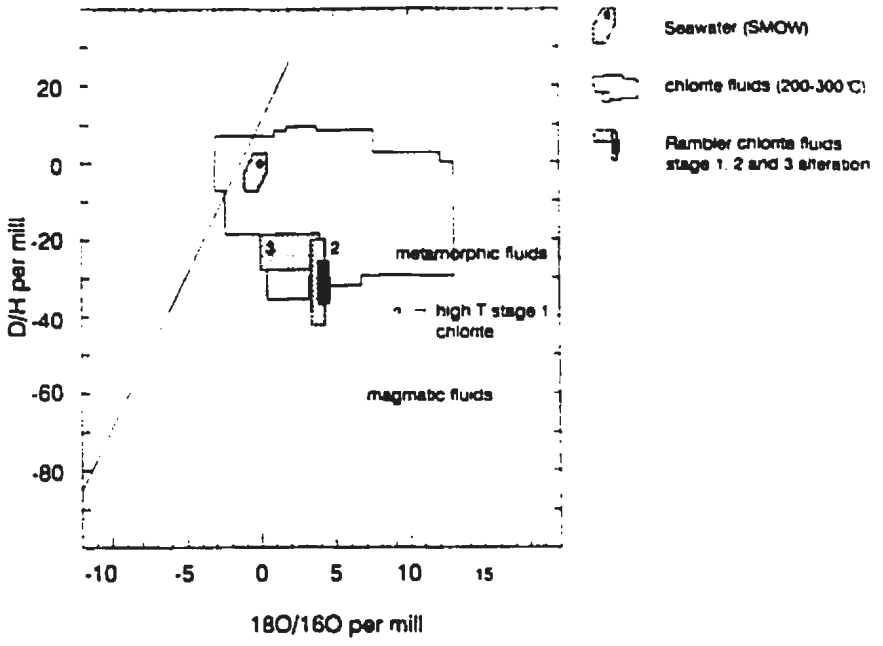

Figure 7.5 a) $\delta^{18}O$ and δD values of fluids in equilibrium with chlorite (alteration stages 1, 2 and 3) in the Rambler deposit. Temperatures are provided in Table 6.4. Also shown are fluids in equilibrium with chlorite analyses at 200 to 300°C (solid outline; Heaton and Sheppard, 1977; Addy and Ypma, 1977; Ripley and Ohmoto, 1979; Stakes and O'Neil, 1982; Kowalik, 1979; Munha et al., 1986).

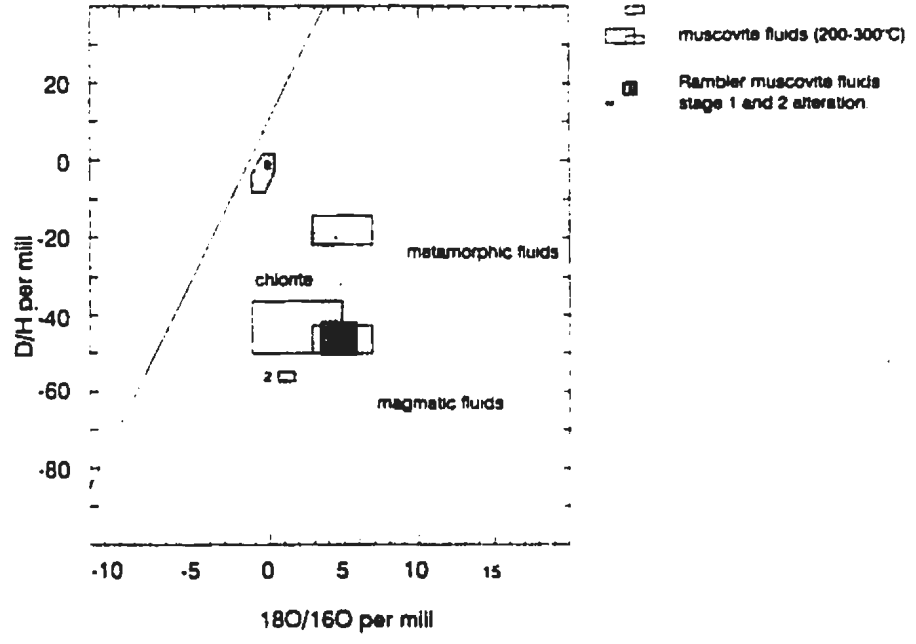

Figure 7.5 b) $\delta^{18}O$ and δD of fluids in equilibrium with muscovite (stages 1 and 2) in the Rambler deposit. Temperatures are provided in Table 6.4. Shown for comparison are fluids in equilibrium with chlorite and compiled chlorite analyses (stippled and stippled outline from Figure 7.5.b) and fluids in equilibrium with compiled muscovite analyses at 200 to 300°C (solid outlines; Addy and Ypma 1977; Munha et al., 1986).

presence of an alternate low D fluid during the formation of muscovite. The replacement of light green chlorite by muscovite (Plate 4.5 and Plate 4.9) suggests that this low D fluid effected the deposit sometime after the fluid which equilibrated with the more pervasive, syn-kinematic light green chlorite.

Calculated $\delta^{18}O$ fluid values of +8.2 to +8.6 ‰, and δD fluid values of -74 to -78 ‰ at temperatures of 300 to 550°C are within range of calculated $\delta^{18}O$ fluid values of +4.5 to +9.8 ‰, and δD fluid values of -45 to -88 ‰ at temperatures of 300 to 550°C from compiled amphibole analyses in similar geologic settings (Figure 7.6.a). The range of calculated fluid values is therefore consistent with a seafloor and/or magmatic fluid origin for the amphibole in the hangingwall sill of the Rambler deposit. The values are distinct from $\delta^{18}O$ fluid values of +10.6 to +13.1 ‰, and δD fluid values of -32 to -66 ‰ calculated from amphibole analyses associated with the Raul VMS deposit (Ripley and Ohmoto. 1977).

$\delta^{18}O$ values of +7.5 and +5.7 ‰ and δD values of -49 and -41 ‰ for the isotopic composition of fluids in equilibrium with biotite at 540 to 560°C are both consistent with high ^{18}O magmatic and/or metamorphic fluid compositions, and similar to calculated $\delta^{18}O$ fluid values of +5.0 to +7.5 ‰, and δD fluid values of -15 to -37 ‰ from compiled analyses at temperatures of 450 to 550°C. Fluids in equilibrium with biotite from the Rambler deposit are slightly higher in ^{18}O than the fluids in equilibrium with muscovite at temperatures of 240 to 310°C (Figure 7.5.b). The overgrowth and replacement of stage 1 and stage 3 assemblages by biotite suggests the introduction of high temperature, high ^{18}O metamorphic fluids sometime after the formation of stage 3 veins (Figure 7.6.a).

The $\delta^{18}O$ fluid values of -1.1 to -1.4 ‰ in equilibrium with quartz, and quartz-chlorite temperatures which range from 180 to 310 °C in stage 3 vein samples are consistent with $\delta^{18}O$ quartz-fluid compositions of -5 to +10 ‰ in the seafloor hydrothermal systems

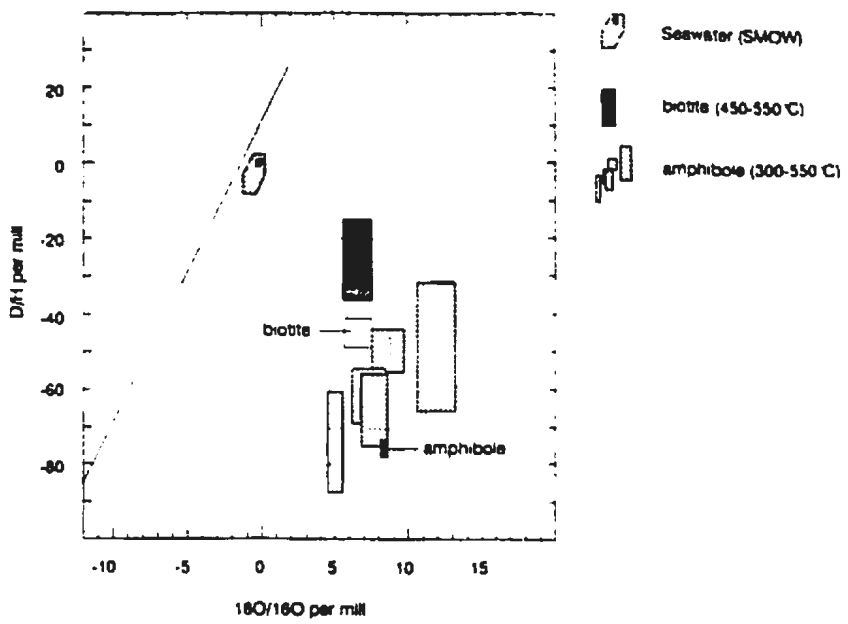

Figure 7.6 a) $\delta^{18}O$ and δD of fluids in equilibrium with amphibole and biotite in the Rambler deposit (labelled). Temperatures are provided in Table 6.4. Also shown are fluids in equilibrium with compiled and recalculated amphibole (stippled) and biotite (densely stippled) analyses at 300 to 550°C and 450 to 550°C, respectively (Heaton and Sheppard, 1977; Addy and Ypma, 1977; Barrett and Friedrichson, 1989).

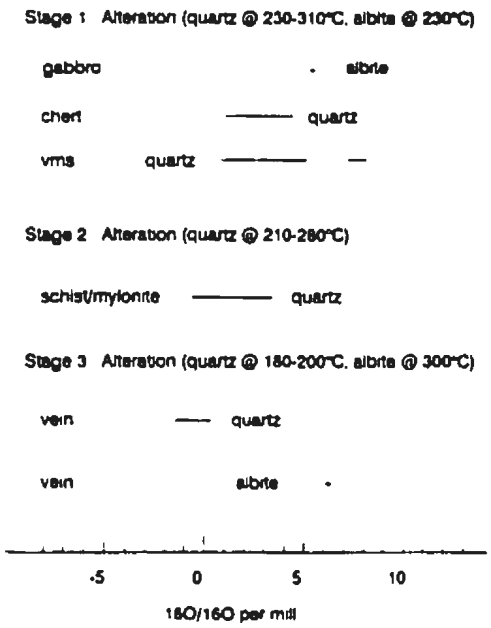

Figure 7.6 b) $\delta^{18}O$ of fluids in equilibrium with quartz and albite at calculated maximum and minimum alteration temperatures in stage 1, stage 2 and stage 3 alteration assemblages. A negative shift in $\delta^{18}O$ values may be related in the influx of meteoric fluids associated with waning fluid activity during stage 2 deformation and stage 3 vein formation.

associated with VMS mineralization (Heaton and Sheppard, 1977; Urabe and Sato, 1978 and others).

A negative shift in calculated $\delta^{18}O$ fluid values in equilibrium with quartz in stage 1 and stage 3 assemblages is consistent with a similar decreases in the $\delta^{18}O$ values of fluids in equilibrium with chlorite and muscovite (Figure 7.6.b). The trends are consistent with cooling and a possible influx of meteoric fluids during stage 2 syn-kinematic alteration and stage 3 syn to post-kinematic vein formation.

7.4 Chlorite-Muscovite Isotopic Equilibria

Chlorite-muscovite disequilibria occurs when the $\delta^{18}O$ and δD values of fluids in equilibrium with chlorite are $\neq$ the $\delta^{18}O$ and δD values of fluids in equilibrium with coexisting muscovite over a common range of temperatures (Kyser, 1987). In Figure 7.7.a a fluid of similar initial composition (in this case seawater) equilibrates with chlorite and muscovite at 200 to 350°C. In all cases the δD fluid values in equilibrium with chlorite are less than the δD fluid values in equilibrium with muscovite. Isotopic data presented in Table 7.1 suggest that chlorite - muscovite equilibrium is the norm in the alteration assemblages associated with other VMS deposits (Addy and Ypma, 1977; Munha et al., 1988). The presence of an additional fluid is indicated when $\delta^{18}O$ and δD chlorite fluid values $\geq$ the $\delta^{18}O$ and δD muscovite fluid values, as suggested by the Rambler data.

The calculation of precise δD values for the low D fluid in equilibrium with muscovite is difficult using the available hydrogen fractionation curves. Extrapolation of the high temperature (400-850°C) muscovite-H_2O fractionation curve of Suzuoki and Epstein (1976) down to 400°C yields a Δ value of approximately -30 ‰. Extrapolation of the smectite-H_2O curve (Yeh, 1980) up to 400°C yields a Δ of -4 ‰. A difference in the two curves is consistent with non-linear behaviour between α and 1/T for many hydrous minerals at temperatures of approximately 200 to 300°C (Valley et al., 1987; Kyser,

Table 7.1 Oxygen and hydrogen isotope analyses of chlorite and muscovite in the Blue Hill, Rio Tinto and Ducktown VMS deposits. All values are reported in standard delta notation relative to SMOW.

		Mineral Analyses			
		$\delta^{18}O$		δD	
Blue Hill Deposit (Munha et al. 1988)					
RAD1	chlorite		6.4		−65
	muscovite		10.0		−54
RAD2	chlorite		5.9		−60
	muscovite		9.9		
RAD3	chlorite		6.7		−68
	muscovite		9.3		
Rio Tinto Deposits (Munha et al., 1988)					
Rio Tinto	chlorite		2.5		−42
Cerro Colorado	chlorite	2.0	2.5		−45
Chanca	chlorite		3.3		−50
Adjustrel	chlorite	3.2	5.0	−37	−39
Feitais	chlorite	6.3	6.9	−32	−41
Salgadinho	muscovite		9.5		−30
Ducktown (Addy and Ypma, 1977)					
Alteration Zone	chlorite	2.2	3.1	−62	−69
	muscovite	5.3	5.8	−51	−54
Host Rocks	muscovite	6.6	8.4	−49	−50

1987). Isotopic fractionation during the formation of smectite (which is chemically and structurally similar to muscovite) in seafloor volcanic and sedimentary rocks occurs at similar temperatures occurs at ΔD values of 15 - 20 ‰ (Friedman and Hardcastle, 1988). Available fractionation data suggests the δD values of muscovite at 200 to 300°C are approximately 10 to 20 ‰ higher than δ D chlorite values under equilibrium conditions (Taylor, 1974; Valley et al., 1987; Kyser, 1987). Analyses of chlorite-muscovite pairs from the Blue Hill, Rio Tinto and Ducktown VMS deposits in similar tectonic settings, all have δD muscovite values ≥ δD chlorite values consistent with the equilibration of the minerals with the same fluid. However, the muscovite in the Rambler has slightly lower δD fluid values than those associated with coexisting chlorite (Figure 7.7.b) suggesting its equilibration with an isotopically distinct fluid of uncertain origin.

7.5 Evidence for a Low D Fluid in the Rambler Deposit

Several syngenetic processes are associated with the production of high ^{18}O (>5 ‰), low D fluids (<-40 ‰) which effect VMS deposits. Proposed fluid origins have included the mixing of seawater with magmatic and metamorphic fluid components, the expulsion of seafloor connate fluids, low W/R ratio high temperature conditions, isotopic exchange with unusual high ^{18}O volcanic or sedimentary rocks, multi-pass convection, shale ultrafiltration, the evaporation of seawater in a restricted basins, and/or boiling (Ripley and Ohmoto, 1979; Barriga and Kerrich, 1981; Beatty and Taylor, 1982; Munha et al., 1986;).

Mixing of seawater and magmatic or metamorphic fluids has been proposed to explain the high ^{18}O and low δD fluid values of the Kuroko fluid inclusions (Ohmoto and Rye, 1974). The expulsion of connate fluids, low W/R ratio high temperature regimes exchange with unusually high ^{18}O rocks, and/or multipass convection are all isotopic fractionation processes which increase $\delta^{18}O$ values, but leave δD fluid values unaffected.

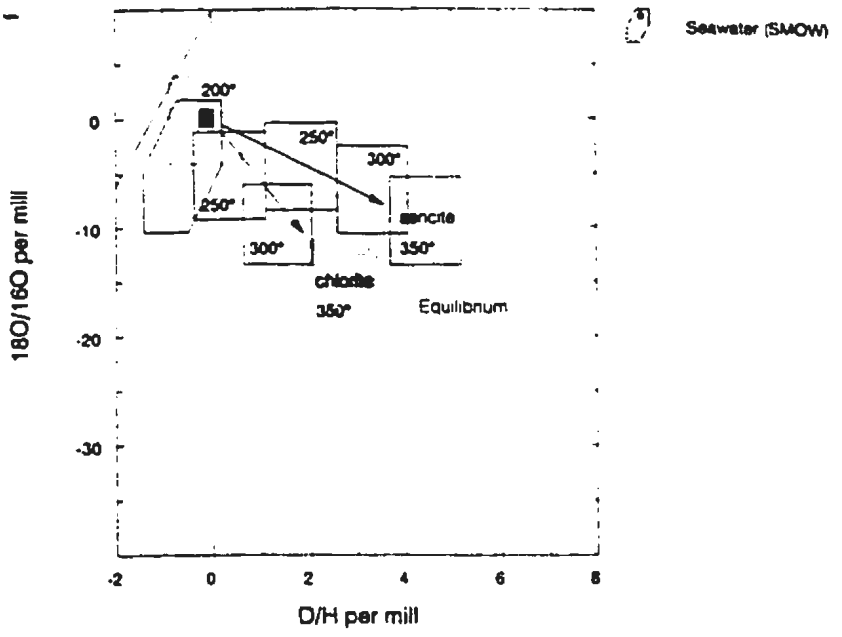

Figure 7.7 a) Shift in the $\delta^{18}O$ and δD compositions of a hypothetical fluid of similar initial composition (in this case seawater) in equilibrium with chlorite (stippled) and muscovite at temperatures of 200 to 350°C.

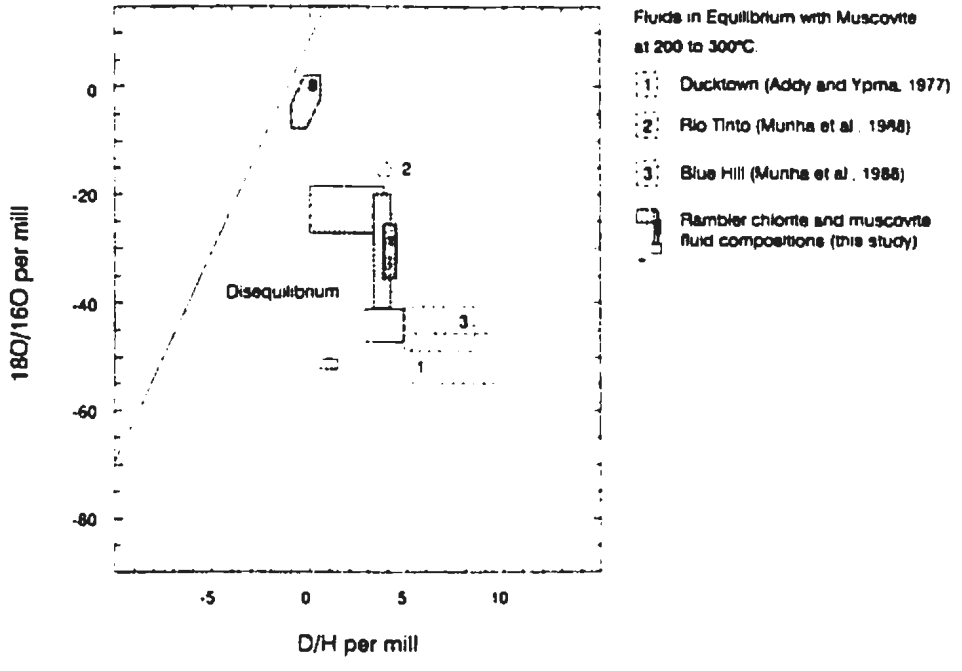

Figure 7.7 b) Calculated $\delta^{18}O$ and δD values of fluids in equilibrium with chlorite (stippled) and muscovite at reported maximum and minimum alteration temperatures in the Ducktown, Blue Hill, Rio Tinto and Rambler MS deposits (Table 7.1; Addy and Ypma, 1977; Munha et al., 1986; this study).

Shale ultrafiltration, evaporation and/or boiling cause net positive increases in D of up to eight times greater than related increases in ^{18}O (Taylor, 1974; Ripley and Ohmoto, 1979 Munha et al., 1986). None of these processes produce fluids with D compositions similar to the fluids which equilibrated with muscovite in the Rambler deposit.

Gregory and Taylor (1981) developed a model for the generation of high ^{18}O, low D fluids during the formation of the Samail ophiolite. Stratigraphic relationships and $\delta^{18}O$ systematics in the ophiolite attribute high ^{18}O fluids to the development of decoupled lower and upper hydrothermal systems at a fast spreading oceanic ridge (Gregory and Taylor, 1981). Fluid convection in the upper system occurred at high W/R ratios, so that seawater was only slightly shifted from its $\delta^{18}O$ and δD fluid composition of 0 ‰ (SMOW) (Craig et al., 1980; Bowers and Taylor, 1985). Fluid convection in the lower hydrothermal system occurred at low W/R ratios (0.3-1.0 mass units) causing ^{18}O enrichments and D shifts of -20 ‰ at temperatures $\geq$ 400°C. ^{18}O depletions associated with normal seafloor alteration and hydration in the Samail are overprinted by ^{18}O enrichments related to the discharge of high ^{18}O fluids from the lower convection system (Gregory and Taylor, 1981). The isotopic data is consistent with the presence of similar high ^{18}O fluids during the formation of the high temperature chlorite in the Rambler VMS deposit. However, the fluids in equilibrium with the pervasive light green chlorite and muscovite in the Rambler deposit are not enriched in ^{18}O ($<$ +5 ‰).

There are also several possible sources for high ^{18}O, low D fluids associated with mesothermal gold deposits during the formation of continental margin orogenic belts (Fyfe and Kerrich, 1985). Fluids from subducting oceanic crust ($\leq$ 100km) cause melting in the lower crust and upper mantle during the generation of arc plutonic complexes (Anderson, 1981; Fryer et al., 1992). Dehydration and anatectic reactions during the formation of these plutonic melts are associated with the generation of high ^{18}O and low D metamorphic and/or magmatic fluids near greenschist-amphibolite transitions at depths of 10 to 15 kilometres (Taylor, 1974; Taylor and Sheppard, 1986).

In general, the isotopic composition of these high ^{18}O low D fluids are not the same as those in equilibrium with muscovite in the Rambler VMS deposit.

Fluids are also expelled from obducted oceanic crust and continental strata during compressive orogenesis and obduction (Kyser and Kerrich, 1992). These may originate from a variety of sources. For example, Timball (1992) distinguishes between fluids related to serpentinization, and later CO_2- rich fluids associated with the obduction of the Coy Pond Ophiolite in Central Newfoundland by demonstrating $\delta^{13}C$ values of 0 to -20 ‰ for the CO_2 - rich fluids in equilibrium with magnesite were caused by the mixing of marine (organic) and igneous carbon from the obducting ophiolite, and subcreted continental margin sediments, respectively.

The complex fluid history in the Coy Pond Complex was likely repeated during the obduction of the Paquet Harbour Group. Isotopic data from the Rambler deposit suggests a mixture of seawater, ^{18}O-shifted seawater and related fluids equilibrated with the light green chlorite during regional deformation. The low D orogenic fluids in equilibrium with stage 2 muscovite may have originated from similar sources, such as repeated greenschist to amphibolite transitions associated with the stacking of ophiolite and underlying sedimentary successions. However, fluids associated with syn-kinematic alteration in the Rambler deposit were not enriched in CO_2, in contrast to the fluids associated with the emplacement and obduction of the Coy Pond Ophiolite Complex and mesothermal gold deposits in general.

Later in the orogenic cycle during transpressive and/or extensional deformation, and at shallow crustal depths where $P_{fluid} \leq P_{litho}$, there may have been an influx of meteoric fluids into regional structures in the Pacquet Harbour Group, resulting in the production of a low ^{18}O, low D fluid during or after peak regional compressive deformation (Kyser and Kerrich, 1992), and prior to peak regional metamorphism associated with the intrusion of large plutonic bodies such as the nearby Burlington Granodiorite. These events are consistent with the formation of the shear zones in the footwall of the Rambler

deposit and the overprinting of stage 1 and stage 2 chlorites, by muscovite. Overprinting relationships suggest the late introduction of high ^{18}O fluids in equilibrium with biotite coincided with the Silurian intrusion of the Burlington Granodiorite providing a minimum age for deformation and accompanying fluid alteration in the Rambler deposit of 432 $\pm$ 2 Ma (per. comm. Dunning, 1993).

The timing and uniqueness of the low D fluid in the Rambler is supported not only by petrographic and isotopic relationships, but also by the $\delta^{18}O$ and δD values of chlorite and muscovite from the alteration assemblages of two epigenetic deposits located in the Baie Vert and Springdale areas (Ramezani, 1993; Ritcey, 1993). δD chlorite values near -70 ‰ and muscovite values near -60 ‰ from the Stog'er Tight, and δD chlorite values near -75 ‰ and muscovite values near -65 ‰ in the Hammer Down gold deposits suggest that chlorite and muscovite in the alteration assemblages of these deposits were in equilibrium with the same fluid. A U/Pb minimum age of 420 $\pm$ 5 Ma for hydrothermal zircon (Ramezani, 1992) in the Stog'er Tight, is consistent with the formation of the deposit sometime after the high ^{18}O fluid event associated with the intrusion of the Burlington Granodiorite (432 $\pm$ 2 Ma) during peak regional metamorphism at 427 to 436 Ma (pers. comm., G.R. Dunning, 1993), well after the stage 2 kinematic alteration in the Rambler.

The lack of carbonate alteration in the stage 2 alteration assemblages, and the isotopic data from this study are both factors not consistent with the presence of mesothermal fluids during the deformation and alteration of the Rambler deposit. Instead, isotopic data suggests the fluids were different from the CO_2 -rich fluids present during the formation of the Stog'er Tight and Hammer Down epigenetic / mesothermal deposits. As such, mesothermal fluids were probably not associated with gold mineralization. It is more likely that gold in the Rambler deposit is syngenetic, and was subsequently remobilized and reconcentrated during alteration and metamorphism. Evidence presented in this study, however, does not rule out the possibility of an alternate source for the

gold during later thermal alteration related to the presence of disseminated metamorphic biotite in the stratigraphy of the deposit.

Conclusions

The Rambler VMS deposit is similar to other deformed VMS deposits which occur in Archean and Phanerozoic volcanic terrains. It occurs in a mixed sequence of mafic and felsic intrusive, volcanic and sedimentary rocks which typify the central portion of the Pacquet Harbour Group. It is deformed to the extent that its alteration and recrystallized sulphide mineralization are the only consistent stratigraphic markers in a structurally intercalated, upright stratigraphic sequence. Mineral assemblages in the deposit are consistent with greenschist to upper greenschist grades of metamorphism which are commonly associated with the alteration in both VMS and epigenetic / mesothermal deposits.

The deposit contains three common types of alteration. Stage 1 alteration is indistinguishable from metamorphic and alteration assemblages normally associated with basalt hydration, greenschist metamorphism and seafloor hydrothermal alteration (Alt et al., 1985). Stage 2 alteration is similar to the alteration associated with epigenetic mineralization in the Baie Verte region and in Central Newfoundland (Huard 1989; Dubé, 1990; Evans, 1992), and the syn-kinematic alteration normally associated with mesothermal gold deposits, except for its complete lack of syn-kinematic carbonate alteration. Stage 1 and stage 2 are dominant alteration assemblages in massive and disseminated sulphide horizons in the deposit and footwall sections of the stratigraphy. Stage 3 albite + quartz $\pm$ calcite $\pm$ chlorite, and/or quartz $\pm$ calcite $\pm$ chlorite veins are common in the alteration associated with both syngenetic and epigenetic varieties of mineralization.

The Rambler also contains two common varieties of sulphide mineralization. The massive sulphide mineralization ($\geq$80% sulphides) is identical to descriptions of similar massive

sulphide assemblages in numerous deformed and recrystallized VMS deposits, and thus probably related to an early seafloor hydrothermal alteration / mineralization. Disseminated sulphides in highly deformed footwall schists and mylonites may be related either to original seafloor or later fluid alteration in the stratigraphy of the deposit during regional metamorphism and local alteration. Both varieties of mineralization are overprinted by secondary sulphide and telluride assemblages with textural and petrographic relationships consistent with a late thermal overprint in the stratigraphy of the deposit. Gold occurs as electrum and telluride phases concentrated in the massive sulphide horizons of the deposit, and as such, is probably syngenetic in origin.

$\Delta^{18}O$ temperatures and calculated $\delta^{18}O$ and δD fluid values confirm the complex multi-stage thermal and fluid history suggested by petrographic relationships among the different silicate alteration assemblages in the Rambler deposit. Early high temperature hydrothermal activity is associated with the presence of a fine grained, dark green chlorite, which occurs only in recrystallized massive sulphides, and which equilibrated with a high ^{18}O fluid; $\delta^{18}O$ and δD fluid values of +9.0 to +9.4 ‰ and -39 ‰, respectively, at 430 to 480°C. A subsequent decrease in temperatures (~200 to 300°C) and shift in $\delta^{18}O$ fluid values to +4.4 and +4.6 ‰, and δD fluid values -26 to -37 ‰ is associated with the formation of the pervasive syn-kinematic light green chlorite, which overprints the dark green chlorite. The light green chlorite appears to have equilibrated with a mixture of seawater, ^{18}O-shifted seawater and metamorphic fluids present during regional greenschist metamorphism and deformation in the Pacquet Harbour Group. Lower $\delta^{18}O$ fluid values of 0 to +4.1 ‰ at 180 to 200°C are related to cooling and an influx of meteoric waters during waning fluid activity and the syn to post-kinematic formation of stage 3 veins.

In contrast to $\delta^{18}O$ and δD silicate and fluid data, $\delta^{34}S$ analyses provide little evidence to suggest a complex thermal and fluid history in the Rambler VMS deposit. Homogeneous $\delta^{34}S$ values suggest disequilibrium among recrystallized sulphide assemblages. $\delta^{34}S$ data from the Rambler are similar to those from the analyses of sulphides in Archean and

Phanerozoic VMS deposits, mesothermal gold deposits, and consistent with $\delta^{34}S$ sulphide values from other Newfoundland VMS deposits in similar settings (Valley et al., 1987; Bachinski, 1977, 1978).

A late thermal event is suggested by the sporadic occurrence of biotite porphyroblass, which yield relatively high $\Delta^{18}O_{qtz\text{-}bio}$ temperatures of approximately 540 to 560 °C. These are in sharp contrast to the lower temperatures which range from 180 to 310 °C for stage 1, stage 2 and stage 3 alteration assemblages, which contain low ^{18}O light green chlorite. Fluids in equilibrium with the biotite have comparatively high $\delta^{18}O$ and δD values of +7.5 and +5.7 ‰ and -41 to -49 ‰, respectively. Similar biotite in the contact assemblages along the margin of the Burlington Granodiorite (pers. comm., M.R. Wilson, 1993) suggest its intrusion may correlate with a high ^{18}O thermal event, indicating a possible minimum age of 427 ± 2 Ma for deformation and syn-kinematic alteration in the Rambler deposit (pers. comm., G.R. Dunning, 1993).

The possible presence of a distinct low ^{18}O (< +5 ‰), low D (< -60 ‰) fluid during deformation in the Rambler deposit is suggested by $\delta^{18}O$ and δD mineral values of +6.4 to +8.2 ‰ and -55 to -70 ‰ for muscovite which are not in equilibrium with values of +2.9 to +7.5 ‰ and -57 to -73 ‰ for the coexisting light green chlorite in stage 1 and stage 2 alteration assemblages. The isotopic composition of this fluid is distinct from those associated with seafloor volcanogenic and metamorphic processes (Ripley and Ohmoto, 1979; Barriga and Kerrich, 1981; Beatty and Taylor, 1982; Munha et al., 1986), and the CO_2-rich, high ^{18}O, low D fluids which equilibrated with chlorite and muscovite during the formation of the Stog'er Tight and Hammer Down mesothermal gold deposits on the Baie Verte peninsula, and in the Springdale area, respectively (Ramezani, 1993; Ritcey, 1993).

The absence of carbonate alteration, petrographic relationships, and isotopic data suggest that overprinting stage 2 alteration in the footwall shear zone of the Rambler was not

associated with a mesothermal fluid event. An interpretation which would seem to negate the possibility of a mesothermal source for the gold in the RAmbler VMS deposit. The preferred interpretation is that gold is syngenetic, and that it was locally remobilized and reconcentrated during the deformation and kinematic alteration associated with stage 2 alteration, and during the subsequent metamorphic recrystallization associated with a late thermal event in the stratigraphy of the deposit (Boyle, 1979; Huston and Large, 1989). However, evidence presented in this study cannot rule out an external source for gold during or after a late thermal event associated with the sporadic formation of biotite porphyroblasts throughout the stratigraphy of the deposit.

References

Addy, S.K., and Ypma, P.J.M., 1977. Origin of massive sulphide deposits at Ducktown, Tennessee: An oxygen, carbon and hydrogen isotope study. Economic Geology, v. 72, p. 1245-1268.

Afifi, A.M. Kelley, W C. and Essene, E.J., 1988. Phase relations among tellurides, sulfides and oxides. Part II: Applications to telluride-bearing ore deposits. Economic Geology, v. 83, p. 395-404.

Alt, J.C., Laverne, C., and Muehlenbachs, K., 1985. Alteration of the upper oceanic crust: Mineralogy and processes in deep sea drilling project hole 504B, leg 83. DSDP Initial Reports, v. 83, p. 217-247.

Anderson, R.N., 1981. Surprises from the Glomar Challenger. Nature, v. 293, p. 261-262.

Bachinski, D. J., 1977. Sulfur isotopic compositions of ophiolitic cuperiferous iron sulfide deposits, Notre Dame Bay, Newfoundland. Economic Geology, v.72, p.243-257.

Bachinski, D. J., 1978. Sulfur isotopic composition of thermally metamorphosed cuperiferous iron sulfide ores associated with cordierite-anthophyllite rocks, Gull Pond, Newfoundland, Economic Geology, v.74, p.64-73.

Baird, D.M., 1951. The geology of the Burlington Peninsula, Newfoundland. Geological Survey of Canada, Paper 51-21, 70 p.

Baragar, W.R.A., 1954. Geological Report - Rambridge Mines Ltd., Consolidated Rambler Mines Ltd. Unpublished report.

Barnes H.L., 1969. Solubilities of ore minerals. In: Barnes, H.L., ed., Geochemistry of Hydrothermal Ore Deposits II. John Wiley and Sons, New York / Toronto, p. 404-454.

Barrett, T.R. and Friedrichsen, H., 1989. Stable isotopic composition of atypical ophiolitic rocks from East Liguria, Italy. Chemical Geology (Isotope Geoscience), v. 80, p. 71-84.

Barriga, F.J.A.S. and Kerrich, R., 1981. High ^{18}O fluids, circulation regimes, and mineralization at Adjustrel, Iberian Pyrite Belt (abs.). Geological Society of America Abstracts with Programs, v.13, p.403-404.

Beane, R.E. and Titley, S.R., 1981. Porphyry copper deposits. Part II. Hydrothermal alteration and mineralization. Economic Geology. 75th Anniversary Volume. p. 235-269.

Beatty, D.W. and Taylor, H.P. Jr., 1982. Some petrological and oxygen isotopic relationships in the Amulet Mine, Noranda, Quebec, and their bearing on the origin of Archean massive sulphide deposits. Economic Geology, v. 77, p. 95-108.

Beatty, D.W. and Taylor, H.P. Jr., 1988. An oxygen isotope study of the Kidd Creek volcanogenic massive sulphide deposit: evidence for a high ^{18}O ore fluid. Economic Geology, v. 83, p. 1-18.

Bell, K. and Blenkinsop, J., 1981. A geochronological study of the Buchans area, Newfoundland. In Swanson, E.A., Strong, D.F. and Thurlow, J.G. (eds.), The Buchans Orebodies: Fifty Years of Mining and Geology. Geological Association of Canada, Special Paper 22, p. 91-112.

Berger, B.R., 1982. The geological attributes of Au-Ag base metal epithermal deposits. In: Erickson, R.L. (ed.). Characteristics of Mineral Deposit Occurrences. United States Geological Survey. Open File Report 82-795, p. 119-126.

Betz, F., Jr., 1948. Geology and mineral deposits of southern White Bay. Newfoundland Geological Survey, Bulletin 24, 24 p.

Bird, J.M. and Dewey, J.F., 1970. Lithospheric Plate-continental margin tectonics and the evolution of the Appalachian Orogen. Geological Society of America Bulletin, v. 81, p. 1031-1060.

Bischoff, J.L., 1969. Red Sea geothermal brine deposits. In Degens, E. T. and Ross, D.A., (eds.), Hot Brines and Heavy Metal Deposits of the Red Sea. Springer Verlag, New York, p. 348-401.

Bischoff J.L. and Dickson, F.W., 1975. Seawater-basalt interaction at 200°C and 500 bars: implications for the origin of seafloor heavy metal deposits and regulation of seawater chemistry. Earth and Planetary Science Letters, v. 25, p. 385-397.

Bostock, H.H., Currie, K.L. and Wanless, R.K., 1979. The age of the Robert's Arm Group, north central Newfoundland. Canadian Journal of Earth Sciences, v. 16, p. 599-606.

Bottinga, Y. and Javoy, M., 1973. Comments on oxygen isotope geothermometry. Earth and Planetary Science Letters, v. 20, p. 250-265.

Bottinga, Y., 1975. Oxygen isotope partitioning among the minerals in igneous and metamorphic rocks. Reviews Geophysics and Space Physics, v. 13, p. 401-418.

Bowers, T.S. and Taylor, H.P., Jr., 1985. An integrated chemical and stable isotope model of the origin of mid-ocean ridge hot spring systems. Journal of Geophysical Research, B14, v. 90, p. 12853-12606.

Boyle, R.W., 1979. The geochemistry of gold and its deposits. Geological Survey of Canada Bulletin, v. 280, 584 p.

Brown, P.A. and Colman-Sadd, S.P., 1976. Hermitage Flexure: figment or fact ? Geology, v. 4, p. 561-564.

Bursnall, J.T., 1975. Stratigraphy, structure, and metamorphism west of Baie Verte, Burlington Peninsula, Newfoundland. Unpublished Ph.D. thesis; Cambridge University, England. 337 p.

Cabri, L.J., 1965. Phase relations in the Au-Ag-Te system and their mineralogical significance. Economic Geology, v. 60, p. 1569-1606.

Cameron, W.E., Nisbet, E.G., and Dietrich, V.J., 1979. Boninites, komatiites and ophiolitic basalts. Nature, v. 280, p. 550-553.

Church, W. R., 1969. Metamorphic rocks of the Burlington Peninsula and adjoining areas of Newfoundland and their bearing on continental drift in the North Atlantic. In: Kay, M., ed., North Atlantic Geology and Continental Drift. American Association of Petroleum Geologists, p. 212-233.

Church, W.R. and Stevens, R.K., 1971. Early palaeozoic ophiolite complexes of the Newfoundland Appalachians as mantle-oceanic crust sequences. Journal of Geophysical Research, B5, v. 76, p. 1460-1466.

Clayton, R.N. and Mayeda, T.K., 1963. The use of bromine pentaflouride in the extraction of oxygen from oxides and silicates for isotopic analyses. Geochemica et Cosmochimica Acta, v. 12, p. 43-52.

Clayton, R.N., O'Neil, J.R. and Mayeda, T.K., 1972. Oxygen isotope exchange between quartz and water. Journal of Geophysical Research, v. 77, p. 3057-3967.

Coates, H., 1990. Geology and mineral deposits of the Rambler property. In: Swinden, H.S., Evans, D.W.T. and Kean, B.F. (eds.), Metallogenic Framework of Base and Precious Metal Deposits, Central and Western Newfoundland. Geological Survey of Canada, p. 184-200.

Coish, R.A., 1977. Petrology of the mafic units of west Newfoundland ophiolites. Unpublished Ph.D. thesis, University of Western Ontario, Ontario, 277 p.

Coish, R.A., 1977. Ocean floor metamorphism in the Betts Cove Ophiolite, Newfoundland. Contributions Mineralogy and Petrology, v. 60, p. 255-270.

Coish, R.A., Hickey, R. and Frey, F.A., 1982. Rare earth element geochemistry of the Betts Cove ophiolite, Newfoundland: Complexities in ophiolite formation. Geochemica et Cosmochimica Acta, v. 46, p. 2117-2134.

Colman-Sadd, S.P., 1980. Geology of south-central Newfoundland and the evolution of the eastern margin of Iapetus. American Journal of Science, v. 280, p. 991-1017.

Colman-Sadd, S.P. and Swinden, H.S., 1984. A tectonic window in central Newfoundland? Geological evidence that the Appalachian Dunnage zone may be allochthonous. Canadian Journal of Earth Sciences, v. 21, p. 1349-1367.

Colvine, A.C., 1988. An empirical model for the formation of Archean lode gold deposits: products of the final cratonization of the Superior Province, Canada. Economic Geology, Monograph 6, p. 37-54.

Colvine, A.C., Fyon, J.A., Heather, K.B., Marmont, S., Smith, P.M. and Troop, D.G., 1988. An integrated model for the origin of Archean lode gold deposits. Ontario Geological Survey, Open File Report 5524, 98 p.

Constantinou, G. and Govett, J.S., 1973. Geology, geochemistry and genesis of Cyprus Sulphide Deposits. Economic Geology, v. 68, p. 843-858.

Cox, D.P., 1982. A generalized empirical model for porphyr copper deposits. In: Erikson, R.L. (ed.), Characteristics of Mineral Occurrences. United States Geological Survey, Open File Report 82-795, p. 27-32.

Coyle, M., 1990. Geology, geochemistry and geochronology of the Springdale Group: An early Silurian caldera in Central Newfoundland. Unpublished Ph.D thesis, Memorial University, St. John's, Newfoundland.

Craig, H., 1957. Isotopic standards for carbon and oxygen and correction factors for mass-spectrometer analysis of carbon dioxide. Geochemica et Cosmoschimica Acta, v. 12, p. 1833-1834.

Craig, H., 1961. Standards for reporting concentrations of deuterium and oxygen-18 in natural waters. Science, v. 133, p. 35-43.

Craig, H., Welhan, J.A., Kim, K., Poreda, R. and Lupton, J.E., 1980. Geochemical studies of the 21°N EPR hydrothermal fluids. EOS Transactions: American Geophysical Union, p. 992.

Dallmeyer, R.D., Hussey, E.M., O'Brien, S.J. and O'Driscoll, C.F., 1981. Geochronology of the Swift Current Granite and host volcanic rocks of the Love Cove Group, southwestern Avalon Zone, Newfoundland: Evidence of a late Proterozoic volcanic-subvolcanic association. Canadian Journal of Earth Science, v. 20, p. 355-363.

De Grace, J. R., Kean, B.F. and Besaw, D.M., 1975. Geology of the Nippers Harbour map area (NTS 2E/13). Newfoundland Department of Mines and Energy, Open File 788, 59 p.

De Wit, M.J., 1974. On the origin and deformation of the Fleur de Lys metaconglomerate, Appalachian fold belt, northwest Newfoundland. Canadian Journal of Earth Science, v. 11, p. 1168-1180.

De Wit, M.J., 1980. Structural and metamorphic relationships of pre-Fleur de Lys and Fleur de Lys rocks on the Baie Verte Peninsula, Newfoundland. Canadian Journal of Earth Science, v. 17, p. 1559-1575.

Dean, P.L. and Strong, D.F., 1975. Springdale, Newfoundland. Geological Survey of Newfoundland, Open File Map 379.

Deer, W. A., Howie, R.A. and Zussman, J., 1966. An Introduction to the Rock Forming Minerals. Longman Group Limited, Essex, England. 528 p.

Dewey, J.F. and Bird, J.M., 1971. Origin and emplacement of ophiolite suites: Appalachian ophiolites in Newfoundland. Journal of Geophysical Research, v. 76, p. 3179-3206.

Dimmel, P. and Hartley, C., 1992. Gold mineralization and exploration potential of the Pine Cove property, Baie Vert Peninsula. In: Swinden, H. S. and Hogan, A. (eds.), Ore Horizons. Newfoundland Department of Mines and Energy, p. 51-62.

Douglas, V.G., Williams, D., Rove, O.N. and others, 1940. Copper Deposits of Newfoundland. Geological Survey of Newfoundland, Bulletin 20, 176 p.

Dubé, B., 1990. Contrasting styles of gold-only deposits in western Newfoundland: A preliminary report. Geological Survey of Canada, Paper 90-1BA, p. 77-90.

Dubé, B., Guha, J. and Rocheleau, M., 1987. Alteration patterns related to Au mineralization and their relation to CO_2/H_2O ratios. Mineralogy and Petrology, v. 37, p. 267-291.

Dubé, B., Koopman S.J., Franklin, J.M., Poulsen, K.H. and Patterson, M.R., 1989. Preliminary study of the stratigraphic and structural controls of the Lyon Lake massive sulphide deposit, Wabigoon Subprovince, northwestern Ontario. Geological Survey of Canada, Paper 89-1C, p. 275-284.

Dunning, G.R., 1988. Advanced Techniques in U/Pb zircon geochronology applied to stratigraphic correlation: examples from the Ordovician of the Appalachians. Fifth International Symposium on the Ordovician System, St. John's Newfoundland, program with abstracts, p. 26.

Dunning, G.R. and Chorlton, L.B., 1985. The Annieopscotch ophiolite belt of southwest Newfoundland: geology and tectonic significance. Geological Society of America Bulletin, v. 96, p. 1466-1476.

Dunning, G.R. and Krogh, T.E., 1985. Geochronology of ophiolites of the Newfoundland Appalachians. Canadian Journal of Earth Sciences, v. 22, p. 1175-1184.

Dunning, G.R., Krogh, T.E., Kean, B.F., O'Brien, S. and Swinden, H.S., 1986. U/Pb ages of volcanic groups from the Central Mobile Belt, Newfoundland. Geological Society of Canada, Program with Abstracts, v. 11, p. 66.

Dunning, G.R., Kean, B.F., Thurlow, J.G. and Swinden, H.S., 1987. Geochronology of the Buchans, Roberts Arm, and Victoria Lake Groups and Mansfield Cove Complex, Newfoundland. Canadian Journal of Earth Science, v. 11, p. 1175-1184.

Dunning, G.R., Swinden, H.S., Kean, B.F., Evans, D.W.T. and Jenner, G.A., 1991. A Cambrian island arc in Iapetus: Geochronology and geochemistry of the Lake Ambrose volcanic belt, Newfoundland Appalachians. Geology Magazine, v. 128(1), p. 1-17.

Epstein, S. and Mayeda, T.K., 1953. Variations of ^{18}O content of waters from natural sources. Geochimica et Cosmochimica Acta, v. 4, p. 213-224.

Eslinger, E.V. and Savin, S.M., 1973. Mineralogy and oxygen isotope geochemistry of the hydrothermally altered rocks of the Ohaki - Broadlands, New Zealand geothermal area. American Journal of Science, 273, p. 240-270.

Eslinger, E.V., Savin, S.M. and Yeh, H., 1979. Oxygen isotope geothermometry of diagenetically altered shales. SEPM Special Publication No. 26, March, p.113-124.

Evans, D.W.T., 1992. Gold metallogeny of the eastern Dunnage Zone, Central Newfoundland. Newfoundland Department of Mines and Energy, Current Research, Report 92-1, p. 231-245.

Evans, D.W.T. and Kean, B.F., 1987. Gold and massive sulphide mineralization in the Tulks Hill volcanics, Victoria Lake Group, Central Newfoundland. Newfoundland Department of Mines and Energy, Current Research, Report 87-1, p. 103-111.

Evans, D.W.T., Kean, B.F. and Dunning, G.R., 1990. Geological studies, Victoria Lake Group, Central Newfoundland. Newfoundland Department of Mines and Energy, Current Research 90-1, p. 144.

Franklin, J.M., Lydon, J.W. and Sangster, D.F., 1981. Volcanic-associated massive sulphide deposits. 75th. Anniversary Volume, Economic Geology, p. 485-627.

Friedman, I. and Hardcastle, K., 1988. Deuterium in interstitial water from deep-sea cores. Journal of Geophysics Research, v. 93, p. 8249-8263.

Fryer, B. J., Kerr, A., Jenner, G.A. and Logstaffe, F.J., 1992. Probing the crust with plutons: Regional isotopic geochemistry of granitoid intrusions across Insular Newfoundland. Newfoundland Department of Mines and Energy, Current Research 92-1, p. 199-140.

Fuller, J.O., 1941. Geology and mineral deposits of the Fleur de Lys area, Newfoundland. Geological Survey of Newfoundland, Bulletin 15, 41 p.

Fyfe, W.S. and Kerrich, R., 1984. Gold: natural concentration processes. In: Foster, R. P., ed., The Geology, Geochemistry and Genesis of Gold Deposits. Geological Society of Zimbabwe, Rotterdam, p. 99-127.

Fyfe, W.S. and Kerrich, R., 1985. Fluids and Thrusting. Chemical Geology, v. 49, p. 353-362.

Fyon, J.A. Crocket, J.H. and Schwarez, H.P., 1983. Application of stable isotope studies to gold metallogeny in the Timmins - Porcupine camp. Ontario Geological Survey, Open File Report 5464, 182 p.

Fyon, J.A., Schwarez, H.P. and Crocket, J.H., 1984. Carbonatization and gold mineralization in the Timmins area Abitibi greenstone belt: genetic links with

Archean mantle CO_2 - degassing and lower crust granulitization. Geological Association of Canada, Program with Abstracts, v. 9, p. 65.

Gale, G.H., 1971. An investigation of some sulphide deposits of the Rambler area, Newfoundland. Unpublished Ph.D. thesis, University of Durham, England.

Gale, G.H., 1973. Palaeozoic komatiite and ocean floor type basalts from northeast Newfoundland. Earth and Planetary Science Letters, v. 18, p. 22-28.

Gieskes, J.M., 1981. Deep sea drilling interstitial water studies: Implications for the chemical alteration of the oceanic crust, layers I and II. In The Deep Sea Drilling Project: A Decade of Progress. Society of Economic Paleontologists and Mineralogists, p. 149-168.

Gjelsvik, T., 1968. Distribution of major elements in the wall rocks and silicate fraction of the Skorovass pyrite deposit, Grong area, Norway. Economic Geology, v. 63, p. 217-231.

Godfrey, J.D., 1962. The deuterium content of hydrous minerals from the East Central Sierra Nevada and Yosemite National Park. Geochemica et Cosmochimica Acta, v. 26, p. 1215-1245.

Goldfarb, M.S., Converse, D.R., Holland, H.D. and Edmund, J.M., 1983. The genesis of hot spring deposits on the East Pacific Rise, 21°N. Economic Geology, Monograph 5, p. 184-197.

Goldfarb, R.J., Leach, D.L., Pickthorn, W.J. and Patterson, C.J., 1988. Origin of the lode gold deposits of the Juneau gold belt, southeastern Alaska. Geology, v. 16, p. 440-443.

Goodwin, L.B. and Williams, P.F., 1990. Strike-slip motion along the Baie Verte Line, Newfoundland. Atlantic Geoscience Society, Colloquium, p. 13.

Gower, D. Graves, G., Walker, S. and MacInnis, D., 1988. Lode gold mineralization at Deer Cove, Point Rousse Complex, Baie Vert Peninsula. In: Swinden, H. S. and Kean, B.F. (eds.), The Volcanogenic Massive Sulphide Districts of Central Newfoundland. Geological Association of Canada / Newfoundland Department of Mines and Energy, p. 43-48.

Graham, U.M., Bluth, G.J. and Ohmoto, H., 1988. Sulphide-sulfate chimneys on the East Pacific Rise, 11° and 13° north latitudes. Part I: Mineralogy and Paragenesis. Canadian Mineralogist, v. 26, p. 487-504.

Gregory, R.T. and Taylor, H.P. Jr., 1981. An oxygen isotope profile in a section of Cretaceous oceanic crust, Samail Ophiolite, Oman: Evidence for $\delta^{18}O$ buffering of the oceans by deep (>5km) seawater - hydrothermal circulation at mid-ocean ridges. Journal of Geophysical Research, B4, v. 86, p. 1737-2755.

Gresens, R.L., 1976. Composition - volume relationships of metasomatism. Chemical Geology, v. 2, p. 318.

Guha, J., Dubé, B., Pilote, P., Chown, E.H., 1988. Gold mineralization patterns in relation to the lithological and tectonic evolution of the Chibougamau Mining District, Quebec, Canada. Mineralium Deposita, v. 23, p. 293-298.

Hajash, A. Jr., 1975. Hydrothermal processes along mid-ocean ridges: An experimental investigation. Unpublished Ph.D. thesis, Texas A and M University, 503 p.

Hannington, M.D., 1989. The geochemistry of gold in modern seafloor hydrothermal systems and implications for gold mineralization in ancient volcanogenic massive sulphide deposits. Unpublished Ph.D. thesis, University of Toronto, Canada.

Hannington, M.D., Herzig, P., Scott, S., Thompson, G., and Rona, P., 1991. Comparative mineralogy and geochemistry of gold-bearing sulphide deposits on the mid-ocean ridges. Marine Geology, v. 101, p. 217-248.

Harland, W.B. and Gayer, R.A., 1972. The Arctic Caledonides and earlier oceans. Geology Magazine, v. 109, p. 289-314.

Hattori, K., 1987. Magmatic felsic intrusions associated with Canadian Archean gold deposits. Geology, v. 15, p. 1107-1111.

Hattori, K. and Sakai, H., 1979. D/H ratios, origins, and evolution of the ore-forming fluids for the Neogene veins and Kuroko deposits of Japan. Economic Geology, v. 74, p. 535-555.

Hattori, K. and Meuhlenbachs, K., 1980. Marine hydrothermal alteration at a Kuroko deposit, Kosaka, Japan. Contributions to Mineralogy and Petrology, v. 74, p. 285-292.

Heald, P., Foley, N.K. and Hayba, D.O., 1987. Comparative anatomy of volcanic-hosted epithermal deposits: Acid-sulfate and adularia-sericite types. Economic Geology, v. 82, p.1-26.

Heaton T.H.E. and Sheppard, S. M. F., 1977. H and O isotope evidence for seawater hydrothermal alteration and deposition, Troodos Complex, Cyprus. In: Volcanic Processes in Ore Genesis; Canadian Press Ltd, p. 42-58.

Heenan, P.R., 1973. The discovery of the Ming zone, Consolidated Rambler Mines Ltd., Baie Verte, Newfoundland. Canadian Institute of Mining and Metallurgy Bulletin, v. 66, p. 78-88.

Herzig, P.H., Becker, K.P., Stoffer, D., Backer, H. and Blum, N., 1988. Hydrothermal silica chimney fields in the Galapagos spreading centre. Earth and Planetary Science Letters, v. 89, p. 261-272.

Hibbard, J. and Bursnall, J.T., 1979. Geology of the Horse Islands, Newfoundland. In: Gibbons, R. V., ed., Report of Activities for 1978; Newfoundland Department of Mines and Energy, Mineral Development Division, p. 64-65.

Hibbard, J., 1983. Geology of the Baie Verte Peninsula, Newfoundland. Newfoundland Department of Mines and Energy, Memoir 2, 279 p.

Huard, A., 1989. Epithermal alteration and gold mineralization in late Precambrian volcanic rocks on the northern Burin Peninsula, southeastern Newfoundland, Canada. Unpublished M.Sc. thesis; Memorial University of Newfoundland, St. John's, Newfoundland.

Huard, A., and O'Driscoll, C., 1986. Epithermal gold mineralization in late Precambrian volcanic rocks on the Burin Peninsula. Newfoundland Department of Mines and Energy, Current Research, 86-1, p. 65-78.

Hudson, K.A., 1988. Gold and Base Metal Mineralization in the Nippers Harbour Ophiolite, Newfoundland. Unpublished MSc thesis, Memorial University of Newfoundland, St. John's, Newfoundland.

Hudson, K.A. and Swinden, H.S. (in prep). The Lake Bond deposit: Superimposed volcanogenic and syn-kinematic base and precious metal mineralization in the Robert's Arm Group, Central Newfoundland. Unpublished manuscript, Newfoundland Department of Mines and Energy, 33 p.

Hughes, C.J., 1972. Spilites, keratophyres and the igneous spectrum. Geology Magazine, v. 109, p.513-527.

Huston, D.L. and Large, R.R., 1989. A chemical model for the concentration of gold in volcanogenic massive sulphide deposits. Ore Geology Review, v. 4, p. 171-200.

Hutchinson, R.W., 1973. Volcanogenic sulphide deposits and their metallogenic significance. Economic Geology, v. 68, p. 1223- 1246.

Hutchinson, R.W., 1987. Metallogeny of Precambrian Au deposits, space and time relationships. Economic Geology, v. 82, p. 1993-2007.

Jemielita, R.A., Davis, D.W. and Krogh, T.E., 1990. U-Pb evidence for Abitibi gold mineralization post-dating greenstone magmatism and metamorphism. Nature, v. 346, p. 831-834.

Jenner, G.A., Kean, B.F. and Evans, D.W.T., 1988. The Lushs Bight Group revisited: new trace element and Sm/Nd isotopic evidence for its tectonic environment of formation. In: Geological Association of Canada, Program with Abstracts, v. 13, p. 61.

Kallioski, J., 1965. Metamorphic features on North American massive sulphide deposits. Economic Geology, v. 60, p. 485-505.

Kamo, S.L., Gower, C.F. and Krogh, T.E., 1989. Birthdate for the Iapetus Ocean ? A precise U-Pb zircon and baddeleyite age for the Long Range dikes, southeast Labrador. Geology, v. 17, p. 602-605.

Kappel, E.S., and Franklin, J.S., 1989. Relationships between geological development of ridge crests and sulphide deposits in the Northeast Pacific Ocean. Economic Geology, v. 84, p. 485-505.

Kashida, A. and Kerrich, R., 1987. Hydrothermal alteration zoning and gold concentration at the Kerr-Addison Archean lode gold deposit, Kirkland Lake, Ontario. Economic Geology, v. 82, p. 649-690.

Kean, B. F. and Evans, D.W.T., 1988. Regional metallogeny of the Victoria Lake Group, Central Newfoundland. Newfoundland Department of Mines and Energy, Current Research 88-1, 24 p.

Kennedy, M.J., 1971. Structure and stratigraphy of the Fleur de Lys Supergroup in the Fleur de Lys area, Burlington Peninsula, Newfoundland. Geological Association of Canada, Proceedings, v. 24, p. 59-71.

Kennedy, M.J., 1973. Pre-Ordovician polyphase structure in the Burlington Peninsula of the Newfoundland Appalachians. Nature, v. 241, p. 114-116.

Kennedy, M.J., 1975a. The Fleur de Lys Supergroup: stratigraphic comparison of Moine and Dalradian equivalents in Newfoundland with the British Caledonides. Geological Society of London, v. 131, p. 305-310.

Kennedy, M.J., 1975b. Repetitive orogeny in the northeastern Appalachians: New plate models based on Appalachian examples. Tectonophysics, v. 28, p. 39-87.

Kerrich, R.W., 1987. The stable isotope geochemistry of Au-Ag vein deposits in metamorphic rocks. In Kyser, T. K., ed., Stable Isotope Geochemistry of Low-Temperature Fluids. Mineralogical Association of Canada, p. 287-336.

Kerrich, R.W., 1989. Geochemical Evidence on the sources of fluids and solutes for shear zone hosted mesothermal Au deposits. In Bursnall, J.T., ed., Mineralization and Shear Zones. Geological and Mineralogical Association of Canada, Short Course Notes, Montreal, p. 129-194.

Kerrich, R.W. and Fryer, B.J., 1981. The separation of rare elements from abundant base metals in Archean lode gold deposits: Implications of low water / rock source regions. Economic Geology, v. 76, p. 160-166.

Kerrich, R.W. and Hodder, R.W., 1982. Archean lode gold and base metal deposits: evidence for metal separation into separate hydrothermal systems. In Hodder, R. W. and Petruck, W., (eds.), Geology of Canadian Gold Deposits. Canadian Institute of Mining and Metallurgy, p. 144-160.

Kerrich, R.W. and Wyman, D., 1990. Geodynamic setting of mesothermal gold deposits: an association with accretionary tectonic regimes. Geology, v. 18, p. 882-885.

Kerrich, R.W. and Feng, R., 1992. Archean geodynamics and the Abitibi Pontiac collision: implications for advection of fluids at transpressive collisional boundaries and the origin of giant quartz vein systems. Earth Science Reviews, v. 32, p. 33-60.

Kidd, W.S.F., 1974. The evolution of the Baie Verte lineament, Burlington Peninsula, Newfoundland. Unpublished Ph.D. thesis, Cambridge University, England.

Kidd, W.S.F., Dewey, J.F. and Bird, J.M., 1978. The Ming's Bight Ophiolite Complex: Appalachian oceanic crust and mantle. Canadian Journal of Earth Sciences, v. 15, p. 781-804.

Kijiwara, Y. and Krouse, H.R., 1971 Sulfur isotope partitioning in metallic sulfide sytems. Canadian Journal of Earth Science, v. 8, p. 1397-1408.

Kinkel, A.R. Jr., 1967. The Ore Knob copper deposit, North Carolina and other massive sulphide deposits of the Appalachians. U.S. Geological Survey Professional Paper 558. p. 1-58.

Knuckey, M.J., Comba, C.D.A. and Riverin, G., 1982. Structure, metal zoning and alteration at the Millenbach deposit, Noranda, Quebec. Geological Association of Canada, Special Paper 25, p. 297-317.

Kowlalik, J., 1979. Geological, mineralogical and stable isotope study of a polymetallic massive sulphide deposit, Buchans, Newfoundland. Unpublished Ph.D. thesis, University of Minnesota, Minnesota.

Kowalik, J., Rye, R.O. and Sawkins, F.J., 1981. Stable isotope study of the Buchans, Newfoundland polymetallic sulphide deposits. In: Swanson, E. A., Strong, D.F. and Thurlow, J.G. (eds.), The Buchans Orebodies: Fifty Years of Geology and Mining; Geological Association of Canada, p. 229-254.

Krogh, T.E., Strong, D.F., O'Brien, S.J. and Papezik, V., 1988. Precise U/Pb dates from the Avalon Terrane in Newfoundland. Canadian Journal of Earth Science, v. 25, p. 442-453.

Kyser, T.K., 1987. Short Course in Stable Isotope Geochemistry of Low Temperature Fluids. Geological Association of Canada, v. 13, 452 p.

Kyser, T.K. and Kerrich, R., 1992. Geochemistry of fluids in tectonically active crustal regions. In: Nesbitt, B.E. (ed.), Fluids in tectonically asctive regimes of the continental crust. Short Course Handbook, Mineralogical Association of Canada, v. 18, p. 133-215.

Lambert, I.B. and Sato, T., 1974. The Kuroko and associated ore deposits of Japan: A review of their features and metallogensis. Economic Geology, v. 69, p. 1215-1236.

Lapierre, H., Cabanis, B., Coulon, C., Brouxel, H., and Albaredi, F., 1985. Geodynamic setting of Early Devonian Kuroko-type sulphide deposits in the eastern Klamath Mountain (Northern California) inferred by the petrological and geochemical characteristics of associated island arc volcanic rocks. Economic Geology, v. 80, p. 2100-2113.

Large, R.R., McGoldrick, P.J., Berry, R.F. and Young, C.H., 1988. A tightly folded, gold rich, massive sulphide deposit: Que River Mine, Tasmania. Economic Geology, v. 83, p. 681-693.

Levinson, A. A., 1974. Introduction to Exploration Geochemistry II; Applied Publishing Limited, Wilmette, Illinois. 924 p.

Lydon, J. W., 1988. Volcanogenic massive sulphide deposits: Parts 1 and 2. In: Roberts, R.G. and Sheahan, P.A., (eds.), Ore Deposit Models. Geoscience Canada Reprint, Series 3, p. 155-181.

McGoldrick, P.J. and Large, R.R., 1992. Geological and geochemical controls on gold-rich stringer mineralization in the Que River Deposits, Tasmania. Economic Geology, v.87, p. 667-685.

MacLean, W.H. and Hoy, D.L., 1991. Geochemistry of hydrothermally altered rocks at the Horne Mine, Noranda, Quebec. Economic Geology, v. 86, p. 506-528.

MacMillan, W.J. and Panteleyev, A. 1988. Porphyry copper deposits. In: Roberts, R.G. and Sheahan, P.A. (eds.), Ore Deposit Models, Geoscience Canada, Reprint Series 3, p. 45-58.

Marumo, K., 1989. Genesis of kaolin minerals and pyrophyllite in the Kuroko deposits of Japan; Implications for the origins of the hydrothermal fluids from mineralogical and stable isotope data. Geochemica et Cosmochimica Acta, v. 53, p. 2915-2924.

Matsuhisa, Y., Goldsmith, J.R., and Clayton, R.N., 1979. Oxygen isotopic fractionation in the system quartz - albite - anorthite - water. Geochimica et Cosmochimica Acta, v. 43, p. 1131-1140.

Matthews, A., Goldsmith, J.R. and Clayton, R.N., 1983. Oxygen isotope fractionations involving pyroxenes: the calibration of mineral pair geothermometers. Geochimica et Cosmochimica Acta, v. 47, p. 631-644.

Mitchell, A.H.G. and Bell, J.D., 1973. Island arc evolution and related mineral deposits. Journal of Geology, v. 81, p. 381-405.

Miyashiro, A., Fumiko, S. and Ewing, M., 1969. Diversity and origin of abyssal tholeiite from the mid-Atlantic Ridge near 24°N and 30°N latitude. Contributions to Mineralogy and Petrology, v. 23, p. 38-52.

Miyashiro, A., 1975. Classification, characteristics and origin of ophiolites. Journal of Geology, v. 83, p. 249-281.

Mottl, M.J. and Holland, H.D., 1978. Chemical exchange during hydrothermal alteration of basalt by seawater. I: Experimental results for major and minor components of seawater. Geochemica et Cosmochemica Acta, v. 42, p. 1103-1115.

Mottl, M. J., 1983. Hydrothermal processes at seafloor spreading centres; application of basalt-seawater experimental results. In: Rona, P.A., Boström, K., Laubier, L. and Smith, K.L. Jr., (eds.), Hydrothermal Processes at Seafloor Spreading Centres. Nato Conference Series, IV: Marine Sciences, Plenum Press, New York, p. 199-224.

Muehlenbachs, K. and Clayton, R.N., 1971. Oxygen isotope studies of fresh and weathered submarine basalt. Canadian Journal of Earth Sciences, v. 9, p. 172-184.

Muehlenbachs, K. and Clayton, R.N., 1972. Oxygen isotope geochemistry of submarine greenstones. Canadian Journal of Earth Sciences, v. 9, p. 471-478.

Mueller, A.G. and Groves, D.I., 1992. The classification of Western Australian greenstone - hosted gold deposits according to wallrock - alteration mineral assemblages. Ore Geology Reviews, v. 6, p. 291-331.

Munha, J., Barriga, F.J.A.S., Kerrich, R., 1986. High ^{18}O ore-forming fluids in volcanic-hosted base metal sulphide deposits: $^{18}O/^{16}O$, and D/H evidence form the Iberian Pyrite Belt; Crandon, Wisconsin; and Blue Hill, Maine. Economic Geology, v. 81, p. 530-553.

Nesbitt, B.E., Murrowchik, J.B., and Muelenbachs, K., 1986. Dual origin of lode deposits in the Canadian Cordillera. Geology, v. 14, p. 506-509.

Nesbitt, B.E., Muehlenbachs, K. and Murrowchick, J.B., 1989. Genetic implications of stable isotope characteristics of mesothermal Au deposits and related Sb and Hg deposits in the Canadian Cordillera. Economic Geology, v. 84, p. 1488-1506.

Norman, R.E., 1973. Geology and petrochemistry of ophiolitic rocks of the Baie Verte Group exposed at Ming's Bight, Newfoundland. Unpublished M.Sc. thesis, Memorial University of Newfoundland, St. John's, Newfoundland.

Norman, R.E. and Strong D.F., 1975. The geology and geochemistry of ophiolitic rocks exposed at Ming's Bight, Newfoundland. Canadian Journal of Earth Sciences, v. 12, p. 777-797.

Ohmoto, H., Stable isotope geochemistry of ore deposits. In: Valley, J.W., Taylor, H.P. Jr. and O'Neil, J.R., (eds.), Stable Isotopes in High Temperature Geological Processes. Mineralogical Society of America, p. 491-556.

Ohmoto, H., 1978. Submarine Calderas: A key to the formation of volcanogenic massive sulphide deposits. Mining Geology, v. 28, p. 219-232.

Ohmoto, H., and Rye, R.O., 1974. Hydrogen and oxygen isotopic compositions of fluid inclusions in the Kuroko deposits, Japan. Economic Geology, v. 69, p. 947-953.

Panteleyev, A., 1988. A Canadian model for epithermal gold-silver deposits. In: Roberts, R.G. and Sheahan, P.A. (eds.), Ore Deposit Models, Geoscience Canada, Reprint Series 3, p. 31-44.

Pisutha-Arnond, V. and Ohmoto, H., 1983. Thermal history, and chemical and isotopic composition of the ore-forming fluids responsible for the Kuroko massive sulphide deposits in the Hokuroko Mining District of Japan. Economic Geology, Monograph 6, p. 523-558.

Pottorf, R. J. and Barnes, H.L., 1983. Mineralogy, geochemistry and ore genesis of hydrothermal sediments from the Atlantis II Deep, Red Sea. Economic Geology, Monograph 6, p. 198-223.

Poulsen, K.H., and Robert, F., 1988. A comparison of the structural style and gold endowment of three Archean gold districts, Superior Province, Canada. In: Bicentennial Gold '88, Extended Abstracts Poster Programme, Melbourne, Australia, v. 1, p. 36-38.

Rafter, T.A., 1957. Sulphur isotope variations in nature. P1: The preparation of sulphur dioxide for mass spectrometer examination. New Zealand Journal of Science and Technology, v. B38, p 849.

Ramezani, J. (in prep.). Petrography and geochemistry of alteration and mineralization, and geochronology of the Stog'er Tight Au prospect, Baie Verte, Newfoundland. Unpublished M.Sc. thesis, Memorial University of Newfoundland, St.John's, Newfoundland.

Ramezani, J., Dunning, G., and Wilson, M.R., 1992. Geochemical and Isotopic Study of the Stog'er Tight Gold Prospect, Baie Verte Peninsula, Newfoundland. Geological Association of Canada / Mineralogical Association of Canada, Program with Abstracts, Wolfville '92, p 10.

Rankin, D.W., 1975. The continental margin of eastern North America in the southern Appalachians: The opening and closing of the Proto-Atlantic Ocean. American Journal of Science., v. 275-A. p. 298-336.

Ripley, E.M. and Ohmoto, H., 1979. Oxygen and hydrogen isotopic studies of ore deposition and metamorphism at the Raul mine, Peru. Geochemica et Cosmochimica Acta, v. 43, p. 1633-1643.

Ritcey, D., (in prep.) Geology, geochemistry, and U/Pb geochronology of the Hammer Down Au deposit, King's Point / Green Bay District, Newfoundland. Unpublished M.Sc. thesis, Memorial University of Newfoundland, St. John's, Newfoundland.

Riverin, G. and Hodgson, C.J., 1980. Wall-rock alteration at the Millenbach, Cu-Zn mine, Noranda, Quebec. Economic Geology, v. 75, p. 424-444.

Rivers, T. and Chown, E.H., 1986. The Grenville Orogen in eastern Quebec and western Labrador: definition, identification and tectono-metamorphic relationships of autochthonous, parautochthonous and allochthonous terrains. In: Moore, J.M., Davidson, A., and Baer, A.J., (eds.), The Grenville Province. Geological Association of Canada, Special Paper 31, p. 31-50.

Roberts, G., 1988. Archean lode Au deposits. In Roberts, R. G. and Sheahan, P.A. (eds.), Ore Deposit Models. Geoscience Canada, Reprint Series 3, p. 1-20.

Roberts, R.G., 1975. Geological setting of the Mattagami Lake Mine: A volcanogenic massive sulphide deposit. Economic Geology, v. 70, p. 115-129.

Roedder, E., 1969. Fluid inclusions as samples of ore fluids. In: Barnes, H. L., ed., Geochemistry of Hydrothermal Ore Deposits II. John Wiley and Sons, New York / Toronto, p. 684-731.

Roedder, E., 1984. Fluid Inclusions. Mineralogical Society of America, Reviews in Mineralogy v. 12, Bookcrafters Incorporated, Michigan. 664 p.

Rona P. A., Boström, K., Laubier, L., and Smith, K.L. Jr., (1983). Hydrothermal Processes at Seafloor Spreading Centres; Plenum Press, New York. p. 177-197.

Rosenbauer, R. J. and Bischoff, J.L., 1984. Uptake and transport of heavy metals by heated seawater: A summary of the experimental results. In: Rona, P. A., Boström, K., Laubier, L., and Smith, K.L. Jr., (eds.), Hydrothermal Processes at Seafloor Spreading Centres; Plenum Press, New York. p. 177-197.

Rui, I., 1973. Geology and structure of the Rostamagen sulphide deposit in the Kvikne district, central Norwegian Caledonides. Norsk Geol. Tidsskr., v. 53, p. 433-442.

Rye, R.O. and Ohmoto, H., 1974. Sulfur and carbon isotopes and ore genesis: A review. Economic Geology, v. 69, p. 826-842.

Sabir, H., 1981. Geology and mineralogy of the pollymetallic sulphide mineralization at Jebel Sa'id. Saudi Arabian Deputy Ministry Mineral Resources Bulletin, v. 26, 101 p.

Sakai, H., 1968. Isotopic properties of sulfur compounds in hydrothermal processes. Geochemical Journal, v. 2, p. 29-49.

Sangster, D.F., 1972. Precambrian volcanogenic massive sulphide deposits in Canada. Geological Survey of Canada, Paper 72-22, 44 p.

Sangster, D.F. and Scott, S.D., 1976. Precambrian stratabound massive Cu-Zn-Pb sulphide ores of North America. In Wolf, K.H., ed., Handbook of Stratabound andstratiform Ore Deposits, Elsevier, Amsterdam, p. 129-222.

Sato, J., 1974. Ores and ore minerals from the Shakanai mine, Akita Prefecture, Japan. Society Mining Geologists Japan, Special Issue 6, p. 323-337.

Saunders, C.M., 1985. Controls of mineralization in the Betts Cove Ophiolite. Unpublished MSc thesis, Memorial University of Newfoundland, St. John's, Newfoundland.

Sawkins, F.J., 1976. Massive sulphide deposits in relation to geotectonics. Geological Association of Canada, Special Paper 14, p. 221-240.

Schoell, M. and Faber, E., 1978. New isotopic evidence for the origin of the Red Sea brines. Nature, v. 275, p. 436-437.

Scott, S.D., 1978. Structural control of the Kuroko deposits of the Hokuroko Mining district, Japan. Mining Geology, v. 28, p. 301-311.

Seyfried, W.E. Jr., Berndt, M.E. and Seewald, J.S., 1988. Hydrothermal alteration processes at mid-ocean ridges: constraints from diabase alteration experiments, hot spring fluids and composition of the oceanic crust. Canadian Mineralogist, v. 26, p. 787-804.

Sibson, R.H., 1987. Earthquake rupturing as a mineralizing agent in hydrothermal systems. Geology, v. 15, p. 701-704.

Sibson, R.H., 1992. Fault-valve behaviour and the hydrostatic-lithostatic fluid pressure interface. Earth Science Reviews, v. 32, p. 141-144.

Spence, C.D. and de Rosen-Spence, A., 1975. The place of sulphide mineralization in the volcanic sequence at Noranda, Quebec. Economic Geology, v. 70, p. 90-101.

Stakes, D.S. and O'Neil, J.R., 1982. Mineralogical and stable isotope geochemistry of hydrothermally altered oceanic rocks. Earth and Planetary Science Letters, p. 285-304.

Stewart, P.W. and Dunning, G.R., 1990. The Lapoile Group, the Hope Brook Mine and geochronology. Program with Abstracts, Atlantic Geoscience Society Symposium 1990, p. 30.

Strong, D.F. and Saunders, C.M., 1988. Ophiolitic sulphide mineralization at Tilt Cove, Newfoundland: Controls by upper mantle and crustal processes. Economic Geology, v. 83, pp 239-255.

Sun, S.S. and Nesbitt, R.W., 1978. Geochemical regularities and significance of ophiolitic basalts. Geology, v. 6, p. 689-693.

Suzuoki, T. and Epstein, S., 1970. Hydrogen isotope fractionation factors (α's) between muscovite, biotite, hornblende and water. American Geophysical Union Transactions, v. 51, p. 451-452.

Swanson, E.A., Strong, D.F. and Thurlow, J.G. (eds.), 1981. The Buchans Orebodies: Fifty Years of Mining and Geology. Geological Association of Canada., Special Paper 22. 350 p.

Swinden, H.S., 1988. Volcanism and mineralization in the Wild Bight Group, Central Newfoundland: A geological, petrological, geochemical and isotopic study. Unpublished Ph.D. thesis, Memorial University of Newfoundland, St. John's, Newfoundland.

Swinden, H.S., 1988. Geology and economic potential of the Pipestone Pond Area (NTS 12A/1 NE; 12A/8 E), Central Newfoundland. Newfoundland Department of Mines and Energy, Report 88-2, 88 p.

Swinden, H.S., 1991. Regional geology and metallogeny of Central Newfoundland. In: Swinden, H.S., Evans, D.W.T. and Kean, B.F. (eds.), Metallogenic Framework of Base and Precious Metal Deposits, Central and Western Newfoundland (Field Trip 1), GSC Open File 2156, p. 7-19.

Swinden, H.S., Kean, B.F., Dunning, G.R., 1988. Geological and paleotectonic settings of volcanogenic sulphide mineralization in central Newfoundland. In: Swinden, H., ed., Volcanogenic Sulphide Districts in Central Newfoundland. Geological Association of Canada, Mineralogical Association Canada, p. 425-439.

Swinden, H.S., Jenner, G.A., Kean, B.F., Evans, D.T.W., 1989. Volcanic rock geochemistry as a guide for massive sulphide exploration in Central Newfoundland. In Newfoundland Department of Mines and Energy, Current Research 89-1, p. 201-219.

Tanweer, A., Hut, G. and Burgman, J.O., 1988. Optimal conditions for the reduction of water to hydrogen by zinc for mass spectrometric analysis of the deuterium content. Chemical Geology (Isotope Geoscience), v. 73, p. 199-203.

Taylor, H.P. Jr., 1967. Oxygen isotope studies of hydrothermal mineral deposits. In: Barnes, H.L. ed., Geochemistry of Hydrothermal Ore Deposits II. Holt Rinehart and Winston, New York, p. 109-142.

Taylor, H.P. Jr., 1974. The application of oxygen and hydrogen isotope studies to problems of hydrothermal alteration and ore deposition. Economic Geology, v. 69, p. 843-881.

Taylor, H.P. Jr. and Sheppard, S.M.F., 1986. Igneous Rocks. I: Processes of isotopic fractionation and isotopic systematics. In: Valley, J.W., Taylor, H.P. Jr. and O'Neil, J.R., (eds.), Stable Isotopes in High Temperature Geological Processes. Mineralogical Association of America, p. 227-269.

Thorpe, R.I. and Harris, D.C., 1973. Mattagamite and telluro-antimony, two new telluride minerals from the Mattagami mine, Quebec. Canadian Mineralogist, v. 12, p. 55-60.

Timball, A., 1992. Serpentinization and carbonitization of tectonic mélanges in the Coy Pond Complex, Central Newfoundland. Unpublished M.Sc. thesis. Memorial University of Newfoundland, St. John's, Newfoundland, 360 p.

Tourigny, G., Brown, A.C., Hubert, C. and Crepeau, R., 1989. Synvolcanic and Syntectonic Gold Mineralization at the Bosquet Mine, Quebec. Economic Geology, v. 84, p. 1875-1890.

Tuach, J., 1976. Structural and stratigraphic setting of the Ming and other sulphide deposits in the Rambler area, Newfoundland. Unpublished M.Sc. thesis, Memorial University of Newfoundland, St. John's, Newfoundland, 128 p.

Tuach, J. 1990. List of gold occurrences and deposits in Newfoundland. Newfoundland Department of Mines and Energy, Open File 1928, 72 p.

Tuach, J. and Kennedy, M.J., 1978. The geological setting of the Ming and other sulphide deposits, Consolidated Rambler Mines, Northeast Newfoundland. Economic Geology, v. 73, p. 126-206.

Tuach, J., Dean, P.L., Swinden, H.S., O'Driscoll, C., Kean, B.F. and Evans, D.T.W. 1988. Gold mineralization in Newfoundland: A 1988 Review. Newfoundland Department of Mines and Energy, St. John's, Newfoundland, p. 192-206.

Upadhyay, H.D., 1973. The Betts Cove ophiolite and related rocks of the Snook's Arm Group, Newfoundland. Unpublished Ph.D. thesis, Memorial University of Newfoundland, St. John's, Newfoundland.

Upadhyay, H.D., Dewey, J.F. and Neale, E.R.W. 1971. The Betts Cove Ophiolite Complex, Newfoundland Appalachian oceanic crust and mantle. Geological Association of Canada, Conference Proceedings, v. 24, p. 27-34.

Urabe, T. and Sato, T. 1978. Kuroko deposits of the Kosaka mine, Northeast Honshu, Japan: Products of submarine hot springs on Miocene sea floor. Economic Geology, v. 73, p. 161-179.

Valley, J.W., Taylor, H.P. Jr. and O'Neil, J.R., 1987. Stable Isotopes in High Temperature Geological Processes. Mineralogical Association of America.

Watson, K. de P., 1943. Mafic and ultramafic rocks in the Baie Verte area, Newfoundland. Journal of Geology, v. 51, p. 116-130.

Watson, K. de P., 1947. Geology and mineral deposits of the Baie Verte - Ming's Bight area, Newfoundland. Geological Survey of Newfoundland, Bull. 21, 48 p.

Weick, R.J., Wilson, M. and Swinden, H.S., 1990. Mineralization and alteration study of the Main Mine orebody, Consolidated Rambler Mines, Baie Verte Peninsula, Newfoundland. Newfoundland Department of Mines and Energy, Current Research 90-1, p. 217-225.

Weick, R.J., 1991. Preliminary report on the geology, petrography and major and trace element geochemistry of the Main (Rambler) deposit. Newfoundland Department of Mines and Energy, Open File Report 9112, 30 p.

Wenner, D.B. and Taylor, H.P. Jr., 1971. Temperatures of serpentinization of ultramafic rocks based on $^{18}O/^{16}O$ fractionation between coexisting serpentine and magnetite. Contributions Mineralogy and Petrology, v. 32, p. 165-185.

White, N.C. and Hedinquist, J.W., 1990. Epithermal environments and styles of mineralization: Variations and their causes and guides for exploration. Journal Geochemical Exploration, v. 36, p. 445-474.

Williams, H., 1964. The Appalachians in Newfoundland - a two sided symmetrical system. American Journal of Science, v. 24, p. 9-25.

Williams, H., 1978. Tectonic lithofacies map of the Appalachian orogen. Map 1.

Williams, H., 1979. The Appalachian Orogen in Canada. Canadian Journal of Earth Science, v. 16, p. 792-807.

Williams, H. and St Julien, P., 1978. The Baie Verte - Brompton Line in Newfoundland and regional correlations in the Canadian Appalachians. Geological Survey of Canada, Paper 78-1A, p. 225-229.

Williams, H. and Hatcher, R.D., Jr., 1983. Appalachian suspect terrains. In Hatcher, R.D., Williams, H., and Zeitz, I., (eds.), Contributions to the Tectonics and Geophysics of Mountain Chains. Geological Society of America, Memoir 158, p. 1044-1047.

Williams, H., Gillespie, R.T. and van Breeman, O., 1985. A Late Precambrian rift-related igneous suite in western Newfoundland. Canadian Journal of Earth Science, v. 22, p. 1727-1735.

Williams, H. and Hiscott, R.N., 1987. Definition of the Iapetus rift-drift transition in western Newfoundland. Geology, v. 15, p. 1044-1047.

Williams, H., Coleman-Sadd, S.P. and Swinden, H.S., 1988. Tectonic-stratigraphic subdivisions of central Newfoundland. Geological Survey of Canada, Current Research, Paper 88-1B, p. 91-98.

Williams, S.H., 1989. New Graptolite discoveries from the Ordovician of central Newfoundland. Newfoundland Department of Mines and Energy, Current Research 89-1, p. 149-157.

Wilson, J.T., 1966. Did the Atlantic close and then re-open ? Nature, v. 211, p. 676-681.

Yeh, H., 1980. D/H ratios and late stage dehydration of shales during burial. Geochemica et Cosmochimica Acta, 44, p. 341-352.

Yeh, H. and Savin, S.M., 1976. The extent of oxygen isotope exchange between clay minerals and sea water. Geochemica et Cosmochimica Acta, 40, p. 743-748.

Young, C.H., 1980. Que River, a synclinally folded stratiform volcanogenic sulfide deposit. Aberfoyle Explor. Pty. Ltd., unpub. Rept., 23 p.

Yui, S., 1983. Texture of some Japanese Beshi-type ores and their implications for Kuroko deposits. Economic Geology, Monograph 6, p. 231-240.

Appendix 1:

Analytical Methods

A1.1 Assay Analyses

Standard commercial assays of the core samples collected during drilling in 1989 on the Rambler VMS deposit were performed by Chemex Laboratories Limited at their laboratory facilities in Pasedena, Newfoundland. Gold and silver were analyzed using standard fire assay techniques, with a gravimetric finish. Copper and zinc were analyzed using a reverse aqua-regia dissolution procedure, followed by atomic absorption (AA).

For gold and silver, a prepared sample (1 assay ton = 29.166 grams) is fused in a litharge, carbonate and siliceous flux. A lead button containing the precious metals is cupelled in a muffled furnace. The resulting bead is weighed, parted in dilute nitric acid, annealed and weighed as gold. The difference in the weights is the weight of silver in the sample. Detection limits are reported at 0.002 oz/ton (0.07g/tonne) for gold, and 0.05 oz/ton (0.3 g/tonne) for silver, with upper detection limits of 20 oz/ton (500g/tonne).

For copper and zinc, a prepared sample (0.5-2.00g) is digested in a hot nitric-hydrochloric acid mixture which is taken to dryness, cooled, and then transferred into a 250ml flask, with a solution matrix of 25% hydrochloric acid. The resulting solutions are analyzed using AA. Detection limits are reported at 0.01% for both copper and zinc, with upper limits of 100%.

A1.2 Major Element Analyses

The fifteen whole-rock samples; five each from the hangingwall, deposit and footwall of the Rambler deposit were analyzed for major element oxides by atomic absorption (AA) spectroscopy in the Department of Earth Sciences at Memorial University.

mixture was diluted with 145mL of distilled water. Analysis of MgO and CaO required further dilution with a lanthanum oxide and distilled water.

During analyses, sample absorptions were compared to standards with predetermined major element concentrations. Initial absorption measurements were taken of the standards, then the sample, and then from standards with absorptions marginally lower and higher than the absorption of the sample. Percent oxide concentrations were calculated using the following equation:

$$\%_{oxide} = \frac{\%_{LS} + (\%A_{sample} - \%A_{LS})}{2(\%A_{HS} - \%A_{LS})(\%_{HS} - \%_{LS})} \quad (1)$$

where %A is absorption, LS is the low standard, and HS is the high standard. Loss on ignition (LOI) was estimated by weighing a portion of the sample in a crucible before and after ignition at 1000°C. The accuracy of individual oxide analyses is illustrated by reference to analyses of the USGS reference sample BE-N (basalt; Table A.1.1).

A1.3 Trace Element Analyses

Splits of the whole-rock samples selected for major element analyses, were sent to Chemex Laboratories in Pasedena, Newfoundland. Trace elements including tellurium, silver, arsenic, bismuth, copper, cadmium, mercury, molybdenum, antimony, and selenium were analyzed using a combination of wet chemistry and atomic absorption spectroscopy (AAS).

For tellurium a prepared sample (5.0g) is digested in concentrated hydrobromic acid and bromine. The iron is then reduced with ascorbic acid and the resulting tellurium bromide complex is extracted into methylisobutylketone (MIBK). The extract is analyzed by AA with a background correction. Detection limits are reported at 0.05 ppm.

TaNe A1.1 Accuracy of major element analyses by Atomic Absorption Spectrophotometry (BE–N basalt)

Oxides	Published Value (wt%)	Mean (wt%)	Difference	Standard Deviation	Range of Values
SiO2	38.2	38.5	0.3	0.18	38.21 – 38.67
TiO2	2.61	2.59	−0.02	0.04	2.56 – 2.64
Al2O3	10.07	10.02	−0.05	0.09	9.85 – 10.1
Fe2O3T	12.84	12.84	0	0.11	12.69 – 12.96
CaO	13.87	13.91	0.04	0.05	13.84 – 13.96
MgO	13.15	13.14	0.03	0.07	13.04 – 13.27
Na2O	3.18	3.25	0.07	0.02	3.22 – 3.28
K2O	1.39	1.46	0.07	0.007	1.45 – 1.47
MnO	0.2	0.19	−0.01	0	0.19 – 0.19

complex is extracted into methylisobutylketone (MIBK). The extract is analyzed by AA with a background correction. Detection limits are reported at 0.05 ppm.

For arsenic, 1.00g of prepared sample is digested with nitric-aqua regia for two hours. The digested solution is diluted to volume and then homogenized. An aliquot of the solution is diluted and reduced with sodium borohydride to liberate arsine gas. The concentration of As is measured through flameless aosorption spectroscopy. Detection limits are reported at 1 ppm, with an upper limit of 10,000 ppm.

For the analyses of mercury a prepared sample (1.00g) is digested with nitric acid with a small amount of hydrochloric acid. The resulting solution is transferred to a flask connected to a closed system absorption cell. Stannous chloride is rapidly added to reduce the mercury, which is measured by cold vapour atomic absorption spectroscopy. Detection limits are estimated at 10 ppb, with an upper limit of 0.01%.

For the analyses of selenium, antimony and bismuth, 2.00g of sample are digested with concentrated hydrochloric acid and potassium chlorate. The solution is cooled and potassium iodide is added to reduce iron. The antimony, bismuth or selenium are then extracted using trioctylphosphine oxide and methylisobutylketone. Concentrations are analyzed with AA with a correction for background absorption. Detection limits are reported as 0.2 ppm for selenium and antimony, and 0.1 ppm for bismuth. The upper limit for the detection of selenium is 0.01%. The upper limit for the detection of antimony and bismuth is 0.1%.

For copper, molybdenum, lead, zinc, silver and cadmium analyses 1.00g of prepared sample is digested with nitric aqua-regia for two hours. The digested sample is cooled and diluted to 25 ml with distilled water. The resulting solution is mixed and its precipitates allowed to settle. Concentrations are determined using atomic absorption spectroscopy. Lead, silver and cadmium concentrations are corrected for background absorption. Detection limits are reported as 1 ppm for copper, molybdenum, and lead,

and 0.2 for silver, and 0.1 for cadmium. Upper detection limits for these elements are 1% for copper and lead, 0.1% for molybdenum, and 0.02% for silver and cadmium.

A1.4 Mineral Separation Techniques

Pure mineral separates for isotopic analyses were collected using a combination of density and magnetic separation techniques (Kowalik, 1978). Sample purity was confirmed at ≥ 80% using X-ray diffraction (XRD) and is summarized in Table A1.1.

Silicates in coarse grained rocks, including gabbros and some quartz veins were easily separated through a combination of density, magnetic separation techniques and hand picking. +60 mesh fractions of amphibole in gabbro were separated from quartz, and albite using bromoform. Quartz was separated from carbonate in coarse grained vein samples by picking and through preferential dissolution using concentrated HCl.

Quartz, chlorite, and muscovite separates were obtained from fine grained samples were obtained by crushing and sieving to +80 to +100 mesh and then separating the sample into pure magnetic fractions using a Franz. Pure quartz separates were obtained by adopting a current setting of 1.4 Amps and retaining non-magnetic fractions at successive axial settings of 10°, 7.5° and 5°. Pure chlorite separates were obtained by setting the current at 0.4 amps and retaining magnetic fractions, at successive axial settings of 10°, 12.5° and 15°. The magnetically separated fractions were picked using a binocular microscope to remove composite grains and other impurities.

The separation of quartz and muscovite from fine grained samples was problematic. Mixtures of quartz and muscovite could be obtained at Franz settings of 1.2 amps, by discarding magnetic fractions over successive axial angles of 10°, 7.5° and 5°. These were placed in about 50 ml of concentrated soap solution in a beaker. The beaker and contents were immersed in an ultrasound to complete sample disaggregation. After 1-2 hours, the solution was decanted and centrifuged at 10,000 rpm for 20 to 30 minutes to

recover the suspended mineral fraction, which XRD analyses confirmed as muscovite. Sample purity was estimated at $\geq$ 80%.

Sulphides were separated from silicates using bromoform. Mixed sulphide samples were separated into pure sulphide fractions, using the Franz. Sphalerite was recovered from pyrite at a setting of 0.9 amps, and an axial angle of approximately 15°. XRD analyses confirmed the purity of the sulphide separates to $\geq$ 90%.

Table A1.2 Mineral Separate Descriptions

		rock	mineral	purity	contaminants
stage 1 alteration					
hanging	25 – 2713	gbbr	qtz	99%	– chl (trace)
wall	28 – 2713	gbbr	alb	98%	– qtz (<2%)
	28 – 2713	gbbr	amp		
	21 – 2749	gbbr			
deposit	21 – 2719	chl	qtz	90%	– mag (<10%)
	21 – 2752	vms	qtz		
	21 – 2752	vms	se		
	21 – 2754	vms	qtz		
	21 – 2754	vms	chl	65%	– se (10%), py (15%)
	21 – 2754	vms	se		
	21 – 2760	vms	qtz		
	21 – 2760	vms	chl	70%	– py (30%)
	21 – 2720	vms	qtz		
	21 – 2720	vms	chl	90%	– py (10%)
stage 2 alteration					
footwall	24 – 1911	myl	qtz	95%	– alb (5%)
	20 – 2762	myl	qtz	95%	– alb (5%)
	20 – 2762	myl	chl	90%	– se (10%)
	20 – 2762	myl	se	95%	– chl / alb (5%)
	26 – 1974	myl	qtz		
	24 – 1925	myl	qtz		
	24 – 1925	myl	se	80%	– chl (18%)
	28 – 2728	myl	qtz		
	28 – 2728	myl	chl	98%	– qtz (<2%)
	24 – 1930	myl	qtz		
	24 – 1930	myl	chl	90%	– qtz (<10%)
stage 3 alteration					
	23 – 2520	vn	qtz		
	23 – 2520	vn	chl	70%	– qtz (30%)
	23 – 2518	vn	chl		
	26 – 1963	vn	qtz		
	26 – 1963	vn	alb		
	26 – 1963	vn	chl		
	23 – 2514	vn	qtz		
	21 – 2835	vn	qtz		
	21 – 2835	vn	bio		
	24 – 1908	vn	qtz		
	23 – 2512	vn	qtz		
	28 – 2542	vn	qtz		
	28 – 2730	vn	qtz		
	28 – 2731	vn	alb		
	24 – 1934	vn	qtz		
	24 – 1934	vn	bio		

A1.5 Gas Extraction

Mineral separates were converted into CO_2, H_2, and SO_2 gas using vacuum line extraction facilities in the Geochemistry Department at Memorial University. O_2 was extracted from pure silicates in a vacuum line by reaction with BrF_5 at 600 °C for 6 to 8 hours. The liberated oxygen was converted to CO_2 by combustion with a carbon rod at approximately 800 °C (Clayton et al., 1963).

Structural H_2O was generated by the inductive heating of hydrous silicates in a vacuum line to temperatures in excess of 1000°C using a Leppel radio frequency (RF) generator (Godfrey, 1962). The H_2O was converted to H_2 gas by reaction with metallic Zn at 460°C for approximately 20 minutes (Hut et al., 1988). SO_2 gas was evolved through the combustion of sulphides and CuO in a vacuum line at 1000°C (Rafter, 1965).

A1.6 Isotopic Analyses

The isotopic compositions of mineral separates were determined by gas source mass spectrometry. Analyses of oxygen and deuterium fractionations were performed on a Finnigan Mat 252 gas source mass spectrometer. D/H analyses were corrected for the formation of H^{+3} in the ion source and all machine, abundance, and standard corrections were applied to the raw data (Craig, 1957, 1961). Individual $^{34}S/^{32}S$ ratios in sulphide separates were determined over a series of runs using a VG 903E mass spectrometer.

All $\delta^{18}O$, δD and $\delta^{34}S$ values for analyzed silicates, carbonates and sulphides are reported using standard δ notation relative to SMOW, PDB and CDT standards. Uncertainties among the measured $\delta^{18}O$, δD, and $\delta^{34}S$ determinations are estimated at $\pm$ 0.2 ‰, $\pm$ 2 ‰, and $\pm$ 0.2 ‰, respectively.

Appendix 2:
Stable Isotope Theory

An isotopic fractionation factor between substances A and B can be written:

$$\alpha_{A\text{-}B} = R_A/R_B. \qquad (1)$$

where R_A is the ratio of the high mass (rare) isotope to the low mass (common) isotope in phase A. In the geothermal / hydrothermal systems, R represents D/H, $^{18}O/^{16}O$, $^{13}C/^{12}C$ or $^{34}S/^{32}S$. If isotopic species are distributed equally among all bonding sites in A and B, α is proportional to an equilibrium constant K, such that for isotopic exchange reactions, $\alpha = K^{1/n}$, where n is the number of atoms exchanged. Since it is more convenient to measure differences in the absolute ratio of isotopes between two substances, isotopic abundances are reported as delta (δ) values in units of per mil (‰), relative to a standard;

$$\delta_A = [(R_A - R_{stnd})/ R_{stnd}] \times 1000, \qquad (2)$$

where R_A and $R_{stnd.}$ represent absolute isotopic ratios in a sample and pre-determined standard, respectively. Isotopic standards used in geological applications typically include SMOW (Standard Mean Ocean Water) for oxygen and hydrogen, PDB (PeeDee Belmnite) for carbon and CDT (Canyon Diablo Triolite) for sulphur (Craig, 1961).

The relationship between the isotopic composition of samples (δ values in ‰ deviations) and fractionation factors is defined as:

$$\alpha_{A\text{-}B} = \frac{(1+\delta_A) / 1000}{(1+\delta_B) / 1000} = \frac{1000 + \delta_A.}{1000 + \delta_B} \qquad (3)$$

Since α is close to unity in most geological systems. Values of $1000\ln\alpha$ approximate per mil deviations, and the difference between the δ values of two co-existing phases equals the fractionation factor. From equation (3), and by defining $\Delta_{A\text{-}B}$ as $\delta_A - \delta_B$:

$$1000\ln\alpha_{A\text{-}B} \approx \delta_A - \delta_B \approx \Delta_{A\text{-}B}, \quad (4)$$

if the fractionation ($\alpha_{A\text{-}B}$) is within 2 % of unity.

Isotopic fractionations in geological systems are a function of temperature. Lnα varies as $1/T^2$ at high temperature, and as $1/T$ at low temperature. Fractionation varies as a function of $1/T$, or $1/T + 1/T^2$ in the hydrous silicate minerals. At high temperatures, $\ln\alpha_{A\text{-}B}$ approaches 0, as bond energies become equal. Equations which equate the fractionation factor (α) between two chemical phases A and B at different temperatures are generally written;

$$\ln\alpha_{A\text{-}B} \sim \delta A - \delta B \sim C + D/T^2 \text{ for T's} \geq 400°C, \text{ and}$$

$$\ln\alpha_{A\text{-}B} \sim \delta A - \delta B \sim C + D/T \text{ for T's} \leq 400°C, \quad (5)$$

where T is temperature and C and D are constants determined through empirical observation. These equations define a series of curves at a specific range of temperatures. Solving the equations for temperature using measured $\delta^{18}O$ data from rocks, minerals and fluids, is the basis for oxygen isotope geothermometry.

Measuring the $^{18}O/^{16}O$ and D/H ratios of fluids extracted from inclusions is a direct method of determining the source of fluids in geological settings (Rye et al., 1974). However, fluid isotopic compositions can also be calculated using the $\delta^{18}O$ and δD values of minerals, and the appropriate mineral-water fractionation curves over a given range of temperatures (Taylor, 1974). Variations in the $\delta^{18}O$ of fluids are a function of the source and chemistry of the fluid and of the isotopic exchange reactions which occur in hydrothermal systems. δD variations are attributed mainly to isotopic fractionations in different crustal fluid reservoirs.

Studies suggest that five isotopically distinct fluids participate in alteration / mineralization processes in the Earth's crust. These include seawater, meteoric fluids, formational fluids and magmatic / metamorphic fluids (Figure A2.1). $\delta^{18}O$ and δD values of seawater are 0 per mil (SMOW) by definition. High $\delta^{18}O$ and similar δD values related to seawater evaporation are shown as a curve originating from SMOW. Meteoric fluids plot close to the meteoric water line (MWL), defined by the equation:

$$\delta D = \delta_p(\delta^{18}O) + 10. \qquad (6)$$

where $\delta_p = 7.95 \pm 0.22$ for North America (Kyser, 1987). The isotopic compositions of formational fluids in continental basins reflect mixing between modern meteoric waters and ^{18}O enriched brines. Formational fluids in Precambrian shields define linear trends to the left of the MWL. $\delta^{18}O$ and δD values of +5.5 to +8 ‰ and -40 to -80 ‰, and +4 to +12 ‰ and -20 to -60 ‰ are associated with the presence of magmatic and metamorphic fluids, respectively (Taylor, 1974; Kyser, 1987).

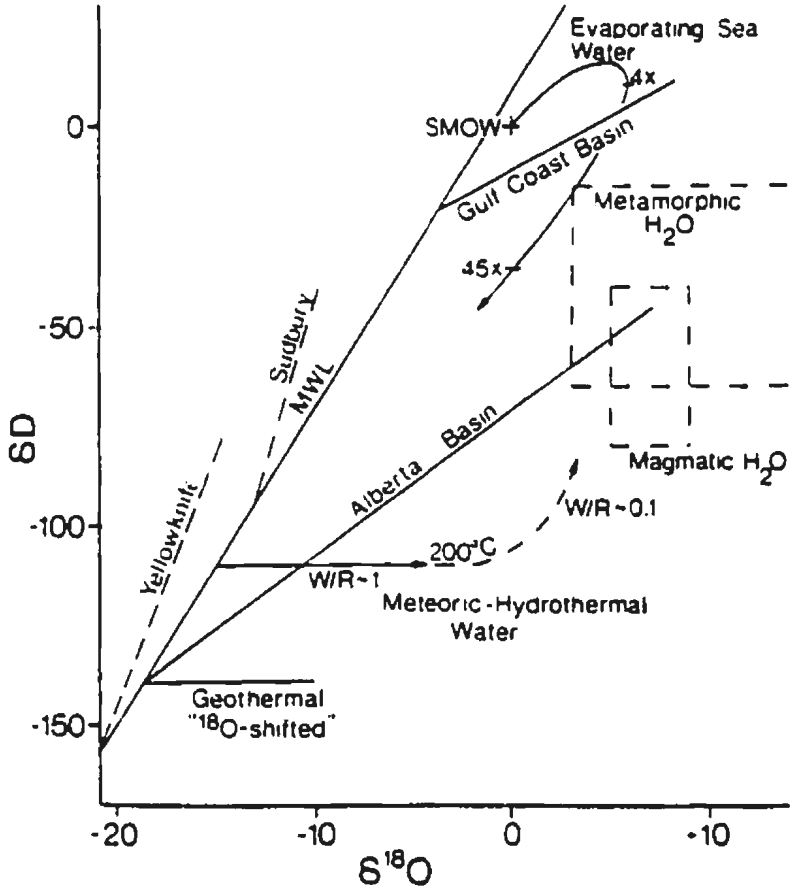

Figure A2.1 $\delta^{18}O$ and δD variations among different fluid reservoirs in the crust (after Kyser, 1987).

Appendix 3:

Major and Trace Element Data

Table A3.1 Major (wt%) and trace element analyses (ppm) of whole-rock samples from the hangingwall, deposit, and footwall stratigraphic sections in the Rambler deposit

	hangingwall					deposit						footwall					
Sample	2703	2706	2707	2709	2710	8885	8886	8887	8888	8889	8915	8916	8918	8919	8924	1925	2810
SiO2	45.30	42.10	35.50	51.40	55.00	25.80	47.80	48.40	40.00	41.80	60.00	62.30	58.00	68.50	54.10	53.90	68.60
Al2O3	14.00	16.90	10.20	14.60	15.90	11.70	6.86	9.05	7.90	8.29	9.27	8.10	9.27	13.70	8.10	5.33	9.87
TiO2	0.84	1.26	0.14	1.66	0.24	0.00	0.00	0.00	0.00	0.00	0.00	0.00	0.00	0.30	1.92	0.02	0.02	0.00
Fe2O3	7.24	9.80	10.03	10.07	9.88	29.16	23.56	20.54	27.18	25.62	15.42	14.54	14.68	15.97	19.56	22.76	13.56
MnO	0.12	0.13	0.12	0.17	0.07	0.04	0.01	0.01	< 0.01	0.04	0.01	0.02	0.06	0.17	0.02	0.01	0.02
MgO	6.65	7.74	12.80	3.63	6.46	2.81	0.36	0.48	0.32	1.98	0.96	1.59	3.98	5.80	2.69	0.38	0.51
CaO	9.70	9.28	5.02	7.62	1.26	0.20	0.08	0.08	0.02	0.06	0.76	0.56	1.88	0.74	0.32	0.06	0.20
Na2O	4.19	3.33	2.14	4.95	4.92	0.38	0.29	0.36	0.34	0.37	2.35	3.26	2.11	0.38	1.01	0.16	3.13
K2O	1.19	0.21	0.05	0.47	1.36	2.88	1.91	2.40	2.09	1.71	1.33	0.10	0.04	0.04	1.46	1.19	0.14
P2O5	0.12	0.11	0.03	0.35	0.07	0.08	0.02	0.04	0.04	0.02	0.02	0.01	0.05	0.24	0.02	0.01	0.08
LOI	7.60	5.50	3.32	2.16	2.50	18.45	13.81	12.73	16.50	15.16	8.74	8.42	6.99	4.71	11.07	12.71	3.52
total	96.95	96.36	89.35	97.08	97.66	91.5	94.68	94.1	94.4	95.06	98.88	98.9	97.36	98.17	98.37	97.13	97.73
Se	< 0.2	0.2	< 0.2	< 0.2	< 0.2	1.4	0.4	1.6	1.6	2	2.8	2.6	1.6	1.2	7	6	< 0.2
Ba	< 0.1	< 0.1	< 0.1	< 0.1	< 0.1	2.7	1.3	0.1	1.3	0.5	0.2	0.3	0.2	< 0.1	0.1	1.2	< 0.2
Cd	< 0.1	< 0.1	< 0.1	< 0.1	< 0.1	54	30	45	16.4	8.3	< 0.1	< 0.1	< 0.1	< 0.1	< 0.1	2	2.3
Mo	< 1	< 1	< 1	< 1	< 1	50	12	18	19	20	22	17	135	22	9	4	6
As	2	1	1	< 1	1	270	180	170	200	170	51	48	17	12	69	82	25
Sb	< 0.2	< 0.2	< 0.2	< 0.2	< 0.2	4	1.2	0.2	0.2	0.4	< 0.2	1.4	< 0.2	< 0.2	< 0.2	0.4	< 0.4
Te	0.05	0.05	0.05	<0.05	0.05	12.5	9.8	9	34.5	13.5	4.25	3.9	2.5	1.4	2.6	26.3	7.6
Ag	< 0.2	< 0.2	< 0.2	< 0.2	< 0.2	7.5	4	2.8	9.4	7	< 0.2	< 0.2	< 0.2	< 0.2	< 0.2	1.4	5.6
Hg	0.04	0.01	0.01	0.02	0.01	0.64	0.51	0.6	0.18	0.13	0.01	0.01	0.01	0.01	0.01	0.02	0.02
Cu	20	38	67	45	4	485	540	700	5900	4000	106	27	104	169	520	> 10000	> 10000
Pb	< 1	< 1	< 1	< 1	< 1	1500	630	24	85	19	< 1	5	< 1	< 1	< 1	< 2	< 1
Zn	67	75	4	44	85	> 10000	> 10000	> 10000	6000	2600	25	35	61	155	35	392	104

< – below detection limits.

Table A3.2: Compiled basalt whole-rock geochemical analyses: major element oxides in wt% (Sun and Nesbitt, 1978; Gale, 1971; Hibbard, 1983; unpub. data from Swinden, 1992).

Sun and Nesbitt (1978).

Sample	1	2	3	4	5	6	7	8	9	10	11	12	13	14	15
SiO2	53.51	52.8	51.2	53.9	49.3	48.3	49.6	55.2	57.4	52.5	50.7	47.7	48.8	47.8	49.7
Al2O3	13.49	9.49	15.92	11.55	15.30	15.90	16.17	7.90	10.53	16.85	14.50	15.88	16.90	16.77	15.64
TiO2	0.18	0.16	0.60	0.31	0.63	1.90	0.76	0.20	0.19	0.34	1.37	0.37	1.03	0.87	1.37
Fe2O3	1.78	10.71	8.98	1.70	5.77	5.00	7.18	11.19	9.17	5.34	1.88	2.19	1.28	10.33	10.80
FeO	6.93	–	–	6.34	2.5	6.27	2.56	–	–	4.87	9.12	7.03	5.39	–	–
MnO	0.2	0.17	0.16	0.16	0.16	0.10	0.12	0.20	0.18	0.18	0.18	0.16	0.16	0.21	0.20
MgO	11.96	14.21	10.02	12.92	9.44	6.27	9.23	19.01	13.52	6.04	7.22	10.98	7.70	10.34	6.27
CaO	7.58	10.22	10.61	9.01	12.87	11.90	9.67	4.75	5.63	11.95	11.55	13.71	11.15	10.98	10.80
Na2O	2.55	2.00	2.08	1.29	1.91	3.60	2.53	0.36	1.70	0.95	3.25	1.02	3.07	2.46	3.27
K2O	0.13	0.12	0.63	0.16	0.17	0.30	0.29	0.48	0.80	0.15	0.17	0.03	0.26	0.05	0.20
P2O5	0.01	0.07		0.03	0.07	0.20	0.11	0.04	0.03	0.04	0.10	0.01	0.12	0.06	0.15

Rambler, Mango Bight, Bay of Islands, Papua New Guinea, Marianas Trench, Bay of Islands, Papua New Guinea,

Marianas Trench, Tonga, Lau, Chun and Indian Islands.

Pacquet Harbour basalt (Gale, 1971).

	1au	1au	1au	1au	1au	1au	1au	1au	1au	1at	1at	1at
Sample	31	32	33	34	35	36	37	38	39	40	41	42
SiO2	53.13	54.09	50.63	51.15	51.41	55.60	52.42	54.42	53.12	48.59	49.23	49.41
Al2O3	8.32	11.11	9.85	10.36	9.03	9.11	10.34	9.59	7.84	15.02	16.95	14.20
TiO2	0.20	0.18	0.15	0.16	0.14	0.13	0.20	0.15	0.16	1.77	1.80	1.49
Fe2O3	11.55	10.28	12.86	11.66	11.24	9.76	9.62	9.16	10.43	11.35	11.98	13.23
MnO	0.18	0.17	–	–	0.22	0.17	0.19	0.16	0.16	0.19	0.16	0.00
MgO	14.52	12.29	13.81	16.40	15.75	13.87	13.40	13.76	14.25	7.02	7.59	8.92
CaO	9.78	8.95	10.71	8.32	10.51	9.64	11.64	10.08	12.02	11.60	7.71	9.60
Na2O	2.21	2.70	1.97	1.79	1.60	1.58	1.97	2.57	1.70	3.96	4.01	2.88
K2O	0.03	0.17	0.34	0.06	0.04	0.04	0.14	0.04	0.19	0.03	0.15	0.09
P2O5	0.06	0.06	0.11	0.10	0.06	0.08	0.08	0.07	0.08	0.24	0.23	0.14

Pacquet Harbour Group. 1at = tholeiitic basalts, 1au = ultramafic basalts (Gale, 1971).

Pacquet Harbour basalt (Hibbard, 1983).

Sample	0001	0002	0003	0005	0006	0010	0013	0014	0015	0016	0017	0018
SiO2	52.60	48.40	47.50	51.40	48.30	49.90	53.80	49.70	51.70	52.00	51.30	50.60
Al2O3	11.95	18.75	17.95	9.40	15.35	10.55	9.90	10.00	8.80	9.25	7.90	9.65
TiO2	0.17	1.30	1.34	0.07	1.59	0.12	0.17	0.18	0.10	0.09	0.07	0.10
Fe2O3	1.07	2.43	1.77	0.89	2.95	12.75	1.87	1.57	1.06	1.42	1.24	1.27
FeO	7.19	6.05	6.94	7.32	8.06	5.27	7.68	–	7.47	7.68	7.84	9.30
MnO	0.13	0.17	0.15	0.17	0.15	0.18	0.13	0.18	0.12	0.12	0.16	0.16
MgO	14.85	7.18	8.14	17.03	8.39	13.35	12.79	16.75	16.88	15.00	16.58	9.86
CaO	9.12	11.57	11.64	8.54	6.89	4.17	9.18	9.42	9.53	10.80	11.86	3.80
Na2O	2.13	2.63	2.39	1.53	3.39	0.21	3.28	1.57	1.73	1.92	1.68	1.00
K2O	0.14	0.56	0.54	0.06	0.10	0.05	0.09	0.06	0.06	0.18	0.33	0.04
P2O5	0.04	0.13	0.14	0.02	0.16	0.05	0.07	0.07	0.04	0.05	0.06	0.08
LOI	2.16	2.15	1.85	3.28	2.54	4.80	2.40	3.36	2.75	1.88	2.01	3.71

Table A3.3: Major and trace element data from unaltered basalts in the southern portion of the Pacquet Harbour Group (Swinden, 1992).

Sample	2141001	2141002	2141003	2141004	2141005	2141006	2141007	2141008	2141009
SiO2	54.63	52.09	51.81	54.14	51.44	50.04	47.47	56.11	48.99
Al2O3	11.87	9.34	12.15	7.87	10.83	12.38	10.27	12.24	11.32
Fe2O3	1.87	1.81	2.00	2.35	2.82	1.88	3.34	1.26	1.64
FeO	6.15	6.53	6.14	7.20	11.29	7.46	11.03	5.27	6.47
MgO	10.82	14.83	13.74	14.62	11.62	14.76	14.26	10.23	15.80
CaO	9.09	10.21	8.00	10.16	6.67	7.04	8.38	9.29	9.65
NA2O	2.43	1.64	2.83	2.00	0.55	2.22	0.94	3.80	1.66
K2O	0.10	0.21	0.08	0.15	0.12	0.04	0.01	0.02	0.05
TiO2	0.16	0.11	0.18	0.09	0.13	0.13	0.19	0.15	0.18
MnO	0.16	0.18	0.16	0.17	0.24	0.19	0.22	0.12	0.14
P2O5	0.02	0.01	0.02	0.02	0.01	0.02	0.02	0.01	0.02
LOI	2.35	2.77	3.39	1.94	4.03	4.24	3.91	1.32	3.26
total	99.65	99.73	100.50	100.71	99.75	100.40	100.04	100.32	99.18

Sample	2141011	2141012	2141013	2141014	2141015	2141016	2141017	2141018	2141019
SiO2	50.96	54.30	71.81	51.26	59.81	51.23	53.16	53.08	46.35
Al2O3	10.03	11.63	11.34	10.43	10.15	12.81	10.79	10.91	15.83
Fe2O3	1.59	0.75	1.39	1.60	1.22	2.79	2.67	1.53	2.64
FeO	7.38	6.99	1.72	6.86	5.62	6.36	6.32	5.81	7.01
MgO	14.90	10.93	2.76	14.98	8.68	13.55	13.02	13.10	10.64
CaO	10.99	7.95	2.64	7.15	6.61	6.67	11.14	11.04	12.52
NA2O	1.00	3.04	5.65	2.88	3.71	1.32	2.01	2.02	2.05
K2O	0.15	0.09	0.15	0.14	0.11	0.82	0.04	0.26	0.15
TiO2	0.10	0.18	0.16	0.10	0.14	0.16	0.10	0.17	1.33
MnO	0.21	0.19	0.03	0.17	0.13	0.17	0.14	0.12	0.16
P2O5	0.01	0.01	0.03	0.02	0.03	0.02	0.02	0.01	0.05
LOI	2.54	2.07	1.89	4.14	1.86	4.56	1.29	1.56	1.45
total	99.86	98.13	99.57	99.73	98.07	100.46	100.70	99.61	100.18

Table A3.4 Mineral analyses from select studies.

Sample		SiO2	Al2O3	TiO2	Fe2O3	FeO	MnO	MgO	CaO	Na2O	K2O	Cr2O3	H2O
Deer, Howie and Zussman (1966)													
1	alb	67.84	19.65	0	0.03	0.02		0.04	0	11.07	0.29		0.86
2	alb	67.81	20.50		0.07			0.10	0.81	10.97	0.36		0.25
3	mus	45.24	36.65	0.01	0.98	0.02	0.12	0.88	0	0.64	10.08		4.56
4	mus	48.42	27.16	0.87	6.57	0.01				0.35	11.23		4.5
5	chl	23.2	24.12		3.48	23.1		22.76	1.04				12
6	chl	27.64	22.58	0.22	0.06	12.06	0.02	24.32		0.17	0.06		13.25
7	chl	25.62	21.19	0.58	3.88	21.55	0.35	19.28	0.16				11.06
8	chl	31.64	17.62				37.64						13.19
9	chl	28.32	19.03	0.09	1.19	14.85	0.09	23.72	0.62	0.01	0		12.01
10	chl	27.11	17.42	0.35	2.91	30.68		9.75	0.21				11.58
11	chl	20.82	17.64		8.7	37.96		4.15					10.31
12	chl	26.4	18.23		5.7	25.87	0.04	11.35	0.42	0.17	0.17		11.11
(Henley et al., 1981)													
2837-1208	mu	51.94	30.8	0		3.79	0	2.35	0.13	0.09	8.95		
2878-406	mu	48.08	34.82	0.1		0.87	0.04	1.24	0.23		7.45	0.09	
2878-406	mu	42.95	33.50	0.09		0.93	0.05	1.23	0.07		7.94	0.07	
(Maclean et al., 1991): microprobe analyses of alteration minerals													
N87-2	chl	22.61	23.38	0.05		39.16	0.2	4.24	0	0.01	0.01		10.78
N87-3	chl	25.14	19.63	0.03		33.27	0.21	9.94	0.06	0.04	0.01		10.95
N87-11	chl	24.51	22.2	0.08		31.31	0.51	9.92	0.03	0.02	0.01		
N87-12	chl	23.72	22.83	0.06		34.65	2.38	5.64	0.01	0.04	0.03		
N87-22	chl	27.85	19.28	0.04		21.95	0.43	18.83	0.02	0.01	0		11.07
N87-25	chl	26.33	21.72	0.03		23.26	0.25	16.43	0.02	0.04	0.01		11.39
N87-26	chl	25.67	21.5	0.05		28.86	0.58	12.07	0.02	0.03	0.09		11.31
N87-27	chl	28.21	21.24	0.04		12.6	0.32	24.54	0.02	0.02	0.02		12.08
N87-2A	ser	47.18	35.94	0.18		2.24	0.02	0.56	0.01	1.17	8.96		4.57
N87-7	ser	45.26	35.66	0.5		1.04	0.01	0.54	0	0.81	10.13		4.45
N87-11A	ser	46.54	34.35	0.18		2.55	0.03	0.38	0.01	0.94	10.16		4.47
N87-12A	ser	48.81	34.67	0.13		2.29	0.06	0.33	0.49	0.55	8.83		4.58
N87-20A	ser	45.87	33.48	0.02		2.66	0	0.92	0	1.12	9.98		4.42
N87-25A	ser	49.77	29.68	0.32		2.7	0.02	1.43	0.58	1.53	9.42		4.49
N87-26A	ser	47.38	32.02	0.25		3.29	0.01	1.24	0.04	0.35	10.54		4.45
N87-3A	plag	67.2	20.11	0.02		0.27	0.01	0	0.55	11.19	0.08		
N87-11B	plag	67.58	19.47	0.02		0.1	0.01	0	0.09	11.53	0.02		
N87-22A	plag	68.27	19.51	0.03		0.21	0.05	0	0.14	11.32	0.04		
N87-26A	plag	61.64	24.43	0.02		0.16	0.05	0	6.07	8.21	0.05		
Svenden (1985), probe data													
C-152-1	chl	26.06	19.33	0.04		26.75	0.32	14.14	0.09	0.09	0.14		
C-152-2	chl	26.34	18.65	0.06		27.95	0.4	13.09	0.08	0	0.07		
C-152-3	chl	25.89	18.29	0.09		27.32	0.41	13.72	0.08	0	0.03		
C70-1	chl	29.77	15.68	0		27.09	0.18	16.34	0.37	0.05	0.03		
C70-2	chl	27.85	15.75	0		26.61	0.13	15.18	0.07	0.04	0.01		
C70-3	chl	31.3	14.99	0		27.12	0.02	14.79	0.26	0.07	0.03		
C70-4	chl	29.64	15.02	0.01		27.65	0.18	14.69	0.27	0.02	0.01		
C70-5	chl	28.43	15.59	0.00		27.65	0.20	13.87	0.20	0.11	0.03		
C70-6	chl	29.49	15.19	0.00		26.57	0.18	14.52	0.24	0.00	0.04		
C70-7	chl	30.39	15.93	0.02		27.83	0.18	14.41	0.30	0.06	0.01		
C70-8	chl	28.60	15.96	0.00		28.41	0.14	15.09	0.24	0.00	0.03		
C177-1	chl	26.54	16.39	0.04		27.48	0.61	13.40	0.13	0.10	0.01		
C177-2	chl	28.29	16.23	0.02		28.24	0.60	13.39	0.09	0.11	0.01		
C177-3	chl	28.38	16.92	0.00		27.52	0.65	13.48	0.04	0.09	0.00		
C177-4	chl	28.23	17.55	0.02		28.65	0.61	14.40	0.06	0.03	0.01		
C177-5	chl	28.18	16.99	0.01		28.55	0.65	13.54	0.05	0.07	0.01		
C177-6	chl	27.85	16.84	0.02		27.73	0.60	13.79	0.09	0.11	0.01		
C177-7	chl	27.69	17.17	0.01		28.13	0.66	14.46	0.07	0.15	0.03		
C177-8	chl	28.70	16.93	0.02		27.00	0.64	13.82	0.10	0.12	0.03		
C52-1	chl	29.44	15.64	0.00		19.51	0.17	18.70	0.05	0.15	0.00		

Table A3 5 Selected trace element concentrations (ppm) of specific sulphide mineral assemblages from VMS Deposits in the Northeast Pacific and Mid – Atlantic (after Hannington, 1990)

	n	Au(ppm)	Ag	As	Sb	Se	Cd	Mo	Hg
Axial Seamount									
sphalerite – marcasit	9	5 17	199	561	375	3	693	37	19
barite – silica	7	4 12	145	605	232	2	193	31	24
Explorer Ridge									
pyrite – chalcopyrite	15	0 18	18	432	4	190	6	290	2
pyrite – marcasite	7	0 52	24	784	13	113	21	190	4
marcasite – sphalerit	8	1 40	303	594	64	75	168	79	8
sphalerite – marcasit	12	1 33	212	610	80	6	506	59	6
barite – silica	6	0 84	92	450	76	3	128	60	58
TAG Hydrothermal Field									
black smoker	7	0 48	13	32	2	201	17	118	
pyrite – chalcopyrite	2	1 43	38	67	6	8	38	144	7
marcasite – sphalerit	4	2 29	35	122	10	< 2	73	82	9
sphalerite – marcasit	10	3 28	151	98	33	< 2	650	35	34
silica – sphalerite	2	0 41	25	82	10	< 2	151	35	9
Snakepit Vent Field									
black smoker	4	0 34	19	48	5	224	34	11	
pyrite – pyrrhotite	1	0 39	10	122	10	136	74	14	–
pyrite – marcasite	2	0 92	<5	324	3	62	5	42	1
sphalerite – marcasit	2	4 62	90	918	46	< 2	219	28	2

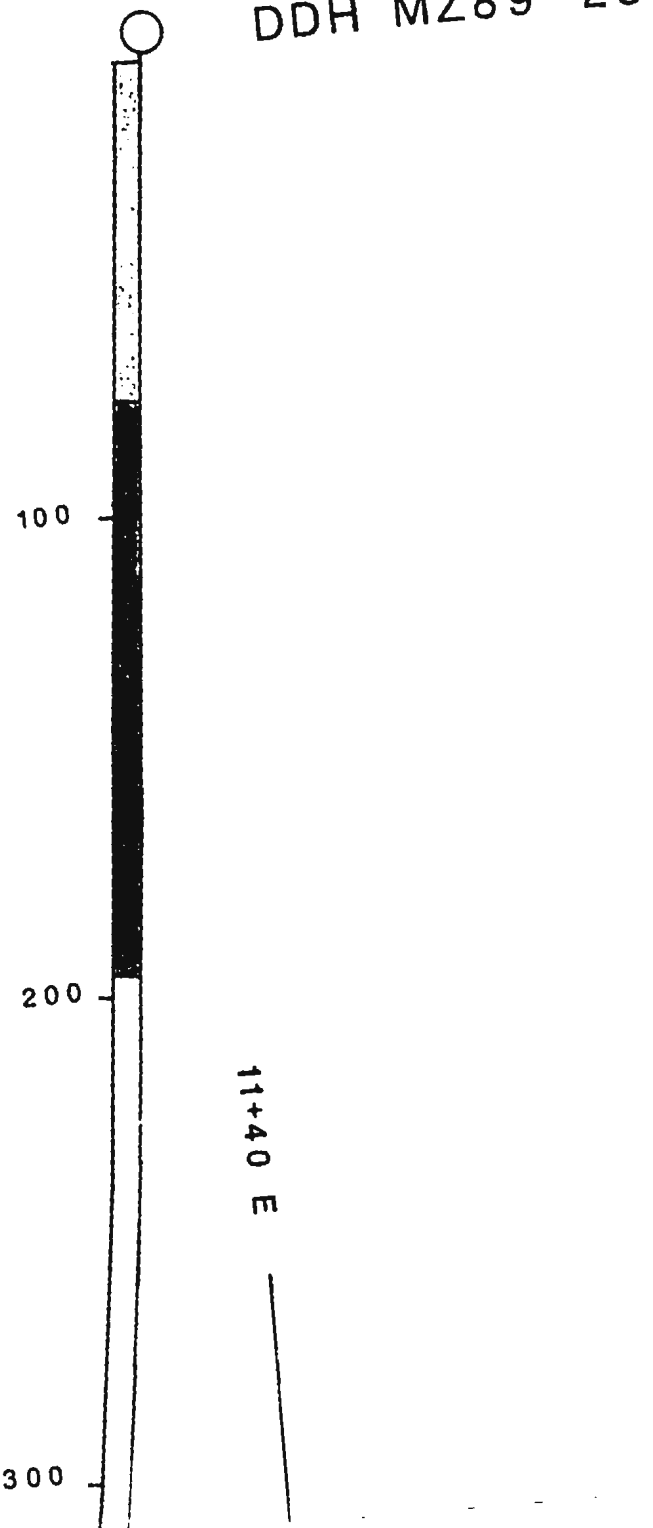
DDH MZ89-28
100
200
300
11+40 E

89-28

FIGURE 5.1: REPRESENTATIVE DRILL SECTION:
RAMBLER DEPOSIT (DDH MZ89-28)

(after MPH Exploration Ltd., 1989)

Lithology / Alteration Summary

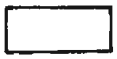

quartz-carbonate veins with chloritic fractures (stage 3 alteration).

dark green, fine massive, mafic dykes with sharp intrusive contacts.

Hangingwall (Stage 1 Alteration)

mixed sediment including polymict conglomerate, felsic agglomerate, wacke, volcanic / epiclastic sediment and tuff.

dark to light green, fine massive to foliated basalt, pillow selvages, relict amygduales, interflow breccia.

dark green coarse cumulate to fine massive, and porphyritic textured gabbro.

Deposit (Stage 1 and 2 Alteration)

dark red to black, amorphous, recrystallized magnetic chert.

breccia textured and sheared ore with intervals of massive ($\geq$ 80 %) to semi-massive ($\geq$ 60, $\leq$ 80 %) and disseminated sulphide ($\leq$ 30 %).

mixed quartz + chlorite ± epidote breccia / schist.

Footwall (Stage 2 Alteration)

quartz + chlorite ± sericite schist; disseminated sulphide; pyrite, with trace chalcopyrite and sphalerite ($\leq$ 20 %).

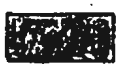

quartz + sericite ± chlorite schist / mylonite with disseminated pyrite ($\leq$ 30%).

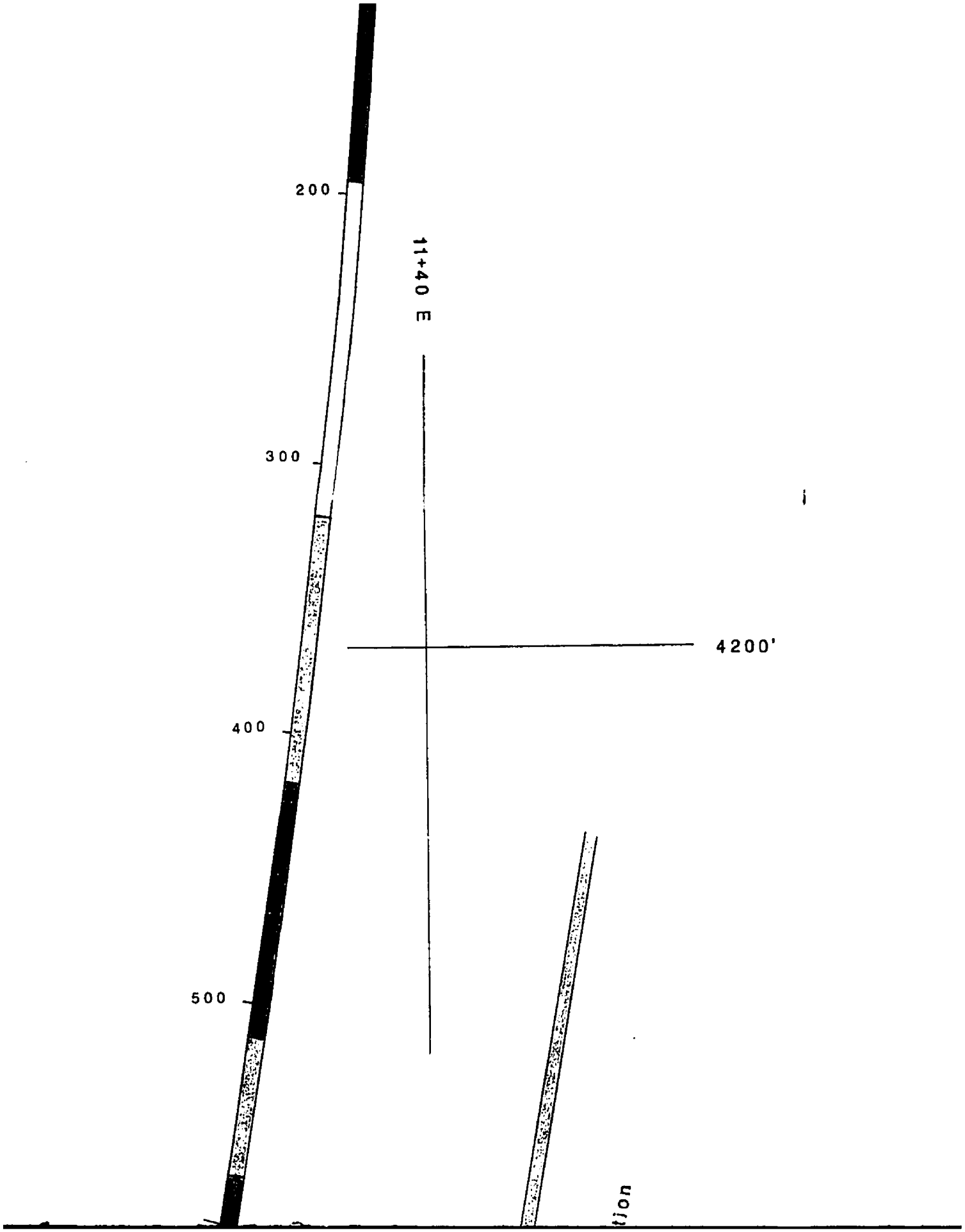
200
300
400
500
11+40 E
4200'
tion

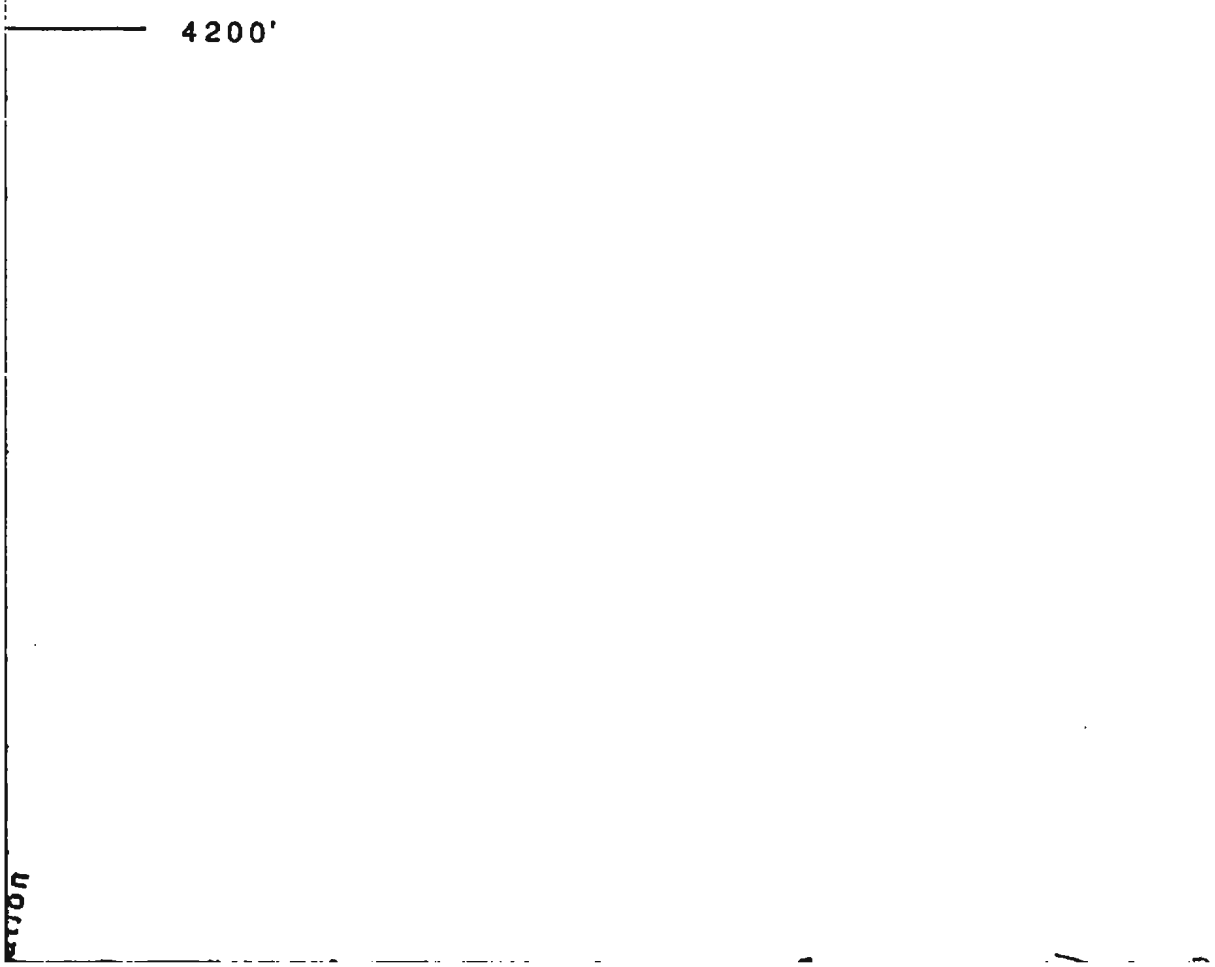
4200'

Deposit (Stage 1 and 2 Alteration)

dark red to black, amorphous, recrystallized magnetic chert.

breccia textured and sheared ore with intervals of massive (≥ 80 %) to semi-massive (≥ 60, ≤ 80 %) and disseminated sulphide (≤ 30 %).

mixed quartz + chlorite ± epidote breccia / schist.

Footwall (Stage 2 Alteration)

quartz + chlorite ± sericite schist; disseminated sulphide; pyrite, with trace chalcopyrite and sphalerite (≤ 20 %).

quartz + sericite ± chlorite schist / mylonite with disseminated pyrite (≤ 30%).

Assay Data

	Au (oz/ton)	Cu (wt%)	Zn (wt%)	Ag (oz/ton)
	≥ 1.000	≥ 2.000	≥ 1.500	≥ 1.000
	≥ 0.250	≥ 1.000	≥ 1.000	≥ 0.250
	≥ 0.075	≥ 0.500	≥ 0.500	≥ 0.075
	≥ 0.025	≥ 0.250	≥ 0.050	≥ 0.025
	≥ 0.010	≥ 0.050	≥ 0.010	≥ 0.010

500
600
700
800
900
hangingwall
stage 1 alteration
stage 1 and stage 2
alteration

Stage 1 alteration

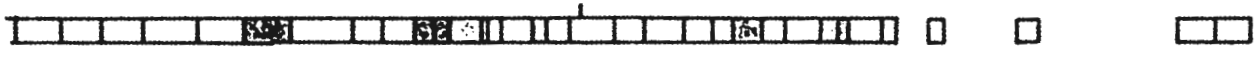

900

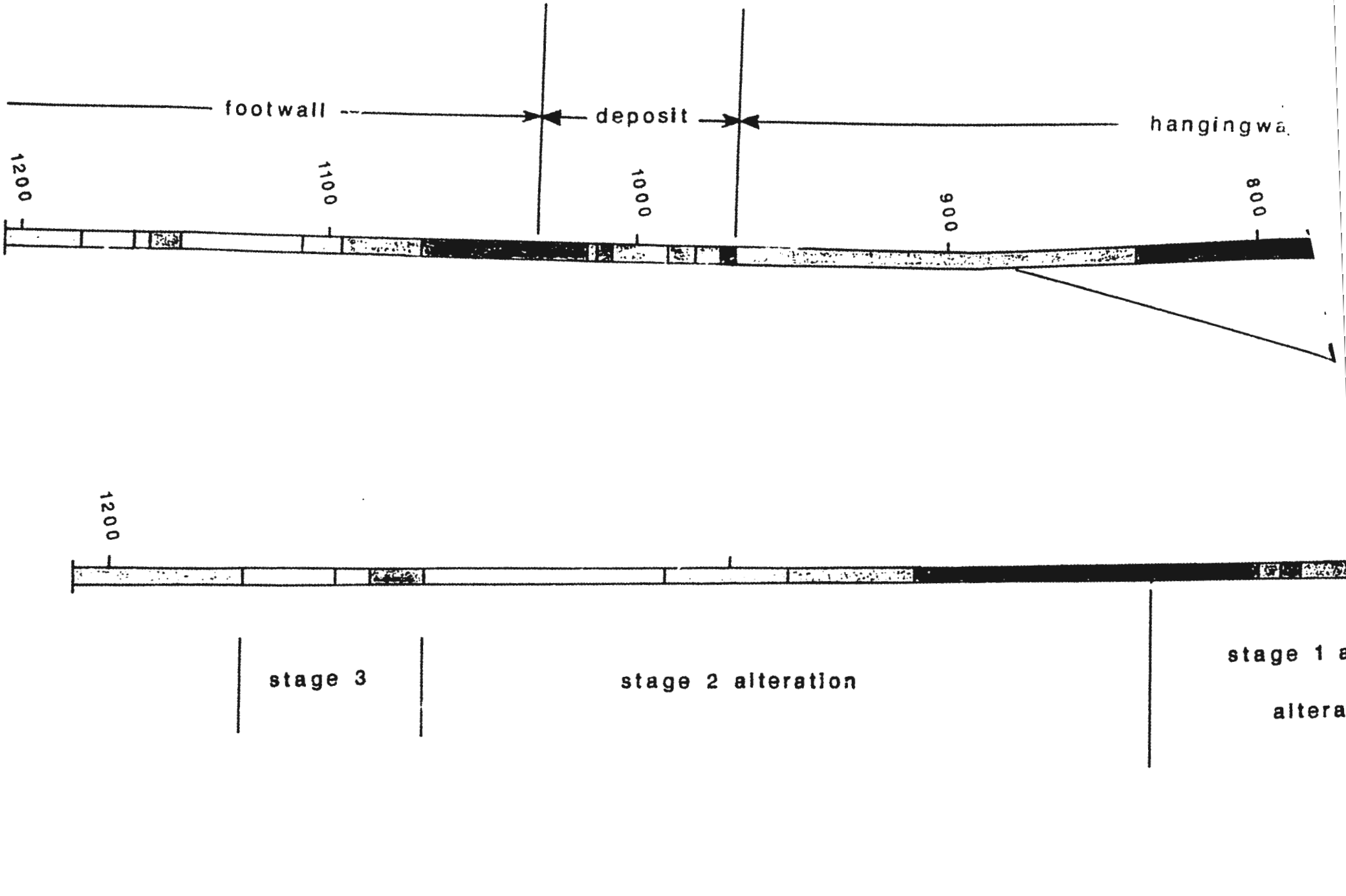
footwall
deposit
hangingwa
1200
1100
1000
900
800
1200
stage 3
stage 2 alteration
stage 1 a
altera

Au oz / ton
Cu wt %

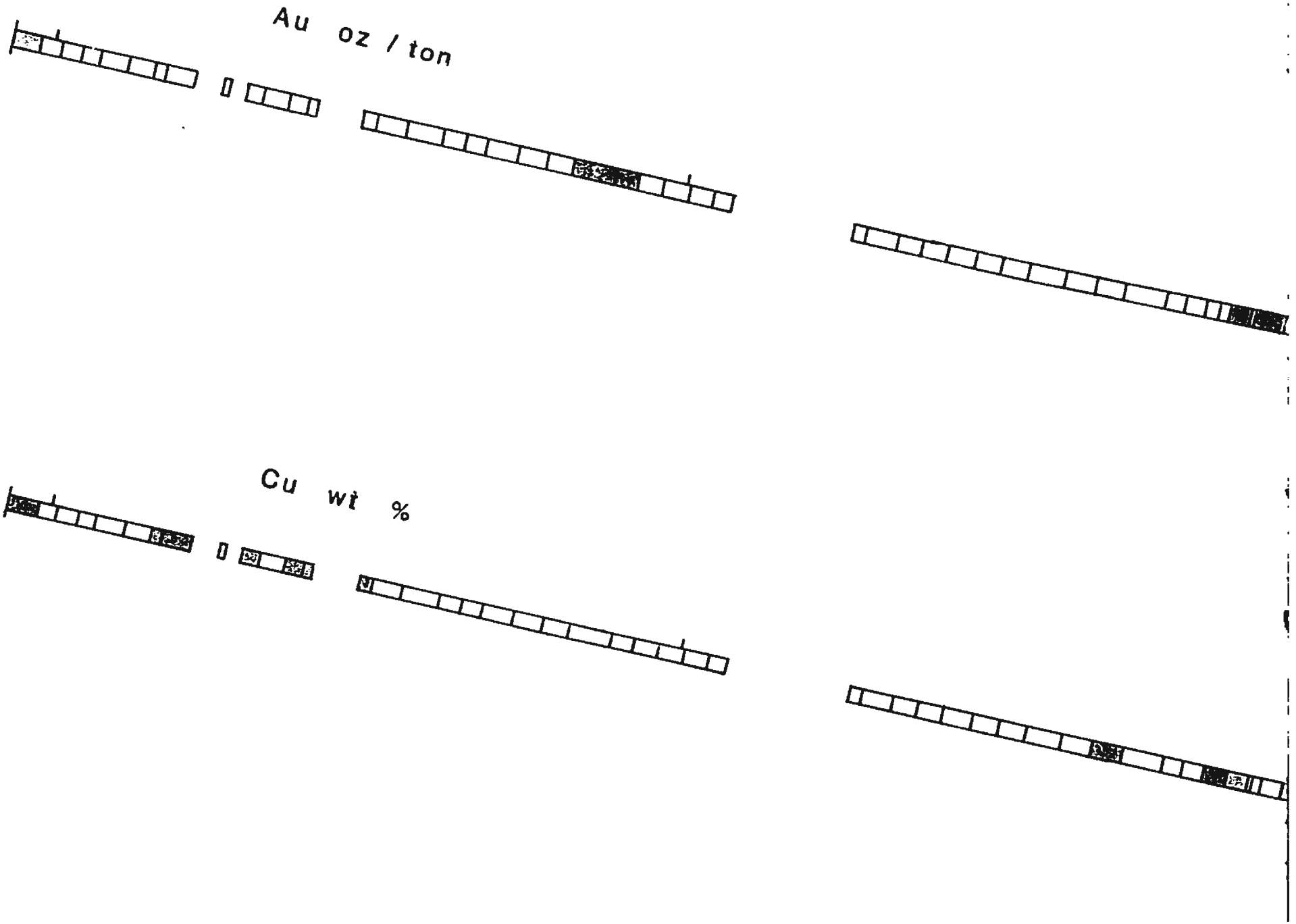
Au oz / ton
Cu wt %

Zn wt %
Ag oz / ton
1200